Methodology for the Seismic Assessment of Earthen and Timber Historic Churches

Application to Peruvian Heritage

by

Carina Fonseca Ferreira

Submitted to the Department of Civil, Environmental and Geomatic Engineering in partial fulfilment of the requirements for the degree of

Doctor of Philosophy in Earthquake Engineering

at

UNIVERSITY COLLEGE LONDON

November 2016

I, Carina Fonseca Ferreira confirm that the work presented in this thesis is my own. Where information has been derived from other sources, I confirm that this has been indicated in the thesis.

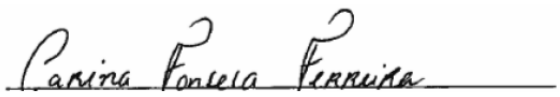

Methodology for the Seismic Assessment of Earthen and Timber Historic Churches

Application to Peruvian Heritage

by

Carina Fonseca Ferreira

Submitted to the Department of Civil, Environmental and Geomatic Engineering in partial fulfilment of the requirements for the degree of Doctor of Philosophy in Earthquake Engineering

Abstract

Historic buildings, and churches in particular, are one of the most complex existing structures not only because of the structural system complexity but also due to the limited documentation on their construction that is normally available. Amongst historic buildings, earthen and timber churches built across Latin-America are one of the least studied and most vulnerable structures, as past earthquakes have shown. For instance, the 2007 Pisco earthquake caused the collapse of many historic earthen and timber colonial churches in Peru. The thesis proposes a new framework for the seismic assessment of historic buildings that measures the uncertainty of the structural analysis and its influence on the structural diagnosis due to incomplete knowledge. The methodology is validated through application to two historic earthen and timber churches built in Peru in the 17th and 18th centuries, of different complexity and cultural value, which are representative of important Latin-American colonial building types. The most important variables that govern the seismic response of these churches are identified by means of numerical simulations. Through the application of the framework, the thesis provides a modeling and structural evaluation solution for planked timber vaults and a hypothesis on the cause of failure of these vaults during the 2007 Pisco earthquake. The influence of lack or shortage of knowledge on the structural diagnosis of the churches is discussed. Alterations to current guidelines for the assessment of historic buildings are proposed from the conclusions drawn from the study.

Thesis Supervisor: Prof. Dina D'Ayala

Acknowledgments

This story is made of enjoyable and sad moments, as all real stories. I moved from Portugal to England with the support of Prof. Humberto Varum, who has always been a reference to me. I met Prof. Dina D'Ayala, my supervisor, several years ago in Bath. She not only built the foundations of this research and participated in each and all steps of it, but also influenced like anyone else the way how I approach any challenge. Logic and commitment are concepts that will follow me forever. After fifteen days in Bath, I went for the first time to Peru. Peru was still trying to recover from a devastating earthquake. I first met Lucho and later on Prof. Daniel Torrealva, Claudia Cancino and Erika Vicente. This was my first contact with the institution that funded this research - The Getty Conservation Institute. During this trip, I discovered the beauty of remote villages in the Andes and the drama of a priest who used to pray every day in a silent and damaged cathedral. I would be back to Peru several times to conduct field surveys and participate in the tests carried out at Pontificia Universidad Catolica del Peru. In Bath, I met Viviana who showed me the best of Napoli, even though I have never had the chance to visit the city. Two years later, we moved with Dina to London. By that time, I became a member of the COST Action FP1101, which allowed me to participate in discussions on the present challenges in timber engineering and gave me the opportunity to work with some of the best experts in Europe. This Action funded my scientific mission to Madrid. Indeed, the first three weeks as a University College London's student were spent in Madrid with Prof. Jose Fernandez Cabo, Marina, Rafael, Almudena and Jorge. Jose and his group tested for the first time a timber planked arch at Universidad Politecnica de Madrid. Back to London, I found the best group of friends in the most remote research room of UCL – GM16. Then I went to China, where I learned about the Chinese masonry pagodas with Shengcai and Prof. Yuan. After completing my research in London, I moved to the USA, where I found in Fernando Ramirez, Laisa, Rashmin and Juan Carlos the strength I needed to finalise this thesis. Along this journey, I always had the unconditional support of my parents, António and Maria da Conceição, and siblings, Célia, Lurdes and Tóne, who are always with me.

This thesis is dedicated to my beloved relatives and friends who passed away during this journey, who I know will never read this thesis but are present in each and all words of it.

To all of you: Obrigada.

Contents

List of tables

List of figures

Glossary

Attribute	It is an intrinsic aspect of the construction that can be characterized in a qualitative or quantitative way in order to inform on the structural performance of the construction.
Control variable	An input or inherent characteristic of a model that influences the results of analysis conducted with this model. The results of structural analysis can be controlled by the value or state of these variables. A control variable can be associated to the geometry, materials, and structural details of the structure, and to actions and modelling techniques used in the analysis.
Fragility	The probability of a structure sustaining a given damage state due to a given hazard level.
Global model	Model of the structure that includes all relevant components and/or interactions that govern its global structural behaviour. This does not necessarily entail that all structural components are modelled. However, it requires the simulation of critical interactions or the influence that each component exerts on the behaviour of others.
Interval of plausibility	Range of plausible values of a control variable or structural performance indicator. It is expected that the unknown 'real' value of the control variable or structural performance indicator lies within this range. The interval of plausibility is characterised by three values: the minimum plausible, the most

	plausible or reference value, and the maximum plausible value.
Local model	Model of a representative portion of a structure used to test alternative hypotheses or to investigate specific local structural behaviour.
Maximum plausible value of a control variable	This value is part of the interval of plausibility of the control variable. It corresponds to the maximum expected value (upper bound) of a control variable in a specific assessment. This value is defined by the analyst.
Maximum plausible value of a structural performance indicator	This value is part of the interval of plausibility of the structural performance indicator. It corresponds to the maximum expected value (upper bound) of the indicator. In the detailed diagnosis, this value corresponds to an increase of the reference value taking into account the overall knowledge-based uncertainty of the assessment.
Minimum plausible value of a control variable	This value is part of the interval of plausibility. It corresponds to the minimum expected value (lower bound) of a control variable in a specific assessment. This value is defined by the analyst.
Minimum plausible value of a structural performance indicator	This value is part of the interval of plausibility of the structural performance indicator. It corresponds to the minimum expected value (lower bound) of the indicator. In the detailed diagnosis, this value corresponds to a reduction of the reference value taking into account the overall knowledge-based uncertainty of the assessment.
Parameter	A control variable characterised by a value. An interval of plausibility can be defined for each parameter.
Reference analysis conditions	These conditions correspond to a structural analysis where the reference values and reference states are assumed for all control variables. The outputs of these analyses are the

	reference values of the structural performance indicators.
Reference results	These are the results of a structural analysis conducted under the reference analysis conditions. The results or outputs of a structural analysis are the structural performance indicators.
Reference value	This value is also called here as the most plausible value. It is selected by the analyst as the value closest to the 'real' value of the control variable. Such selection is based on the best knowledge available and experience of the analyst.
Reference state	This state is selected by the analyst as the state closest to the 'real' state of the control variable. Such selection is based on the best knowledge available and experience of the analyst.
Sensitivity	The variation of the value of an output due to variations of inputs.
State	Condition of a control variable that does not have a numerical representation. Such condition aims to simulate a given state of the structure. For instance, alternative boundary conditions of the model correspond to alternative states of the structure.
Structural performance indicator	It is a quantitative measure of structural behaviour that indicates a given performance.
Uncertainty	The uncertainty of the diagnosis is here considered as the variation of the outputs within the intervals of plausibility of the control variables (i.e. interval of plausibility of the outputs) given a certain level of knowledge.
Value	Numerical representation of a control variable. For instance, the material properties of a structure, such as the modulus of elasticity, are defined by a value.
Vulnerability	The degree of loss sustained by a structure under a given hazard level.

Key Notation

$I_{jmn,Ki}$ Structural performance indicator j, which is an output of structural analysis

$I_{jmn,Ki}$ Value of the structural performance indicator j corresponding to the minimum value assumed for the control variable Ki

$I_{jmx,Ki}$ Value of the structural performance indicator j corresponding to the maximum value assumed for the control variable Ki

$I_{jref,Ki}$ Reference value of the structural performance indicator, calculated from the reference analysis conditions.

n_{pr} Number of variables of the preliminary diagnosis

m_{pr} Number of macroelements of the preliminary diagnosis

I_j 'Real' value of the structural performance indicator

m_p Total number of macroelements in the preliminary diagnosis

m_{uj} Knowledge-based uncertainty associated to a specific structural performance indicator j:

$$m_{uj} = \left\lceil \left(1 + \frac{\sum_{ki=1}^{n_c} \delta I_{j,ki}}{n_c} \right) \times \left(1 + \frac{\sum_{ki=1}^{n_c} \lambda_{ki}}{n_c} \right) \right\rceil - 1$$

m_u Knowledge-based uncertainty of the results, which takes into account multiple structural performance indicators:

$$m_u = \left[\left(1 + \frac{\sum_{j=1}^{p} \delta I_j}{p} \right) \times (1 + \lambda) \right] - 1 \text{, or } m_u = \left[\left(1 + \frac{\sum_{ki=1}^{n_c} \alpha_{ki}}{n_c} \right) \times (1 + \lambda) \right] - 1$$

m_{urmn} Minimum reference value of the knowledge-based uncertainty

m_{urmx} Maximum reference value of the knowledge-based uncertainty

n Total number of control variables

n_c Total number of critical variables

n_p Total number of attributes in the preliminary diagnosis

p Total number of structural performance indicators

V_{Ki} Control variable, where K denotes the class and i the number

V_{Kimn} Minimum plausible value

V_{Kimx} Maximum plausible value

V_{Kiref} Most plausible or reference value

w_j Weights of the structural performance indicators

α_{ki} Influence of a control variable Ki on the output:

$$\frac{\sum_{j=1}^{p} \delta I_{j,Ki}}{p}$$

$\delta I_{j,Ki}$ Sensitivity of a structural performance indicator j to the variation of a control variable Ki:

$$1 - \left(\frac{I_{jmn,Ki}}{I_{jmx,Ki}} \right)$$

δI_j Overall sensitivity of a structural performance indicator *j*:

$$\frac{\sum_{Ki=1}^{n} \delta I_{j,Ki}}{n}$$

$\delta Ip_{j,i}$ Uncertainty on the judgement of attribute *j* as far as macroelement *i* is concerned, in the preliminary diagnosis

δIp_j $$\frac{\sum_{i=1}^{mp} \delta Ip_{j,i}}{mp}$$

δIp_i $$\frac{\sum_{j=1}^{np} \delta Ip_{j,i}}{np}$$

δIp $$\frac{\sum_{i=1}^{np} \delta Ip_{j}}{np}, \text{ or } \frac{\sum_{i=1}^{mp} \delta Ip_{i}}{mp}$$

δV_{Ki} Range of variation of a control variable *Ki*:

$$1 - \left(\frac{V_{kimn}}{V_{Kimx}} \right)$$

λ_{ki} Knowledge index of a critical variable *Ki*

Acronyms and abbreviations

DEM	Discrete Element Method
DS	Damage states
EAI-SRP	Earthen Architecture Initiative – Seismic Retrofitting Project in Peru
FEM	Finite Element Method
GCI	The Getty Conservation Institute
GM	Global model
ICOMOS	International Council on Monuments and Sites
ISCARSAH	International Scientific Committee on the Analysis and Restoration of Structures of Architectural Heritage
LM	Local model
MCP	Ministerio de Cultura del Perú
MDOF	Multi-degree-of-freedom
MMI	Modified Mercalli Scale
MRSA	Mean response spectral acceleration
NRSA	Nominal range sensitivity analysis

OAT	One at a time
PGA	Peak ground acceleration
PUCP	Pontificia Universidad Católica del Perú
SDOF	Single-degree-of-freedom
SPI	Structural performance indicator
UCL	University College London
UPM	Universidad Politécnica de Madrid

Many issues still need good answers; explanations require new scientific developments; and simple and cheap interventions are needed. But the international knowledge has already reached a level that, if placed at the easy of professionals and seismic code-makers, and applied without restrictions by their owners, there is a great potential for an important mitigation of our architectural heritage.

Carlos Sousa Oliveira[1]

[1] Sousa Oliveira C. (2003). Seismic vulnerability of historical constructions: a contribution. *Bulletin of Earthquake Engineering*, 1, p.37-82

CHAPTER 1

Introduction

1.1 Historic buildings: preserving values and assuring safety

Historic buildings have a unique identity and recognized importance by present communities, even though their everyday use might have changed over the years. Such importance emerges from the wide recognition of their cultural significance, which regards the aesthetic, historic, scientific, social or spiritual value of a construction for past, present or future generations, as defined by the Burra Charter issued in 1979 (ICOMOS, 2004a). Cultural significance includes the value of hidden parts (the structural part) whose preservation is often neglected (Hume, 2007). The cultural significance of a historic building is related to the predominant conservation values of society at any given time, and these tend to evolve over the years.

On the one hand, conservation values have changed throughout the history of humankind. On the other hand, alternative conservation values, often regulated by dichotomous philosophies, have coexisted in different geographical locations. Often, different groups of conservators defend alternative conservation values within the same period of time and location. From the purist approach that advocates that all original parts should be preserved and supported by a more modest and clearly different material, to the "stylistic restoration" of Viollet-le-Duc's, in which the restorer was allowed to create a historic falsehood (D'Ayala and Forsyth, 2007), conservation practices have historically found alternative solutions for similar structural problems.

At present, the principles of conservation disseminated by the Venice Charter issued in 1964 (ICOMOS, 2004b) are almost accepted worldwide. The principles of authenticity, minimum intervention, like-for-like repairs, compatibility, reversibility or rectractability, and durability are well established and widely applied; even though the application of the principles in practice is deeply related to the expectations and perceptions of the authorities, citizens and owners, in terms of real cost and cultural significance.

The compliance with conservation principles is met with increased challenges in the case of buildings located in seismic prone areas, since they often require high levels of upgrading to ensure the present and future safety of the occupants and of the structure itself. Earthquakes have caused and continue to cause extensive losses of cultural heritage. Noticeable examples are the Mausoleum of Halicarnassus in Turkey and the Lighthouse of Alexandria in Egypt, which are among the seven wonders of the ancient world. More recently, the destruction of the Bam Citadel in Iran by an earthquake in December 26th 2003, and of many historic temples and palaces in Nepal by an earthquake in April 25th 2015 (Figure 1.1 and Figure 1.2), have dramatically shown that historic buildings continue to be vulnerable to earthquakes.

Stabilization and repair interventions are often insufficient to prevent life and/or cultural losses caused by poor structural performance of historic buildings during earthquakes. In this case, upgrading interventions must be undertaken in order to eliminate or reduce the level of deficiencies and improve the structural performance of the buildings (see for instance ISRCHB, 2006). The upgrading of a historic building normally requires a case-by-case deliberation, which is based on the following aspects (D'Ayala and Forsyth, 2007):

(i) The life safety judgment;
(ii) Prevention of damage to building components and contents (damage control);
(iii) Cultural significance;
(iv) Foreseen use;
(v) Predominant conservation values, expectations and perception of value;
(vi) Timeframe; and
(vii) Economic context.

As far as seismic upgrading is concerned, the timeframe can directly or indirectly affect all other aspects, since it is associated with the risk of occurrence of natural hazards. This case-by-case deliberation should be supported by a robust and consistent method for a thorough assessment of the historic construction. The development and validation of such method is the objective of this thesis.

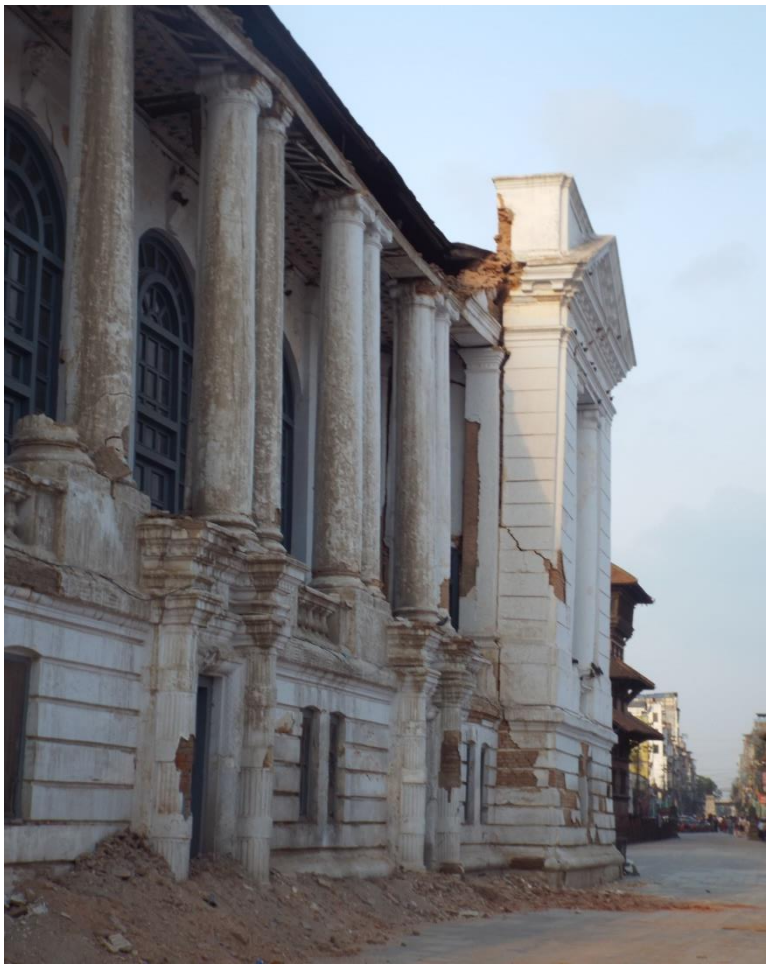

Figure 1.1 Hanuman Dhoka Palace damaged by the April 25th earthquake (Kathmandu, May 2015)

Figure 1.2 Collapsed temple in Durbar Square after the April 25th earthquake (Kathmandu, May 2015)

1.2 Investigating the state of historic buildings

The idea of performing a thorough investigation of the actual state of "health" of a historic building and the causes leading to such state can be traced back to the sixteenth century with the work of Leon Battista Alberti (D'Ayala and Forsyth, 2007; Alberti, 1988). In modern times, ICOMOS promotes the principle stating that the "*recording [of a heritage construction or site] should be undertaken to an appropriate level of detail in order to provide information for the process of identification, understanding, interpretation and presentation of the heritage [construction]*" (ICOMOS, 2004c). A medical-like and holistic approach is currently widely applied to investigate the state of conservation of a historic building. Complying with the previous principle, the process of assessing, identifying and planning treatment measures for a historic building can be categorized into the following four phases (ICOMOS-ISCARSAH, 2003):

(i) Acquisition and interpretation of original and historical data;
(ii) Interpretation of the current structural layout, construction and condition;
(iii) Diagnosis and safety evaluation; and
(iv) Planning, design and execution of interventions.

The first three phases can be supported by historical investigations, surveys, field and experimental research, structural analysis and monitoring. Taking into account this approach, the judgment of the level of current and future safety of a historic building requires that the analyst possesses both traditional building knowledge and current engineering knowledge and a robust method of acquiring, interpreting and applying the traditional knowledge (D'Ayala and Forsyth, 2007). Traditional building knowledge is the basis of historical and qualitative analysis, as defined by the ICOMOS-ISCARSAH (2003) principles. Qualitative analysis regards the comparison between the present condition of the structure and the condition of other similar structures which response is already understood.

Surveying, field and experimental research are important procedures to characterise the present state of the building, because the building has been subjected to long-term decay and damage in different ways and to an extent that is hardly comparable to any other site, although might find useful precedents in literature. Nevertheless, "opening up" or in situ testing are constrained in their application by the extent to which they might compromise any inherent cultural value. Furthermore, the benefits of experimental testing are often limited due to the anisotropic nature of traditional materials, the typical heterogeneity of

historic buildings, and economic or technical constraints. It has been discussed in literature that it is difficult to conclude on whether an experimental sample is representative of the best, the worst or the average of the structure as a whole (Beckmann and Bowles, 2004).

Advances in numerical methods and computer science provide the theory and tools to perform structural analyses of increasing complexity and detail of large structures composed of thousands of degrees-of-freedom and several sub-structures interacting with each other. Results of these analyses contribute, sometimes in a decisive way, to several phases of the investigation, especially to the phase of diagnosis and safety evaluation.

Historic buildings have been studied using the most advanced tools contemporarily available for structural analysis due to their relevant cultural significance (see for instance Roca *et al.*, 2010). An important amount of time and resources are therefore usually allocated to their assessment with the final aim of performing a diagnosis and safety evaluation. If interventions are required to improve the structural response or condition of a historic building, the interventions must comply with the principles of conservation.

However, although advanced structural analysis of historic buildings, on the basis of numerical models for instance, has been extensively performed especially in the past two decades, many concerns remain at present due to the high level of uncertainty normally present in such analyses. The high level of uncertainty normally compromises the reliability of the diagnosis and safety evaluation, which subsequently can compromise the safety of the occupants and the cultural significance of a historic building.

Thus, it could be argued that increasing the complexity of the calculation method is *per se* insufficient and not condition *sine qua non* for performing an accurate structural analysis. The accuracy of the results will increase only if the increased sophistication of the model is accompanied by an increased level of confidence in the value of the additional parameters required to define the refined model.

The requirements and compliance criteria of modern codes and guidelines can be used for the diagnosis and safety evaluation of a historic building, by taking advantage of the synergy of different expertise that is usually present in these documents. In addition, the foreseen use of a historic building could be considered in the evaluation of the structure and design of treatment measures by means of importance factors (see for example E.030, 2003 and EN 1998-3, 2005). Notwithstanding this possible application, importance factors proposed by modern codes do not take into account the cultural significance of historic buildings, which might be important to the diagnosis. Moreover, specifications of modern codes demand higher levels of reliability or structural performance in terms of damage

control, which could increase the level of intrusiveness of the interventions required for compliance. Such level of intrusiveness could compromise the cultural significance of the building.

1.3 Research motivation

Historic buildings and their analysis present the principal challenges summarized in Table 1.1, which emerge from the considerations developed in previous sections. These challenges originated from several factors, some of which include difficulties or limitations that compromise the reliability of the assessment, and ultimately the precision of the diagnosis.

Table 1.1 Principal challenges for the structural analysis and preservation of historic buildings

Principal challenges	Factors
(i) Knowledge of the present layout of the structure as a whole and materials is limited	▪ Original or historical information with details about the structure is normally limited; ▪ Original construction normally undergoes extensive changes over the years, which are not often recorded in detail; and ▪ Surveying and experimental work can be carried out up to an extent that it does not involve significant losses of historic materials or elements of the structure.
(ii) The present condition of the building is difficult to evaluate	▪ The structure normally undergoes complex processes of decay and damage that are different throughout the structure; and ▪ Evidences of decay or damage are often hidden and not easily visible.
(iii) High seismic fragility is typically ascribed to historic buildings	▪ Poor conceptual design and construction for earthquake resistance; ▪ Poor maintenance over the years, which lead to significant levels of deterioration; and ▪ Inadequate alteration of the original structural system.
(iv) Diagnosis is normally poorly supported by results of structural analysis	▪ Several assumptions in terms of structural performance are normally considered due to lack of knowledge and guidelines for traditional materials and structural systems; ▪ Structural analysis methods are not sufficiently developed for structural systems composed of traditional materials; ▪ Effect of decay or damage on the structural performance of the buildings is often difficult to assess; and ▪ Existing specifications of engineering codes in terms of damage control and reliability are not tailored to historic constructions.

Although there has been remarkable progress on the analysis of historic constructions made in recent decades, these challenges are still significant obstacles to the preservation of historic buildings especially in developing seismic prone countries. Peru is a prominent example of this due to the following main reasons:

(i) Peru has a high seismic hazard, being frequently affected by strong, damaging and deadly earthquakes;
(ii) Past earthquakes have shown that most existing historic buildings in Peru are vulnerable to earthquakes; and
(iii) The structural system of Peruvian historic buildings and their performance of largely under researched in Peru, which has led to wrong seismic retrofitting measures in the past.

Peru has a long documented history of strong earthquakes that have caused severe damage to existing constructions. Historical records summarized in Figure 1.3 show that Peru has been affected by many not only strong but also deadly earthquakes (see for instance Dorbath *et al.*, 1990; Utsu, 2002 and USGS Historic World Earthquakes List, 2011). The Global Seismic Hazard Map (Giardini *et al.*, 1999) shows that the Western coast of South America is one of the most active seismic areas of the world. According to this map, a PGA of 0.24g-0.4g with 10% chance of exceedance in 50 years is associated to a vast area of the Peruvian territory. In general, seismic activity in Peru is related to the subduction of the Nazca plate under the South American plate and also with tectonic structures accommodating this convergence process (Tavera *et al.*, 2009).

Earthen construction has performed a significant role in Peru for almost four thousand years, having spread throughout the country. In particular, earthen and timber historic buildings erected during the Spanish Viceroyalty, a period spanning from 1534 to 1821, have been constantly used over the years. Past earthquakes have shown that earthen and timber historic buildings are vulnerable to earthquakes. For instance, the Arequipa earthquake of June 23, 2001, of magnitude 6.9 in the Richter scale and maximum intensity VII-VIII MMI (Tavera *et al.*, 2002) caused severe damages, including the total collapse of colonial churches and houses. According to Aguilar and Farfan (2002), 36 of the 246 historic houses of the city of Arequipa were severely affected by the earthquake.

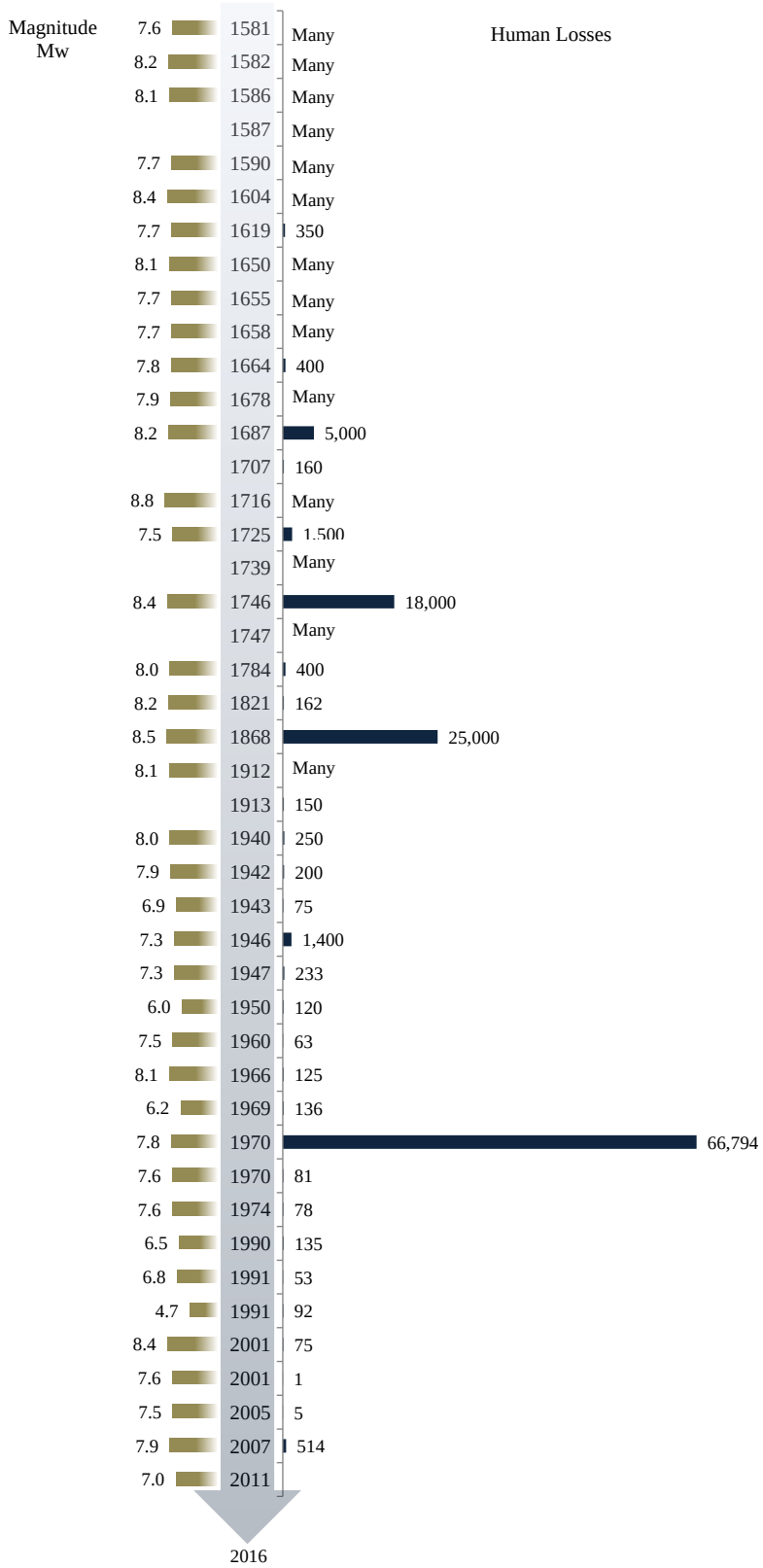

Figure 1.3 Magnitude and human losses of historical earthquakes in Peru since 1500 to present (*Source of the data:* Dorbath *et al.*, 1990; Utsu, 2002; USGS historic world earthquakes list, 2011)

The recent Pisco earthquake of August 15, 2007, of 7.9 M_W and maximum MMI of VIII in Pisco and VII in Ica, Chincha and San Vicente de Cañete (Tavera *et al.*, 2009) caused severe damage to historic churches. The San Clemente Cathedral, an adobe colonial church with planked timber vaults, collapsed during a service at the time of the earthquake, causing the death of 160 people (30% of the total fatalities) (Tavera *et al.*, 2009). This was the single largest death toll of any structure during the earthquake (Taucer *et al.*, 2009). During the Pisco earthquake, 42 churches in Ica and 44 in Yauyos, Cañete and Huarochirí were damaged, according to the Ministry of Culture of Peru, former National Institute of Culture (INC, 2007).

In terms of historic churches, the most important lesson of the 2007 Pisco earthquake was the collapse of many planked timber vaults (Figure 1.4). This problem has not been only observed in Peru but also in Chile after the February 2010 earthquake (for details the reader can refer to D'Ayala and Benzoni, 2012).

Figure 1.4 Examples of planked timber vaults that collapsed during the 2007 Pisco earthquake

Research on the seismic performance of existing constructions in Peru done by Peruvian universities was triggered by several strong earthquakes that happened between 1940 and 1978 (Torrealva *et al.* 2006). In particular, investigations on the seismic response of earthen constructions began in early 1970s in the aftermath of the 1970 Huaraz earthquake. Most of this research has focused on experimental testing of adobe houses (e.g. Vargas *et al.* 1983). However, research on the response of historic constructions would only be initiated at the beginning of the 21st century. Nevertheless, to the author's knowledge, no significant attempts have been made so far to model and analyse Peruvian historic earthen and timber churches by means of advanced models and detailed analyses.

The extreme shortage of information on existing structural systems and condition of earthen and timber churches in Peru exacerbates the challenges of **Error! Reference source ot found.** and jeopardizes the future preservation of this vast heritage. The 2007 Pisco Earthquake opened a unique, even though dramatic, opportunity to progress on the understanding of the seismic performance of not only earthen and timber churches but also other historic buildings in Peru. Advances made on the interpretation and analysis of the structural performance of these buildings will have a potential high impact not only in many local communities but across several Latin American countries where similar historic building types can be found (see for instance D'Ayala and Benzoni, 2012).

The research reported in the present thesis was developed within the 'Earthen Architecture Initiative – Seismic Retrofitting Project in Peru' (EAI-SRP), which is a collaborative project of The Getty Conservation Institute (GCI), University College London (UCL), Pontificia Universidad Católica del Perú (PUCP), and the Ministerio de Cultura del Perú (MCP). For further details of the EAI-SRP the reader can refer to Cancino *et al.* (2012).

1.4 Research aim and objectives

This research seeks a response to the following questions:

(a) *How can the seismic performance of heritage constructions be assessed in the presence of many uncertainties, and uncertainties be measured?*
(b) *What is the structural concept and seismic response of historic Peruvian earthen and timber churches?*

The response to question (a) provides the strategy to answer question (b). In order to reach a solution to the aforementioned questions, this research aims to:

(i) Interpret the structural system of historic earthen and timber churches in Peru;

(ii) Propose a strategy to model and analyse earthen and timber churches;

(iii) Propose a systematic seismic assessment strategy, tailored to conduct the diagnosis of existing historic constructions and to explain the causes of existing damage, which can be used by the technical community in earthquake prone countries;

(iv) Propose a strategy to measure the uncertainty present in the assessment of historic constructions; and

(v) Formulate and validate a hypothesis to explain the failure of historic planked timber vaults during the 2007 Pisco earthquake.

These specific objectives serve the purpose of developing and validating the assessment approach while investigating some of the most complex and under researched heritage constructions in the world.

1.5 Overview of the thesis

This thesis is organized into eight chapters, including the present introduction. The literature review in Chapter 2 addresses the historical development of seismic analysis of masonry and timber structures, discussing the present limitations and inherent uncertainties of the various approaches from a theoretical and practical viewpoint. A conclusion is made at the end of the chapter on the most adequate assessment strategy tailored to the diagnosis of historic earthen and timber constructions in developing earthquake prone countries.

Based on recommendations of guidelines accepted worldwide, a general framework for seismic assessment of historic constructions is proposed in Chapter 3. The framework seeks to overcome current limitations of the assessment of historic constructions through a logic sequence of stages that can be applied by practitioners in both developing and developed countries. A procedure for uncertainty analysis is formulated and included in the framework in order to monitor, quantify and control the level of uncertainty present at various stages.

Chapters 4, 5, 6 and 7 aim at validating the general framework for seismic assessment of historic constructions by applying it to the prominent case of earthen and timber Peruvian

churches. This validation is done through the analysis and diagnosis of both a representative structure of Andean adobe churches (the Church of Kuño Tambo) and a representative historic timber structure (Cathedral of Ica). The assessment of each of these representative structures presents different challenges. The aim is to show that the same general framework can be applied to historic buildings of different complexity, made of different materials, and with distinct structural behaviour.

Chapter 4 presents a detailed investigation and interpretation of the principal structural characteristics of the Church of Kuño Tambo and Cathedral of Ica. The structural system and current condition of these buildings is interpreted on the basis of historical documentation, oral testimonies and surveys conducted by the EAI-SRP team, including the author, in Peru. A preliminary diagnosis of the Church of Kuño Tambo and Cathedral of Ica is presented in Chapter 5. This consists of the first diagnostic exercise which is based on initial interpretation of available information by the analysts. The preliminary diagnosis is a collegial activity conducted by a team with different expertise. It precedes more specialized and detailed investigations as for instance the structural modelling and analysis. The preliminary diagnosis is accompanied by an initial qualitative evaluation of uncertainty.

The structural modelling and analysis of the Church of Kuño Tambo and Cathedral of Ica are initiated in Chapter 6 with local finite element models. The objective of these analyses at the local level is to investigate alternative hypotheses to simulate the global response of the structures and identify critical aspects that must be taken into account in the structural analysis in order to make a final meaningful diagnosis. The uncertainties of the assessment due to lack of knowledge and their relative influence are quantified, showing that some inputs of the analyses are more critical than others to the accuracy of the diagnosis. The conclusions of this chapter allow identifying hypotheses related to the structural response of the churches to be further investigated with the global models, as for instance the influence of specific aspects on the failure of planked timber arches during the 2007 Pisco earthquake.

Chapter 7 presents the analysis of the Church of Kuño Tambo and Cathedral of Ica at the global level. Based on these results, a detailed diagnosis of the adobe structure of Kuño Tambo and timber structure of the Cathedral of Ica is conducted. A hypothesis for the conservation of these historic building types is proposed.

Finally, Chapter 8 presents the principal conclusions of the thesis and the opportunities for further research.

CHAPTER 2

A literature review on structural assessment of historic buildings

2.1 Introduction

The principal challenges in the structural assessment of historic buildings highlighted in Chapter 1 can be summarized in one word: knowledge. This knowledge is associated not only to available information of the building structure but also to present engineering understanding of the behaviour of historic materials and structural systems. However, the level of knowledge should be discussed within a wider perspective of the assessment and the respective purpose. It is reasonable to assume that the final aim of any assessment is to make a diagnosis of the historic building. In another words, the aim is to decide whether the building requires or not remedial interventions. To make this diagnosis, the analyst will use best engineering knowledge and tools taking into account the available resources. The analyst will therefore seek available knowledge and tools and decide what resources and tools can be used. This chapter attempts to anticipate the analyst's search for an adequate methodology to make the diagnosis of a specific historic construction. It will therefore discuss what tools are available and what the use of these tools implies in terms of uncertainty. While doing so, this chapter will discuss the best engineering knowledge and tools available to study historic buildings and identify the principal limitations. This concept of engineering tools is here used to denote methods available to model and conduct structural analysis of historic buildings. These structural analysis methods deal with idealisations or models of the building, in terms of geometry, materials and structural behaviour, and use estimates of the actions that act on the structure at a given time or which are foreseen in the

future. More refined models would in principle demand more detailed information about the building and actions, and more experienced analysts; even though for historic buildings much of the available information is qualitative and anecdotal and the uncertainty of any data is variable and may depend on expert opinion (D'Ayala and Forsyth, 2007).

In structural analysis of historic buildings, the constitutive model used to reproduce the mechanical behaviour of the building materials is a critical source of uncertainty. Any attempt to reproduce this behaviour faces limitations in terms of characterization of the building materials and the ability of the models to estimate the response to given actions.

This chapter focus on the most common traditional building materials: masonry and timber. In the specific case of masonry, emphasis is given to adobe, which is one of the most vulnerable and least studied historic masonry types. Masonry and timber have different mechanical behaviour, and the structural system made of either one or the other requires a different modelling and structural analysis strategy. Nonetheless, masonry and timber structural systems in real structures do interact with each other and this interaction phenomenon is often more difficult to reproduce than the isolated structural behaviour of either masonry or timber structures.

In the following, an overview and discussion of the constitutive models and structural analysis approaches most applied to the assessment of historic masonry and timber structures are discussed. An overview of seismic assessment procedures for this type of structures is then presented, highlighting the corresponding limitations and applicability to the objectives of this thesis. While discussing the advantages and limitations of the various approaches, the uncertainties associated to the use of these models and methods are also discussed. A brief discussion on the uncertainties present in the assessment of historic constructions and provisions of current codes and guidelines to take into account these uncertainties conclude the chapter.

2.2 Structural analysis of masonry structures

2.2.1 Constitutive modelling of masonry

Masonry is a composite non-homogeneous material, normally with a spatially regular arrangement of units and bonding agent. Such arrangement results in an orthotropic material with different mechanical characteristics in three orthogonal directions and different strength and stiffness in compression, tension and shear. The spatial arrangement can also be irregular, such as in the case of rubble stone masonry or where two leaves of wall with rubble infill exist, with a typical anisotropic behaviour. Analytical formulations of the mechanical behaviour of masonry are normally based on plasticity theory and continuum damage mechanics.

Classical failure criteria based on plasticity theory have been successfully applied to the analysis of masonry constructions over the years. For instance, soil-like material models such as Mohr-Coulomb and Drucker-Prager (Drucker and Prager, 1952) can simulate well the seismic behaviour of unreinforced masonry, especially of historic masonry where the interfaces have typically low friction coefficient due to the type of mortars used and due to deterioration (D'Ayala and Tomasoni, 2008). The Drucker-Prager material model allows the adoption of different relationships for calculation of strength parameters based on cohesion and friction angle. These relationships can be formulated on the basis of a desired match with a Coulomb-type criterion. For instance, the relationships can be formulated with the aim of getting a good match with uniaxial tensile and/or compressive strength of the material. Some difficulties might however be found when trying to predict the response of the masonry under both uniaxial and biaxial stress states. These limitations can however be overcome by intersecting two Drucker-Prager surfaces with independent strength parameters (see for instance Genna *et al.*, 1998).

Formulations based on multi-surface plasticity theory have the main advantage of allowing different failure mechanisms of masonry to be considered which may act simultaneously (Mistler *et al.*, 2006). Multi-surface formulations were first introduced by Mann and Müller (1978) and Ganz (1985) for two-dimensional and three-dimensional problems, respectively. However, these formulations were verified by means of experimental data gathered by tests performed on new masonry (Zimmermann *et al.*, 2010). More recently, Lourenço (1996) proposed a non-linear model for in-plane loaded walls based on a multi-surface composed of a Hill-type criterion for compression and a Rankine-type criterion for tension. D'Ayala (1998) also used a Rankine-type failure criterion to define the state of

stress internal to the single element of mortar or brick, while the bond between mortar and unit and the shear behaviour of the units are defined by a Mohr-Coulomb type criterion.

A drawback of the plasticity theory is the inherent limitation to reproduce stiffness degradation of masonry related mainly to cracking, which is an important aspect when masonry is subjected to reverse loading, such as earthquake for instance. Continuum damage mechanics is suitable for applications where this behaviour must be taken into account.

The approach is based on continuum mechanics theory. Smeared crack behaviour is assumed, where progression of cracking is simulated by the change of deformational and strength properties of the material. For instance, an isotropic continuum damage mechanics law was adopted by Callerio and Papa (1998) to simulate the decreasing of stiffness of masonry subjected to in-plane reverse loading. In this work, the behaviour of bed joints in shear is governed by a Mohr-Coulomb criterion.

Despite their more complex formulation, orthotropic damage models have also been applied to the analysis of masonry structures. For instance, Berto *et al.* (2002) developed an orthotropic damage model to study the response of masonry composed of bricks stiffer than mortar under plane stress conditions, where the directions of the bed and head joints are assumed as the main directions of the damage. In each direction, a parameter for compression and a parameter for tension are used to simulate the crack opening/closure. The model takes into account the capacity of transmission of shear due to friction phenomena through an open crack, assuring minimum shear strength for a completely damaged material.

The material properties of masonry's components and the equivalent continuum can be characterised by means of:

(i) Experimental tests on representative models;
(ii) Statistical studies of properties of bricks and mortar; and
(iii) Homogenisation techniques.

Experimental testing has traditionally been the most successfully applied method for characterising the material properties of masonry. However, as discussed in Section 1.2, experimental work is often of limited application due to the anisotropic nature of traditional materials, the typical heterogeneity of historic buildings, and economic, technical and conservation constraints. At a technical level, the main issue regards the representativeness of the samples or experimental models and the adequacy of the experimental setup and program for the purpose of the test.

As far as statistical studies are concerned, a representative example can be found in work by D'Ayala and Carriero (1995a), who conducted an extensive review of literature related to experimental work on historic masonry in order to develop a database of geometric and mechanical properties. From the statistical analysis of the data collected, correlations between ranges of parameters were identified and regression curves derived (Figure 2.1). This work enables the definition of mechanical parameters for masonry when mechanical and geometric properties of the corresponding components are available. As a result of this work, D'Ayala and Carriero (1995b) developed a numerical tool to study the non-linear response of masonry structures by devising a simple step by step procedure that can be applied using commercial finite element software.

However, a major limitation of statistical studies is the need for having a comprehensive database of relevant properties for bricks and mortar that represent well the heritage construction. Such database is not available for traditional materials like adobe, as will be further discussed in Chapter 6.

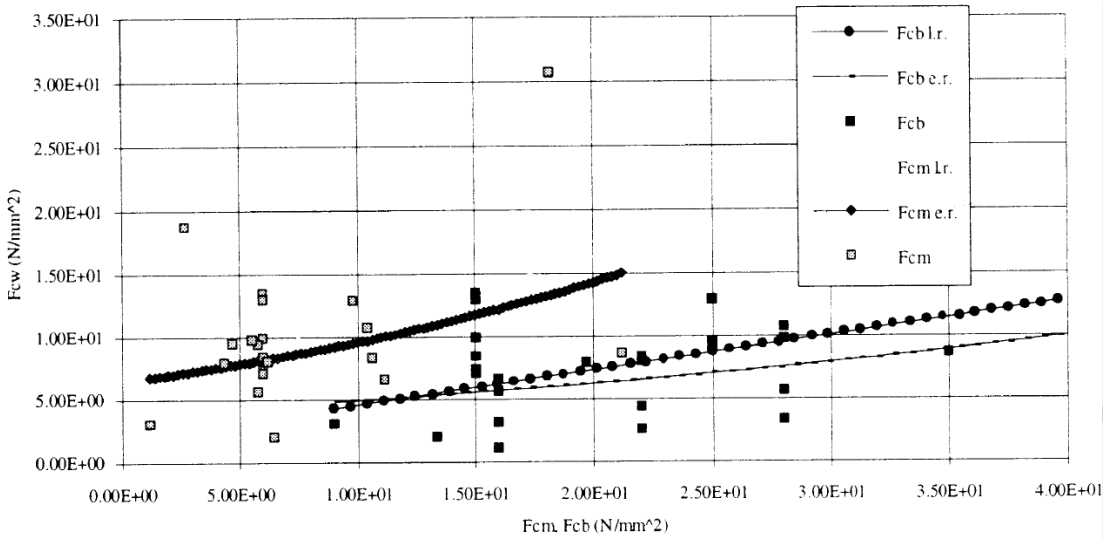

Figure 2.1 Relation between the compressive strength of the components (*Fcm* for mortar and *Fcb* for brick) and the strength of masonry, *Fcw* (after D'Ayala and Carriero, 1995a)

Homogenisation techniques have been formulated for masonry in order to analytically obtain the properties of a macro-scale continuum from the properties of some components using alternative approaches, such as Limit State Mechanism approaches, Finite Element and Discrete Element based approaches. These techniques are based on the principle that the macroscopic structural behaviour of regular masonry can be characterised by a basic cell that

is representative of the masonry pattern. This concept of a representative cell for periodic media was described by Anthoine (1995) by using the example of a masonry wall's portion under plane stress conditions (Figure 2.2). In this case, the mechanical properties of a periodic media are invariant along any translation $m_1v_1+m_2v_2$, where v_1 and v_2 are two independent vectors and m_1 and m_2 are integers. The characterisation of the periodic masonry hence requires only the definition of the mechanical properties of the media on a small domain S (representative cell), associated to a frame of reference (v_1, v_2) and with an area equal to the norm of the vector product $|v_1 \Lambda v_2|$.

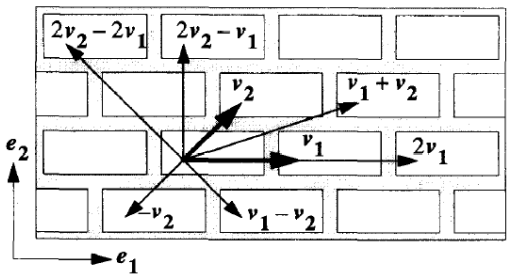

Figure 2.2 Masonry under plane stress conditions and frame of reference (after Anthoine, 1995)

Examples of homogenization techniques can be found in work by Pande *et al.* (1989), Anthoine (1995), Lee *et al.* (1996), Chudyba *et al.* (1998), Casolo and Milani (2010), and Milani (2011).

Among the various homogenization techniques, finite element nonlinear approaches, also known as 'multi-level' approaches are one of the most disseminated and powerful. It consists of getting stress-strain relations at the representative cell level and using this information at a macroscopic level. The most important limitation of this homogenization technique is the fact that the double computational effort needed due to the existence of a micro and macroscale mesh does not allow for study of real complex three-dimensional buildings, as quoted by Lourenço *et al.* (2007).

2.2.2 Structural analysis approaches

In literature normally three approaches have been taken so far for the modelling and structural analysis of masonry structures:

(i) Simplified limit state mechanism approaches;
(ii) Finite element method based approaches; and
(iii) Discrete element method based approaches.

These approaches are listed according to their complexity. The origin and basic principles of the various approaches, as well as the main advantages and disadvantages are discussed in the following.

2.2.2.1 LIMIT STATE MECHANISM APPROACHES

Limit state mechanism approaches assume that the failure of masonry structures is caused by instability of the units, in the case of dry masonry or masonry with poor mortar, or portions of the masonry, in the other cases. The units or portions are modelled as a system of rigid bodies articulated by hinges, and equilibrium states are expressed in terms of stress-resultants. Since equilibrium equations relate stress-resultants rather than stresses they only ensure, in general, that equilibrium is satisfied in an overall sense (Livesley, 1978).

Heyman (1966) quotes the work of Frézier in the 18th century to demonstrate that the identification of typical mechanisms of collapse of masonry structures through model experiments is a quite old idea (Figure 2.3). The origins of limit state mechanism approaches can be traced back to equilibrium methods or stability methods for structural analysis of vaulted masonry constructions developed by the end of the 17th century. These methods use the thrust line theory to find equilibrium states and possible collapse mechanisms. Among all equilibrium methods, graphic statics was one of the most widely applied in the 19th century and beginning of the 20th century. Recent work by Block *et al.* (2006) applies graphic statics to the analysis and design of masonry constructions by means of an interactive computational geometry software in which the geometry of the structure can be adjusted in real-time. Based on this tool, DeJong (2009) applied tilting thrust analysis as a first order seismic assessment method to study the stability of sub-structures, such as vaults and buttresses, and the influence of the interaction of structural components upon the stability of

the whole structure. However, local sliding and crushing are not simulated and it is also limited to two-dimensional problems.

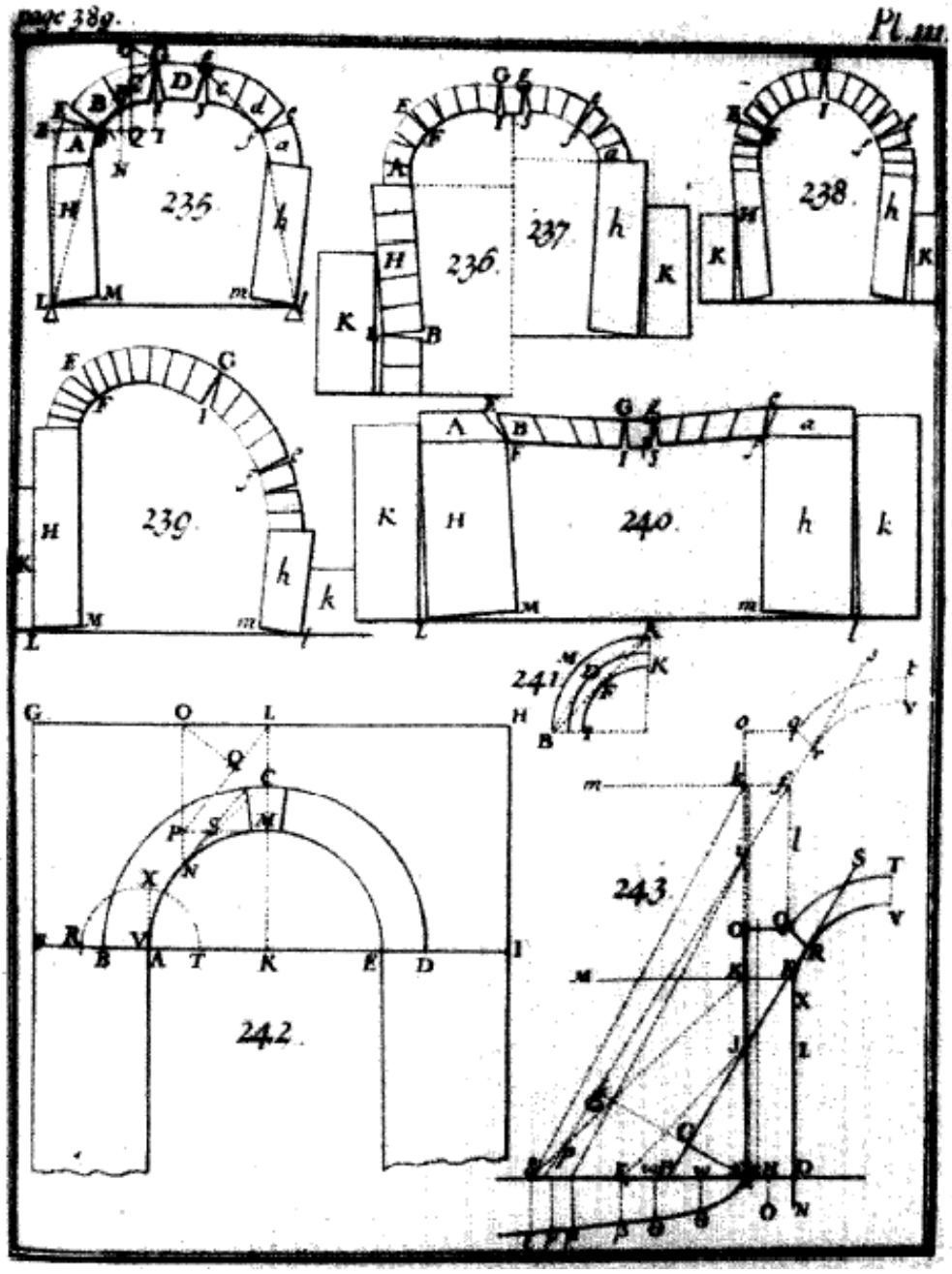

Figure 2.3 Collapse mechanisms of arches after Frézier (Heyman, 1966)

Limit analysis of masonry structures was first formulated by Heyman (1966, 1995) assuming that the limit theorems of plasticity (lower-bound theorem and upper-bound theorem) can be applied to masonry structures on the premises that masonry has no tensile strength but infinite compressive strength and sliding failure does not occur. These assumptions are usually valid for masonry structures with high values of friction coefficient subjected to self-weight; however shear failure and crushing of masonry structures normally occur under earthquake loading for instance.

Limit analysis evolved towards formulations based on premises of possibility of sliding in presence of friction, limited compressive strength and non-associated flow rules with absence of dilatancy. Livesley (1978) considered for the first time a Coulomb friction law to characterise the behaviour of the interface of rigid blocks in shear. More recent advances on limit analysis formulations can be found in work by D'Ayala and Tomasoni (2008), Casapulla and D'Ayala (2006), Gilbert *et al.* (2006) and Orduña and Lourenço (2005a, 2005b).

In summary, limit state mechanism approaches seek the identification of ultimate stress-resultants and load capacities when collapse mechanisms have formed. An important advantage of limit analysis for practitioners is the simplicity of the approach, which allows the development of practical computational tools, and especially the reduced number of input parameters. A major disadvantage is the fact that these approaches do not assess initiation and progression of damage and therefore they are suited to evaluate only ultimate states, which occur for modest levels of displacement. It is assumed that no local failures occur before the critical mechanism is completely triggered. However, in the case of historic buildings, the assessment pursues mainly the evaluation of the initiation and progress of damage; such as to identify remedial measures that prevent the occurrence of major damage, which would compromise the preservation of valuable assets. Moreover, limit state mechanism approaches are inherently not suited for the analysis of large three-dimensional structures, but for specific structural components, such as buttresses and arches.

Nevertheless, as reported by Roca *et al.* (2010), independently of the level of refinement, the results of any analysis method will produce, at ultimate condition, results foreseeable by means of limit analysis. An interesting example of the complementary use of finite element modelling with limit analysis can be found in work by De Luca *et al.* (2004) to analyse triumphal arches of Neapolitan churches. In this work, finite element analyses allow to localise potential cracks and identify collapse mechanisms. On the other hand, limit analysis provides a collapse multiplier for each identified collapse mechanism.

2.2.2.2 FINITE ELEMENT METHOD BASED APPROACHES

Original mathematical and engineering ideas that led to the Finite Element Method (FEM) can be traced back to the late 18th and 19th centuries (Zienkiewicz and Taylor, 2000). However, the basic ideas of the method as known today were developed in the 20th century by Argyris and Kelsey (1955) and Turner *et al.* (1956). The first book dealing with present-day FEM was published in 1967 and authored by Zienkiewicz and Cheung (1967). Since the origins to present-day, research on FEM has rapidly evolved and its application expanded across many professional and academic fields solving multiple engineering problems, as described in Gupta and Meek (1996).

Zienkiewicz and Taylor (2000) describe FEM as a general discretization procedure of continuum problems posed by mathematically defined statements. A building structure is therefore discretized into a finite number of elements, where each element is characterised by a force-displacement relationship. The assembly of all elements by following a well-defined procedure of establishing local equilibrium at each node or connecting point of the structure allow solving the resulting equations for the unknown displacements. FEM is based on the principles of continuity, in which all elements are connected at the nodes, and compatibility in which equilibrium is established at each node.

FEM based approaches assume that the performance of masonry structures is governed by the behaviour of the constituent materials and contacts between them. Equilibrium states are expressed in terms of displacement/stress distributions and contact phenomena (Figure 2.4 and Figure 2.5). An important advantage of these approaches is that the whole performance of the structure, from damage initiation and progression to failure can be predicted; even though the large displacements normally accompanying the collapse of the structure can be hardly simulated. However, the choice of material models is an important issue of FEM analysis in order to realistically simulate by means of isotropic or orthotropic models a material which is typically anisotropic.

In literature, the Drucker-Prager and Mohr-Coulomb models are two of the most successfully applied material models on the analysis of masonry constructions through FEM. Some examples can be found in work by Roberti *et al.* (2005), Mallardo *et al.* (2008), Krstevska *et al.* (2008), Pallarés *et al.* (2009) and Sevim *et al.* (2011). In alternative, concrete-based models have also been successfully used in the analysis of masonry structures. Some examples can be found in work by Mele *et al.* (2003), Bayraktar *et al.* (2010), Silva *et al.* (2012) and Tarque *et al.* (2013).

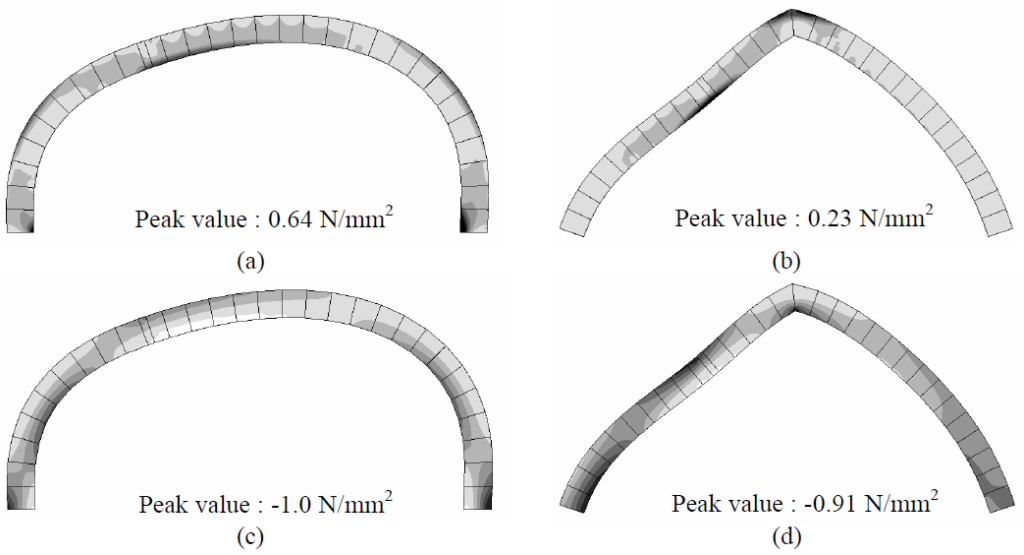

Figure 2.4 Results of linear elastic finite element analysis for a quarter span point load: (a,b) maximum and (c,d) minimum principal stresses for semi-circular and pointed arch, respectively (after Lourenço, 2001)

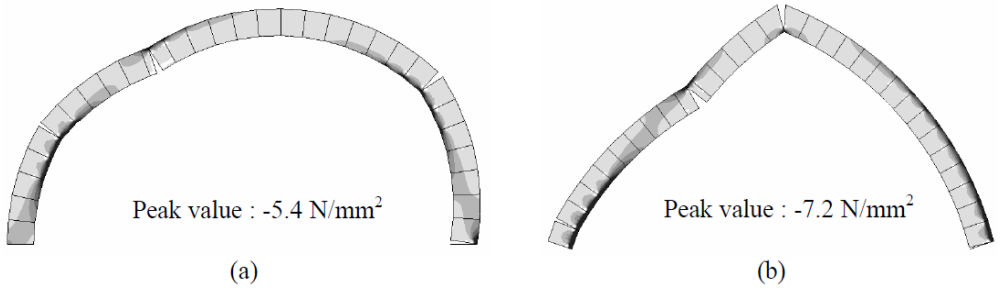

Figure 2.5 Results of non-linear finite element analysis for a quarter span point load. Minimum principal stresses and failure mechanisms for (a) semi-circular and (b) pointed arch (after Lourenço, 2001)

According to Rao (2005), one of the main reasons for the popularity of the FEM in different fields of engineering is that once a general computer program is written, it can be used for the solution of any problem simply by changing the input data. Perhaps for this reason, FEM software is almost worldwide known by the engineering community.

This popularity of the FEM is an important advantage for the assessment of historic constructions, since the analysis of the three-dimensional structural behaviour of historic constructions by practitioners requires an approach suitable for the modelling of large and complex structures using current available computational tools. Current finite element method based software packages have good three-dimensional graphic interface, which

allows complex geometries to be simulated and a suite of linear and non-linear material models and finite elements, which can be adapted to different analysis' purposes.

2.2.2.3 DISCRETE ELEMENT METHOD BASED APPROACHES

Approaches based on the discrete element method have been applied to analyse the structure of different types of masonry by assuming the material as a discontinuous media composed of rigid or deformable blocks and contact surfaces between the blocks for simulation of the joints. Material, geometric and boundary non-linearities, including large displacements, can be modelled by these techniques under both static and dynamic conditions. Under these conditions, individual masonry blocks can separate from each other or slide along their contact area. In the case of deformable blocks, a constitutive model is applied to simulate the internal stress and deformation of the blocks. A Coulomb's friction law is normally applied on the interfaces when the blocks are in contact to simulate the response of the masonry in shear. Following this law, relative sliding of the blocks occurs when the frictional resistance is exceeded by the loads.

Alternative formulations such as the Distinct Element Method, Discontinuous Deformation Analysis, and Discrete Finite Element Method have also been used in the analysis of masonry constructions (Cundall, 1971; Shi, 1992; Mamaghani *et al.*, 1999).

The Distinct Element Method (DEM) was initial formulated by Cundall (1971) based on Newton's second law. A direct derivation of this work was implemented into a computer program UDEC – Universal Distinct Element Code. More recent work by Azevedo *et al.* (2000), Zhuge (2008) and Furukawa *et al.* (2010) use approaches which are based on this method (Figure 2.6).

Discontinuous Deformation Analysis (DDA), formulated by Shi (1992), is an alternative displacement-based method formulated on the basis of the principle of minimum total potential energy. The method was applied by Ma *et al.* (1996) to the analysis of two-dimensional masonry structures. This allowed the authors to explain through numerical simulations the typical behaviour of masonry characterized by the occurrence of local failures. The authors concluded that although discontinuities or joints between blocks inherently reduce the integrity and strength of masonry structures, sliding occurring along those joints consumes seismic energy and therefore the probability of overall structural collapse is low compared to the occurrence of local failures.

The Discrete Finite Element Method, developed by Mamaghani *et al.* (1999), uses the principles of continuity and compatibility of the Finite Element Method for analysis of

blocky systems, incorporating contact elements to model block interactions such as sliding and separation for the purpose of conducting stability studies.

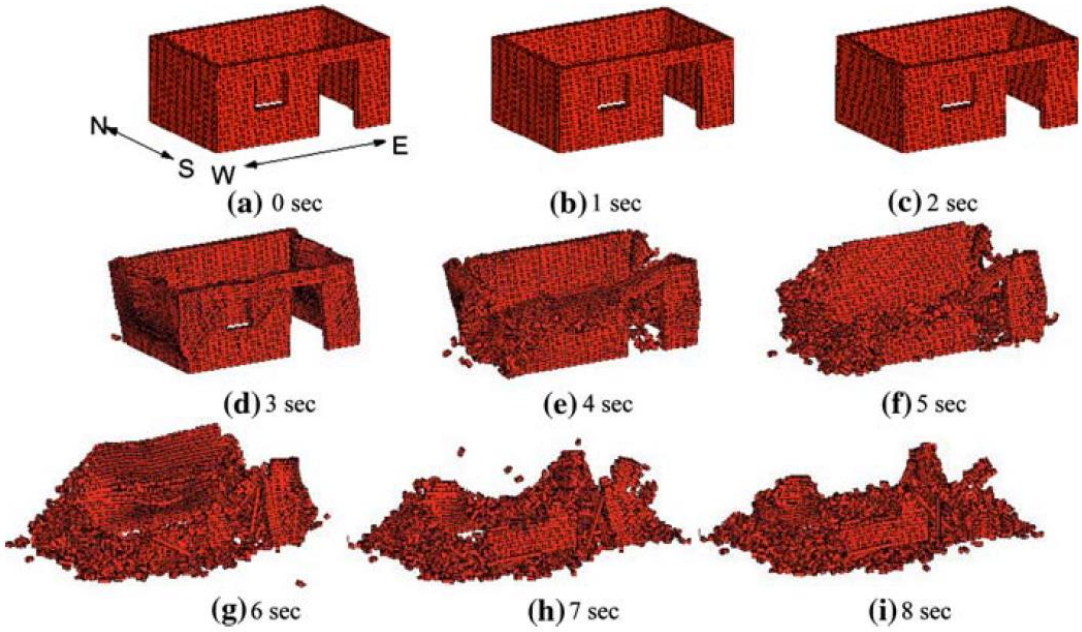

Figure 2.6 Structural performance of an adobe building model (5m width x 3m depth x 2.4 height) subjected to ground motion recorded during the 2003 Bam earthquake in Iran (after Furukawa and Ohta, 2009)

The main advantage of discrete element method based approaches is the ability to simulate the collapse of the structure, which is typically accompanied by large displacements. However, these approaches require a large number of inputs to characterize the behaviour of blocks and joints and their interaction, which are not normally available for historic buildings. These uncertainties on the inputs resulting in cumulative errors derived by repetitive iterations lead to significant inaccuracies on the evaluation of failure initiation and progression. In the case of the assessment of historic buildings, where the aim is to protect the assets from future damage, the evaluation of failure initiation and progression is more important than the simulation of the collapse. Moreover, in practice these approaches can only be applied to relatively small cells, with a limited number of elements due to very high computational burden required. This does not allow simulating large three-dimensional historic structures and the complex interactions occurring among the various components at a macro-level (e.g. interactions among orthogonal walls). Thus, discrete element method based approaches are not currently viable to assess the performance of historic buildings.

2.2.3 The specific case of adobe constructions

Taking into account the previous discussion of the various analysis approaches, and in order to evaluate possible best approaches for the seismic assessment of historic adobe constructions in countries like Peru, three main aspects must be taken into account:

(i) The material behaviour of adobe;
(ii) The structural characteristics of historic adobe constructions; and
(iii) The availability of resources in seismic prone countries with historic adobe constructions.

The following discussion will address each and all of these aspects.

Historic adobe is a type of masonry characterised by a relatively low compression strength compared to other types of masonry, such as fired brick masonry. In addition, adobe is often not well bonded and can easily lose the cohesion of the material in the presence of water. These facts can create multiple critical points and local failures in the structure, especially in the case of complex geometries and presence of concentrated loads. Although adobe has low compression strength if compared to other types of masonry, crushing of adobe in historic Peruvian structures might not occur as compression stresses are expected to be generally low due to the large thickness of the walls and the low weight of typical Peruvian historic roof structures and their applied loads.

Experimental evidences from shaking table tests performed on historic adobe structures (Tolles *et al.*, 2002) indicate that, when cracking develops, the natural frequency of vibration decreases and the displacements substantially increase. Although cracking typically develops for very low values of tension, thick adobe walls admit large displacements without the formation of a failure mechanism. However, such large displacements would compromise the conservation of assets with cultural significance; and hence it is more important to identify when large displacements can initiate than to simulate those large displacements.

The mortar of adobe structures has normally the same or similar material composition, and hence strength characteristics of the units, which leads to combined failure mechanisms. However, the joints may often be the weakest constituents of adobe structures since rapid drying during the building of the structure can lead to shrinkage and cracking of the mortar (Tolles *et al.*, 2002). Although shrinkage phenomenon can also occur in the adobe units, its effect is usually less evident due to the typical addition of straw, crushed bone or/and other organic materials. Indeed, animal, vegetable, mineral or synthetic fibres increase the tensile

strength of the units, hinder cracking on drying by distributing the tension arising from the shrinkage of the clay throughout the bulk of the material, and accelerate drying since they improve the drainage of moisture towards the outer surface through the channels afforded by the fibres (Houben and Guillaud, 1994).

Considering a similar material behaviour of joints and units, FEM based approaches, where adobe is simulated as a homogeneous material have been successfully applied both in the elastic (e.g. Islam and Watanabe, 2004) and inelastic range (e.g. Tarque *et al.*, 2013), using both soil-like material models such as the Drucker-Prager model, and concrete-based models.

On the other hand, exploring the fact that the joints may also be the weakest component, and hence that adobe structures may fail by instability caused by the separation of the units (as observed in buildings after earthquakes by for instance Furukawa *et al.*, 2010), DEM based approaches have also been applied to the analysis of the collapse of small adobe houses (e.g. Mayorca and Meguro, 2004; Furukawa *et al.*, 2010).

Although important developments have been recently made on non-linear analysis of adobe structures using advanced numerical simulations, detailed studies on historic adobe constructions, such as churches, lack in literature when compared to stone or fired brick masonry constructions. In the case of these constructions, important developments can be traced back to more than two decades ago with the modelling and analysis of the Colosseum in Italy by Croci *et al.* (1995), Mexico Cathedral by Meli and Sánchez-Ramírez (1997) and Mallorca Cathedral in Spain by Roca (2001).

The lack of detailed seismic analysis of historic adobe structures can be justified by economic and scientific reasons. Economic reasons can be explained by comparing the distribution of adobe constructions in the world with the distribution of wealth. Simplified maps showing the distribution of earth construction in the world and a map of the world combining population density and wealth developed by the National Geographic Society are shown in Figure 2.7. These maps show that some of the most densely populated and poorer areas in the world have an important building environment built from earth, namely adobe.

a) Distribution of earth construction in Africa, Asia, Europe and Oceania (Houben and Guillaud, 1994)

b) Distribution of earth construction in North, Central and South America (Houben and Guillaud, 1994)

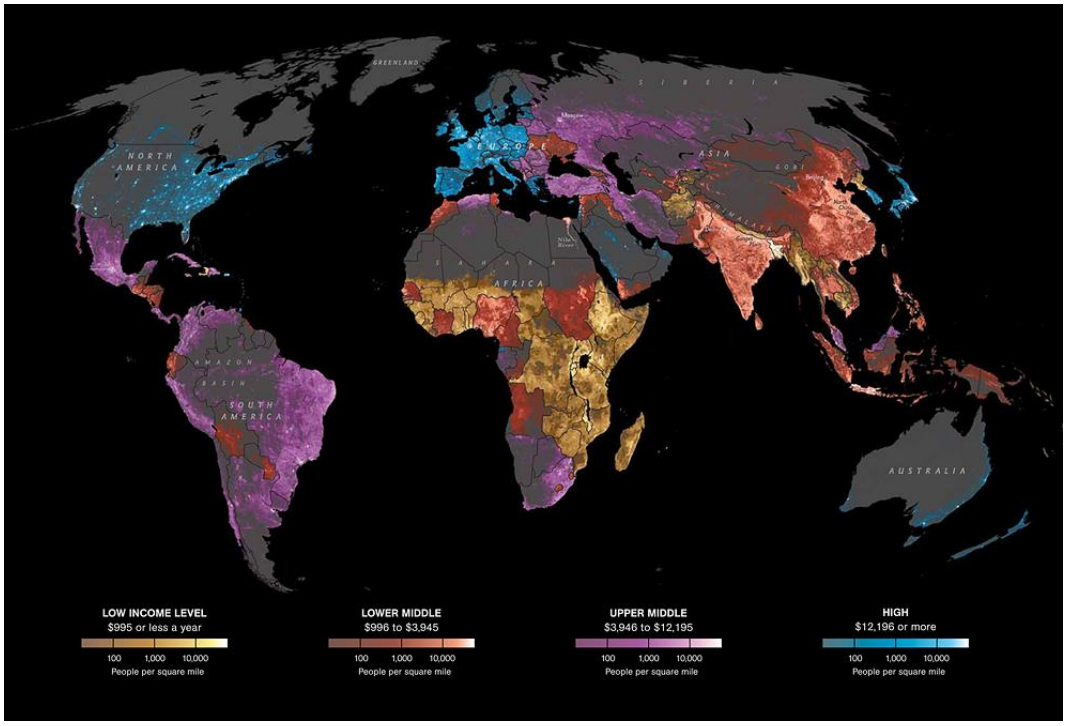

c) Distribution of wealth (in Gross Domestic Product per capita) and population density (people per square mile) in the world (NGM, 2011)

Figure 2.7 Distribution of earth construction, wealth and population density in the world

This means that most historic adobe constructions are located in countries where the engineering community lack resources to develop detailed and expensive experimental and numerical analyses. In seismic prone countries, like Peru, experimental and analytical work

conducted by universities have been mainly focused on the testing of retrofitting solutions for adobe houses (Torrealva *et al.* 2006). A direct consequence of this fact is the lack of available datasets on material properties of adobe.

Scientific or technical reasons are specially related to lack of knowledge about performance of historic structural systems within the engineering community. Such knowledge is currently available only within specific research groups or accessible to a limited number of practitioners.

2.3 Structural analysis of timber structures

2.3.1 Constitutive modelling of wood

Timber is an anisotropic material with defects, such as knots, grain shakes, spiral grain and wane. Microscopically, wood is composed of cells oriented in the longitudinal direction, whose structural arrangement could be considered as a fibre-reinforced composite system with cellulose fibrils as reinforcement in the hemicelluloses and lignin matrix. In the longitudinal direction, cellulose determines the strength properties of the wood fibre, whereas in the transverse direction the hemicelluloses and lignin play a more dominant role than cellulose (Mishnaevsky and Qing, 2008).

Due to the manner in which a tree grows and the arrangement of the wood cells within the stem, wood can be considered locally as an orthotropic material that possesses three principal directions (Holmberg *et al.*, 1999), oriented in the longitudinal direction along the fibres, in the radial direction parallel to the rays and in the tangential direction to the growth rings. The strength and stiffness of wood are greater in the longitudinal direction, which can be explained by the fact that 90-95% of the fibres are oriented longitudinally (Holmberg *et al.*, 1999). There is also a difference in properties between the radial and tangential directions due to the presence of the rays, as well as the difference in cellular structure between the radial and tangential directions and the differences of the orientation of the microfibrils on the various sides of the cell (Holmberg *et al.*, 1999).

For compression perpendicular to the fibres, three basic failure patterns can be distinguished, depending on the orientation of the growth rings in relation to the direction of loading: a) crushing of earlywood; b) buckling of growth rings; and c) shear failure. Tensile loading perpendicular to the grain gives rise to three different failure patterns: a) tensile fracture for radial loading in earlywood; b) tensile failure in the wood rays for tangential

loading; and c) shear failure along a growth ring when loading is at an angle to the growth rings (Holmberg *et al.*, 1999).

The yield stress and strength of wood in compression and tension significantly differ. Above the elastic limit, wood behaves in a nonlinear way, having a typical more brittle response and lower strength in tension than in compression.

Depending on the structural system and the purpose of the analysis, wood can also be assumed as an isotropic material. Homogenisation techniques have been applied to derive the properties of an equivalent homogeneous continuum from analysis at micro-level, which consider the microstructure of wood. Some examples can be found in work by Holmberg *et al.* (1999) and Hofstetter *et al.* (2005).

Adverse effects in timber structures are not only related to critical load-strength combinations but also to moisture-induced strength and stiffness degradation of structural elements and connections (Kohler, 2010). Degradation of timber, caused by fungi or insect attack, which is common in historic buildings, can hence contribute to their failure.

2.3.2 Approaches for the modelling and analysis of timber structures

The structural behaviour of timber structures is normally governed by the joints, which can connect two or more members at different angles or lengthen the members. The stiffness and strength of the joints is normally more modest than the stiffness and strength of the members. Thus, permanent deformation and failure normally occur at the joints. Timber joints are a complex system, which perform differently according to the location within the structure and the type of imposed loading (see for instance Chang *et al.*, 2009). This behaviour is typical of both historic timber systems composed of carpentry joints, and more modern systems with fasteners such as screws. The case of historic systems with carpentry joints is the most relevant for this thesis; and hence the following discussion builds on literature addressing this type of timber structures.

The need of appropriately simulate the semi-rigid behaviour of timber joints (i.e. the difference of stiffness between joints and members) when modelling seismic action on timber structures has been emphasised in work by Parisi and Piazza (2002) in the analysis of traditional carpentry joints of roof structures in Italy.

A similar approach was also applied by Tsai and D'Ayala (2011) in the assessment of the seismic performance of Taiwanese Dieh-Dou temples. Tsai and D'Ayala developed a FEM

model of a temple in which the joints were simulated by translational and rotational springs with stiffness and maximum capacity obtained from experimental testing of full scale joints.

However, in most available literature, structural analyses are performed with timber joints assumed as either rigid or pinned. A relevant example for this thesis is the work of Proaño *et al*. (2007) related to the modelling and analysis of the Cathedral of Lima (Figure 2.8). To the author's knowledge, this work is the first comprehensive analysis of a historic masonry and timber church in Peru; even though the behaviour of masonry is assumed as linear elastic and the timber joints are simply assumed as pinned or rigid depending on the location. This work allowed the making of some general conclusions on the overall elastic response of the church, identifying areas of greater demand; even though no conclusions in terms of non-linear behaviour or failure of the structure have been made.

Among historic timber structures located in seismic prone developing countries like Peru, structures with planked arches are one of the most important at a cultural level. Detailed studies on timber planked vaults have investigated the evolution of this construction form through history (see for example Marussi Castellán, 1981, 1989; Gómez Sánchez, 2006; Hahmann, 2006; Hurtado Valdez, 2011) and clearly highlighted the relevance of the joints to the overall stability of the arch systems. However, to the author's knowledge, work on their structural assessment has so far assumed the arches as continuous, so the connections between the planks are modelled as rigid (Marzo, 2006; Fabbri, 2010).

The simplifications made in the modelling of historic timber structures by available literature might be justified by the need to carry out expensive experimental work to characterize the mechanical response of historic timber joints. For instance, the Peruvian historic churches have systems composed of many different timber joints, requiring the testing of many specimens to realistically simulate the response of one single church.

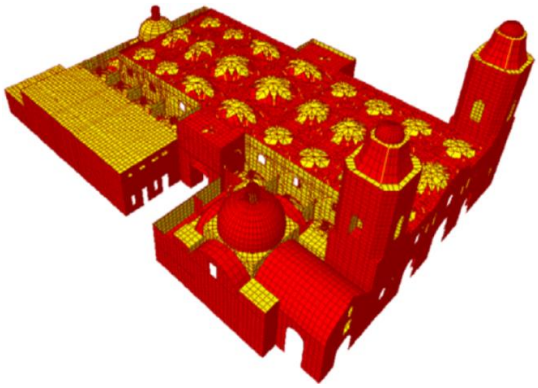

Figure 2.8 Finite element model of the Cathedral of Lima (by Proãno *et al.*, 2007)

2.4 Seismic assessment of historic buildings

The previous sections focused on alternative strategies to model the structural behaviour of historic buildings, their advantages and limitations. This section will focus on the seismic assessment of historic buildings, especially historic churches, conducted with the final purpose of making a diagnosis of the structure. Building on the previous discussion, the aim here is to understand how this assessment is normally conducted, what the gaps are, and how this knowledge can be used to meet the objectives of this thesis.

An assessment can be understood as the total set of activities performed in order to verify the reliability of an existing structure for future use (ISO 13822, 2010). For this purpose, several sources of information (historical or other existing documentation, survey of the structure, field research, laboratory testing and monitoring) and different types of analysis (historical, qualitative, quantitative and experimental) are used to make a diagnosis of an existing individual or group of historic buildings (ICOMOS-ISCARSAH, 2003), as discussed in Chapter 1.

Recurring damage patterns observed in masonry churches after earthquakes have indeed shown that the performance of churches to earthquakes can be understood by considering the individual behaviour of macroelement-architectural parts that make the building; even though such individual behaviour is not fully independent but rather a result of the interaction of the various macroelements. Lourenço (2006) outlines that although the evaluation of a historic building frequently requires a holistic approach considering the building as a whole, the assessment of the performance of individual elements is also commonly required due to the frequent lack of box-like structural response of historic constructions.

Following this idea, the seismic assessment of historic buildings has been historically based on the identification of relevant damage mechanisms, and formulation of mechanical models to obtain the corresponding seismic capacity, described in terms of horizontal acceleration. The mechanism with the lowest seismic capacity is the critical or most likely to occur, and therefore the one that characterises the fragility of the structure. The damage limitation state, which triggers the activation of the mechanism, can be obtained by limit state mechanism approaches, whereas the ultimate or near-collapse limit state can be obtained by formulations based on displacement capacity. As outlined by Lagomarsino and Resemini (2009), the initial damage phase of masonry structures may be generally far from the ultimate condition, because of the structural resources in the post-cracked state. In line

with this, a procedure for seismic assessment of historic buildings should incorporate the principles of performance-based approaches.

2.4.1 Performance-based assessment

By the end of the 1960's, it was already recognised that strength-based seismic design procedures were limited to a reasonable representation of linear-elastic response and dependent on special detailing requirements to provide a somewhat unknown degree of resistance to strong motion inelastic response (Freeman, 1998). Furthermore, the extremely large economic losses associated to earthquakes such as the 1989 Loma Prieta (7 billion dollars) and the 1994 Northridge (30 billion dollars) when compared to the fatalities (fewer than 100) indicated that code provisions of that time for zones of high seismicity were relatively reliable in avoiding life threatening damage and collapse, but not to limit damage to the building (Hamburger, 1996).

Performance-based procedures were therefore devised with the purpose of evaluating not only the safety of the occupants but also the performance of the building for a given earthquake hazard level. According to ASCE/SEI 41-06 (2007), building performance can be described qualitatively in terms of the safety afforded building occupants during and after the event; the cost and feasibility of restoring the building to its pre-earthquake condition; the length of time the building is removed from service to effect repairs; and economic, architectural, or historic impacts on the larger community.

Performance-based assessment of an existing building checks if the structure is able to fulfil some selected performance levels in case of occurrence of properly defined earthquake hazard levels. The implementation of performance-based assessment for historic constructions with cultural significance needs to extend the rehabilitation requirements usually adopted for ordinary buildings, related to use and safety of people, also to conservation requirements, related to architectural and artistic cultural value (Lagomarsino and Cattari, 2015).

Within the framework of the PERPETUATE European research project, Lagomarsino and Cattari (2015) defined performance levels with reference to the following safety and conservation requirements:

(i) *Use and human life*: also for a cultural heritage asset, similarly to ordinary buildings, the possibility of an immediate occupancy after an earthquake and the protection of human life have to be considered;

(ii) *Building conservation*: due to the intangible value of a cultural heritage asset, the preservation from building damage is not related, as for ordinary buildings, to the costs of repair or rebuilding but to the possibility of restoration or to the collapse prevention, in order to maintain, at least, the monument as a ruin; and

(iii) *Artistic assets conservation*: in many cases, severe damage to artistic assets occurs also in the case of moderate damage to structural elements; moreover, damage to artistic assets is related to the local scale, while the other requirements are related to the whole architectural asset; therefore it is necessary to define specific performance levels for each relevant artistic asset in the building.

Performance levels are related to the extent of damage that would be sustained by the building. CEN (2005b) specifies the damage state of the structure through the following three limit states:

(i) *Near collapse*: the structure is heavily damaged, with low residual lateral strength and stiffness, although vertical elements are still capable of sustaining vertical loads. Most non-structural components have collapsed. Large permanent drifts are present. The structure is near collapse and would probably not survive another earthquake, even of moderate intensity;

(ii) *Significant damage*: The structure is significantly damaged, with some residual lateral strength and stiffness, and vertical elements are capable of sustaining vertical loads. Non-structural components are damaged, although partitions and infills have not failed out-of-plane. Moderate permanent drifts are present. The structure can sustain after-shocks of moderate intensity. The structure is likely to be uneconomic to repair; and

(iii) *Damage limitation*: The structure is only lightly damaged, with structural elements prevented from significant yielding and retaining their strength and stiffness properties. Non-structural components, such as partitions and infills, may show distributed cracking, but the damage could be economically repaired. Permanent drifts are negligible. The structure does not need any repair measures.

Damage states can be identified by proper thresholds of structural performance indicators, such as drift and total base shear, which describe the structural behaviour of the construction. These indicators can be quantified through structural analysis methods that take into account the inelastic response of the structures and the progress of damage. Pushover analysis is currently considered the standard tool for performance-based assessment (Lagomarsino and Cattari, 2015). It allows determining realistic values of permanent deformations of structures with a prevalent non-linear behaviour, such as masonry structures. An important complement to pushover analysis is modal superposition analysis which allows characterizing the dynamic response of structures composed of several parts of different relative stiffness and a non-uniform distribution of masses, which is for instance the case of timber structures.

It will be seen in the following that procedures that incorporate the principles of performance-based assessment have been mainly applied to the analysis of masonry buildings in historic urban centres.

2.4.2 Fragility assessment

Observation of damage to masonry churches after the 1976 earthquake in Friuli (Italy) led to the conclusion that the response of the churches to earthquakes can be described by a number of typical damage patterns and collapse mechanisms associated to specific macroelements (Figure 2.9).

An empirical approach based on this premise was successively applied to the damage and vulnerability assessment of churches in the aftermath of the earthquakes in 1987 in the provinces of Modena and Reggio Emilia, 1995 in the region of Tuscany and territory of Lunigiana, and in 1997 in the regions of Umbria and Marche (see for instance Lagomarsino, 1998). This work led Lagomarsino (1998) to propose the first systematic methodology to describe the fragility of historic churches by correlating a damage index and a vulnerability index on the basis of empirical observation and data. The damage index measures the average level of damage to the church and the vulnerability index describes in a qualitative way the propensity of the church to be damaged by the earthquake. The vulnerability index is based on the evaluation of two indicators of specific structural deficiencies that may activate a given damage mechanism (Figure 2.10). The evaluation is done for all possible damage mechanisms, providing a qualitative measure of the vulnerability of the church to those mechanisms.

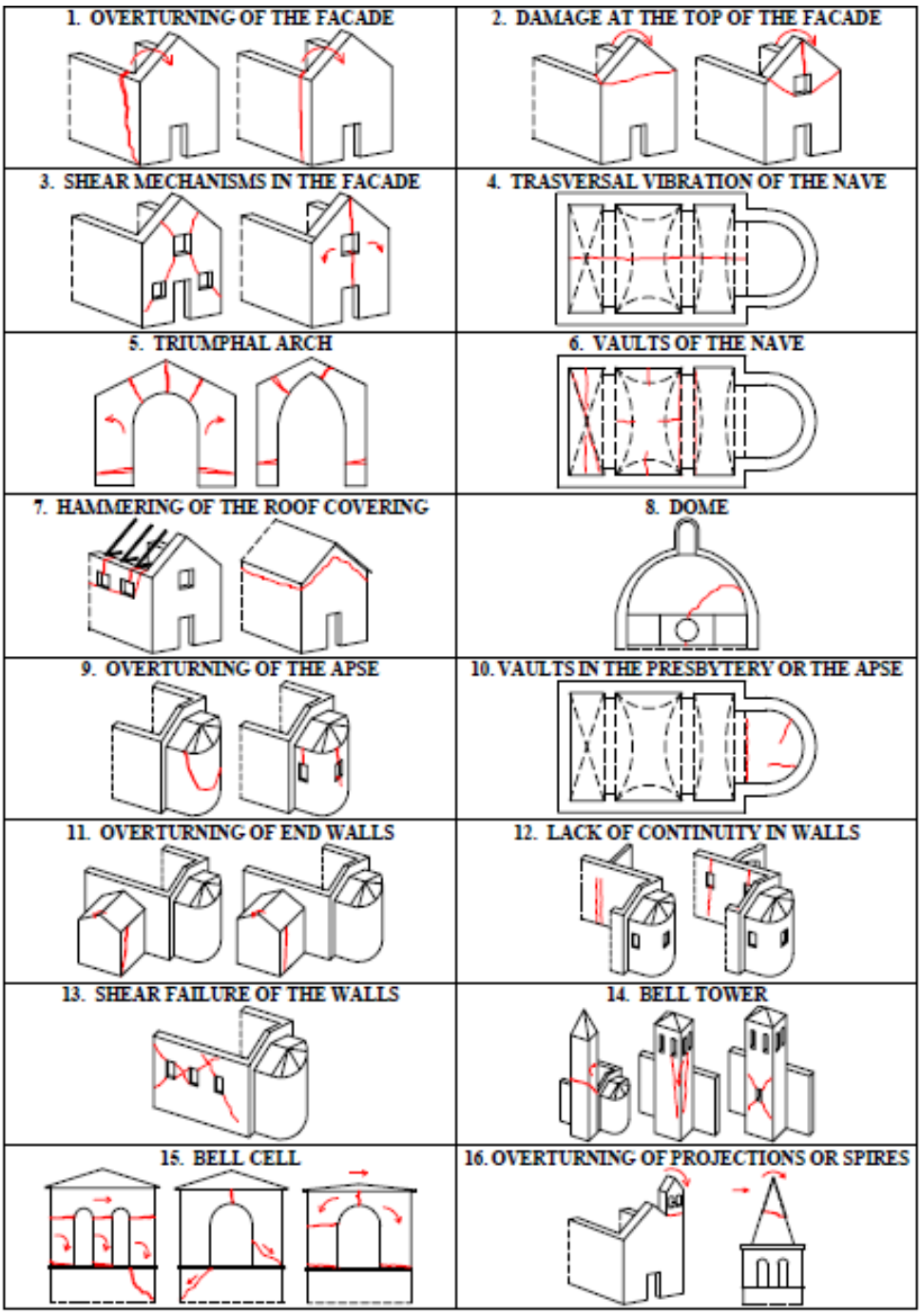

Figure 2.9 Illustration of typical damage mechanisms in churches after Lagomarsino (1998)

1. OVERTURNING OF THE FACADE	•	**2. DAMAGE AT THE TOP OF THE FACADE**	•
DETACHMENT OF THE FACADE FROM WALLS	•••	CRACKS IN THE TOP PART OF THE FACADE	•••
• Poor clamping between facade and nave walls • Lack of longitudinal chains or efficient buttresses		• Facade weakened by wide openings • Lack of a connection with the roof covering	
3. SHEAR MECHANISMS IN THE FACADE	•	**4. TRANSVERSAL VIBRATION OF THE NAVE**	•
SLOPING, VERTICAL AND ARCHED CRACKS	•••	CRACKS IN ARCHES, DEFORMED WALLS	•••
• Presence of many openings (also filled) • Possibility of rotation of the side walls		• Very thin side walls • Lack of transversal chains or efficient buttresses	
5. TRIUMPHAL ARCH	•	**6. VAULTS OF THE NAVE**	•
CRACKS IN KEY AND SPINE	•••	CRACKED VAULTS, DETACHMENT FROM ARCHES	•••
• Arch of insufficient thickness or poor masonry • Chains missing or badly placed; weak shear walls		• Vaults lowered excessively or thin • Presence of concentrated loads of roof covering	
7. HAMMERING OF THE ROOF COVERING	•	**8. DOME**	•
BEAM SLIDING; DISCONNECTION OF TIE BEAMS	•••	CRACKS IN: DOME, TAMBOUR, LANTERN	•••
• Roof thrusting; new roof covering rigid and heavy • Lack of connection between tie beams and masonry		• Tambour very high and with large openings • Lack of hoops or external buttresses	
9. OVERTURNING OF THE APSE	•	**10. VAULTS IN THE PRESBYTERY OR APSE**	•
VERTICAL OR ARCHED CRACKS IN APSE WALLS	•••	CRACKS IN THE VAULT OR APSE BASIN	•••
• Lack of hoops or chaining • Weakening from many wall openings		• Vaults lowered excessively or thin • Presence of concentrated loads by the roof covering	
11. OVERTURNING OF END WALLS	•	**12. LACK OF CONTINUITY IN WALLS**	•
DETACHMENT OF END WALL	•••	MOVEMENT OF JOINTS OR DISCONNECTEDNESS	•••
• Poor clamping between wall and orthogonal walls • Lack of chains or efficient buttresses		• Great difference of stiffness between two parts • Lack of clamping or chains	
13. SHEAR FAILURE OF THE WALLS	•	**14. BELL TOWER**	•
SHEAR CRACKS OR LOCAL DISCONTINUITY (OLD OPENINGS etc.)	•••	CRACKS ON CONTACT WITH THE CHURCH; VERTICAL CRACKS; EXPULSION OF EDGE	•••
• Masonry poor or of limited thickness • Great weakening due to the presence of openings		• Lack of connections with the church • Masonry decayed, poor, of limited thickness	
15. BELL CELL	•	**16. OVERTURNING OF PROJECTIONS/SPIRES**	•
CRACKED ARCHES; PIER ROTATION OR SLIDING	•••	PERMANENT ROTATION OR SLIDING	•••
• Lack of chains or hoops; thin piers • Roof covering heavy or thrusting		• Lack of buttress or other connection • Projection too thin	

Figure 2.10 Vulnerability indicators for typical damage mechanisms of churches after Lagomarsino (1998)

D'Ayala (2000) applied an analytical approach to analyse the damage to historic masonry churches in Umbria due to the 1997 Umbria-Marche earthquake and aftershocks, using a simple collapse mechanism model and establishing a correlation between fragility and the corresponding damage to the façade (Figure 2.11). Fragility is expressed in terms of the lowest equivalent shear capacity associated to relevant collapse mechanisms. The equivalent shear capacity is calculated with an approach based on limit state analysis. Thus, the mechanism with the lowest shear capacity is considered the most critical or likely to occur. Another important outcome of this work is the evaluation of the benefit of existing retrofitting solutions to the seismic response of the church.

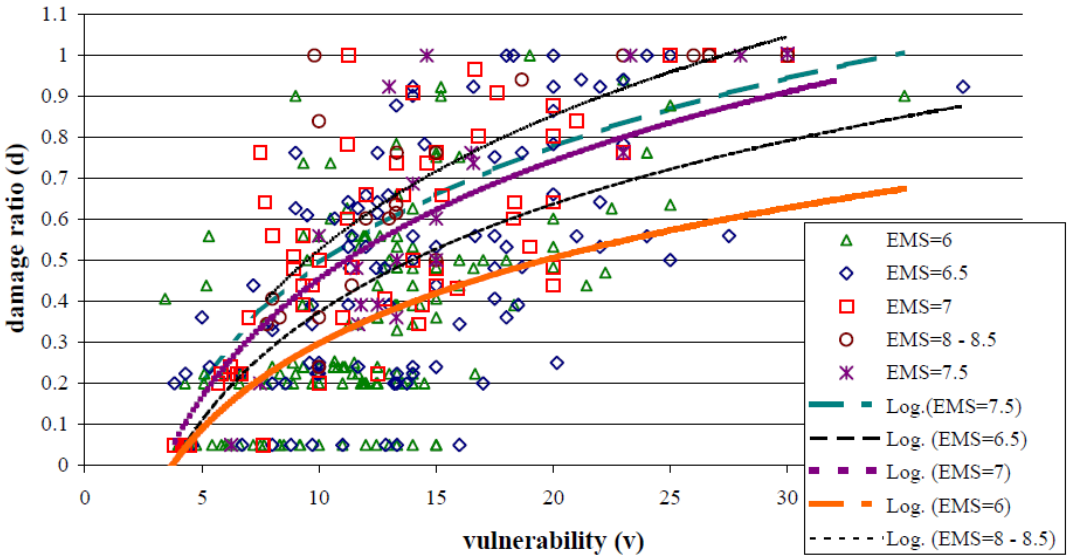

Figure 2.11 Correlation between the mean damage ratio of the facades of churches affected by the 1997 Umbria-Marche earthquake, *D*, and the corresponding vulnerability, *V*, expressed in terms of the lowest equivalent shear capacity associated to relevant collapse mechanisms (after D'Ayala, 2000)

As outlined by D'Ayala (2005), the definition of a holistic procedure for the performance-based seismic assessment of existing building stock and prediction of losses relies on the following steps: (i) classification of buildings, by typology and seismic design; (ii) definition of damage states; (iii) assignment of capacity curves; (iv) definition of demand spectra (with performance related level); and (v) evaluation of building response. The procedure provides as output fragility curves and damage scenarios.

Limit state analysis has been extensively applied to the fragility assessment of historic masonry buildings. FaMIVE (D'Ayala and Speranza, 2003) is a prominent example of this type of procedure. D'Ayala and Speranza (2003) identified typical partial and total collapse

mechanisms of facades made of dry stone or weak mortared masonry with non-rigid floor slabs under seismic loading, and calculated the collapse-load factor associated to each mechanism by means of limit analysis. The collapse load factor is expressed as a percentage of gravity acceleration, *g*. The procedure identifies the most critical collapse mechanisms of the facades of individual or groups of buildings, relating specific structural characteristics (e.g. type of masonry fabric, level of connection among orthogonal walls, and presence of strengthening) with vulnerability.

Incorporating the principles of performance-based assessment, D'Ayala (2005) also defined limit displacement conditions that corresponds to damage states and compares these values with the displacements demands obtained through non-linear displacement spectra (Figure 2.12). In particular, the author defines capacity curves for each façade on the basis of the strength capacity, a_y, which is equal to the collapse load factor obtained with FaMIVE, the elastic limit displacement at the top of each façade, Δ_y, and the ultimate displacement, Δ_u, which is assumed as the displacement that determines the collapse of the façade.

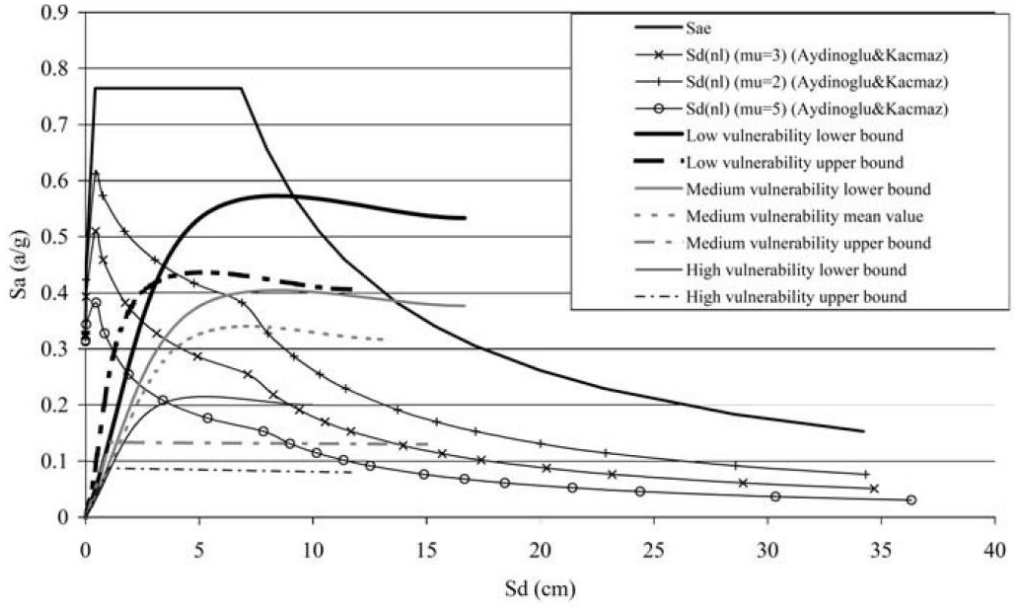

Figure 2.12 Fragility curves obtained for classes of vulnerability Low, Medium, High and Extreme, using mean values and standard deviations of collapse load factors (after D'Ayala, 2005).

For monumental buildings, such as masonry churches, Lagomarsino and Resemini (2009) developed limit state based models for assessing the damage limitation state corresponding to relevant out-of-plane mechanisms. Based on these models, the authors analysed the influence of a tie-rod in an arch mechanism, the influence of interlocking in the

façade overturning and the influence of the compressive strength of masonry. The authors concluded that if the steel tie-rod is pre-stressed, the spectral acceleration corresponding to the activation of the mechanism increases. In terms of typical overturning of the churches's façade, Lagomarsino and Resemini (2009) analysed the two failure mechanisms illustrated in Figure 2.13, where *H* is the height of the overturning part. The models showed that mechanism 2 (Figure 2.13b) is more likely than mechanism 1, except in the case of interlocking conditions at the corner similar to Figure 2.13d, where the frictional surface is reduced. Finally, the authors also concluded that neglecting the limited compressive strength of masonry leads to an overestimation, on the unsafe side, that may be unacceptable in the case of medium to low quality masonry.

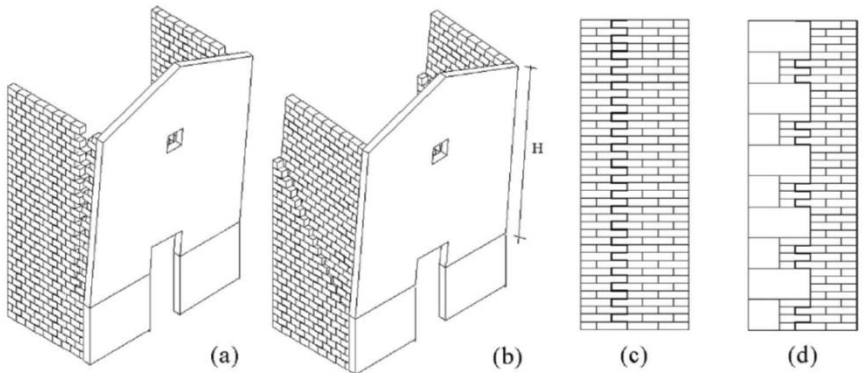

Figure 2.13 Out-of-plane overturning of the church façade after Lagomarsino and Resemini (2009): (a) mechanism 1; (b) mechanism 2. As far as mechanism 1 is concerned, figure (c) shows a possible failure surface in the case of façade and lateral wall made up of blocks of similar dimensions; and figure (d) shows a the case of façade and lateral wall made up of blocks of different dimensions.

These examples of seismic analysis of historic constructions based on limit state mechanism approaches further show the possibilities of using limit analysis to evaluate the damage limitation state of specific macroelements, in addition to more global analysis using other approaches such as the FEM.

2.5 Uncertainty of the assessment

Limitations on the information available to assess the structural behaviour of historic constructions, and limitations associated to the intrinsic formulation of the assessment approaches have been discussed in previous sections. These limitations would naturally become uncertainties of the assessment, compromising the quality of the diagnosis.

Reliability is a term commonly use in the structural design of new constructions, and can be expressed as the conditional probability, at a given confidence level, that an element or structural system will perform its required function within specified performance limits for a stated time interval, function period or mission time (Kececioglu, 2002; Birolini, 2004). In this context, the structural system is not intended to resist all possible occurrences without any damage, but a disproportionate collapse consequent to a localised triggering failure should be avoided, i.e. the structural system should prove a robust behaviour (Bontempi *et al.*, 2007).

In summary, the diagnosis of an existing historic building provides a measure of the reliability and robustness of the structural system. However, the quality of this diagnosis is dependent on the presence of uncertainties throughout the assessment process, as mentioned before.

Uncertainty is commonly considered as aleatory or epistemic (Apostolakis, 1993). Aleatory uncertainty refers to the variables involved in the modelling process that are of a stochastic nature. For instance, the uncertainties regarding actions or material properties in the process of design of a new structure are aleatory. Epistemic uncertainty reflects the confidence on the appropriateness of the model to represent the real physical system.

If the system is a historic building, some of the aleatory uncertainties could be of an epistemic nature. For instance, the uncertainty associated to material properties is usually described by normal distributions in the design of a new structure. However, such uncertainty is related to the level of knowledge on the constituent materials within the assessment of a historic building, and hence it is of an epistemic nature. Similarly, the characterisation of the actions could be of either an aleatory or epistemic nature; or the aleatoric uncertainty can be reduced by the knowledge of the current use.

In engineering codes and standards, for both the design of new constructions and the assessment of existing structures, uncertainties are usually taken into account by means of global or partial factors. Several procedures for characterising these factors are available in literature (e.g. CEN, 2005b; ASCE/SEI 41-06, 2007; CIB 335, 2010). Although both CEN

(2005b) and ASCE/SEI 41-06 (2007) provide a comprehensive procedure to evaluate the current level of knowledge of a structure and to achieve higher levels if needed, their provisions are not directly applicable to historic buildings. The reasons are that they do not evaluate the relevance of several sources of knowledge, such as historical documentation and oral testimonies, both fundamental contributors for the analysis of historic constructions, and they are not set to deal with the diverse nature of the uncertainty as outlined above. Moreover, the knowledge levels are defined on the basis of comprehensive experimental tests, which are normally unreasonable to undertake in historic constructions due to conservation principles.

A few interesting references on the evaluation of uncertainties related to the assessment of existing reinforced concrete (e.g. Franchin *et al.*, 2010; Jalayer *et al.*, 2010) and masonry structures (e.g. Tondelli *et al.*, 2012) are available in literature. The evaluation is based on the assessment of a reference structure, assumed to be perfectly known, and comparison with the assessment of an imperfectly known structure. Alternative hypotheses and decisions made by the analysts during the assessment are considered in accordance with the Eurocode 8 procedure (CEN, 2005b). Results of these comparisons show that geometric uncertainty is at least of the same order of importance of uncertainties associated with material properties and structural details, and that the effect of epistemic uncertainties is dependent on the analysis method and the reference structure used, as would be expected.

2.6 Conclusions

This chapter has provided an overview of assessment procedures for historic constructions, including analysis approaches widely applied in literature. A summary of the principal advantages and limitations were discussed in the relevant sections. It has been shown that, independently of the approach used, there are inevitable limitations that become uncertainties of the assessment. More detailed and specific literature review can be found in the relevant chapters of this thesis.

The most important conclusions of this chapter for the objectives of this thesis are:

(i) Structural analysis approaches have significantly evolved in the past decades from a mathematical and computational viewpoint. However, such progress was not accompanied by a similar evolution of the capability of analysing the structural performance of a historic construction in practice. On the one hand, this is due to the fact that the analysis of large and complex historic constructions is always based on

many assumptions and simplifications related to the intrinsic limitations of the various approaches. On the other hand, this can also be explained by the fact that only a few researchers and practitioners in the world have proper ability and resources to conduct advanced structural analyses on the basis of detailed and reliable data.

(ii) This capability of analysing large and complex historic constructions is most critical in seismic prone developing countries, where shortage of resources is more critical and some of the least studied historic structural systems are located. A prominent example is the Peruvian historic adobe and timber churches. Adobe is one of the least studied and modelled traditional materials, and the analysis of timber structures do not have significant precedents in Peru. Moreover, experimental work is still the most viable method to collect information about the mechanical behaviour of traditional materials and components, while being simultaneously the most expensive and intrusive.

(iii) FEM based approaches are currently the most viable approach to assess the structural performance of historic constructions. These approaches are able to evaluate the initiation and progression of damage that can compromise the cultural significance of historic assets, and to identify local failures typical of adobe. Using appropriate constitutive models, these approaches can simulate the predominant behaviour in shear of adobe under earthquake loading. Moreover, commercial FEM software is the most worldwide disseminated tools for structural analysis. These tools can be used to model large and complex structures, simulating multiple interactions among different types of components.

(iv) The lack of information about the historic construction and the various limitations of the assessment approaches result in several uncertainties, especially of an epistemic nature, which are present throughout the assessment, compromising the quality of the final diagnosis of an historic construction. Current codes and guidelines do not have specific provisions that address the diverse nature of the uncertainties present in the analysis of historic constructions as compared to the analysis of other existing constructions. Moreover, such provisions lack a proper strategy to evaluate the effect of the uncertainties on the diagnosis of a specific historic construction.

Create your own method. Don't depend slavishly on mine. Make up something that will work for you! But keep breaking traditions, I beg you.

Constantin Stanislavski

CHAPTER 3

Structural assessment of heritage constructions with appraisal of the knowledge-based uncertainty of the results

3.1 Introduction

A holistic approach is currently widely applied to make a diagnosis and safety evaluation of historic buildings, as discussed in Section 1.2. Such approach includes the interpretation of the current structural layout, construction and condition, and the application of some qualitative and/or quantitative method in support of the analyst's judgment, as discussed in Chapter 2.

The accuracy of the diagnosis or safety evaluation of an historic building (or any heritage construction) depends on the different assumptions made throughout the assessment process. If the uncertainties can be first clearly identified, then in some way quantified, the accuracy of the results can be monitored and controlled.

The uncertainties, principally of an epistemic nature, present in the assessment of heritage constructions can be summarised as follows:

(i) uncertainties on geometry;
(ii) uncertainties on material properties and current condition;
(iii) uncertainties on the characterisation of loading;
(iv) uncertainties on structural details, which will lead to different internal and external constraint and interaction conditions;

(v) uncertainties on the ability of the mathematical model to reproduce the real system; and

(vi) uncertainties related to the analyst's judgement.

Following the aforementioned holistic approach, it can be inferred that a procedure for evaluation of the accuracy of the diagnosis of heritage constructions should be adaptable to the nature and complexity of each individual case study, and at the same time based on the judgment capacity of the analyst. This means that the use of a pre-defined confidence factor as a measure of uncertainty might be inappropriate for the specific case of heritage constructions, especially monumental buildings such as churches. The current use of confidence factors in the diagnosis, as for instance in Eurocode 8 (CEN, 2005b), is based on the assumption that any uncertainty present in the diagnosis leads to the erroneous idea of a state that is 'better' than the real state. However, the inaccuracy of the results of the assessment due to the presence of uncertainties can lead to both an overestimation and underestimation of the performance of the structure. Moreover, the traditional conservative approach can lead to excessive retrofitting and compromise the cultural significance of a construction. A strategy that should be explored as an alternative to this conservative approach is to use available knowledge of the construction to evaluate whether the quantitative analyses lead to an overestimation or underestimation of the 'real' structural performance of the construction. For this purpose, it is essential having a methodology to evaluate the uncertainties that is tailored to each specific assessment and that takes into account the holistic nature of the problem and the specific constraints in terms of data and knowledge. Moreover, this methodology should include and deal with the various sources of uncertainty outlined above in a similar way. These considerations can find evidence in existing work, for instance by Tondelli *et al.* (2012), who emphasised that geometric uncertainty is as important as other types of uncertainty, and that the effect of epistemic uncertainties is dependent on the analysis method and reference structure used, which is ultimately a decision made by the analyst.

Recently, Cattari *et al.* (2015) proposed an approach for existing masonry buildings that uses sensitivity analysis to identify the most influent variables to the structural response of the building. This identification is essential to optimise the work plan of the assessment, in order to gather more detailed and reliable data for the most sensitive variables, or at least to find a compromise between sensitivity and level of knowledge. Sensitivity classes are assigned to the variables on the basis of their respective level of influence. This allows

confidence factors to be obtained that take into account both the sensitivity and the level of knowledge associated to the inputs of the assessment. The approach is oriented to applications where the vulnerability of the buildings is expressed by a unique fragility measure, for instance the seismic capacity that leads to a certain performance level.

This work by Cattari *et al.* (2015) builds on the idea of correlating sensitivity to level of knowledge in order to measure uncertainty. This idea can be further developed to establish a more general framework that takes into account all the aforementioned uncertainties, and that can be applied to complex cases that require the consideration of several macroelements and structural performance indicators such as churches.

The methodology proposed in this chapter and tested in the rest of this thesis provides a complete framework for the assessment of heritage constructions, from the gathering of data to the final diagnosis. It is applicable to all types of heritage constructions and adaptable to different methods of analysis. A procedure for evaluation of the influence of different knowledge-based uncertainties and for estimation of a final uncertainty measure of the diagnosis is proposed within this framework. The uncertainty is determined by monitoring the existing knowledge and influence associated to a number of control variables. Uncertainties associated with inputs, modelling choices and analysis' conditions are taken into account. The analyst's capacity of judgment is critical to the assessment of heritage constructions, and therefore this source of uncertainty is also indirectly considered in this framework. All uncertainties are treated in a similar way, which reduces the complexity and increases the versatility of the framework. In this context, variables with different statistical distributions can be treated in an identical way. As the modelling choices are critical to the results, a strategy to determine most appropriate choices with reduced computational effort is also proposed.

3.2 A framework for the structural assessment of heritage constructions

The diagnosis of heritage constructions should be supported by quantitative analyses that describe in mathematical and physical terms the structural behaviour of the construction. These quantitative analyses can be simple hand-made calculations or more sophisticated numerical models. Numerical modelling is currently the most common approach used in the analysis of heritage constructions, as discussed in Chapter 2. In this context, the modelling strategy is one of the critical decisions made by the analyst at an early stage of the assessment process. Such decision is partly influenced by existing data, but also determines

what further data is needed, and hence the cost of the investigation. Due to the usual complexity of heritage constructions, it is more efficient to conduct initial sensitivity analysis and testing of different hypotheses and modelling strategies using a model of a portion of the heritage asset, sufficiently representative of the whole behaviour of the structure. Moreover, the influence of the uncertainties on the diagnosis must be evaluated taking into account the variability of the input and the corresponding effect on the output.

Based on these premises, the proposed framework for the global assessment of a heritage structure is outlined in Figure 3.1. The framework is a staged process including several phases, in which decisions regarding forthcoming phases are taken from results of the current phase. This helps the analyst to make more informed, fit for purpose and tailored data collections. At each phase, the level of uncertainty is identified either in a qualitative or quantitative way in order to keep track of the quality of the assessment. The framework follows a logic sequence of phases of increasing complexity and refinement. In line with this logic, the uncertainty is also evaluated with an increasing level of detail. Depending on the level of uncertainty identified by the analyst at any phase of the assessment, more information about the structure should be collected in order to increase the accuracy of the results, whenever this is deemed necessary to make a meaningful diagnosis.

The initial phase regards collection of data about the heritage construction from different sources, as recommended by ICOMOS-ISCARSAH (2003), namely historical data, oral testimonies, *in-situ* surveys and testing, laboratory testing and monitoring. These sources provide information on the geometry, constituent materials, structural details, damage and decay of the construction. If there is shortage of information, especially in relation to a specific aspect of the structure, different sources can be used to make reasonable assumptions; even though such assumptions have an inherent level of uncertainty depending on the quality of the sources. For instance, the geometry of the building and the year of construction might provide useful information regarding typical structural details and materials, which are often difficult to check on site without "opening up". Moreover, evidences of damage and decay may inform on structural details, depending on where the damage or decay occurs.

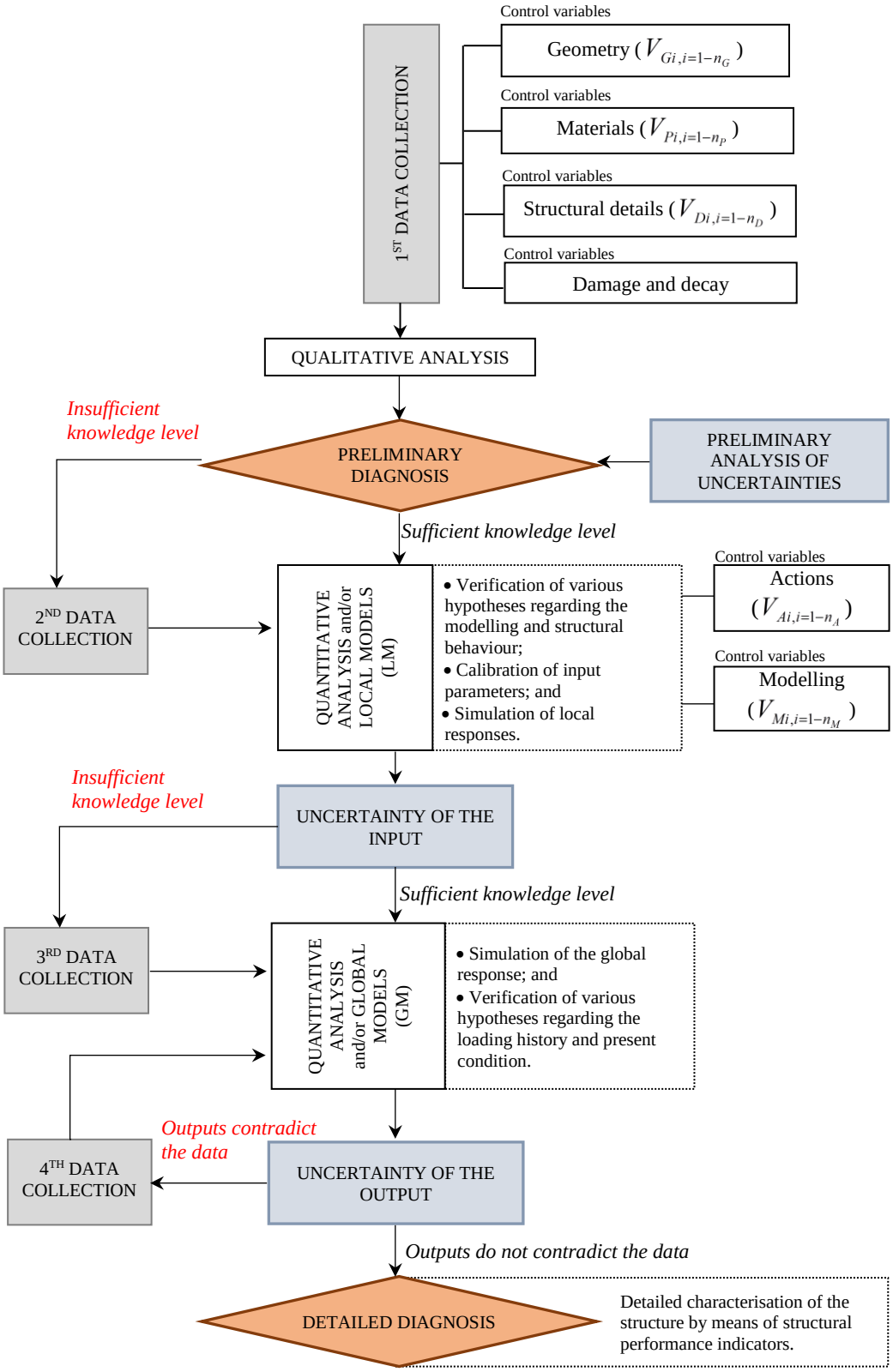

Figure 3.1 Framework for structural assessment of heritage constructions

Based on information gathered at the beginning of the assessment in an activity called here as '1st data collection' a qualitative analysis supported or not by simple hand-made calculations can be conducted. This analysis will inform a preliminary diagnosis of the heritage construction, which provides a first judgement of the structural behaviour and condition of the structure and identifies the issues that need further investigation by means of structural analysis or experimental testing. Moreover, this preliminary diagnosis also helps to understand whether more information must be collected.

The preliminary diagnosis might be sufficient to evaluate whether a construction represents or not an eminent threat for the occupants, but it would not be normally sufficient to evaluate the need for specific remedial measures for the building to achieve a given performance level. In the aftermath of a disaster, this preliminary diagnosis can be seen as an initial rapid assessment of the structure for the purpose of evaluating possibilities of re-occupancy. For a more detailed assessment of current structural performance, a more detailed diagnosis based on structural analysis is required. For this purpose, models of representative portions of the structure, from now on called local models (LM), can be used to test the relevance of different geometric and/or structural hypotheses, material models, hypotheses for contact simulation and boundary conditions.

The results of these local analyses will inform the strategy for evaluating the global structural response of the construction by means of global models (GM). Local models allow to expeditiously testing different modelling hypotheses and selecting control variables. Moreover, local models can be directly used in the uncertainty appraisal to evaluate the sensitivity of the modelling strategy to the variation of the inputs with relatively low computational burden and time requirements. At the local level, the impact of more detailed modelling strategies (micro-modelling for instance) or simplified alternatives can be investigated in order to optimise the strategy for the global model. Input parameters can also be calibrated at a local level by comparing the results of structural analysis with experimental testing or other types of data.

The global models may be essential to test various hypotheses regarding the loading history and present condition of the structure, which ultimately and decisively helps the analyst to make a detailed diagnosis. However, the results of the global models are difficult to validate, as the modelling in itself is aimed at explaining and demonstrating a structural behaviour which might be qualitatively understood by the analyst, but which is to a large extent unknown in quantitative terms and often cannot be reproduced or simulated in other ways, by means of laboratory testing for instance. Usually the verisimilitude of the results is

judged on the basis of the ability of the model to reproduce specific failures or deformations observed on site, as done by Croci *et al.* (1995) more than two decades ago in the analysis of the Colosseum of Rome. In alternative, *in-situ* dynamic identification can be used to determine whether the stiffness and mass distribution of the model represents the real distribution by modal vibration correlation. However, this method only validates the elastic behaviour of the model (see for instance Martinez *et al.*, 2006). Simplified hand-made calculations are important at this stage to verify specific results of the model and to compare the demands with the capacity of the structure. The results of these analyses will ultimately inform the detailed diagnosis of the heritage construction. If the results of the global models contradict existing data, such as *in-situ* observations, more information must be collected in order to calibrate and refine the model.

In the following, a comprehensive discussion of the principal steps of the framework is presented.

3.3 Preliminary diagnosis

In the proposed framework for structural assessment of heritage constructions (Figure 3.1), a diagnostic exercise is conducted at two different phases – preliminary diagnosis and detailed diagnosis. Nevertheless, each of these phases may include a number of iterations that go along with the progress on the collection and interpretation of information. The formulation of possible alternative diagnoses during these iterations can inform the process of further gathering of information, testing and analysis to be carried out to prove or disprove a given diagnostic hypothesis.

The preliminary diagnosis exercise indicated in Figure 3.1 builds on information collected through initial *in-situ* visits and/or other qualitative data drawn from archives, historic sources, tests, and precedents from literature, and on simplified qualitative analysis of structural performance. It provides a first synthetic judgement on the structural behaviour and condition of the construction, and relies largely on the expertise and experience of the analysts and their ability to interpret these data sources.

The preliminary diagnosis might be a joint team activity to ensure that all disciplinary skills and concerns are properly represented in the assessment and decision making about future steps of the project or investigation. The preliminary diagnosis conducted within the EAI-SRP is described in Quinn *et al.* (2015), where the procedure is applied to the diagnosis of a historic Peruvian church and house.

The first step in the preliminary diagnosis is the identification of the macroelements of the construction. A macroelement is a portion of the structure that can be considered independent from the rest, since for instance in the event of an earthquake it will show a distinct seismic behaviour while interacting with other macroelements (Novelli and D'Ayala, 2011). This division into macroelements is particularly relevant to historic buildings with complex lay-outs where parts of the buildings behaving independently can be clearly identified.

Thus, the structure can be seen as a structural system that can be decomposed into a number of entities that interact with each other. This decomposition can be done at different levels, namely at the level of the structural system (whole structure), substructures (nave, altar, baptistery, sacristy, roof, floor, etc.), components (trusses, walls, buttresses, arches, tie-beams, etc.) and elements (arches' planks, rafters, joints, etc.). Large scale levels are typically distinguishable from a simple observation of the geometry of the construction, whereas more detailed levels require knowledge about materials and existence of discontinuities, which are often difficult to observe and lack information in historical documents.

The preliminary diagnosis is based on the establishment of a relationship between macroelements and the attributes described in Table 3.1. More attributes can be added or some of them removed according to their relevance and applicability to a specific case study. However, the attributes chosen in this framework allow the determination of the global and local structural behaviour, the interaction between macroelements, the integrity of the structure and its condition over time, delivering a holistic diagnostic tool.

A first element of judgement of the relevance of the attributes to the structural response of a specific macroelement is required. To this end, the attributes are ranked through classes of influence according to Table 3.2. The attributes that are not ranked are considered by the analysts as having no influence on the performance of the macroelement.

The second element of judgement relates to the nature of the influence, i.e. the favourable or unfavourable nature of the influence of an attribute over a given macroelement is qualified by the symbols "+" (favourable) and "-" (unfavourable), following the letter.

The third component of judgement is the uncertainty with which the first two judgements are made by the analysts. This procedure is called in Figure 3.1 as the preliminary analysis of uncertainties and it is described in Section 3.4.1.

Table 3.1 Attributes of the diagnosis

Attributes	Definition
(i) Robustness of the structure (Robustness)	This variable evaluates how well the structure was originally conceived and constructed and how this influences the structural response.
(ii) Interaction of macroelements (Interaction)	This variable evaluates the nature and mechanisms of interaction of the various macroelements of the construction. Emphasis is here put on the connections between macroelements, which determine the global structural behaviour of the construction, and its ability to respond to external actions.
(iii) Type of connections (Connections)	The variable evaluates the original conceptual design and construction of the connections between structural elements within a given macroelement, and relates to the local response of the macroelement which in some circumstances can lead to partial collapses.
(iv) Quality of materials (Materials)	The variable evaluates the layout and integrity of the materials and fabric constituting a given macroelement. In particular for masonry it evaluates the quality of the units, mortar and bond and the general layout of the fabric.
(v) Level of deterioration (Condition)	The condition of the structure changes the structural performance of the system. Although this attribute is related to 'Robustness', since a structure that is well-conceived and constructed would have less propensity for deterioration, external actions can trigger the deterioration of the materials and connections up to a point where safety is compromised even if the structure is robust.

Table 3.2 Classes of influence of the attributes in the preliminary diagnosis

Classes of influence	Relevance
A	Critical
B	Relevant
C	Influential but not relevant
D	Negligible influence

The uncertainty is judged by the analyst by means of an uncertainty factor $\delta Ip_{j,i}$ which represents the percentage of uncertainty present in the judgement of a macroelement *i* as far as attribute *j* is concerned. This judgment is simply based on the experience and perception of the analyst.

The level of uncertainty at macroelement level is a measure of the level of uncertainty associated with the diagnosis, and hence together with the relevance of a specific attribute provides an indication of further numerical, experimental or field investigations that should be pursued in order to improve the accuracy of the diagnosis. The preliminary diagnosis can be summarised in a matrix similar to Table 3.3.

Table 3.3 Matrix of the preliminary diagnosis

MACROELEMENTS	ATTRIBUTES			
	Attribute (i)		[…]	Attribute (j)
Macroelement (1)	Class of influence	+ or -		
	$\delta Ip_{j,i}$ (%)			
[…]				
Macroelement (*i*)				

3.4 Control variables of the structural analysis

Epistemic uncertainties are present at various phases of structural analysis of a heritage construction and are related to input parameters and analysis conditions or modelling hypotheses. During the first data collection, input parameters related to geometry, materials, structural details, damage and deterioration are characterised based on interpretation of existing information and simple hand-made calculations. If numerical analyses are required to make a meaningful diagnosis, and information is deemed sufficient to conduct such analyses, local models should be first developed. During the preparation of these local models, modelling hypotheses and actions to be applied to the models are selected by the analyst. If information is not sufficient, a second data collection should be conducted. This

logic sequence of steps is shown in the framework of Figure 3.1. However, there is normally an important component of looping in this process, since the models and the analyses might be iteratively and continuously adjusted while more information is collected and interpreted.

Input parameters and modelling hypotheses are here called control variables of the structural analysis, as indicated in Figure 3.1 and Table 3.4. Control variables are similar to what is commonly denominated 'basic variables' in literature (e.g. ISO 13822, 2010; CEN, 2005a), with the difference that these 'basic variables' are all essential inputs of structural analysis, whereas not all control variables are needed. Some control variables are just alternative modelling hypotheses identified by the analyst to improve the quality of the results. Following this rationale, the 'basic variables' can be seen as a sub-set of the control variables. The term 'control' reflects the fact that these variables 'control' the quality of the structural analysis and its ability to successfully inform the diagnosis.

Table 3.4 Control variables and respective plausible values or states for evaluation of uncertainty

Class of variables	Control variables	Plausible modelling states of the control variables	Plausible values
Geometry, *G*	$V_{Gi}\ ,i=1-n_G$		
Materials, *P*	$V_{Pi}\ ,i=1-n_P$		
Structural details, *D*	$V_{Di}\ ,i=1-n_D$	Most plausible or reference state	Interval of plausibility:
Actions, *A*	$V_{Ai}\ ,i=1-n_A$	Alternative plausible states	$[V_{Kimn}\ , V_{Kiref}\ , V_{Kimx}\ ]$
Modelling, *M*	$V_{Mi}\ ,i=1-n_M$		
Variable class: $K = G, P, D, A, M$	Total number of control variables: $n = n_G + n_P + n_D + n_A + n_M$		

The control variables, V_{Ki}, where K denotes the variable's class and i the variable's number within a given class, are identified for each case study. The complete set of control variables, composed of n variables, is divided into five classes (Table 3.4): geometry, materials and structural details (defined in accordance with Eurocode 8 (CEN, 2005b)), actions and modelling.

The 'actions' class regards the mechanical agents, such as forces, displacements and accelerations, which produce stresses and strains in the structure. The ICOMOS-ISCARSAH

(2003) recommendations also identify physical, chemical and biological actions which affect the deterioration of the mechanical behaviour of the materials and are usually related to long-term or cyclic processes.

The effect of these actions may be taken into account in a simplified way by means of the following two strategies:

(i) changing the material properties at specific locations or of specific members and therefore directly affecting material strength and deformability; or

(ii) modifying the cross-section of the structural components in order to approximate the mechanical behaviour of materials with reduced mechanical characteristics.

Thus, depending on the strategy, these actions become control variables of the 'materials' class or 'geometry' class.

The 'modelling' class investigates alternative modelling hypotheses, which are associated to the approach used for structural analysis. Variables of the 'modelling' class are not directly related to the structure itself but to contemporary scientific/technological capacity to simulate an assumed structural behaviour for a given heritage construction and depend on the quantitative method used. For instance, the type of finite elements to be used in the modelling of an adobe wall by means of the finite element method is an example of a variable belonging to a 'modelling' class. In current engineering practice, structural analysis is usually performed using commercial packages with pre-existing codes, over which the analyst has modest control and with a limited library of elements and material constitutive laws to choose from. In principle, if the analyst does not have substantial experience on the modelling approach used, more control variables are likely to be defined for this class.

Each class of variables can be linked to a specific phase of the modelling approach used, independently of the corresponding formulation and complexity. For instance, if a FEM based programme is used, the modelling phases can be related to the classes of control variables, as shown in Figure 3.2, where continuous arrows indicate a direct relation and dotted arrows indicate a relevant influence. A relevant influence is attributed to a class of control variables that has significant influence or interdependencies with a given modelling phase; even though none of the variables have a direct correlation. The 'modelling' variables are a special case since they can be similarly associated to all modelling phases.

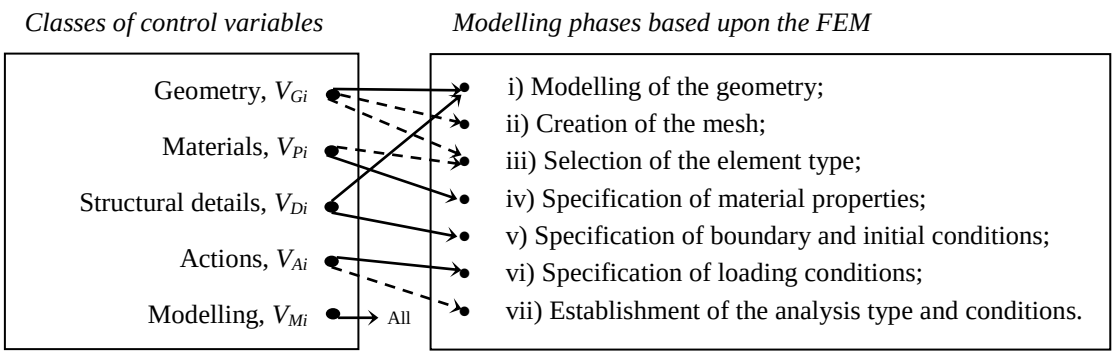

Figure 3.2 Ontological diagram of the relationship between FEM modelling phases and classes of control variables (continuous arrows indicate a direct relation and dotted arrows indicate a relevant influence)

A consequence of the interdependency of the modelling phases is the fact that in order to properly identify and quantify the uncertainties present during a specific phase, it is necessary to propagate the uncertainties of previous phases. Moreover, although the modelling phases are presented as a sequence, they can inform each other, and this feedback between the phases in the modelling process allows the reduction of some of the uncertainties.

A control variable can be characterised by either a range of values, called interval of plausibility, or a number of states, as shown in Table 3.4. A 'state' is a hypothesis assumed for a control variable that does not have a numerical representation, called a 'value'. Since a state can be an alternative model, the choice of the model is treated as one source of uncertainty. The interval of plausibility can be composed of several values. In this formulation, three are considered:

(i) minimum plausible value, V_{Kimn};
(ii) most plausible or reference value, V_{Kiref}; and
(iii) maximum plausible value, V_{Kimx}.

In literature, the reference value is usually called 'base-case', 'nominal value' or 'baseline' (e.g. Hoffman and Gardner, 1983; Helton, 1993; Frey and Patil, 2002; Campolongo *et al.*, 2011). The reference value or state can be seen as the 'best estimate' (Saltelli and Annoni, 2010), which is a function of the amount of available information and its credibility (Pilch *et al.*, 2011). The results of an analysis performed under the reference

analysis conditions are the reference results, where the reference values and/or states are assumed for all control variables.

This is illustrated in Figure 3.3 for the case of a given control variable characterised by an interval of plausibility. Such control variable can be for instance the modulus of elasticity of the main structural material of the heritage construction. Prior to a 1st data collection, there is a space or universe of possible values of modulus of elasticity known for building materials. This space is represented by the grey area in Figure 3.3a. At this point of the assessment there is no information about the specific heritage structure. But the analyst knows that the real or exact value of the modulus of elasticity of any specific heritage construction lies within this space. The 1st data collection allows the analyst to reduce the possible space to a plausible interval (Figure 3.3b).

For instance, the analyst might know at this point that the main structural material is adobe, even though the exact value of the modulus of elasticity of this specific heritage construction is still unknown. However, based on information available in literature and field observations or tests, the analyst is able to select a reference value and the upper and lower bounds of the interval of plausibility. At this point, the initial input variability is reduced to an interval of plausibility. If more information is collected, through more detailed *in-situ* investigations and/or experimental tests, the analyst can review the reference value and reduce the interval of plausibility (Figure 3.3c). Sensitivity analysis conducted with the local models can also be used to further reduce the interval of plausibility to a range of values that significantly change the output. For instance, it can be seen in Figure 3.3c that values above V_{Kimx} and below V_{Kimn} do not significantly change the value of the structural performance indicator (SPI). Conversely, it is also reasonable to consider that values between V_{Kiref} and V_{Kimx} do not significantly change the value of the SPI. In this case, it is possible to further reduce the interval of plausibility assuming V_{Kimx} equal to V_{Kiref}. How far the reference value is from the exact value is still unknown. In practice, it is impossible to know the exact value, since it is impossible to reach a complete level of knowledge about an existing heritage construction. This is the fundament of the uncertainty analysis described in detail in the following.

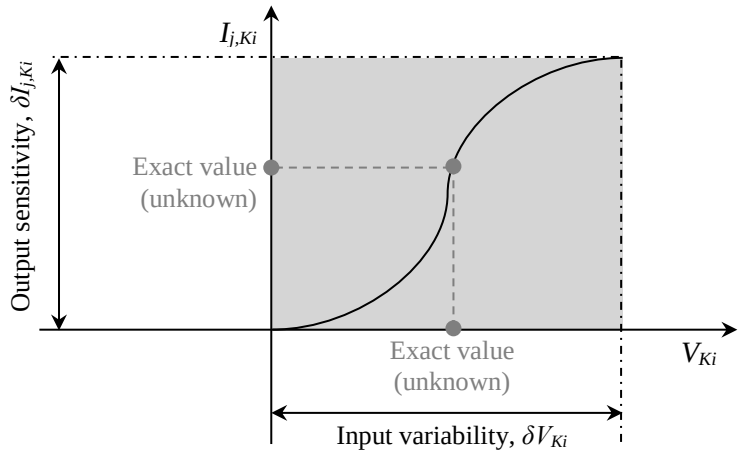

a) Possible control variable's space and output sensitivity before the 1st data collection

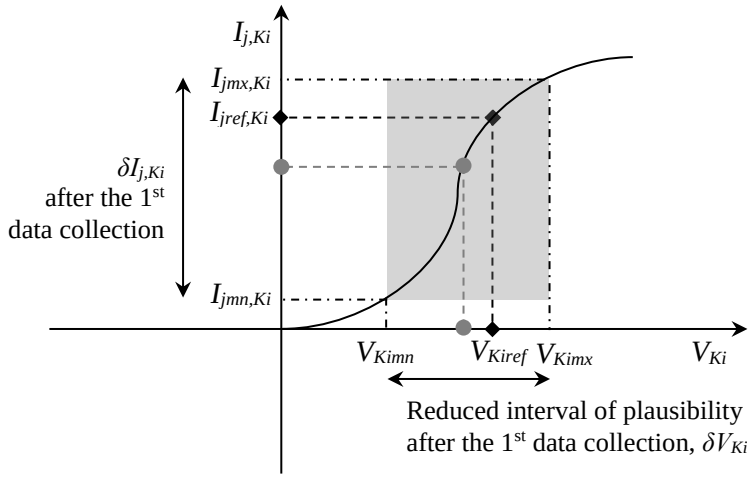

b) Interval of plausibility of the control variable and corresponding sensitivity of the output after the 1st data collection

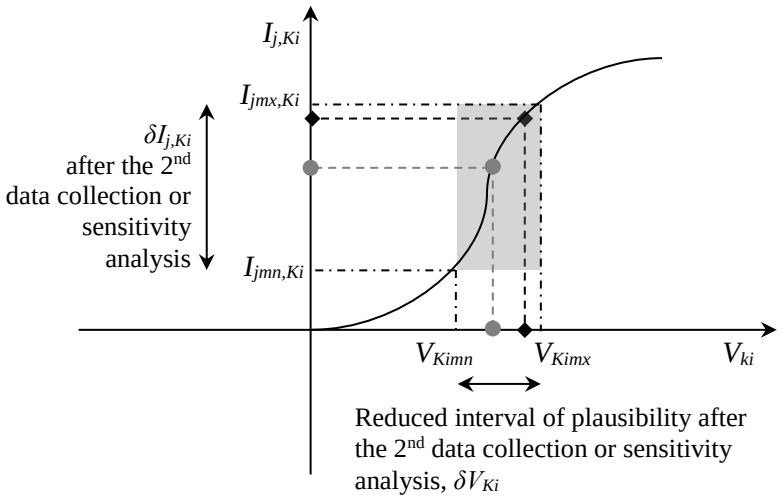

c) Interval of plausibility of the control variable and corresponding sensitivity of the output after the 2nd data collection or sensitivity analysis

Figure 3.3 Reduction of uncertainty due to increasing level of knowledge regarding a control variable characterised by a given interval of plausibility

3.5 Knowledge-based uncertainty analysis

The framework of Figure 3.1 includes three phases of uncertainty analysis, which are defined in Table 3.5. Each of these phases is described in detail in the next sections.

3.5.1 Preliminary uncertainty analysis

This uncertainty is quantified in the preliminary diagnosis in terms of a percentage of uncertainty assigned to the diagnosis of macroelement *i* as far as attribute *j* is concerned, $\delta Ip_{j,i}$, by the analyst. It is a perceptive measure of the level of uncertainty of the judgement. The combined uncertainty associated to a given attribute, δIp_j, or macroelement, δIp_i, is obtained by means of equation 3.1 and equation 3.2, respectively.

$$\delta Ip_j = \frac{\sum_{i=1}^{mp} \delta Ip_{j,i}}{m_p} \quad [3.1]$$

$$\delta Ip_i = \frac{\sum_{j=1}^{np} \delta Ip_{j,i}}{n_p} \quad [3.2]$$

, where n_p is the total number of attributes of the preliminary diagnosis, and m_p is the total number of macroelements. An overall level of uncertainty, δIp, can likewise be obtained by applying equation 3.3.

$$\delta Ip = \frac{\sum_{i=1}^{np} \delta Ip_j}{n_p} \text{ or } \delta Ip = \frac{\sum_{i=1}^{mp} \delta Ip_i}{m_p} \quad [3.3]$$

Table 3.5 Phases of knowledge-based uncertainty analysis within the framework for structural assessment of heritage constructions

Uncertainty analysis phase	Definition and objectives	Uncertainty measure
1st Phase: Preliminary analysis of uncertainties	This analysis provides a measure of the uncertainty with which the analyst(s) conduct(s) the preliminary assessment. In particular, it informs on the lack of confidence of the analyst(s) in the assignment of a class of relevance and nature of influence to an attribute to characterise its influence on the structural behaviour of a given macroelement.	A percentage of uncertainty defined by the analyst(s) in a qualitative way.
2nd Phase: Uncertainty of the input	This analysis provides a quantitative measure of the uncertainty present in specific structural analysis used to support the detailed diagnosis which can be used in a similar way as the current confidence factors of existing codes and guidelines. This measure takes into account the plausible range of variation (interval of plausibility) or alternative states of the inputs, the sensitivity of the outputs to this variation, and the level of knowledge with which the interval of plausibility and the alternative states are identified.	A quantitative measure of uncertainty which can be used in a similar way as current confidence factors of existing codes and guidelines. This uncertainty is however tailored to the assessment of heritage constructions.
3rd Phase: Uncertainty of the output	This analysis is based on the evaluation of the outputs or results of structural analysis used in the detailed diagnosis and comparison with existing knowledge on the structural response of the heritage construction. The detailed diagnosis takes into account that the response of the model varies within the range defined by the uncertainty of the previous phase (uncertainty of the input). If the behaviour of the model is not comparable to observations and evidences collected directly from the heritage construction, the model is not accurate enough to be used in the detailed diagnosis. In this case, the interval of plausibility or alternative states must be redefined and the uncertainty of the input recalculated. This process should be repeated up to a point that the model exhibits a behaviour that is comparable to the real response of the heritage construction.	The outputs of the model used in the structural analysis are here used as an uncertainty measure of the accuracy of the model. If the outputs contradict existing data (e.g. field observations of the level of damage of a building after an earthquake), the uncertainty is high and the inputs of the model must be calibrated.

3.5.2 Uncertainty of the input

The uncertainty of the input is calculated as part of the analysis at the local level, in which alternative hypotheses of the modelling are investigated, input parameters are calibrated and local behaviour is simulated to answer specific questions of the preliminary diagnosis (see framework of Figure 3.1). The procedure for evaluation of the uncertainty of the input is summarised in the flowchart of Figure 3.4. Each of the steps of this flowchart is described in detail in the following sections.

3.5.2.1 LEVEL OF INFLUENCE OF CONTROL VARIABLES AND SENSITIVITY OF OUTPUTS

To determine the influence of a given control variable, it is necessary to evaluate the change in the results of the analysis due to a predefined change in value or state of the variable. Various sensitivity analysis methods are available in literature for this purpose.

The present approach uses the 'nominal range sensitivity analysis' (NRSA) (Frey and Patil, 2002) with the "one at a time" (OAT) method (Saltelli *et al.*, 2000), in which one variable is changed at a time. An inconvenience of the OAT method is that interdependency among control variables can not be detected since the variables are not changed simultaneously (Critchfield *et al.*, 1986; Saltelli, 2005; Morio, 2011). Furthermore, perturbations of the control values near the reference values are not able to detect a different pattern of sensitivity that might exist in some point of the input variables' space when using a nonlinear model (Saltelli, 1999). This is illustrated by Figure 3.3a, where a given output or SPI j varies in a non-linear way depending on the value of control variable V_{Ki}. Hence, depending on the interval of plausibility of V_{Ki}, the SPI j will have a different pattern of sensitivity (i.e. it will vary slightly or exponentially).

However, the objective here is to analyse the pattern of sensitivity within a relatively small interval of the variables' space. It can be argued that linear dependency could be safely assumed when analysing sensitivity near specific reference values (Ingalls, 2008). The lower is the level of knowledge the wider will be the interval of the variables' space, and therefore larger will also be the uncertainty. Following this logic, the uncertainty associated to the sensitivity method used can be integrated into the uncertainty associated to the identification and characterisation of the control variables due to insufficient knowledge, as discussed in the next section.

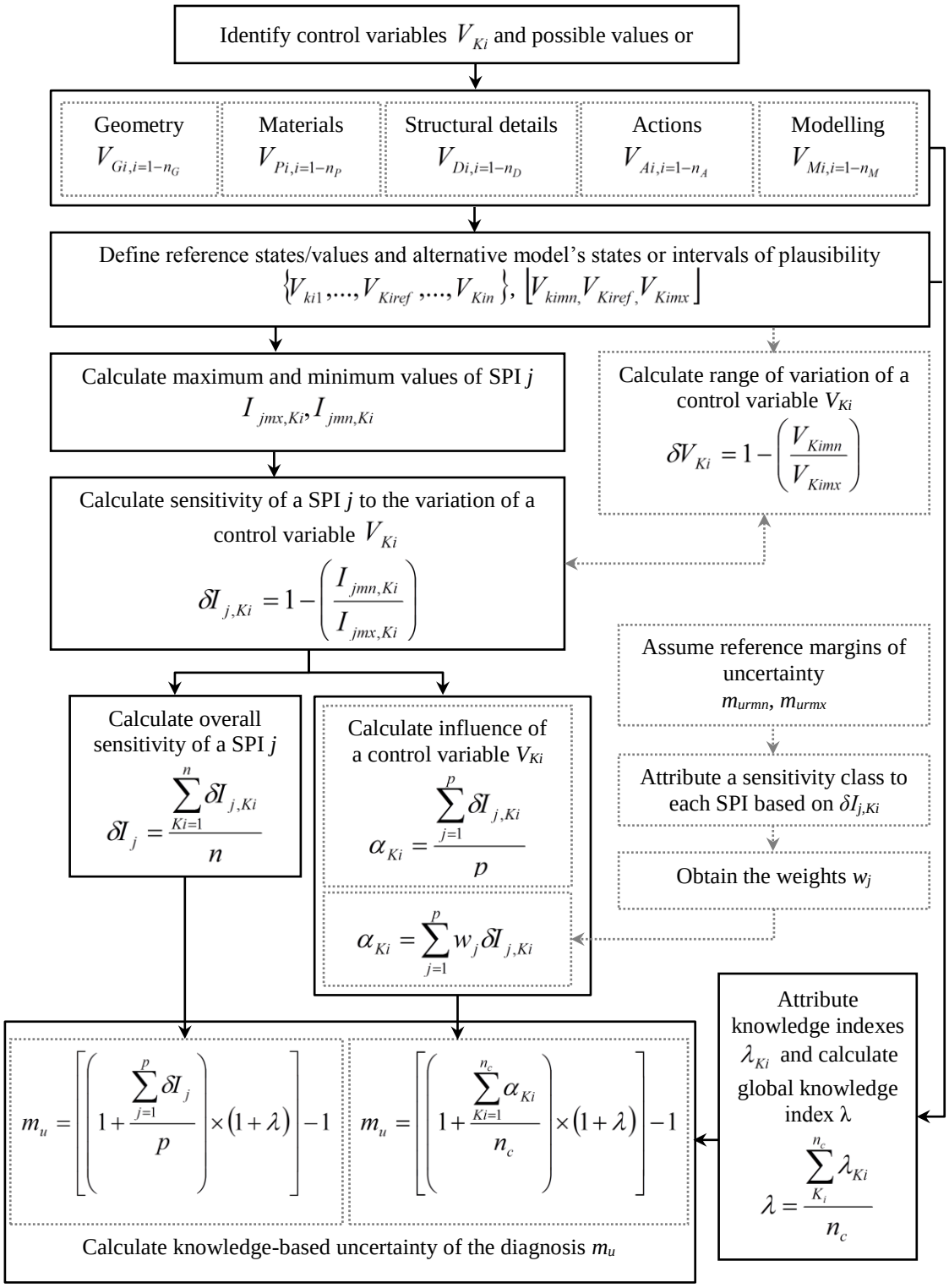

Figure 3.4 Procedure for evaluation of the uncertainty of the input

A convenient advantage of the OAT method in a deterministic model is that whatsoever effect is observed in the output, it is solely due to the variable that has been changed, and all OAT sensitivities are referred to the same reference model (Saltelli and Annoni, 2010).

The choice of the outputs of the model representing the performance of the structure is as important as the choice of control variables. Structural systems can be characterised by several types of SPIs. Since the sensitivity of different SPIs might vary for the same control variable, the SPIs should be carefully selected so that they are meaningful with respect to the question asked of the model (Saltelli and Tarantola, 2002).

In the present approach, the sensitivity of the outputs to variations of the inputs is evaluated on a case by case basis by selecting SPIs judged by the analyst as representative of the target performance considered.

The values of the SPIs computed under the reference analysis conditions, which are part of the reference results, are the reference structural performance indicators (RSPIs).

There are two relevant aspects for evaluation of uncertainty:

(i) the sensitivity of each SPI to the variation of the control variables; and

(ii) the relative influence of each control variable to the variation of the SPIs.

The first aspect is essential to define the error or uncertainty of the structural analysis solution, whereas the second aspect allows identifying the critical variables and optimizing the plan for data collection.

The range of variation of a control variable V_{Ki}, δV_{Ki}, with an interval of plausibility [V_{kimn}, V_{Kiref}, V_{Kimx}] can be given by equation 3.4.

$$\delta V_{Ki} = 1 - \left(\frac{V_{kimn}}{V_{Kimx}} \right) \qquad [3.4]$$

This range of variation, δV_{Ki}, is illustrated in Figure 3.3. Sensitivity indexes are usually used to represent the percentage of difference between maximum and minimum output values when varying one input parameter from the minimum to the maximum value (Hoffman and Gardner, 1983; Hamby, 1995), or by the percentage of change compared to the RSPI (Frey *et al.*, 2003).

Following the formulation of Hoffman and Gardner (1983), the sensitivity of a SPI *j* to the variation of a control variable *Ki*, $\delta I_{j,Ki}$, can be obtained by means of equation 3.5.

$$\delta I_{j,Ki} = 1 - \left(\frac{I_{jmn,Ki}}{I_{jmx,Ki}} \right) \quad [3.5]$$

, where $I_{jmx,Ki}$ is the maximum and $I_{jmn,Ki}$ is the minimum value of the SPI after analyses are performed under the assumption of minimum and maximum plausible values or alternative states of the control variable V_{Ki}. As illustrated in Figure 3.3, the initial sensitivity of the SPI includes all possible values of the SPI given all possible values of V_{Ki}. An interval of plausibility is identified for the SPI through sensitivity analysis depending on the interval of plausibility or alternative states defined for V_{Ki}.

In the case of control variables characterised by an interval of plausibility, the following conclusions in terms of propagation of uncertainties can be made when comparing the variation of a control variable V_{Ki}, δV_{Ki}, with the corresponding sensitivity of a SPI, $\delta I_{j,Ki}$:

- If $\frac{\delta I_{j,Ki}}{\delta V_{ki}} > 1$, the output varies more than the input – uncertainty is amplified;
- If $\frac{\delta I_{j,Ki}}{\delta V_{ki}} = 1$, the output varies the same as the input – uncertainty is constant;
- If $\frac{\delta I_{j,Ki}}{\delta V_{ki}} < 1$, the output varies less than the input – uncertainty is diminished.

The way in which the uncertainties propagate provides an initial indication of the relevance of the control variable or SPI. For instance, the reduction of uncertainty can indicate that:

(i) a control variable is irrelevant;
(ii) a SPI is irrelevant; or
(iii) both are irrelevant.

However, the actual variation of the output must be analysed in order to reach final conclusions, for independently of the way how the uncertainty propagates large values of $\delta I_{j,Ki}$ indicate that either/both the control variable or/and SPI are relevant.

The overall sensitivity of a SPI *j* can be obtained by means of equation 3.6.

$$\delta I_j = \frac{\sum_{Ki=1}^{n} \delta I_{j,Ki}}{n} \quad [3.6]$$

, where *n* is the total number of control variables. This index provides an overall measure of the relevance of the SPI to the assessment. In this context, δI_j also provides a measure of the uncertainty of the diagnosis regarding this specific SPI *j*.

Following this rationale, the influence of a control variable V_{Ki} on the output (i.e. on the variation of the SPIs) is described in terms of an overall influence index α_{ki} that can be obtained by means of equation 3.7.

$$\alpha_{Ki} = \frac{\sum_{j=1}^{p} \delta I_{j,Ki}}{p} \quad [3.7]$$

, where *p* denotes the total number of SPIs.

In this case it is assumed that all SPIs are equally important to evaluate the relevance of the control variable. An alternative formulation to obtain α_{ki} can be however applied, considering the index as a weighted sum of the sensitivity indexes of the SPIs, as shown in equation 3.8.

$$\alpha_{Ki} = \sum_{j=1}^{p} w_j \delta I_{j,Ki} \quad [3.8]$$

The weight, w_j, is a measure of the relative importance of the SPIs for the objective of the structural assessment. They can be defined according to the case study in hands and their sum should be equal to unity. These weights should reflect the relative importance of the SPI to evaluate a specific performance level. For instance, if the objective is to evaluate whether a structure exceeds or not the limit state of near collapse, the drift might have a greater weight than the total base shear. The opposite can be assumed if the aim is to evaluate the

limit state of damage limitation. Procedures to combine the sensitivity of all SPIs can also be based on the attribution of a sensitivity class to each SPI, as explained in the following.

A knowledge-based uncertainty m_{uj} can be seen as a percentage of variation of the results of structural analyses, such that the 'real' value of the SPI, denoted as I_j, is within the range of equation 3.9.

$$\frac{I_j}{1 + m_{uj}} \leq I_j \leq I_j \times (1 + m_{uj}) \qquad [3.9]$$

Following this rationale, a reference range $\{m_{urmn}, m_{urmx}\}$ of existence can be established *a priori* for m_u based on confidence factors proposed in current codes (e.g. CEN, 2005b) and guidelines (e.g. CIB 335, 2010). These reference thresholds can be used to attribute a sensitivity class that qualifies the sensitivity of a given SPI, according to the criterion proposed in Table 3.6.

Table 3.6 Criteria for attribution of a sensitivity class to a SPI *j* for a given control variable V_{Ki}

		Sensitivity classes		
		Low	Medium	High
Sensitivity indexes	$\delta I_{j,Ki}$	$\delta I_{j,Ki} < m_{urmn}$	$m_{urmn} \leq \delta I_{j,Ki} < m_{urmx}$	$\delta I_{j,Ki} \geq m_{urmx}$

The criterion is based on the premise that if the sensitivity of a SPI *j* to the variation of a control variable V_{Ki}, expressed by means of the sensitivity factor $\delta I_{j,Ki}$, is equal or greater than the level of uncertainty usually assumed as the minimum required to assure reliability by current codes and guidelines, the SPI *j* belongs to a 'Medium' or 'High' sensitivity class as far as control variable V_{Ki} is concerned. The SPI *j* belongs to a 'High' class if its sensitivity is higher than the maximum reference uncertainty.

Taking into account the sensitivity classes, the following procedures to obtain the weights, w_j, of equation 3.8 are proposed:

(Proc. I) attribution of a w_j to a SPI *j* that corresponds to the percentage of control variables with the highest sensitivity associated to the particular SPI *j* under consideration;

(Proc. II) attribution of a w_j to a SPI j that corresponds to the percentage of control variables with 'Medium' and 'High' sensitivity classes associated to the particular SPI j under consideration; and

(Proc. III) attribution of a w_j to a SPI j that corresponds to the percentage of control variables with 'High' sensitivity classes associated to the particular SPI j under consideration.

The first procedure can underestimate the importance of SPIs that, even though not being the most sensitive to the variation of any control variable, are still being substantially influenced by the variability of the input. The second and third procedures require the attribution of a sensitivity class to each SPI regarding all control variables on the basis of the criterion indicated in Table 3.6.

A critical variable of the assessment is a control variable that has a significant influence on the detailed diagnosis of the heritage construction. If the diagnosis is based on the results of structural analysis, it is logical to assume that a control variable with an influence factor α_{Ki} above m_{urmn} is a critical variable. A high level of knowledge should therefore be pursued for the critical variables in order to reduce the overall uncertainty of the diagnosis.

3.5.2.2 LEVEL OF KNOWLEDGE ASSOCIATED TO THE CRITICAL VARIABLES

Existing standards and guidelines provide general criteria for identification of the level of knowledge associated to 'geometry', 'materials' and 'structural details' classes (e.g. Ordinance 3274, 2003; CEN, 2005b). The level of knowledge is linked to the quality and detail of the information available about the heritage construction. Procedures for deepening this knowledge through interpretation of existing information, inspection and experimental work are well documented in literature (see for example NIKER, 2012; CIB 335, 2010; ICOMOS-ISCARSAH, 2003; Tolles *et al.*, 2002).

The sources of information can be categorised as:

(i) preliminary data collection;
(ii) detailed inspection;
(iii) monitoring; and
(iv) analyst judgment and experience.

Three levels of knowledge can be defined, as in Eurocode 8 (CEN, 2005b):

(i) L (Low Knowledge);
(ii) M (Medium Knowledge); and
(iii) H (High Knowledge).

Table 3.7 shows how the various categories can be related to the levels of knowledge.

Table 3.7 Knowledge level of the critical variables depending on the source of information

		CLASSES OF CRITICAL VARIABLES				
		Geometry	Materials	Structural details	Actions	Modelling
PRELIMINARY DATA COLLECTION	Historical documentation and oral testimonies	L	L/M	L/M	L/M/H	L/M/H
	Construction and specialised documentation	L	L/M/H	L/M	L/M/H	L/M/H
	Visual condition assessment	L/M	L/M	L	L/M/H	L/M
	On-site measurements	L/M/H	L/M	L/M	L/M/H	L/M
DETAILED INSPECTION	Opening-up and recording	M/H	M/H	M/H	L/M/H	L/M/H
	Experimental work (NDT, SDT and DT)	L/M/H	M/H	M/H	M/H	L/M/H
MONITORING		M/H	M/H	M/H	M/H	M/H
ANALYST JUDGEMENT AND EXPERIENCE		L/M/H	L/M/H	L/M/H	L/M/H	L/M/H

On-site measurements is assumed here as part of a preliminary data collection procedure, since they normally entail non-intrusive activities in which the analysts simply record geometric aspects of the constructions. On the other hand, ‘opening-up’ such as removal of plasters and valuable finishes is considered a typical activity of a detailed inspection, since it entails a modification of the current state of the construction with some degree of loss.

Non-destructive (NDT) and semi-destructive testing (SDT) are assumed as part of a detailed inspection due to the substantial cost and/or timeframe that can be devoted to the

assessment, even though the aim is to keep the level of intrusiveness of the procedure as moderate (SDT) or negligible (NDT) as possible.

Monitoring could be either performed independently or within a preliminary or detailed survey as a means to measure the performance of the structure over time and/or interpret the causes of visible damage.

Finally, the analyst's judgement and experience is a valuable resource throughout the process of assessing a heritage structure, especially in the presence of incomplete or low quality information. Nevertheless, the value of heuristic knowledge is closely dependent on the level of qualification and specific experience of the analyst and thus it is difficult to properly evaluate its overall contribution. Though the analyst's judgement and experience is relevant for the quantification of all classes of variables, it is particularly important for the 'modelling' class, since the variables are chosen by the analyst as a means to improve the quality of the model and the results of the simulation, often after analysis and interpretation of initial results.

The rationale behind the attribution of a given knowledge level to a variable of the 'geometry' class is based on the premise that no complete knowledge can be achieved from historical documentation, oral testimonies and/or construction documentation without on-site checking of the overall geometry and member sizes, since heritage structures can undergo several interventions during their lifetime which are often not reported. Furthermore, although a preliminary data collection might provide a thorough geometrical description of the overground structure when in good condition, a detailed inspection is often required to record in detail the geometry of the foundations and the change in geometry due to deterioration of elements with time.

As far as the 'materials' class is concerned, an high knowledge is only achievable by means of detailed inspection, sample extraction and testing, even if a large amount of material data from similar constructions is available. It is assumed that the current material behaviour is a result of a convergence of causes which are usually inherent to a given site, and thus best acquired by means of experimental work on material samples from the site. Furthermore, materials of hidden parts of the construction, such as the foundations, are often only identified by means of a detailed survey involving opening-up. Nonetheless, a higher level could be assumed by the analyst if, for instance, the purpose of the structural analysis is to assess the response of the original state of the construction which is satisfactorily characterised by means of available documentation, and the current condition of the

materials is to an extent irrelevant. In addition, in particular cases, specialized literature might provide the properties of the materials with a high level of confidence.

The attribution of a knowledge level to the critical variables of 'structural details' class is governed by the assumption that a preliminary assessment is unable to provide a complete overview and characterisation of the major structural details, since usually some opening-up or NDT is required.

Uncertainties on dead loads can be associated with control variables of the 'geometry' and 'materials' classes and therefore they can be taken into account by the corresponding knowledge levels. As far as live and dynamic loads are concerned, they would normally be best characterised by on-site experimental tests, such as live load tests, dynamic identification and micro-zonation studies; even though historical information and a thorough condition assessment could be sufficient for a good estimation of the current or past actions. For this reason, the four levels of knowledge are considered feasible for all types of sources except when related to 'experimental work' and 'monitoring', since these would normally result in a more detailed characterisation of the actions.

Finally, the knowledge level associated to the critical variables of the 'modelling' class is related to the knowledge acquired in other classes, and to the way in which the analyst interprets this information and uses it to improve the model. Hence, the knowledge level associated to these variables is dependent on the analyst's field of expertise and experience, which influences his/her abilities to foresee and interpret results, to detect misleading outputs and to seek best strategies for the simulation.

A knowledge index, λ_{ki}, is assigned to each critical variable taking into account the criteria set forth in Table 3.8. This index is an indicator of the uncertainty with which the analyst defines the control variables. The index is within the reference interval of uncertainty $\{m_{urmn},m_{urmx}\}$ assumed at priori by the analyst for the calculation of the influence index, α_{Ki}. The criterion is based on the premise that a low level of knowledge yields a level of uncertainty that can be assumed similar to reference maximum uncertainty margins suggested in literature. Conversely, it is considered that some level of uncertainty, even if negligible, can be present if the characterisation of a given critical variable is based on a high level of knowledge. Hence, the knowledge index associated to this knowledge level is equal to the minimum reference value assumed by the analyst. In alternative, if the analyst is confident with the level of knowledge achieved, m_{urmn} can be considered null. The index of a medium level is assumed as the average of the range characterised by the m_{umn} and m_{umx} thresholds.

Table 3.8 Knowledge indexes

Level of knowledge	Knowledge index λ_{ki}
LK – Low Knowledge	m_{urmx}
MK – Medium Knowledge	$\frac{m_{urmx} + m_{urmn}}{2}$
HK – High Knowledge	m_{urmn} or null

A global knowledge index, λ, can be set by means of equation 3.10, where n_c denotes the total number of critical variables.

$$\lambda = \frac{\sum_{Ki=1}^{n_c} \lambda_{ki}}{n_c} \qquad [3.10]$$

3.5.2.3 UNCERTAINTY OF THE INPUTS

The uncertainty of the detailed diagnosis is governed by the sensitivity of the SPIs used in the diagnosis and the corresponding level of knowledge present when measuring this sensitivity. Since at this stage of the assessment process the critical variables are known, this uncertainty can take into account the sensitivity of the SPIs to the variation of the critical variables only.

This knowledge-based uncertainty of the diagnosis, m_{uj}, is such that equation 3.9 applies. The 'real' value of the SPI used in the diagnosis, I_j, is therefore within an interval defined by m_{uj}.

The uncertainty m_{uj} can be obtained by means of equation 3.11.

$$m_{uj} = \left[\left(1 + \delta I_j\right) \times \left(1 + \lambda\right)\right] - 1 \qquad [3.11]$$

Taking into account that only the critical variables are analysed at this point of the assessment, equation 3.11 has the format of equation 3.12 or equation 3.13.

$$m_{uj} = \left[\left(1 + \frac{\sum_{ki=1}^{n_c} \delta I_{j,ki}}{n_c}\right) \times \left(1 + \frac{\sum_{ki=1}^{n_c} \lambda_{ki}}{n_c}\right)\right] - 1 \quad [3.12]$$

$$1 + m_{uj} = \left[\left(1 + \frac{\sum_{ki=1}^{n_c} \delta I_{j,ki}}{n_c}\right) \times \left(1 + \frac{\sum_{ki=1}^{n_c} \lambda_{ki}}{n_c}\right)\right] \quad [3.13]$$

In the case of a diagnosis based on results of multiple SPIs, an overall uncertainty measure, m_u, can be calculated using equations 3.14 or 3.15 in case of all SPIs being equally relevant, or equation 3.16 in case of SPIs with different weights.

$$m_u = \left[\left(1 + \frac{\sum_{j=1}^{p} \delta I_j}{p}\right) \times (1 + \lambda)\right] - 1 \quad [3.14]$$

$$m_u = \left[\left(1 + \frac{\sum_{ki=1}^{n_c} \alpha_{ki}}{n_c}\right) \times (1 + \lambda)\right] - 1 \quad [3.15]$$

$$m_u = \left[\left(1 + \sum_{j=1}^{p} w_j \delta I_j\right) \times (1 + \lambda)\right] - 1 \quad [3.16]$$

It is assumed that the exact value of the SPIs lay within an interval defined by equation 3.9 taking into account this uncertainty m_u. Thus, at the end of this uncertainty analysis, the analyst can calculate a factor equal to '$1+m_u$' that is comparable to the confidence factors available in literature. It has however the advantage of being tailored to the heritage construction in hand and the purpose of the diagnosis.

3.5.3 Uncertainty of the output

The third phase of uncertainty analysis, as indicated in Figure 3.1 and Table 3.5, evaluates whether the values of the SPIs, which are outputs of structural analysis carried out with global models under the reference analysis conditions, contradict evidences of field work, experimental and/or monitoring data. This checking is conducted during the detailed diagnosis. Intervals of plausibility are defined for the outputs by means of equation 3.9 taking into account the uncertainty calculated in the previous phase, m_u. By comparing the reference results and upper and lower bounds of the SPIs with existing information, it is possible to evaluate whether the model presents a behaviour that is 'worse' or 'better' than the real structure. If the intervals of plausibility of the SPIs show a response that contradicts existing data, the reference values and intervals of plausibility or alternative states of the critical variables must be adjusted in order to match to the better possible extent the outputs with existing data.

3.6 Detailed diagnosis

The detailed diagnosis thoroughly investigates the current state of a heritage construction by evaluating the same five attributes of the preliminary diagnosis (Table 3.1) on the basis of structural analysis and experimental work. In order to render this diagnostic process systematic, robust and repeatable over the diverse case studies and assessment process, a decision-tree approach is introduced, whereby the judgement arrived at in the process of the detailed diagnosis could be thoroughly documented, justified and communicated, providing reliable support for the choices to be made in terms of measures.

The decision tree is shown in Table 3.9 in the format of a matrix, where an influence measure and a vulnerability measure are associated to each decision point. Each tier of the matrix is one of the five attributes of Table 3.1.

The attributes are ranked according to the sequence of the diagnosis. While it might appear from the structure of the matrix in Table 3.1 that there is a hierarchy in influence going from the robustness to condition, indeed this only reflects a focus from the global structural form to the local quality of the materials and the workmanship, rather than their subordinate relevance to the seismic behaviour. This notwithstanding, the sequence of the diagnosis may vary from case to case depending on the relative relevance of the attributes to a specific diagnosis. In addition, although the final outcome at each extreme (left and right)

end of the matrix represents the best and worst possible cases, the other possible outcomes are not ranked since there is no hierarchy. Therefore, it cannot be assumed that the outcomes furthest to the left of the matrix represent the best behaviour, as this obviously depends on the relative relevance of the five attributes in each judgment.

The diagnosis of the whole structure or macroelements regarding each attribute requires the evaluation of the respective vulnerability in terms of positive or low vulnerability (marked as '+' and following a green path) or negative or high vulnerability (marked as '–' and following a red path). Sixteen different diagnoses are possible for five SPIs.

In the matrix of Table 3.9, condition is considered as an attribute similar to the other four attributes. However, the condition of the construction is distinct since it can change over time and influence the state of the other attributes.

A consequence of the use of the matrix in its present state is that the same building could have vastly different results if the diagnosis is done at a different time, unless only the original state of the structure is analysed, in which case the condition is considered positive. These five attributes are judged on the basis of local and global criteria which include the evaluation of one or several SPIs (e.g. drift and base shear). Local criteria consider the existence of concentration of stresses and local fragilities, whereas global criteria evaluate the global response of the structure or macroelements in terms, for example, of drift and capacity. The 'Robustness' attribute is evaluated by means of global criteria, whereas attributes such as 'Interaction' and 'Connections' can be evaluated by means of local criteria. Different criteria may need to be formulated for different case studies.

Table 3.9 Matrix for the detailed diagnosis of heritage constructions

1.ROBUSTNESS	2.INTERACTION	3.CONNECTIONS	4.MATERIALS	5.CONDITION
-	-	-	-	-
				+
			+	-
				+
		+	-	-
				+
			+	-
				+
	+	-	-	-
				+
			+	-
				+
		+	-	-
				+
			+	-
				+
+	-	-	-	-
				+
			+	-
				+
		+	-	-
				+
			+	-
				+
	+	-	-	-
				+
			+	-
				+
		+	-	-
				+
			+	-
				+

3.7 Conclusions

This chapter proposes a new methodology for the systematic structural assessment of heritage constructions that evaluates the uncertainty of the analysis at various phases of the assessment. The main characteristics of this methodology are:

(i) It is tailored to heritage constructions, taking into account all important sources of knowledge and uncertainty;

(ii) It is applicable to different form of heritage construction;

(iii) It is applicable to both qualitative and quantitative methods;

(iv) It is a logic sequence of phases with increasing level of complexity, so that results of previous phases inform in a consistent way the planning of the next activities;

(v) It measures the uncertainty of the analysis' results by directly evaluating the sensitivity of the results to variations in inputs and the analysts' level of knowledge while conducting such analysis; and

(vi) It allows determining the impact of uncertainty on the evaluation of multiple structural performance indicators, which inform the diagnosis.

A major element of novelty is the ability of the proposed methodology to identify whether the level of uncertainty can or cannot ultimately lead to alternative diagnoses and whether this is acceptable or not. Moreover, while identifying a 'best' and 'worst' performance of the structure and evaluating whether the 'worst' leads to an acceptable structural performance, this methodology helps the analyst to avoid the planning of remedial measures that can compromise the cultural significance of the constructions.

This assessment methodology can be used both in a pre and post-earthquake scenarios. In a post-earthquake scenario, the preliminary diagnosis can be used as a rapid damage assessment to evaluate whether the building can be reoccupied or not. The following quantitative analyses and the final diagnosis should explain the cause of the damage and the interventions (repair, reconstruction, retrofitting) needed to rehabilitate and improve the performance of the structure. Since there is evidence of the damage caused by a specific event and, in some cases, many structural details are visible due to the collapse of portions of the structure, in principle there is more information available to verify whether the results of

quantitative analyses are realistic or not and to calibrate the models. The existence of this evidence will normally reduce the uncertainties of the assessment. Moreover, if some structural elements have partially collapsed during the earthquake, it is often feasible to take samples from these collapsed portions that can be tested in a laboratory. This allows a more detailed mechanical characterisation of the structure, therefore decreasing the uncertainty associated to the properties of the materials.

In pre-earthquake scenarios, since the level of knowledge is expected to be lower than in a post-earthquake scenario, historical data and the experience of the analyst are key aspects to evaluate whether the final diagnosis is realistic or not.

Although all steps of the methodology can be conducted by a single analyst, it is recommended that multiple analysts carry out the activities, especially if the principal analyst does not have significant experience on the specific structure or analysis method in hand. The synergy produced by experiences from multiple analysts will in principle reduce the uncertainties, since this assessment methodology depends mainly on the analysts' judgment. Moreover, the initial steps, namely the 1st data collection and the preliminary diagnosis, normally require the participation of analysts with different expertise (e.g. historians, engineers, architects, etc.), such that different sources of information can be considered and structural issues that require further investigation can be identified.

In practice, the composition of the teams and the amount of time dedicated to each step of the methodology should be optimized, such that a reasonable balance between the uncertainties present in the assessment and the cost and time needed to conduct the activities is reached.

Me propongo – los ojos azules del Obispo, enfocados en la nada, habían adquirido un inspirado brillo – levantar hermosas iglesias en cada uno de los pueblos y reducciones de indios, por humildes que estos sean, para que vean ellos que tienen abiertas las puertas de la casa de Dios. [...] Vigilaré con obstinación que se destruyan sus huacas y adoratorios, que se quemen sus ídolos, que sus templos sean abolidos y, en su lugar, se levanten iglesias de altos campanarios, para hacerlos así merecedores de gozar de la bienaventuranza que, como hijos de Dios, les corresponde también a ellos. Veré…

Alberto E. Massa, in 'El último día de Francisco Pizarro'[2]

[2] Massa A.E. (2003). *El último día de Francisco Pizarro*. Alfaguara

CHAPTER 4

Historic earthen and timber ecclesiastical buildings in Peru: a structural understanding

4.1 Introduction

In order to validate the framework for structural assessment of heritage constructions proposed in Chapter 3 (Figure 3.1), two structurally distinct earthen and timber Peruvian churches are assessed following each and all steps of this framework. The first step regards the 1st data collection where information about the historic structure is collected and interpreted. As discussed in Chapter 1, interpretation of original and historical data, current structural layout, construction and condition of a historic building is an initial and essential phase of the assessment, which determines the level of uncertainty of the diagnosis. In the present case, the principal sources of information are historical data and oral testimonies of Peruvian engineers and architects, and surveying and field research conducted within the framework of the EAI-SRP. The EAI-SRP project team performed extensive campaigns of condition survey, opening up and recording of essential construction components and connections of the case studies (Cancino *et al.*, 2012). The author has participated in these campaigns in Peru, visiting not only the case studies but also other similar historic churches. In particular, the author has observed and recorded the geometry of the most relevant structural elements and their overall damage state and condition. The author has also made an inventory of all timber connections of the Cathedral of Ica, measuring the structural elements and recording their condition, which was essential data to develop a detailed model of the timber structure.

This chapter explains the rationale of the selection of the Church of Kuño Tambo and timber structure of the Cathedral of Ica to test and validate the framework for assessment of historic constructions proposed in this thesis. This explanation is based on the cultural significance of the churches, the characteristics and vulnerability of the structure and the location in seismic prone areas. A detailed description and interpretation of the structure of the two selected churches is presented in the rest of the chapter.

4.2 Selection of case studies

Historic earthen and timber churches were built during the Hispanic Viceroyalty of Peru, which spanned a period in history from the first half of the 16th century until the first half of the 19th century. The viceroyalty was composed of several current South and Central America countries which were under Spanish rule, such as Argentina, Bolivia, Chile, Colombia, Ecuador, Guyana, Panama, Paraguay, Peru, and Uruguay. During this period, many ecclesiastical buildings were built for the purpose of Christianisation of the native people or as part of settlements built for the Catholic settlers. The *reducciones indígenas* (indigenous settlements) were large villages established by Spaniards in order to relocate a native population which was formerly living in small and dispersed settlements. More detailed information about these indigenous villages can be found in work by Málaga (1974) and Villacorta (2005) for example. An example of a remote village in the Andean Cordillera is shown in Figure 4.1.

The settlements were planned in a way that the streets would go towards the *plaza principal* (main square) where the church was located (Málaga, 1974). However, in some cases, the church was built in areas previously occupied by pre-colonial temples, which may not have had any relationship to the new square (Cancino *et al.*, 2012). Thus, the front façade of the church does not always face the main square.

Most of these churches have been constantly occupied since their construction four or five centuries ago. The churches were normally built with local materials, being adobe, stone masonry, timber, canes and mud or lime plasters the most common building materials.

The use of these materials in Peru can be traced back to four thousand years ago (see for instance Shimada and Cavallaro, 1985). The use of wood, canes and mud mortar in walls can be traced back to even earlier periods, as the work in the archaeological site of Caral by Solis *et al.* (2001) shows. However, past earthquakes, creep and weather demands have jeopardised the structural performance of those churches over the years. Past earthquakes,

such as the recent 2007 Pisco earthquake, have shown that those structures are vulnerable, especially if their condition is poor due to lack of maintenance and repair.

Figure 4.1 Typical village in high lands

The following earthen and timber historic building types of ecclesiastical constructions built during the Viceroyalty of Peru have a very high cultural significance at present:

(i) Churches composed of adobe walls and timber trussed roofs that were built on the Andean Cordillera (high lands); and
(ii) Churches composed of adobe walls and timber vaults and framings that were built on coastal cities (low lands).

Diverse structural typologies can be identified within these building types as summarized in Figure 4.2. In high lands, the churches normally have adobe walls and buttresses with a single nave covered by a traditional *par y nudillo* (rafter and collar-tie) roof. A bell tower is either attached or built near and physically separated from the church. In low lands, single nave churches have timber vaults sitting on adobe walls. In the case of churches with lateral aisles, the timber vaults are normally supported by timber pillars. These churches normally have towers attached to the main façade made of timber on the top of a masonry base. Examples of these typologies are shown in Figure 4.3 and Figure 4.4, respectively.

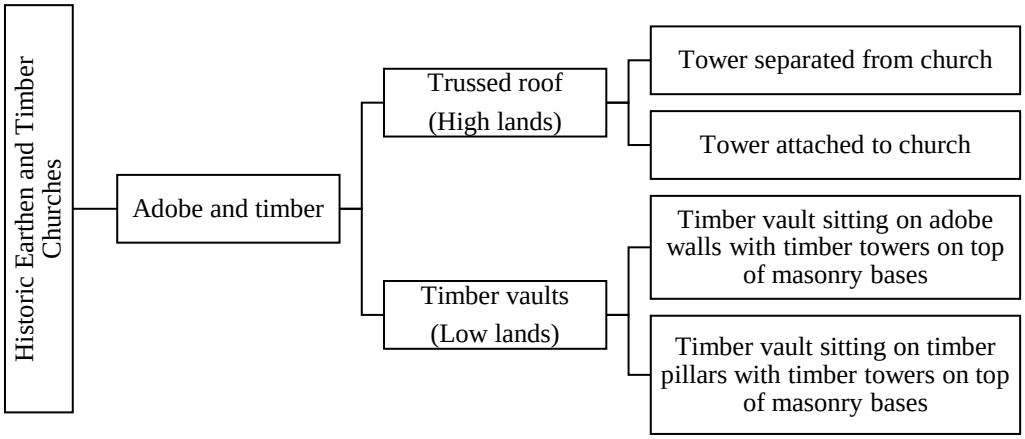

Figure 4.2 Typologies of historic earthen and timber churches

a) Church of San Jeronimo de Acopia, Cusco (courtesy of Juan Carlos Miranda)

b) Church of Virgen Asunción de Choquekancha, Cusco (courtesy of Juan Carlos Miranda)

c) Church of San Miguel de Pitumarca, Cusco (courtesy of Juan Carlos Miranda)

d) Church of Rondocan (Cusco)

Figure 4.3 Examples of historic earthen and timber churches in high lands

a) Church of El Carmen Santuario de Yauca (Ica)

b) Church of San Antonio (Cañete)

c) Cathedral of Ica (courtesy of Claudia Cancino)

d) Church of San Luis (Cañete)

Figure 4.4 Examples of historic earthen and timber churches in low lands

As discussed in Chapter 1, the structural performance of these earthen and timber churches are to a great extent unknown, especially due to lack of knowledge on typical structural systems. To the author's knowledge, this research conducted within the framework of the EAI-SRP in the aftermath of the 2007 Pisco earthquake constitutes a first significant attempt to investigate the structural systems and seismic performance of these historic churches.

Churches in high lands and churches in low lands have different levels of structural complexity and distinct structural behaviour. In the case of churches in high lands, the main challenge of the assessment is to evaluate the performance of thick adobe walls restrained by buttresses and tie-beams. On the other hand, in the case of churches located in low lands, the timber structure has a key structural role; either the vaults are supported by the walls or by a timber frame.

The most complex case of timber structures is present in churches with lateral aisles, where the vault is supported by a timber frame; and hence this typology is preferred for analysis in this research.

Taking into account these considerations, the following case studies were selected:

(i) The Church of Kuño Tambo located in Acomayo (Cusco), which is representative of churches built in high lands with separated towers; and

(ii) The Cathedral of Ica located in Ica, which is representative of churches built in low lands with timber vaults supported by timber pillars.

4.3 Historic adobe churches in high lands: the Church of Kuño Tambo

In the village of Kuño Tambo, a church dating from 1681 and located near but not directly facing the main square stands out of the landscape (Figure 4.5 and Figure 4.6). This church has a significant religious and social role in the local village, being a centre of interaction of the village's community.

4.3.1 Plan and elevations

The church of Kuño Tambo is composed of nave, chancel, baptistery and sacristy, as shown in Figure 4.7. The main body of the nave and chancel are composed of four walls, the South elevation with the main entrance (Figure 4.7a), the North elevation (Figure 4.7c) and the longitudinal East and West walls (Figure 4.7b and Figure 4.7d). The sacristy and the baptistery are adjacent to the East elevation.

Figure 4.8 shows the plan of the church. The walls are identified by the symbol $W_{i,j}$, where i regards the body (nave, baptistery or sacristy) to which a wall belongs and j regards the number of the wall within the corresponding body.

The buttresses are identified by the symbol B_k, where k is the number of the buttress. The adobe blocks of WII.1 and WII.2 of the sacristy are interlocked with the adobe blocks of wall WI.4 of the main nave, which might indicate that the sacristy was built at the same time of the nave and chancel. In contrast, no interlocking between the walls of the baptistery and WI.4 might indicate that the baptistery was added to the original church at a later stage.

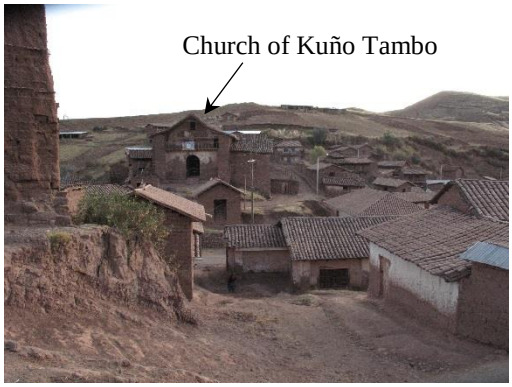

a) View of the front façade of the church

b) View of the village from the church's balcony

Figure 4.5 The village of Kuño Tambo

Figure 4.6 The Church of Kuño Tambo (courtesy of GCI)

a) Frontal façade, WI.1 (facing South)

b) Longitudinal wall, WI.2 (facing West)

c) Back façade, WI.3 (facing North)

d) Longitudinal wall, WI.4 (facing East)

e) Baptistery

f) Sacristy

Figure 4.7 External views of the Church of Kuño Tambo

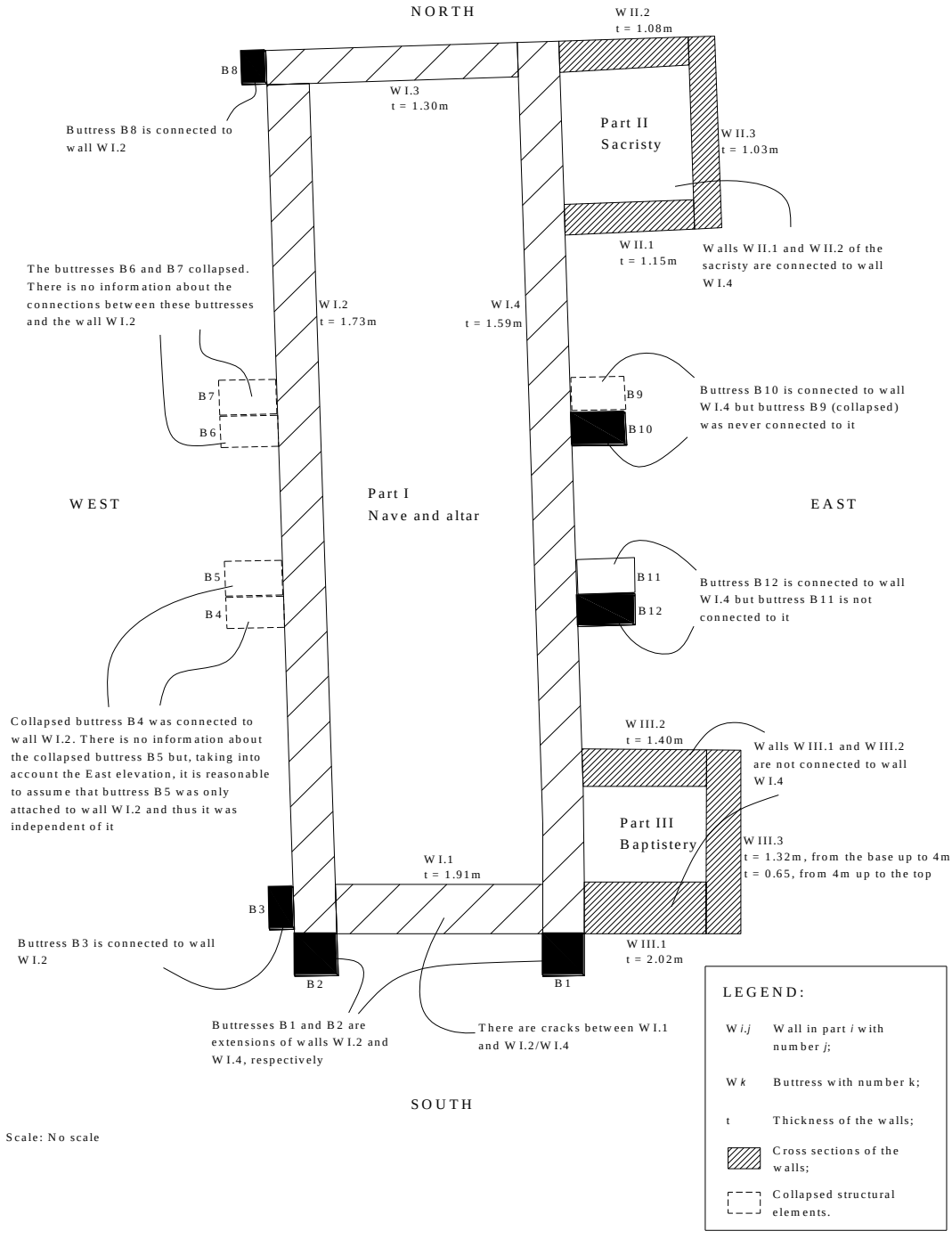

Figure 4.8 Floor plan and structural details of the Church of Kuño Tambo

4.3.2 Adobe walls with rubble stone base courses

Typically in this type of church, the adobe walls have high base courses, continuous along the walls, of thickness similar to the thickness of the walls (Figure 4.9). The base course is normally made of rubble stone masonry laid in mud mortar. It protects the adobe wall from rising damp and superficial water erosion.

In the case of the Church of Kuño Tambo, the base course is bearing directly on the rocky soil or compacted clay fill following the natural slope of the site (Figure 4.10). The bottom of the base course and its relationship with the interior floor level and the exterior grade level is variable. In some locations, the bottom of the base course extends below both the interior floor level and the exterior grade. At other locations, primarily at the East wall, the bottom of the base course is higher than both the interior floor level and the exterior grade, and the rocky soil or compacted clay fill on which it bears is exposed.

The base course is made of rubble stone, with some stones exceeding 0.64m in width, laid in mud mortar with head and bed joints varying in thickness from 20 to 60mm (Figure 4.9b). The base course typically varies in height from 1.20m to 1.50m.

The walls of the Church of Kuño Tambo are made of adobe with units of 0.70x0.35x0.20m laid in mud mortar joint 15mm thick on average. The adobe units are set in an English bond pattern, with alternating courses of header and stretcher (Figure 4.11). From the layout of the units on the face of the wall, it can be inferred that there are layers of at least two headers alternating with layers of two stretchers + one header or four headers across the thickness of the wall. Such arrangement avoids the continuity of the joints.

The units are made of soil rich in clay with small stones and reinforced with straw. The straw resists tensile forces, improving the cohesion of the components of the units. Crushed bone was also found in the composition, contributing further to the binding of the various components.

The thicknesses of the walls are shown in Figure 4.8. WIII.1 is the thickest wall with 2.02m; since the staircase that provides access from the nave to the mezzanine is embedded in the wall (0.75m is the thickness without staircase). It is followed by WI.1, the South façade of the nave, with 1.91m. The thinnest walls of the church are the gable wall of the sacristy with 1.03m and the upper part of the gable wall of the baptistery with 0.65m.

The height of the walls is variable since the church was built on a hill (Figure 4.10). It varies from 4.0m to 8.5m, as measured from the top of the base course up to the top of the gables.

a) General view b) Ground prospection

Figure 4.9 Rubble stone base course

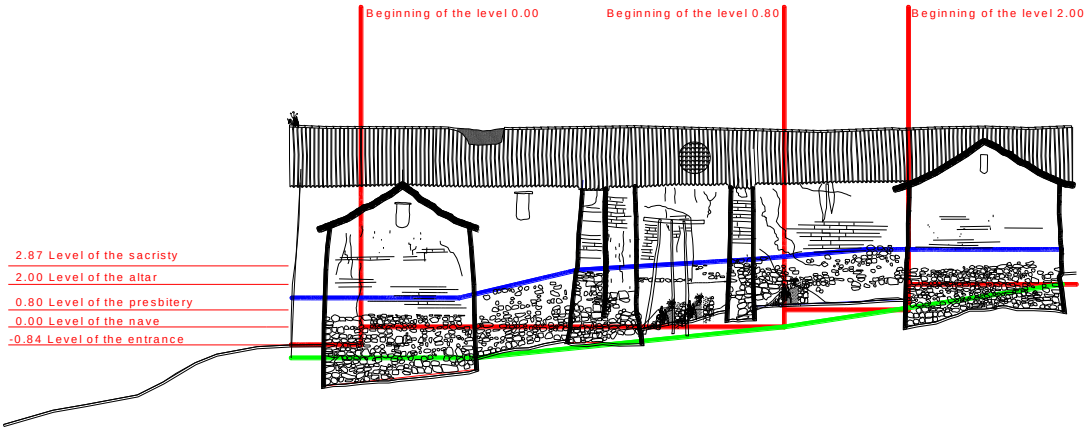

Figure 4.10 Floor levels and limits of the base course of the East façade (grade levels in meters)

a) b)

Figure 4.11 Adobe layout: a) English bond pattern; and b) adobe layout of the Church of Kuño Tambo

Wooden lintels are used to span the openings. A large arched opening was located in the centre of both WI.2 and WI.4; however these openings have been infilled with adobe blocks (see Figure 4.7b and Figure 4.7d).

In their current condition, the exterior faces of the walls are largely unplastered and the adobe units and mortar are exposed; however, some exterior plaster remains in WI.1, which is sheltered by the roof overhang. The interior finish typically consists of one 20-30mm thick layer of mud and straw plaster and one layer of 1-2mm thick painted gypsum; however, where later plaster coats have been applied over the original plaster, the thickness typically reaches 60mm. Much of the interior wall plaster is decoratively painted.

4.3.3 Buttresses with rubble stone base courses

The buttresses of the Church of Kuño Tambo are composed of a rubble stone base course, continuous along the walls and buttresses, and adobe at the upper portion. The materials have similar characteristics to the walls.

B1, B2 and B8 correspond to extensions of the walls WI.4, WI.2 and WI.3, respectively, beyond the intersection of the planes of perpendicular walls. In the other cases, the buttresses are transversely projecting from the walls. On-site observations showed that buttresses B10 and B12 are connected to WI.4 by interlocking of adobe blocks (Figure 4.12a and Figure 4.12c). It is reasonable to assume that collapsed buttresses B4 and B6 were also connected to WI.2 in a similar way (Figure 4.12b). B9 and B11 are only attached to WI.4, being reasonable to assume that collapsed buttresses B5 and B7 were also merely attached to the perpendicular wall WI.2.

Information about the collapsed buttresses on the West side and respective connections to transversal walls could only be collected by observing the present situation of the opposite wall due to the lack of historical documentation clarifying this issue. The lateral forces are therefore not effectively transmitted from the walls to those unconnected buttresses. A pounding effect rather than a counteracting of forces is likely to occur between those components during an earthquake.

a) Buttresses B11 (right) and B12 (Left)

b) Base course of collapsed buttress B4 and B5

c) Interlocking of units between buttress B12 and wall WI.4

Figure 4.12 Details of the buttresses of the Church of Kuño Tambo

4.3.4 Wooden trussed roofs

The most traditional roof's structural system in high lands for both ecclesiastical buildings and houses is the *par y nudillo* system. The system is based on pre-Hispanic building practices, being typically composed of ridge beam, principal rafters, secondary rafters, purlins, collar-ties and tie-beams (Figure 4.13).

The system may also have wall plates, which redistribute vertical loads and prevent concentration of stresses. If the wall plates are continuous along the walls' perimeter and well connected at the corners, they may behave as ring beams. This would help to prevent the out-of-plane overturning of the walls and to minimise in-plane offsets of cracked portions of the walls.

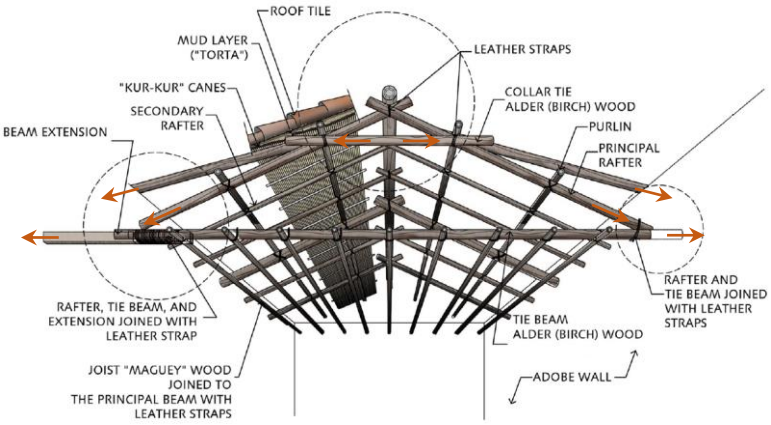

Figure 4.13 Typical *par y nudillo* roof system of historic buildings in Peruvian high lands (adapted from Cancino *et al.*, 2012)

Various types of joints are used to connect the wooden members together, such as nailed joints or vegetal straps. Slender confinement wooden elements, passing all way through the thickness of the walls, are also used to connect the roof's structure to the adobe walls (Figure 4.14a and Figure 4.14b).

According to traditional building practices, these elements are introduced into the structure during the construction of the walls, being connected to the roof's purlins in both sides of the wall by means of straps of vegetal fibres. These connections are therefore working in tension and preventing the uplift of the roof under wind loads for instance. Stone elements were used in Inca's building practices for the same purpose (Figure 4.14c and Figure 4.14d).

In the case of the Church of Kuño Tambo, a traditional *par y nudillo* wooden structure was used to cover the nave and chancel, and the baptistery and sacristy. The nave and chancel have 47 roof-trusses, spaced 0.65m approximately apart, which are composed of two rafters and one collar-tie located at approximately 1/3 of total height from the top of the truss (Figure 4.15 and Figure 4.16a).

a) Wooden confinement elements in the Church of Kuño Tambo

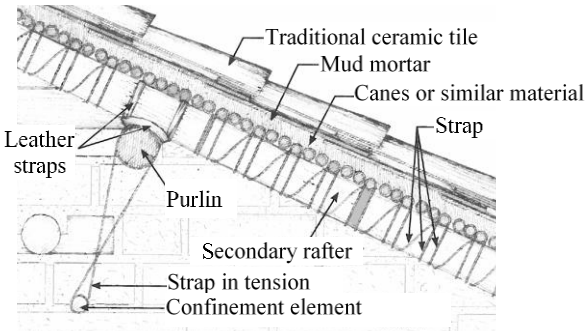

b) Traditional building technique of the historic village of Vilcashuamán (adapted from INC, 2008)

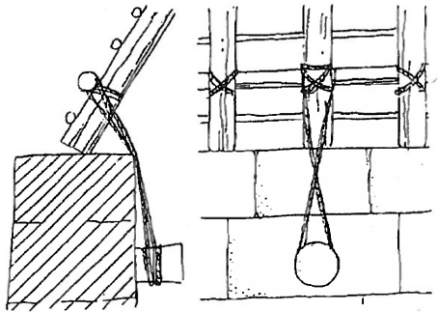

c) Confinement elements made of stone typical of the Inca's building practices (Gasparini and Margolies, 1977)

d) Confinement elements made of stone in Machu Picchu, Peru

Figure 4.14 Traditional confinement techniques of roof structures in Peru

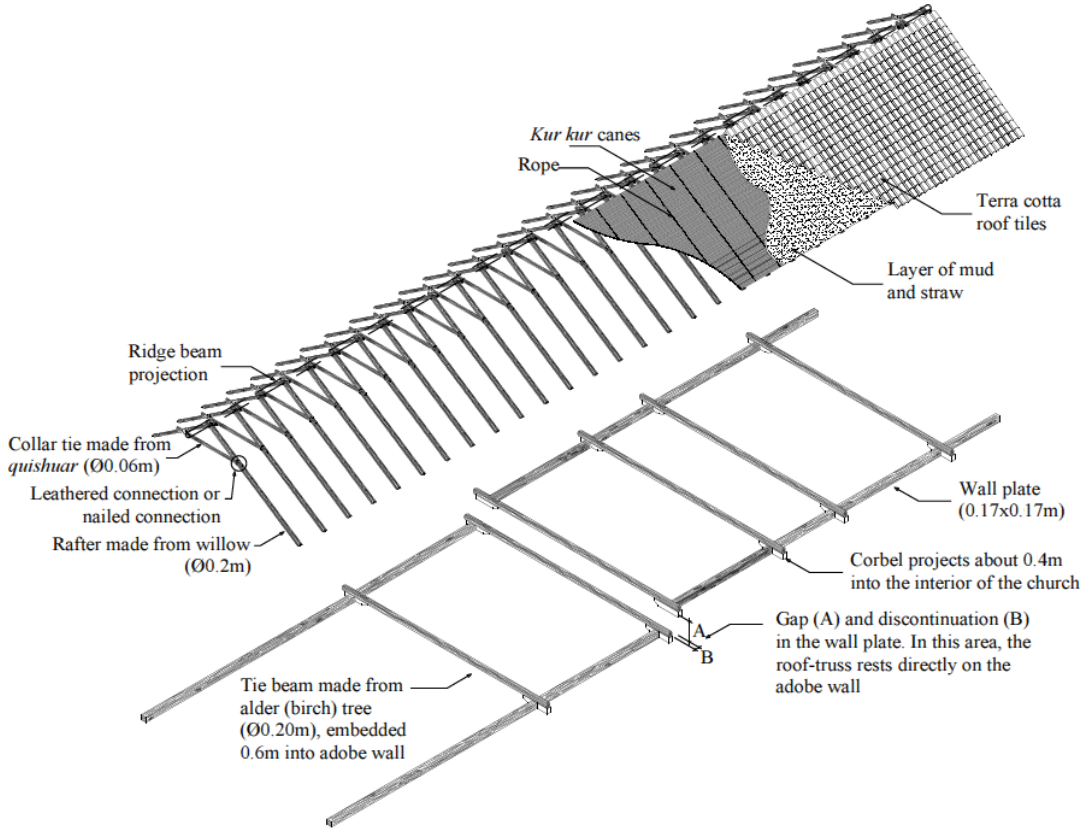

Figure 4.15 General view of the roof's structure of the Church of Kuño Tambo (Courtesy of Mirna Soto and Percy Iparraguirre, adapted from Cancino *et al.*, 2012)

The rafters are made from 0.20m diameter willow tree trunks; and they overlap one another with half-lap joints at their intersection. The rafters are tied to one another and the ridge beam above with leather straps or ropes and wrought iron nails (Figure 4.16b). The collar-ties are made from 0.06m diameter *quishuar* (name in quechua of a local species) and strapped or nailed to the rafters (Figure 4.16c). The rafters are scarfed at the ends and sit on 0.17x0.17m wooden wall plates that sit on the adobe walls (Figure 4.16d).

The wall plates are neither continuous nor the various segments, each of them supporting either four or five rafters, are connected together. Hence, the wall plates do not behave as ring beams, since they distribute the load that comes from the roof along the top of the walls but the system does not absorb the roof's thrust.

The baptistery and sacristy's roof structure is composed of 6 roof-trusses similar to those built in the nave and chancel with one more truss without collar-tie. In this case, the rafters are sitting directly on the adobe walls since there are no wall plates.

The roof's cover is made of *Kur Kur* canes that are woven and tied together with rope, a mud and straw layer and Spanish style terra cotta roof tiles.

a) Interior view of the roof

b) Connection rafter/rafter/ridge beam (half-lap joint tied with leather straps)

c) Connection rafter/collar-tie (nailed joint)

d) Connection rafter/wall plate (scarf joint)

Figure 4.16 Structural details of the roof's structure of the Church of Kuño Tambo (courtesy of the GCI)

4.3.5 Wooden tie-beams and anchors

The longitudinal walls of the nave and chancel of the Church of Kuño Tambo are restrained by 6 wooden tie-beams. Additional tie-beams connect buttresses B1 and B2, which are extensions of those walls, and restrain the lateral walls of the baptistery.

All tie-beams are 0.20m diameter alder or birch tree trunks. In the nave and chancel, the tie-beams sit on wooden corbels, and both the beams and corbels extend approximately 0.6m into the depth of the adobe walls (Figure 4.15 and Figure 4.17b).

In the central portion of the nave, two of the tie-beams are closely placed together, almost forming a pair, which causes a discontinuity in the wall plate which is placed at the same height. For this reason, the rafter located in-between the pair of tie-beams is directly embedded in the wall.

a) Tie-beams at the far North side of the church b) Connection tie-beam&corbel/adobe wall

Figure 4.17 General view and structural details of the tie-beams

External wooden anchors in the West and East elevations of the nave and North elevation of the baptistery were observed during the surveys (anchors AN1.1, AN1.2, AN2.1 and AB1.1 shown in Figure 4.18). The anchors placed at the external facades of the nave are located at the far South side of the church.

The existence of anchor AN2.1 indicates that possibly a tie-beam was connecting walls WI.2 and WI.4 at the location of the mezzanine. However, the tie-beam failed most probably due to the decay of WI.4 at the location of the tie-beam's anchorage. This is further shown by the failure of the wall plate and supported rafter in this portion of the wall (Figure 4.19).

a) Anchor AN1.1, West side of B2 b) Anchor AN1.2, façade of WI.4

c) Anchor AN2.1, façade of WI.2 d) Anchor AB1.1, façade of WIII.2

Figure 4.18 Observed external wooden anchors of the Church of Kuño Tambo

Figure 4.19 Failure of rafter, tie-beam and anchor due to deterioration of the wall

4.3.6 Chancel arch

An arch is normally separating the chancel from the nave. The arches can have alternative forms, as shown in Figure 4.20 which shows an example of a round and a segmental arch. They are typically composed of adobe pillars with timber arches. The Church of Kuño Tambo had a chancel arch in the past, of which only the adobe pillars are still standing at present as shown in Figure 4.21.

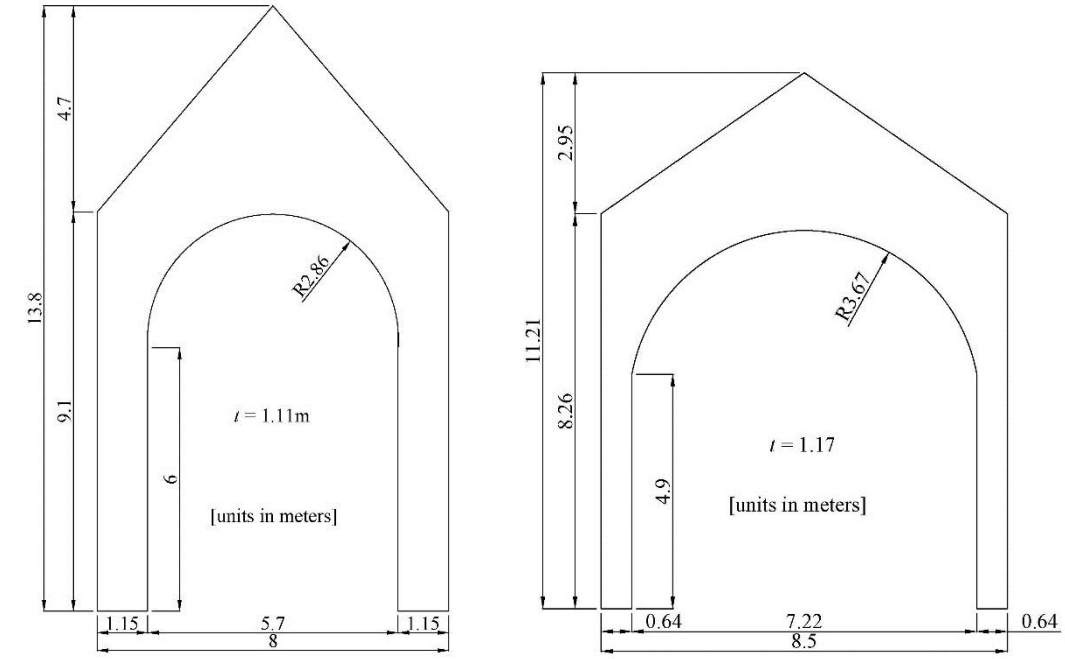

a) Round chancel arch of the Church of San Miguel de Pitumarca

b) Segmental chancel arch of the Church of San Jeronimo de Acopia

Figure 4.20 Examples of chancel arches

Figure 4.21 Remaining adobe pillars of the chancel arch of the Church of Kuño Tambo

4.3.7 Mezzanine and balcony

Churches in high lands typically have an internal wooden mezzanine and an external balcony. The Church of Kuño Tambo has a wooden mezzanine (Figure 4.22a) and balcony (Figure 4.23) in the South façade (WI.1 wall).

The mezzanine's joists are supported by WI.1 and supported by a beam that runs in the West-East direction. The beam is embedded in both WI.2 and WI.4 and supported by two wooden columns with mud brick bases and decorative wooden capitals (Figure 4.22b).

A beam running in the North-South direction support the joists of the Northwest extension of the mezzanine (Figure 4.22b). The beam's South end is tied to the beam supporting the main structure with ropes and the North end rests on a pillar located at the Northeast of the mezzanine's extension. The joists of the extension run in the West-East direction and are embedded in WI.2. Both the beam supporting the joists and the column below are unsawn tree trunks, suggesting that this mezzanine's extension is a later addition to the main structure.

The balcony's structure is composed by cantilevered joists, which are embedded in the main façade (WI.1 wall), as shown in Figure 4.23.

a) General view

b) Details of the structure

Figure 4.22 Mezzanine of the Church of Kuño Tambo

Figure 4.23 Balcony of the Church of Kuño Tambo

4.4 Historic earthen and timber churches in low lands: the Cathedral of Ica

In low lands, the churches are mainly composed of masonry walls (generally adobe and in some cases brickwork main façade) and planked timber vaults either supported by the walls or by a timber frame. The timber structure of these churches has therefore a primary structural role. However, this structural system of planked timber vaults has been to a large extent ignored by the engineering community in several countries in modern times. In the case of Peru, the damage caused to this type of structures by the 2007 Pisco earthquake, showed that churches built with this system and the people attending services in these churches are at risk.

The structural system of planked timber vaults (*bóvedas encamonadas* in Spanish) is often mistakenly named in literature by *quincha* (see for instance Marussi Castellán, 1989 and San Cristobal, 2003). The etymology of the word *quincha* can be traced back to the *quechua* or *runa-simi* (name used at the time of the Inca Empire), a native language of the Andean region and it was originally associated to the idea of a fence. In the pre-Hispanic period, the *quincha* technique was a rudimentary system of timber trunks, connected together by means of vegetal straps (Marussi Castellán, 1989). The system was commonly used in houses in the coast, being still used in rural areas at present. The meaning of the word has however changed to denote a structural system similar to European construction practices. The *quincha* developed at the time of the Hispanic Viceroyalty of Peru consists of a partially braced frame, with timber members connected together by mortice and tenon and nailed joints, with an infill of canes and mud mortar. The system was applied as a walling solution at upper floors of traditional houses in coastal areas.

Hurtado Valdez (2011) has conducted a comprehensive study of the origin, evolution and principal geometry and construction characteristics of historic planked timber vaults in Peru. The author emphasizes the misuse of the term *quincha* to name the *bóvedas encamonadas*, which are composed of *camones* and *contracamones* (planks in English).

4.4.1 Origin and evolution of historic planked timber vaults in Peru

Historic buildings composed of timber vaults with planked arches are an important part not only of Latin-American but also European heritage. The first reference to timber vaults in Europe can be traced back to the 1st century BC, to the work of Vitruvius in his treatise '*De architectura*'. However, this construction system, as interpreted by Rowland and Howe

(1999) and Hurtado Valdez (2011), corresponds to a curved ceiling made of canes and longitudinal ribs suspended by means of vertical ties from horizontal beams. Hence, there are no timber arches.

During the Medieval period, structural solutions to cover large spans in churches, palaces and public buildings normally included the use of long linear or curved timber members together with shorter elements, such as rafters, posts and braces. Shortage of long timber pieces began to be felt by the end of the Medieval period (Gómez Sánchez, 2006), which triggered the conception of systems composed of small timber members assembled together to make long spans (Hurtado Valdez, 2011). A prominent example of a timber roof composed of relatively short members connected together to form a vaulted ceiling is the hammerbeam roof of the Westminster hall in London, which was completed in 1402 (Heyman, 1967).

The treatises of Philibert De L'Orme in France and Sebastiano Serlio in Italy, published in the 16th century, are currently recognised as the first references to timber planked arches. The vault is composed of planks curved both in the intrados and extrados that are assembled together in two or more alignments of planks by means of carpentry joints to make an arch (Figure 4.24a). Parallel arches are longitudinally braced by means of ribs, which pass through holes made both at the centre of the planks and at their extremities. This bracing is fixed to the planks by means of wooden keys (Figure 4.24b). The arches are mortice and tenon into wooden wall plates supported by masonry walls, which counteracts the roof thrusts. De L'Orme suggested the following advantages of the system when compared to masonry vaults (Hahmann, 2006; Hurtado Valdez, 2011): (i) the modest weight; (ii) the modest thrust produced at the spring points; and (iii) the relatively simple replacement of deteriorated members.

However, Jean-Baptiste Rondelet suggested in the 19th century connecting the longitudinal bracing at the top of the arches by means of notched joints, since the holes made in the planks of the De L'Orme system create vulnerable points at these locations. Furthermore, Rondelet also suggests connecting the primary structure to a system of rafters and ties, which supports the roof, in order to increase the stability of the vault (Hurtado Valdez, 2011). This idea of a planked timber vault restrained at the top by the roof's structure can be traced back to the treatise of Lorenzo de San Nicolás, published in the 17th century in Spain. Systems of planked arches connected to roof's trusses or timber frames hidden by the roof (Figure 4.25) became popular in Spain from the 17th century onwards.

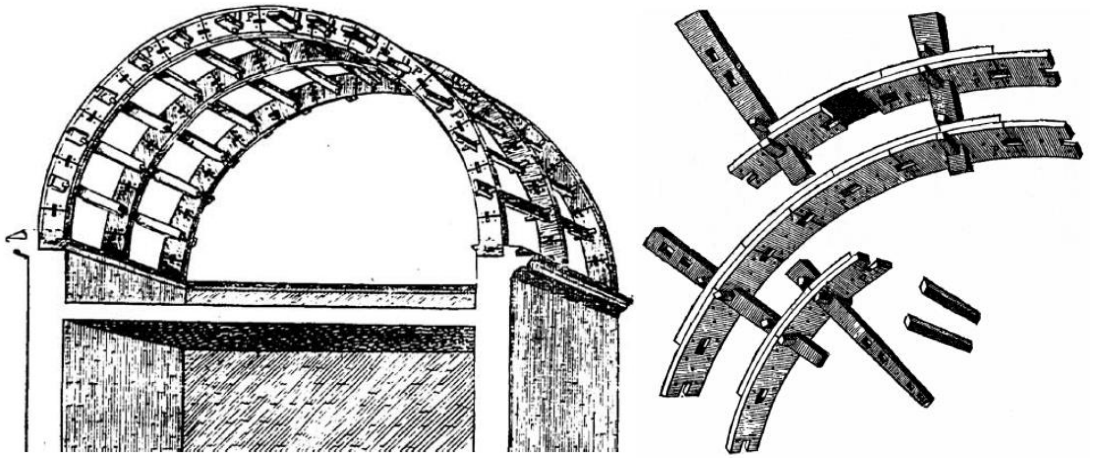

a) b)

Figure 4.24 Planked timber vault of De L'Orme: a) General view of the vault (Hurtado Valdez, 2011); b) Detail of the arches and bracing (Hahmann, 2006).

Figure 4.25 Vault of the Rojas Theatre in Toledo (courtesy of Marina Arce-Blanco, UPM)

The justification for the increasing use of timber vaults to cover large spans is economical as well as architectural, as timber vaults were approximately 4 times cheaper to construct in the 17th century, and more flexible to fulfil the demand of the new Baroque style (Hurtado Valdez, 2011). The formation of the Hispanic Viceroyalty in Latin America, with capital Lima, in the 1st half of the 16th century promoted the exchange of knowledge on construction methods between Spain and present day Peru.

The first timber vaults built in Lima were similar to the typical Spanish system (Hurtado Valdez, 2011), with planked arches connected to the roof's structure. However, timber vaulted systems evolved in Peru in the direction of systems more similar to the De L'Orme's proposal. The vaults of the Church of San Francisco in Lima built by Manuel de Escobar and Constantino de Vasconcellos in 1675 are composed of arc-shaped planks nailed to each other and forming arches that are braced longitudinally. The arches are connected to wall plates, which are supported by the walls. This type of vaults presents also some local characteristics, such as adobe infill near the spring line to counteract the lateral thrust (Hurtado Valdez, 2011). Examples can be found in Figure 4.4a, Figure 4.4d and Figure 4.26.

The good structural behaviour of timber vaults to destructive earthquakes that occurred in the 17th century in Peru, if compared to the masonry vaults initially built in the 16th century, also raised the popularity of the timber systems, which were then widely used in the rebuilding of damaged structures and in new constructions (San Cristóbal, 2003).

A thorough description of the structural system of a representative church with planked timber vaults supported by timber pillars is provided in the following section of the present chapter.

4.4.2 The structure of the Cathedral of Ica

The Cathedral of Ica dates from 1759 and it is representative of historic churches with a central nave and lateral aisles built in low lands throughout the Viceroyalty of Peru. The church has a prominent religious and social role in the city of Ica, with the frontal façade facing the main square of the city (Figure 4.27). It has been used as a place of worship until it was severely damaged by the 2007 Pisco earthquake.

4.4.2.1 PLAN AND EXTERNAL STRUCTURE

A three-dimensional structural model of the cathedral is shown in Figure 4.28. The building is composed of external masonry walls and base of towers, towers' top made of timber, and internal timber structures, which make the roof and divides internally the building into several spaces.

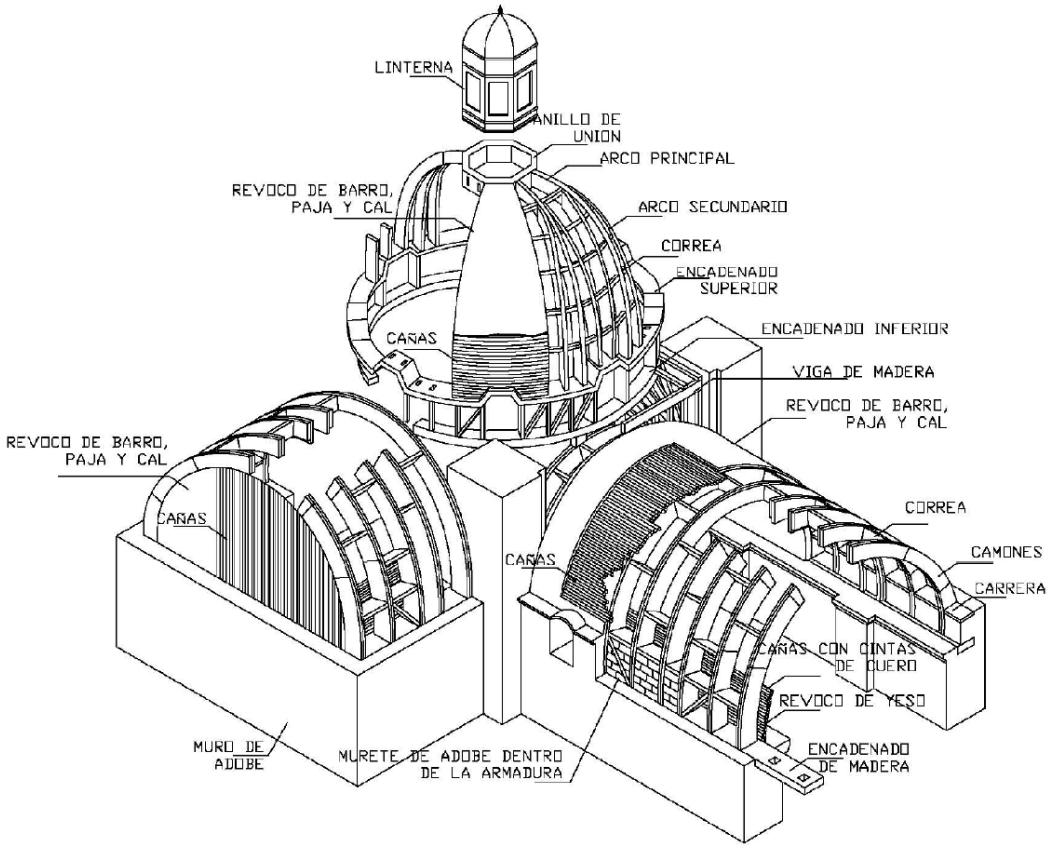

Figure 4.26 Typical church with planked timber vaults sitting on walls by Hurtado Valdez (2011)

a) In 2005, before the earthquake

b) In 2007, after the earthquake

Figure 4.27 View of the cathedral from the main square (Courtesy of the GCI)

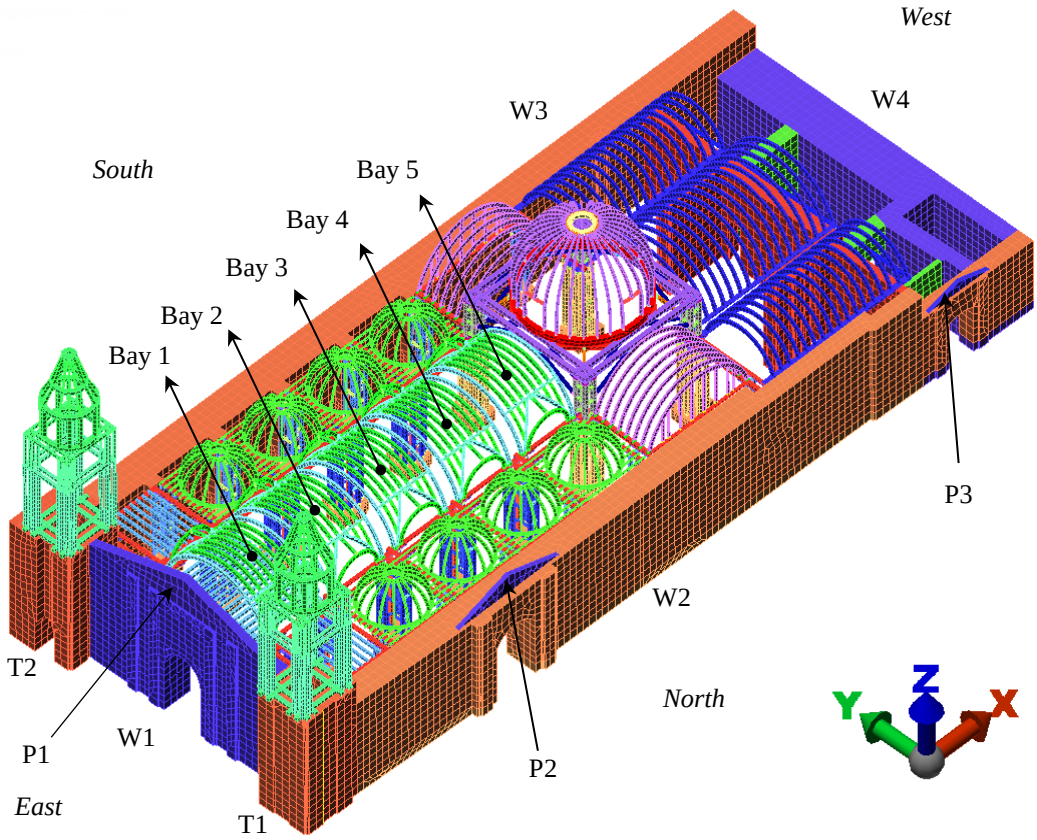

Figure 4.28 Three-dimensional model of Cathedral of Ica

The walls and pillars are sat on brickwork base courses, laid in sand and lime mortar, and rubble stone masonry foundation. The height and material composition of the base courses change at the transitional area between the fired brick base of the North bell tower (T1) and the adobe lateral wall (W2). In this area, the base course is composed of an alternating system of stone masonry interspersed with courses of brickwork and the rest of the wall is made of brickwork, reaching a total height of 3m.

The main façade W1 (Figure 4.29a) is made of brickwork laid in lime mortar. The lateral walls (Figure 4.29b and Figure 4.29c) are made of adobe laid in mud mortar.

There are two bell towers which flank the front façade, built of a wood framing structure on top of a lower brickwork base (Figure 4.29d).

a) Frontal façade (W1, facing East)

b) Longitudinal wall (W2, facing North)

c) Longitudinal wall (W3, facing South) (courtesy of Claudia Cancino)

d) Tower (T2, view of the North and West façades)

Figure 4.29 External views of the Cathedral of Ica in 2010

The plan of the building consists of a choir loft (Figure 4.30a), one central nave covered by timber vaults with four bays (Figure 4.30b), a transept, crossing and altar. Each side of the nave is flanked by an aisle (Figure 4.30c) that is covered with a series of small timber domes. The transept is covered by vaults and a large timber dome (Figure 4.30d).

a) Choir loft

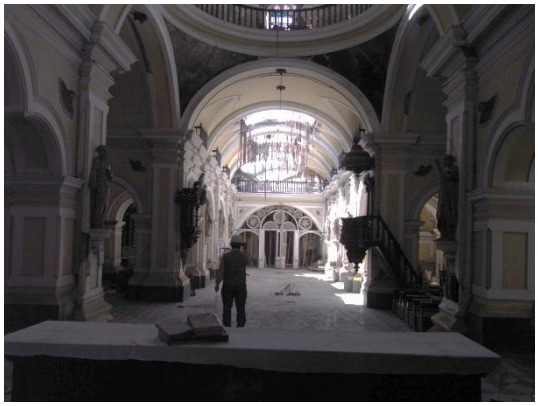

b) Central nave

c) Lateral aisle

d) Main dome of the crossing

Figure 4.30 Internal views of the Cathedral of Ica in 2010

4.4.2.2 INTERNAL STRUCTURE

The timber framing of the nave, lateral aisles, transept, crossing, and roof of the Cathedral of Ica are shown in Figure 4.31. Timber-framed pillars, connected between each other by timber frames, are supporting the vault, the central and lateral domes and the choir loft by means of beams that run in the longitudinal and transversal directions. The domes are composed of meridians braced horizontally by timber ribs.

The pillars are composed of several timber posts, which are braced by horizontal and diagonal timber elements. Three different pillar's layouts are present in the church, as shown in Figure 4.32, namely the central pillars of the nave, the crossing's pillars and the lateral

pillars. The pillars between the nave and the lateral aisles have also a central trunk made of guarango, a hardwood species indigenous of Peru. All pillars have a brickwork base course which is 0.7m high and a rubble stone foundation, which form the base of the structure. The lateral pillars are located adjacent to adobe piers, which are part of the South wall (W3), or immediately adjacent to the lateral North wall (W2).

In the nave, longitudinal beams support transversal beams where the joists of the lateral aisles rest. These longitudinal beams are resting on the guarango trunk and on two of the posts of the central pillars. The internal longitudinal beams of the nave, which are connected to two posts of the central pillars, support the vault. Furthermore, the transversal beams of the aisles are connected to four posts of the central pillars and to the lateral pillars.

The base of the central dome is composed of a system of beams and pillars with four posts. These pillars are sitting on the crossing's pillars at the intersection of the longitudinal beams of the nave with the transversal beams of the transept.

At the central nave, the vaults are composed of bay-edge and internal timber arches and lunettes, as shown in Figure 4.33. The lunettes' ribs and diagonals and the internal arches are connected to a beam at the top of lunettes. This beam is connected to the bay-edge arches. The arches, lunette's ribs and domes' meridians are composed of arc-shaped timber planks, as shown in Figure 4.34.

Adjacent bays of the vault are longitudinally braced by means of two systems of struts:

(i) the first system is composed of longitudinal timber elements connecting the bay-edge arches of adjacent bays, shown in Figure 4.35a; and

(ii) the second system is composed of longitudinal timber elements connecting the bay-edge arches of each bay, shown in Figure 4.35b.

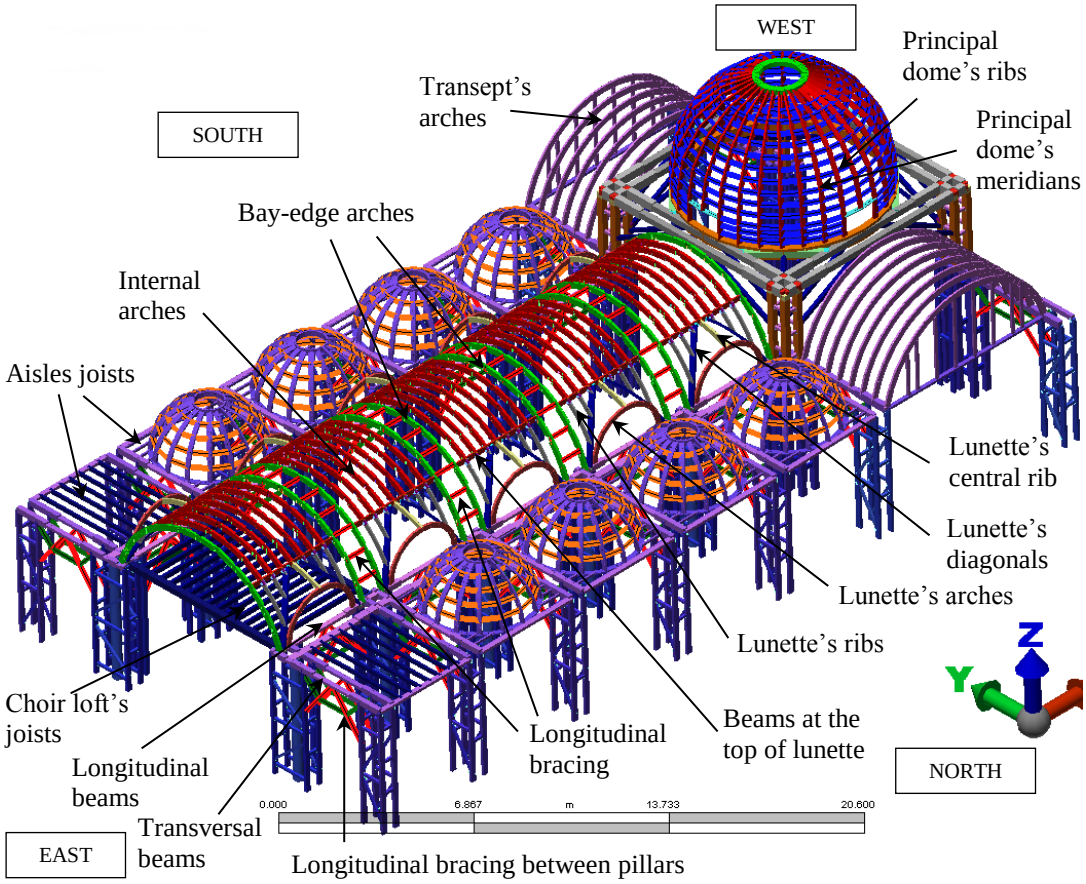

Figure 4.31 Structural model of the timber framing of the Cathedral of Ica (extruded beam elements and springs)

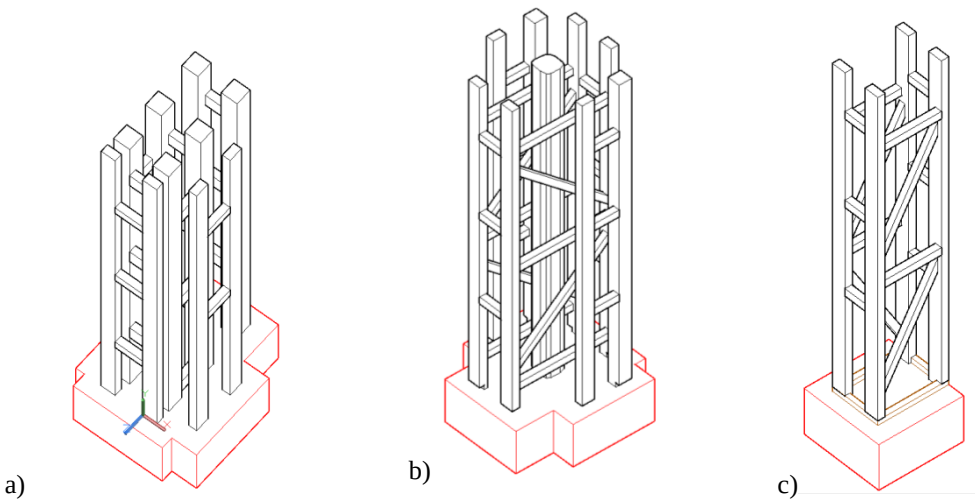

Figure 4.32 Representative timber pillars of the Cathedral of Ica – a) pillars of the crossing's bay, supporting the central dome; b) central pillars of the nave, which separate the nave from the lateral aisles; and c) lateral pillars, which are adjacent to the lateral walls

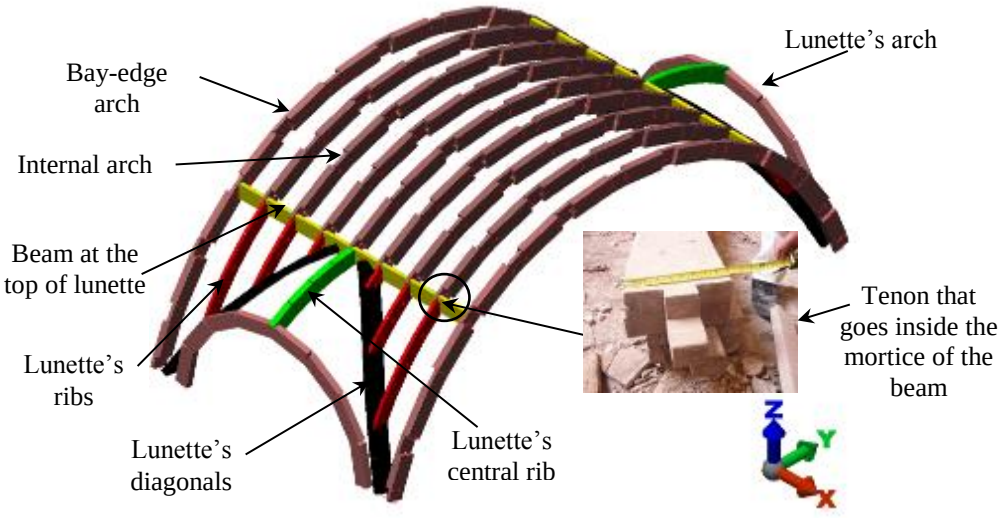

Figure 4.33 Structural model of a representative bay of the nave's vault

Figure 4.34 Representative bay-edge arch of the Cathedral of Ica (courtesy of Erika Vicente, PUCP)

a) b)

Figure 4.35 Longitudinal bracing of the timber vault of the Cathedral of Ica (courtesy of Erika Vicente, PUCP): a) connection of the bay-edge arches of adjacent bays; and b) connection of the bay-edge arches within each bay

The interior and exterior surface of the timber structure is covered with cane attached with nailed leather straps and plaster. The roof has an additional layer of sand, lime and cement mortar, introduced after the construction, which added 1.7kN/m^2 weight to the structure of the vault. The roof of the aisles has a layer of timber planks, fired bricks, mud mortar and lime and cement mortar in a total of 2.5kN/m^2.

4.4.2.3 TIMBER JOINTS

A typical bay of the nave of the cathedral of Ica is shown in Figure 4.36. Six parts of the complex timber framing can be distinguished for an easier understanding of the structure (drawn with different colour in Figure 4.36):

(i) the vault composed of 2 bay-edge arches supported by the longitudinal beams, 7 internal arches connected to the lunettes, 2 beams (1 at each side) located at the top of lunettes and the lunettes' structure (6 ribs, 2 diagonals, 1 strut, and 1 arch on each side);

(ii) the lateral domes;

(iii) the joists of the aisles;

(iv) the system of longitudinal and transversal beams supporting the vault and the roof of the aisles;

(v) the central and lateral pillars; and

(vi) the base course of the pillars.

All members in each part of the timber framing are connected to adjacent members by means of different types of timber joints. The arches forming the vault, the diagonals, ribs and arches of the lunette, the bottom ring and meridians of the domes, and the arches of the transept are composed of several segments made of arc-shaped planks connected together by plain lap joints with four wrought handmade nails (detail 5 of Figure 4.36). There are approximately 1580 nailed joints such this in the cathedral. The arches and lunettes' members are connected to beams by means of mortice and tenon joints of different dimensions and layout, either with or without nails (details 1, 2, 3 of Figure 4.36), counting in total 130 similar joints in the cathedral.

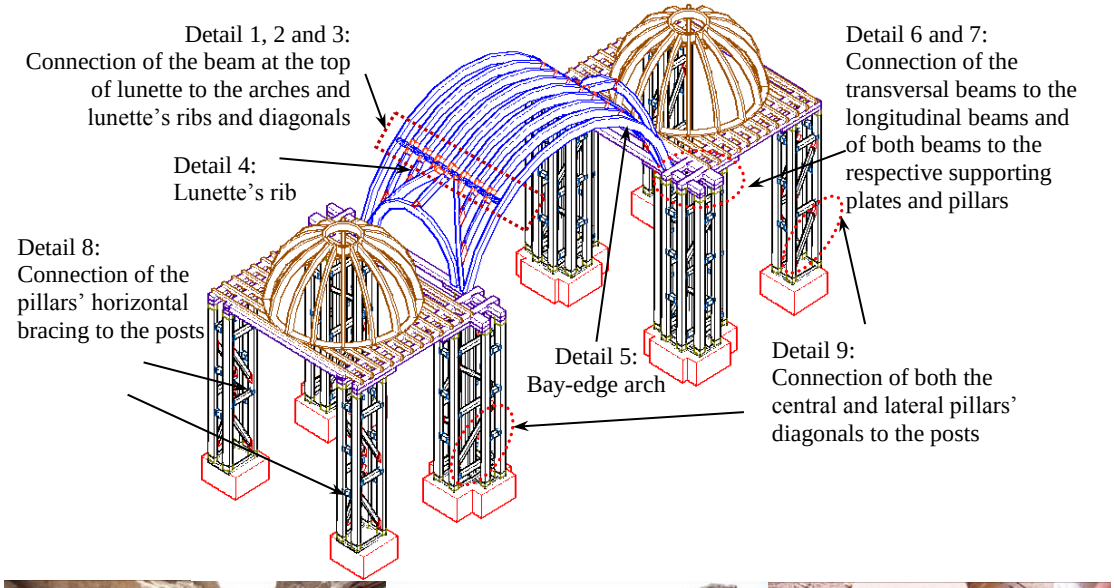


Detail 1
Credits: GCI, 2012


Detail 2
Coutesy: GCI, 2012


Detail 3


Detail 4


Detail 5
Courtesy: GCI, 2012


Detail 6


Detail 7


Detail 8


Detail 9

Figure 4.36 Timber framing of a bay of the Cathedral of Ica's nave: principal structure's layout and details of the timber joints

The mortices of the beam at the top of lunettes are filled by the tenon of the arches and the tenon of the lunette's ribs and diagonals (detail 1 and 2 of Figure 4.36). The meridians of the domes are also connected to the bottom ring by means of mortice and tenon joints.

As depicted in detail 4 of Figure 4.36, the lunette's ribs are connected to the lunette's diagonals by means of nailed joints, which can have one or two nails, depending upon the position of the rib. Furthermore, the longitudinal and transversal beams are connected to the pillars' posts by means of mortice and tenon joints (detail 6 of Figure 4.36), counting in total 186 similar joints in the cathedral. Notched joints connect the transversal beams to the longitudinal beams, as also shown in detail 6 of Figure 4.36. Both the longitudinal and transversal beams are connected to supporting plates of same cross section by means of leather straps (detail 7 of Figure 4.36). These supporting plates allow doubling the cross section of the beams at the connections.

The horizontal bracing of all pillars of the cathedral is connected to the respective posts by means of pegged mortice and tenon joints (detail 8 of Figure 4.36), counting in total 752 similar joints in the cathedral. The diagonals are connected to the posts by nailed joints (detail 9 of Figure 4.36), counting in total 192 similar joints in the cathedral.

4.4.2.4 INTERACTION OF THE TIMBER FRAMING WITH THE MASONRY WALLS

The timber framing and the masonry walls of the cathedral are connected at two locations:

(i) connection of the façade (W1) with the first bay of the timber framing. It was observed during the field campaigns that the choir loft floor joists are sitting on W1 (Figure 4.37);
(ii) connection of the transversal beams of the transept's bay with the longitudinal adobe walls (Figure 4.38). According to *in situ* observation of the North longitudinal wall, the transversal beams of the transept's bay are directly sitting on the adobe wall without wall-plate.

During the field campaigns, some links between the lateral pillars and the longitudinal walls were also observed, as shown in Figure 4.39. However, these links were only observed at one single position along the height of the columns. Moreover, these links are relatively short, and therefore they do not perform as a proper connection. It is likely that the mortar around the links will fail locally for low values of ground shaking.

Figure 4.37 Choir loft's joists sitting on the façade

Figure 4.38 Damage on the North longitudinal wall, where it can be seen the end of the transversal beams of the transept bay

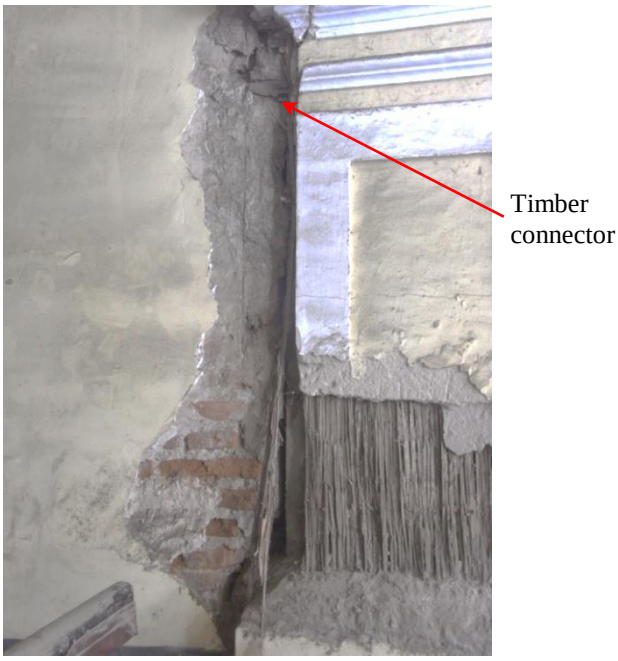

Figure 4.39 Timber links between a lateral pillar and the North longitudinal wall

4.4.3 State of the Cathedral of Ica after the 2007 Pisco Earthquake

The vault and central dome of the Cathedral of Ica partially collapsed during the mainshock of the 2007 Pisco earthquake, as shown in Figure 4.40a. The cathedral has not yet been repaired and a minor shoring and propping system was put in place only after a strong tremor in 2011 has caused the complete collapse of the central dome.

The almost complete collapse of the vault of bay 1, observable in Figure 4.40a ,was due to the failure of the nailed connections of the bay-edge arches in shear and tension perpendicular to the grain, as shown in Figure 4.40b. The beam at the top of lunettes failed in shear in bays 2, 3 and 4 as shown in Figure 4.41. This failure could be identified in bay 2 after the earthquake by the visible settlement of the top of the vault (Figure 4.40a); however the internal arches did not collapse immediately due to the existence of a layer of canes connected to the bay-edge arches. The whole weight of the roof at the top of bay 2 was therefore completely supported by the bay-edge arches. Subsequent minor shacks in 2010 caused the collapse of the East bay-edge arch of bay 2 in a similar way as in the case of bay 1 (Figure 4.42 and Figure 4.43). This collapse was due to the failure of the nailed joints in shear and tension perpendicular to the grain, which shows that these connections were not capable of supporting the forces produced by the masses being supported by the arches. It is reasonable to assume a similar but quicker progress of damage in bay 1 during or immediately after the earthquake.

The internal arches of bays 3 and 4 collapsed during the earthquake due to the failure of the mortice and tenon joints that connect these arches to the beam at the top of the lunette (Figure 4.40a). Due to this collapse the mass of the roof insisting on the bay-edge arches of these bays was substantially reduced and this can explain their survival without significant damage to the main shock and subsequent aftershocks and tremors which have affected the cathedral in the last 9 years. No significant damage was observed in the nailed joints between planks of the internal arches.

The earthquake also caused the collapse of the roof of the left aisle of bay 1 (Figure 4.44a), which appears to have been triggered by the collapse of the longitudinal beam running between the lateral pillars and supporting the joists of the internal ceiling, as shown in Figure 4.44b. The collapse of the beam was caused by the failure of the connection of the horizontal bracing of the lateral pillar, where the beam was sitting (Figure 4.44c).

a)

b)

Figure 4.40 Damage state of the vault of the Cathedral of Ica shortly after the 2007 Pisco earthquake: a) general view of the nave (courtesy of Claudia Cancino, GCI); and b) partial collapse of the East edge arch of bay 1

Figure 4.41 Failure of the mortice and tenon connection at the top of lunettes (courtesy: GCI)

Figure 4.42 Damage state of the timber vault and principal dome of the Cathedral of Ica in 2011 (courtesy: Erika Vicente, PUCP)

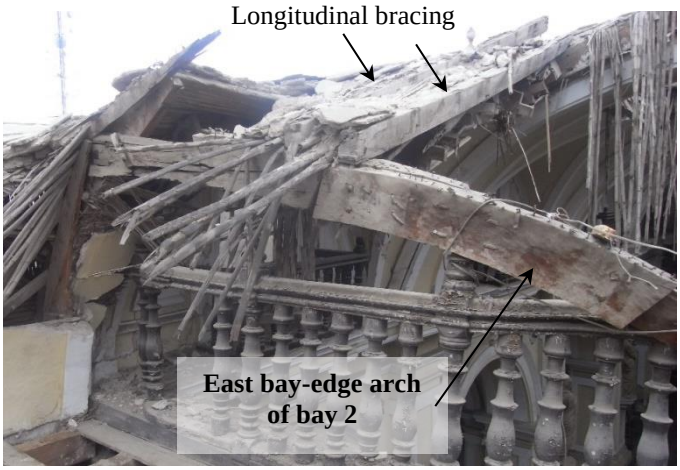

a)

b)

Figure 4.43 Failure of the bay-edge arches of bay 2: a) partially collapsed arch at the Eastern end; and b) failure of the nailed connections near the spring point of the arch at the Western end

a)

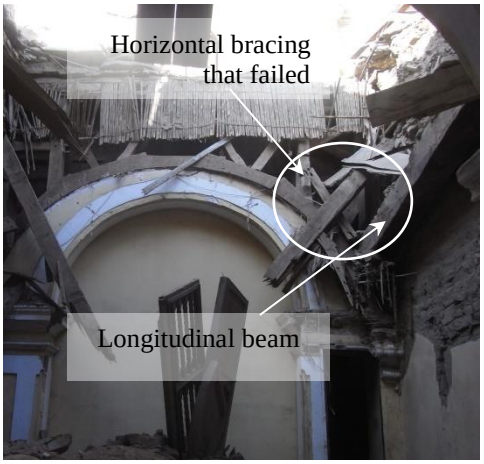

c)

b)

Figure 4.44 Collapse of the roof of the left aisle of bay 1

As far as the walls of the cathedral are concerned, Figure 4.45 shows the principal damage caused by the earthquake. Detail 1 shows the vertical crack caused by the interaction of the brickwork base of the tower with the adobe wall. Details 2 and 5 show the cracks induced by the interaction of the crossing bay with the wall. Detail 3 shows the crushing of the pediment caused by the interaction with the tower. Finally, detail 4 shows the horizontal crack caused by the out-of-plane vibration of the pediment.

Detail 1

Detail 2 and 5

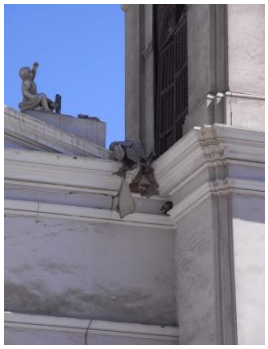

Detail 3

Detail 4

Figure 4.45 Damage in the walls of the Cathedral of Ica after the 2007 Pisco earthquake

4.5 Conclusions

The previous sections have shown that historic churches built in the same period of time but in different geographical locations in Peru have different levels of complexity in terms of structural layout and arrangement. These differences emerge from the topographical characteristics of the places – the high and remote lands of the Andes and the low and more accessible lands of the coast located in areas that were deserts in the past -, and the type of settlements – small and dispersed settlements in high lands inhabited by a majority of indigenous people and large settlements in low lands where the settlers established their homes.

From the detailed description and interpretation of the structural systems of the Church of Kuño Tambo and Cathedral of Ica, the following main conclusions are important for the next phases of the assessment:

(i) Churches in high lands are typically composed of a single nave, chancel, baptistery and sacristy. The structure is characterized by the response of thick adobe walls, which are typically restrained by buttresses and wooden tie-beams.

The traditional *par y nudillo* system, with origin on pre-Hispanic construction techniques, is the typical structural solution of the roof. The locally available stone is used on high rubble stone masonry base courses;

(ii) Churches in low lands have a more complex structure of adobe and brick or stone masonry walls with planked timber vaulted systems. The most complex typology of this type is exemplified by the Cathedral of Ica, which has an internal timber structure with only a few and modest links with the external masonry walls. The cathedral was severely affected by the 2007 Pisco earthquake, especially at the level of the vault where several arches failed. In general, the failure of the timber structure is concentrated at the joints. The earthquake exposed for the first time in decades or even centuries a structural system that was unknown up to that date. It also showed the high level of deterioration that is affecting a significant portion of the timber structure due to poor maintenance.

In order to assess the seismic performance of these historic churches and explain the damage observed especially in the Cathedral of Ica, more detailed investigations based on structural analysis are required. In the next chapter, a preliminary diagnosis of the Church of Kuño Tambo and Cathedral of Ica are conducted with the purpose of identifying the critical aspects that require a detailed analysis in order to understand the seismic response of these churches from the construction details observed.

CHAPTER 5

Preliminary diagnosis of Peruvian earthen and timber historic churches

5.1 Introduction

The present chapter shows the preliminary diagnosis of the Church of Kuño Tambo and Cathedral of Ica. The preliminary diagnosis is normally a collegial activity of people with different expertise. It corresponds to the first diagnostic exercise based on qualitative analysis of initial available information, field observations and primarily on experts' judgment.

This activity was initially carried out collegially during an EAI-SRP partners meeting and adjusted later on, after reinterpretation of available data at the time.

This chapter is organized into two main sections, one for the Church of Kuño Tambo and another for the Cathedral of Ica. Taking into account that the structural behaviour of churches to earthquakes can be understood by considering the individual behaviour of macroelements, as discussed in Section 2.4, both the Church of Kuño Tambo and the Cathedral of Ica are initially divided into macroelements. The preliminary diagnosis is then carried out following the approach described in Section 3.3. The most important remarks for the next step of the assessment, as per the framework of Figure 3.1, conclude the chapter.

5.2 Historic adobe churches in high lands: the Church of Kuño Tambo

A detailed description and interpretation of the principal construction details of the Church of Kuño Tambo was presented in Section 4.3. The following diagnosis will make reference to this section as appropriate for more clarity.

5.2.1 Macroelements

The Church of Kuño Tambo is assumed as a system composed of the following macroelements, illustrated in Figure 5.1:

1. Adobe façade of the nave;
2. Adobe back wall of the nave;
3. Lateral adobe walls of the nave;
4. Rubble stone base course;
5. Adobe buttresses;
6. Adobe walls of the baptistery/sacristy;
   6a. Baptistery
   6b. Sacristy
7. Wooden tie-beams; and
8. Wooden roof structure.

The façade of the building (WI.1) and the back wall of the nave (WI.3) are assumed as macroelements distinguishable from the lateral walls (WI.2 and WI.4). In the case of the façade, such assumption is due to the existence of cracks at the interface between the façade and those lateral walls (Figure 5.2), and due to the masonry fabric itself, because the façade presents a plaster and painting which is not currently present elsewhere. Moreover, the shape ratio of the façade and back wall and the presence of the gables lead to the assumption of a behaviour different in respect to the lateral walls.

The base course is assumed as a macroelement independent of the rest of the structure, because it is composed of rubble stone masonry whereas the rest of the wall is made of adobe. The difference in material composition creates a surface of discontinuity and interaction between the base course and the other macroelements.

The baptistery and sacristy are assumed as unique macroelements, since their influence on the response of the principal body of the church is more important for the global response of the building than the individual performance of each of these two construction parts.

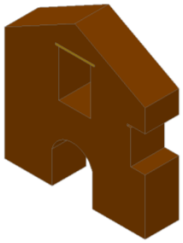

1. Adobe façade of the nave

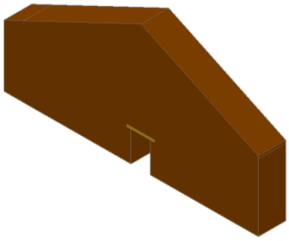

2. Adobe back wall of the nave

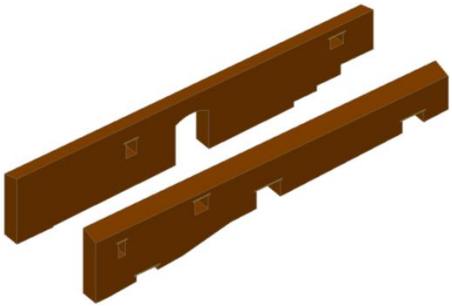

3. Lateral adobe walls of the nave

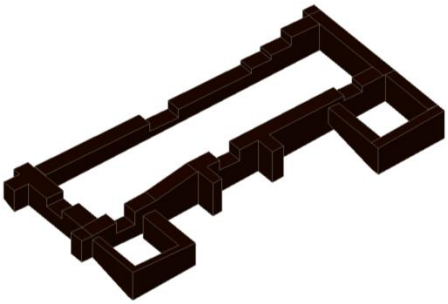

4. Rubble stone base course

5. Adobe buttresses

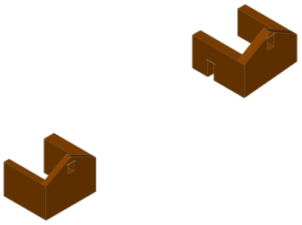

6. Adobe walls of the baptistery/sacristy

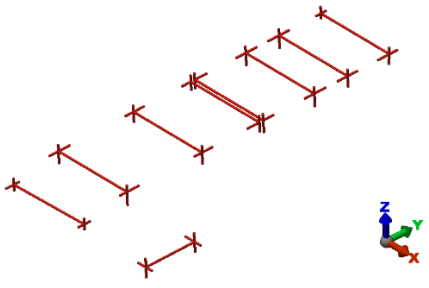

7. Wooden tie-beams

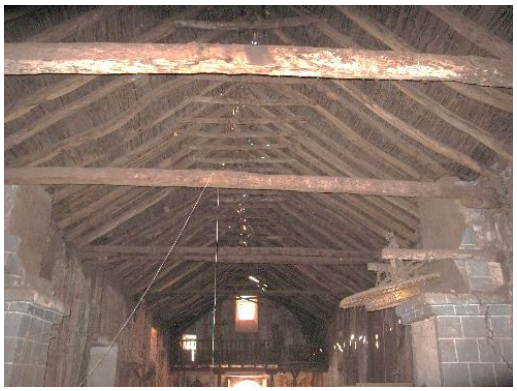

8. Wooden roof structure

Figure 5.1 Macroelements of the Church of Kuño Tambo

Figure 5.2 Crack at the interface WI.1/WI.4

Hence, the connection between the various walls composing either the baptistery or the sacristy is evaluated within the "Connections" attribute rather than within "Interaction".

The tie-beams are a distinct macroelement made of a different material, which interacts with the lateral walls.

The roof is composed of several components connected together by flexible joints. The entire structure of the roof is assumed as a unique macroelement because the failure of one of its components is likely to cause local deformations and collapses and not global failure modes. Inversely, a global mechanism can be triggered if the connection between the roof and other macroelements fails.

5.2.2 Diagnosis

The preliminary diagnosis of the Church of Kuño Tambo is summarised in the matrix of Table 5.1. This matrix includes: (i) the five attributes described in Table 3.1; (ii) the macroelements; (iii) the classes of influence A to D of the attributes, described in Table 3.2; (iv) the nature of the influence of the attributes over the macroelements; and (v) the uncertainty, $\delta Ip_{j,i}$, with which the analyst makes the judgment.

In Table 5.1, the 'Interaction' attribute evaluates the way how each macroelement interacts with the other macroelements (e.g. how the baptistery interacts with the lateral walls). When a given macroelement interacts in different ways with other macroelements, the most important interaction for the global response of the structure is the one evaluated in

the matrix of Table 5.1. The 'Connections' attribute evaluates the conceptual design and construction quality of the connections between structural elements that belong to the same macroelement (e.g. it evaluates the connections between the walls of the baptistery).

Table 5.1 Matrix of preliminary diagnosis of the Church of Kuño Tambo

MACROELEMENTS	ATTRIBUTES				
	Robustness	Condition	Interaction	Connections	Materials
1. Façade	A + 30%		C + 30%	D + 30%	B + 30%
2. Back wall	A - 20%	C - 30%	A - 30%		C + 30%
3. Lateral walls	A - 20%	C - 30%	A - 30%		C + 30%
4. Base course	C + 30%	B - 30%	C - 40%		A - 30%
5. Buttresses	B - 20%	C - 30%	A - 20%		C - 30%
6a. Baptistery	C + 30%	D - 30%	A - 30%	B - 30%	D - 30%
6b. Sacristy	C + 30%	D - 30%	A + 30%	B - 30%	D - 30%
7. Tie-beams	B + 20%		A - 20%	C + 40%	
8. Roof	B - 20%	D - 40%	A - 20%	C - 20%	

The vertical slenderness of the walls, S_L, defined as the height to thickness ratio, is shown in Table 5.2, considering both the total height of each wall, including the base course, and the height of the adobe portion. The height of the base course and adobe wall indicated in the table are average dimensions; since the respective heights are not constant along the length of the walls.

The classification of the walls as 'thick', 'moderate' or 'thin' follows the criteria of Tolles *et al.* (2002):

- thick: $S_L < 6$;
- moderate: S_L = 6-8; and
- thin: $S_L > 8$.

According to this classification, a 'thick' wall is stable under earthquake loading, and hence it is not likely to collapse.

Table 5.2 Vertical slenderness of the walls

Wall	Height of adobe wall, H_a (m)	Height of base course, H_b (m)	Total height of the wall, H (m)	Thickness, t (m)	H_a/t	Classif.	H/t	Classif.
WI.1	8.55	2.45	11.00	1.90	4.5	Thick	5.8	Thick
WI.2	5.00	2.50	7.50	1.60	3.1	Thick	4.7	Thick
WI.3	6.00	3.05	9.05	1.30	4.6	Thick	7.0	Moderate
WI.4	5.00	2.80	7.80	1.60	3.1	Thick	4.9	Thick
WII.1	4.00	2.40	6.40	1.15	3.5	Thick	5.6	Thick
WII.2	3.30	3.10	6.40	1.08	3.1	Thick	5.9	Thick
WII.3	5.80	3.10	8.90	1.03	5.6	Thick	8.6	Thin
WIII.1	4.10	2.55	6.65	0.75	5.5	Thick	8.9	Thin
WIII.2	4.10	2.60	6.70	1.4	2.9	Thick	4.8	Thick
WIII.3	6.00	2.90	8.90	0.65	9.2	Thin	13.7	Thin

Robustness is the most important variable for the façade (WI.1) due to the existence of a crack between this macroelement and the lateral walls (Figure 5.2), which perhaps makes the stability of the façade to rely mostly on its geometry and fabric. This crack appears to be caused by the deformation of the lateral walls over the years, either due to the roof thrust or other external actions such as modest ground shakes. Nevertheless, interaction between macroelements is considered favourable due to the foreseen buttressing effect caused by the extension of the lateral walls beyond the façade (these extensions are denoted as B1 and B2 in Figure 4.8). Robustness has a positive influence, since the façade is a thick wall with a low slenderness ratio of 4.5 or 5.8 without and with base course, respectively. Hence, under good conditions of maintenance, the façade is likely to remain stable, even if some parts, such as the gable, might fail. The façade is the most well preserved wall of the building, retaining most of the plaster and painted finishing, which protects it from weather demands, and therefore the 'Materials' attribute is positive. The mezzanine's timber structure can

provide some connection between the façade and the lateral walls; however this benefit is uncertain because little information is available at this stage about the nature of the connection of the mezzanine's joists to the façade and of the mezzanine's beam to the lateral walls.

Although the vertical slenderness of the lateral walls is low, with a maximum of 4.9, these walls are 30m long and lacking effective lateral restraint. This is most evident in the case of the West wall (WI.2). As far as the East wall (WI.4) is concerned, there is evidence of connection by intercalation of adobe units to the sacristy and buttresses B10 and B12 (Figure 4.8). The walls present many holes, made to accommodate niches and large closed openings that are former doors. This has created weak areas and more complex load paths. The roof appears to be unable to provide a good connection between the lateral walls and to support their lateral movement due to the inexistence of roof ties and connectors between the wall plates and the lateral walls. It could be argued that a good connection between the lateral walls and other macroelements would compensate the modest robustness of the walls. In this case, it would be appropriate to assign an 'A' class to 'Interaction' and a 'B' class to 'Robustness'. On the other hand, a good robustness can compensate an unsatisfactory interaction. However, both attributes, as they stand, have a negative influence on the seismic response of the lateral walls, and therefore neither 'Robustness' nor 'Interaction' compensates each other. Thus, the relevance of one over the other is more difficult to recognise. The 'Materials' attribute has a positive influence, since the walls are in general made of a regular arrangement of units and joints. 'Condition' on the other hand is considered negative, since no special measures were taken to protect the core of the walls from weather demands, triggering deterioration.

For the back wall (WI.3), a similar judgment of all attributes can be done. It should be emphasised that it is assumed that the lateral and back walls did never have the same material quality of the façade and, for this reason, the façade is less deteriorated. Alternatively, if it is assumed that weather demands have affected more the lateral and back walls than the façade, especially because the latter is protected by the buttresses at the front and by the roof's gable, a different diagnosis can be done. In this case, 'Condition' can be assumed as 'B-' and 'Materials' as 'C+'.

The 'Materials' attribute of the base course is considered negative, since the base course is composed of heterogeneous stones laid on mud mortar with joints of dimensions that vary within a range of 20 to 60mm. Apart from the high anisotropy of the material, the mortar and the bond mortar/unity is of poor quality. The 'Materials' attribute has a strong influence on

the deterioration of the base course, which is very high at some locations where the mortar of the joints was almost totally lost. At these locations, the stability of the base course relies on friction and on the degree of locking of the aggregates. The deterioration of the base course was especially caused by the action of superficial water, which means that even a better masonry fabric would be strongly affected by erosion under the same conditions.

'Robustness' is considered positive, since the existence of a high base course instead of an adobe wall starting from the foundation has prevented more severe deterioration of the walls due to improper superficial water drainage. Nevertheless, the existence of a base course made of a different material created a plane of discontinuity between the adobe wall and the rubble stone masonry, which compromises the overall interaction between the macroelements. This plane of discontinuity can become a plane of failure when the cohesion between the two materials is overcome by the lateral forces, and rotation or sliding may occur.

The buttresses appear to be poorly designed and not well connected to the lateral walls. When present, these connections are made by means of intercalation of adobe units at the intersections. Historical information shows that this type of connection could be limited to the adobe units located at outer layers and therefore the core of the buttresses might not be connected to the walls. 'Interaction' has the most influential class, since if the interaction between buttresses and walls is poor the purpose of building the buttresses is not accomplished, even if they are robust.

'Interaction' is critical both for the baptistery and sacristy, being negative in the case of the baptistery and positive in the case of the sacristy. Although intercalation of adobe units is present at the intersections of the sacristy with the lateral walls; the same conclusion could not be drawn for the connection of the baptistery with the lateral walls. Hence, the lateral walls do not benefit from the existence of this connection and a phenomenon of hammering can occur. Here, the 'Connections' attribute refers to the connections between the walls of the baptistery and between the walls of the sacristy. Cracks between the façade of the baptistery and sacristy and the corresponding transversal walls show that these structural elements are poorly connected. 'Interaction' is more relevant than 'Connections', since the losses caused by the failure of the lateral walls of the main church may be more severe than the failure of the façade of the baptistery or sacristy. 'Robustness' is considered positive, since the baptistery and sacristy can provide lateral support to the lateral walls of the nave, providing that the interaction between these macroelements is favourable.

The interaction of the tie-beams with the lateral walls is critical and negative, since only a few tie-beams seem to be connected to the walls by means of wooden anchors; whereas the others are resting in the wall without any type of anchorage. The tie-beams without any anchorage can easily slide in relation to the wall, as the connection relies on friction only. Moreover, the tie-beams are located near the top of the walls and therefore the surface of the wall mobilised by earthquake loading can be smaller than the one required to restrain the lateral movement of the walls without the local failure of the anchors. On the other hand, the number, distribution and design of the existing tie-beams, including the collapsed one, appear to be sufficient to restrain laterally the walls if they are properly anchored. For this reason, the 'Robustness' attribute is considered positive. The 'Connections' are also assumed positive, since there are no evidences of the failure of the connection of the anchors with the tie-beams. However, a high level of uncertainty is assigned to this last judgment because information regarding the anchoring conditions is still incomplete.

'Interaction' is the most influential attribute for the structural response of the roof, since the failure of any connection within the roof structure might cause a local failure (for instance the failure of one connection of the rafter to a wall-plate can cause the failure of one roof-truss), whereas the failure of one connection between the roof and the lateral walls can cause a global failure mechanism (for instance the failure of the connection of a wall-plate to the wall can cause the failure of several roof-trusses). 'Interaction' is classified in a negative way, since there are no evidences of a positive connection of the wall-plates to the walls. The wall-plates seem to be resting on the top of the walls without any level of embedment or any vertical element reinforcing the connection. Moreover, the wall-plates are discontinuous and therefore do not behave as a ring beam. 'Robustness' is considered more important than 'Connections' in the case of the roof's structure, since for instance the existence of a ring beam would be beneficial for the response of the walls, which conversely would limit the deformation of the roof. 'Robustness' is also negative since a roof-tie is missing at a lower level of the roof-trusses, as the collar-ties located near the ridge of the roof seem to be unable to resist alone the roof thrust. Moreover, the purlins do not provide longitudinal stability, as they are connected to the rafters by means of leather straps, and their aim is merely to serve as a support to attach the roof cover made of canes. The 'Connections' are also considered negative due to the high flexibility of the roof's structural system, where local failures are likely to occur. Finally, the 'Condition' of the roof is evaluated with a higher level of uncertainty, since the roof was not surveyed with the same level of detail of the other macroelements. The roof is not in poor condition overall; even though some local failures

have occurred, which could be related more to the type of connections than with the level of deterioration. This also justifies the assignment of the lowest influence class to this attribute.

The most influential attribute to the overall structural response of the church is the interaction between macroelements, followed by their robustness, since these attributes present the first and second highest percentage, respectively, of classes A within the total set of attributes, as shown in Figure 5.3. Conversely, the less influential attribute is the condition of the macroelements. Although deterioration has contributed to the partial or total collapse of some macroelements such as the buttresses, the lack of robustness of those elements and the conditions for their interaction are the most important attributes for their structural response and present condition.

As shown in Figure 5.4, the robustness of 56% of the macroelements influenced by this attribute has a favourable effect on the seismic behaviour. On the other hand, the interaction between macroelements is considered unsatisfactory in 78% of the relevant cases. Thus, taking into account its high influence and unfavourable nature, 'Interaction' is a major concern for the improvement of the response of the church to earthquakes.

Table 5.3 shows the average uncertainty or lack of confidence of the EAI-SRP team while making a judgement of the various attributes. It can be seen that 'Condition', 'Materials' and 'Connections' are the attributes judged with larger uncertainty.

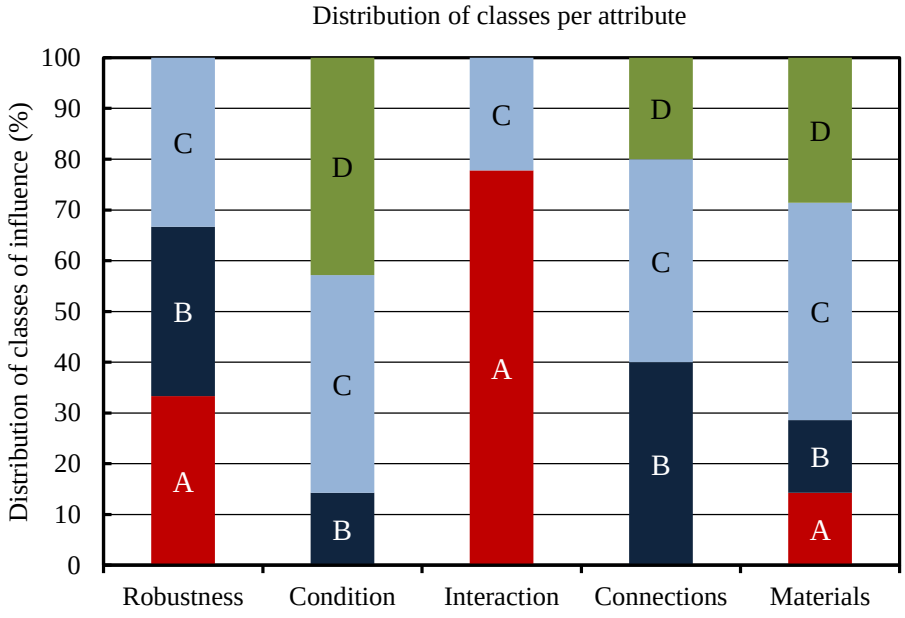

Figure 5.3 Distribution of classes of influence per attribute

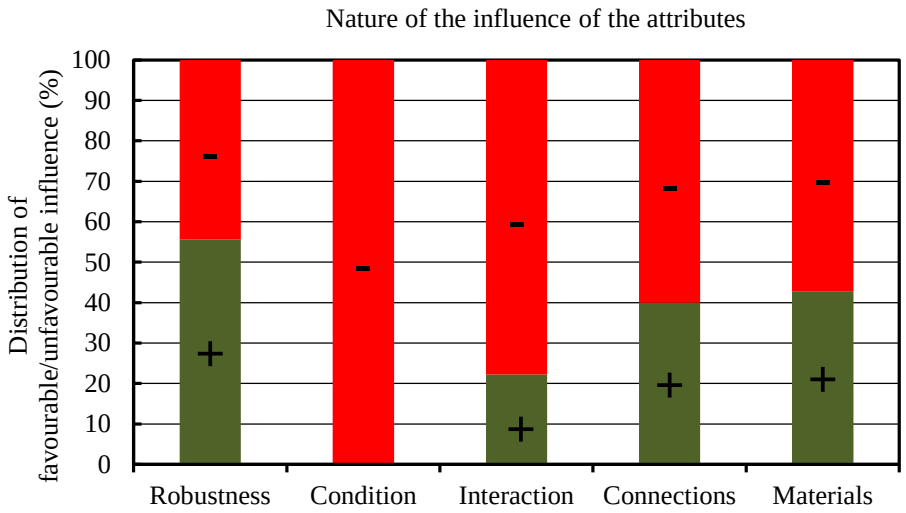

Figure 5.4 Distribution of the nature of the influence of the attributes

Table 5.3 Preliminary analysis of uncertainties of the assessment of the Church of Kuño Tambo

	ATTRIBUTES				
	Robustness	Condition	Interaction	Connections	Materials
δIp_j [equation 3.1]	24%	31%	28%	30%	30%

5.3 Historic earthen and timber churches in low lands: the Cathedral of Ica

A detailed description and interpretation of the principal construction details and damage of the Cathedral of Ica was presented in Section 4.4. The following diagnosis will make reference to this section as appropriate for more clarity.

5.3.1 Macroelements

The cathedral of Ica is assumed as a system composed of the following macroelements, illustrated in Figure 5.5:

1. Main brickwork façade (W1);
   1a. Wall
   1b. Pediment
2. Adobe lateral walls (W2 and W3);
   2a. Walls
   2b. Pediments (shown in green)
3. Towers;
   3a. Brickwork base
   3b. Timber top structure
4. Timber framing, composed of pillars, respective bracing, and horizontal beams;
   4a. Lateral aisles of Bay 1
   4b. Nave and lateral aisles
   4c. Transept
5. Timber vaulting system
   5a. Vault (including bay-edge arches, internal arches, lunette's members, beam at the top of lunettes and bracing between/within bays)
   5b. Central dome
   5c. Lateral domes

The macroelements were sub-divided into several components, according to the distinct construction features and condition after the 2007 Pisco earthquake. For instance, the timber framing is divided into three main components: (a) the lateral aisles of Bay 1, containing the mezzanine and where the left aisle collapsed (Figure 4.44); (b) the nave and lateral aisles; and (c) the transept which interacted with the lateral walls during the earthquake causing damage to wall W2 (Figure 4.45). Similarly, the timber vaulting system can be divided into three main components: (a) the timber vault, which partially collapsed during the 2007 Pisco earthquake (Figure 4.42); (b) the timber lateral domes, which did not undergo significant damage; and (c) the timber central dome, which partially collapsed (Figure 4.42).

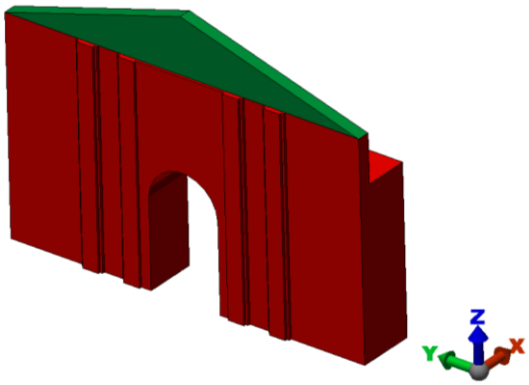

1. Main façade (W1)

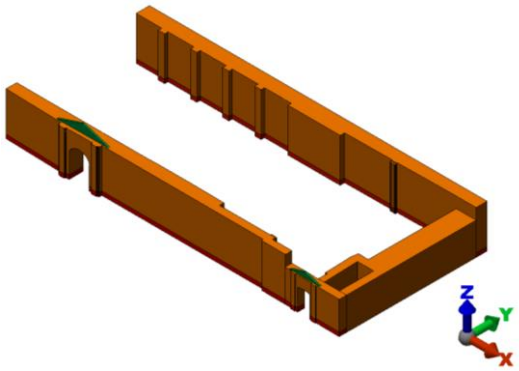

2. Adobe walls (W2 and W3)

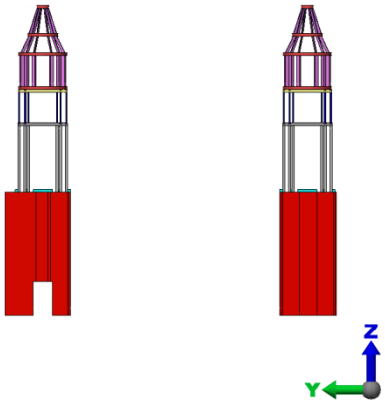

3. Towers (T1 and T2)

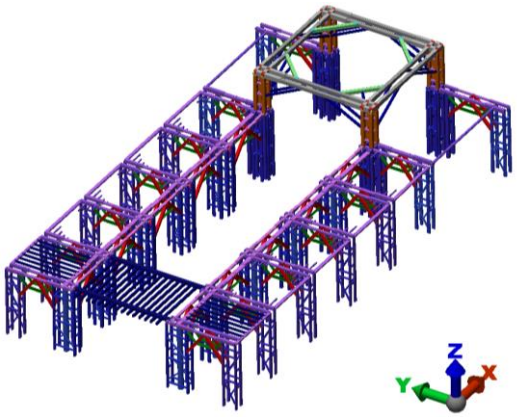

4. Timber framing

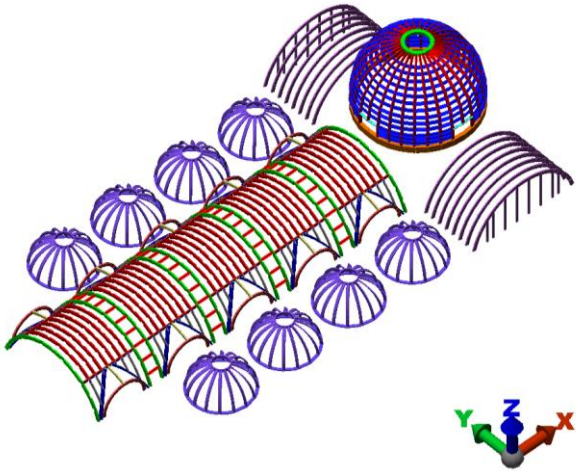

5. Timber vaulting system

Figure 5.5 Macroelements of the Cathedral of Ica

5.3.2 Diagnosis

The preliminary diagnosis of the Cathedral of Ica is summarised in the matrix of Table 5.5. This matrix includes: (i) the five attributes described in Table 3.1; (ii) the macroelements; (iii) the classes of influence A to D of the attributes, described in Table 3.2; (iv) the nature of the influence of the attributes over the macroelements; and (v) the uncertainty, $\delta Ip_{j,i}$, of the analyst in making the judgment.

The vertical slenderness of the walls is shown in Table 5.4. All walls are considered thick and therefore likely to keep stable for large ground motions, according to the definition of Tolles *et al.* (2002); except one quarter of the length of W2 located in the West extremity, which has slenderness greater than 6.

Table 5.4 Vertical slenderness of the masonry walls of the Cathedral of Ica

Wall	Height, *h* (m)	Thickness, *t* (m)	Slenderness (*h*/*t*)	Definition of Tolles *et al*. (2002)
W1a	6.6	1.92 (up to 6.6m)	3.4	Thick wall.
W1b	1.85	0.5 (6.6-8.45m)	3.7	Thick wall.
W2a	6.75	1.0	6.75	Moderate for a length of 11.75m (West portion).
W2b	6.75	1.7	4.0	Thick for a length of 32.5m (East portion).
W3	6.75	1.72-2.0	3.4-3.9	Thick wall.

The brickwork façade is a robust macroelement, laterally restrained by the base of the towers. It is a wall of low slenderness, made of homogeneous and regular fired brick masonry, with a fair condition. Hence, all relevant attributes are considered favourable with a relatively low level of uncertainty. 'Robustness' is considered as the most critical attribute, followed by 'Interactions', since even if the towers did not provide any lateral restraint, the walls would be expected to keep stable due to its robustness.

The base of the pediment has a crack along the intersection with the façade, which shows a weak point of the structure. On the one hand, there is no longitudinal restraint for the pediment, and therefore 'Interaction' is the most critical attribute and negative.

Table 5.5 Matrix of preliminary diagnosis of the Cathedral of Ica

MACROELEMENTS	ATTRIBUTES				
	Robustness	Condition	Interaction	Connections	Materials
1. Main brickwork facade (W1)					
1a. Wall	A + 10%	D + 20%	B + 15%		C + 15%
1b. Pediment	B - 30%		A - 20%		
2. Adobe lateral walls (W2 and W3)					
2a. Walls	A + 20%	B - 20%	C - 30%		D + 30%
2b. Pediments	B + 30%		A + 30%		
3. Towers					
3a. Brickwork base	A + 10%	D + 30%	B - 30%		C + 30%
3b. Timber top structure	A + 30%	D + 30%		B + 40%	C + 50%
4. Timber framing					
4a. Lateral aisles of Bay 1	D - 40%	C - 30%	B - 50%	A - 30%	C + 40%
4b. Nave and lateral aisles	A + 30%	C - 50%	D + 50%	B + 40%	C + 40%
4c. Transept	A + 30%	C - 50%	D - 30%	B + 40%	C + 40%
5. Timber vaulting system					
5a. Vault	A - 10%	A - 10%	D + 40%	B - 40%	C - 40%
5b. Central dome		A - 30%	D - 30%	B - 50%	C - 40%
5c. Lateral domes		A - 30%	D + 30%	B + 40%	C - 40%

On the other hand, the pediment has a thickness smaller than the thickness of the façade and therefore a discontinuity is present at this location, which creates a weak point, even if some longitudinal restraint is present. 'Robustness' is therefore considered important and negative.

The lateral adobe walls (W2 and W3) have a good overall robustness, with low slenderness except in specific portions. These walls remained stable during and after the 2007 Pisco earthquake. 'Robustness' is hence considered the most critical and favourable attribute.

However, deterioration caused by water and salts, especially affecting wall W3, reduced the strength of the wall, contributing in a negative way to its structural response. It is reasonable to conclude that it was the deterioration of the wall that led to the construction of a reinforced concrete frame adjacent to the South face of wall W3 at the location of the transept, in order to provide additional lateral stability. 'Condition' is therefore considered relevant and negative. Interaction of the lateral walls with the timber structure of the transept was unfavourable, as cracks were observed on the face of wall W2. This damage seems to be caused by hammering of the adjacent timber framing and masonry walls. Moreover, poor interaction was also observed at the interface of the lateral adobe walls with the brickwork base of the towers (Figure 4.45). 'Interaction' is therefore considered negative. On the other hand, the pediments of wall W2, of smaller dimensions than the pediment of the main façade, appear to be robust and to interact well with the wall, since no visible damage was observed.

The bell towers had a good structural response to the 2007 Pisco earthquake. The base is a robust fired brick masonry structure in overall fair condition. The only negative attribute of the towers' base is associated to the poor interaction with the lateral adobe walls, which caused vertical cracks and separation of these two macroelements, as explained above. As far as the towers' top timber structure is concerned, it appears to be a robust structure with no significant permanent deformations after the earthquake. No evidence of failure of the timber joints was observed; and hence the 'Connections' variable is considered positive. The timber members appear to be in overall good condition, even though no detailed information about wooden species is available.

The roof of the left aisle of bay 1 collapsed due to the collapse of the longitudinal beam running between the lateral pillars, as shown in Figure 4.44b. The collapse of the beam was caused by the failure of the joint connecting the beam to the horizontal bracing of the lateral pillar (Figure 4.44c). Since the joint failed, the 'Connections' attribute is considered the most

critical and negative. It is followed by the 'Interactions' attribute with an unfavourable influence due to the potential negative effects of the interaction of a flexible timber framing with a façade that vibrates with higher frequency.

The timber framing of the nave and lateral aisles appears to be a robust system of braced posts and beams, with timber joints that had an overall good structural performance during the 2007 Pisco earthquake, since no significant permanent deformations were observed in the framing. Thus, all attributes are considered positive except the condition, since deterioration of longitudinal beams were observed in a few locations (Figure 4.36, detail 6). However, it should be emphasized that there is no detailed information about the timber joints and wooden species. Hence, further investigations are required to address this lack of information.

The performance of the timber structure of the transept appears to have been similar to the performance of the framing of the nave and lateral aisles. However, the transept had a negative interaction with the lateral adobe walls, causing cracks in wall W2, as discussed above. Hence, the 'Interaction' attribute is considered negative for the transept.

'Robustness' and 'Condition' are considered critical to the structural behaviour of the vault, followed by the timber 'Connections'. This judgment is mostly based on evidences observed on site that the weakest point of the structure is the top of lunettes, where the internal arches and the lunettes' members are connected to a longitudinal beam. Although the failure of the joints at the top of lunettes might have been triggered by material deterioration (Figure 4.41), the structural arrangement consisting of several mortice and tenon joints closely spaced reveal a weak structural point, even if the material is in good condition and the timber joints are well designed. The information collected on site is insufficient to formulate a hypothesis for the failure of the bay-edge arches. More detailed structural analyses are required to reach a conclusion. The interaction of the vault with the timber framing is considered favourable since no local failures of the mortice and tenon joints connecting the arches and lunettes' members to the beams were observed on the site (Figure 4.36, detail 6). However, this judgment is made with a high level of uncertainty due to the impossibility of observing the condition of those joints on the site. Further field investigations must be conducted to verify this judgment.

The partial collapse of the main dome seems to have been triggered by deterioration of the timber members. The timber joints were not surveyed in detail and therefore the 'Connections' attribute is classified with high uncertainty.

Finally, although the lateral domes have also some evidences of deterioration, no major damage or deformation was observed in this macroelement. Hence, it is considered that the connections of the elements of these domes are well designed and constructed, and the lateral domes interact well with the timber framing.

The most influential attribute to the structural response of the Cathedral of Ica is 'Robustness', followed by 'Connections', 'Interaction' and 'Condition', as shown in Figure 5.6. Robustness is a critical attribute for 70% of the macroelements which are influenced by this attribute. For macroelements influenced by the performance of connections, the 'Connections' attribute is either critical or relevant, as per the classes of influence of Figure 5.6. Figure 5.7 shows that the condition is poor in 70% of the macroelements that are influenced by this attribute.

Table 5.6 shows the average uncertainty or lack of confidence of the EAI-SRP team while making a judgement of the various attributes. It can be seen that 'Connections' and 'Materials' are the attributes judged with larger uncertainty. The uncertainty of the diagnosis of the Cathedral of Ica is overall higher than the uncertainty of the assessment of the Church of Kuño Tambo. This reflects the fact that most of the timber structure of the cathedral was hidden by plaster, and therefore could not be observed on the site.

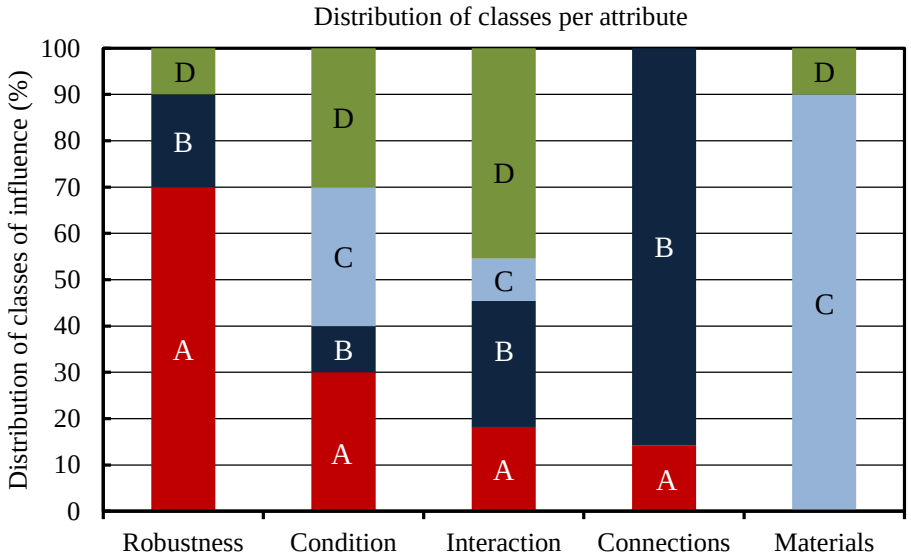

Figure 5.6 Distribution of classes of influence per attribute

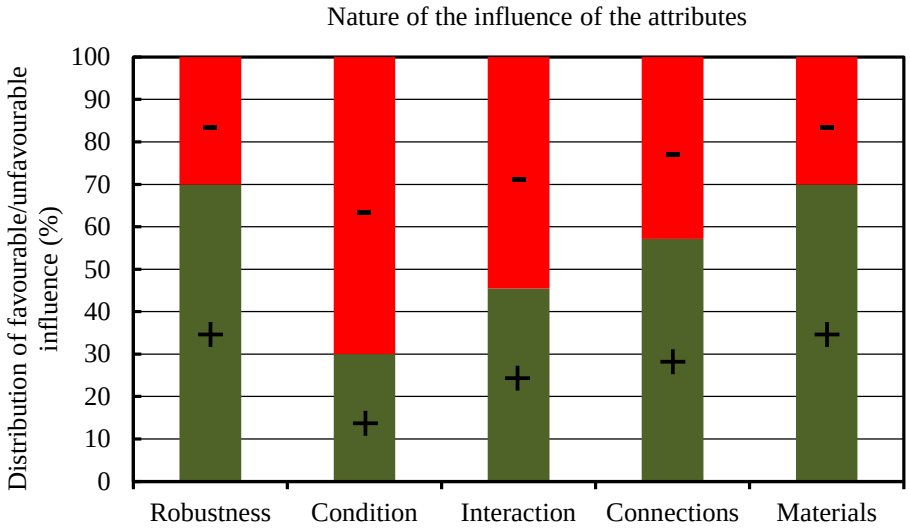

Figure 5.7 Distribution of the nature of the influence of the attributes

Table 5.6 Preliminary analysis of uncertainties of the assessment of the Cathedral of Ica

	ATTRIBUTES				
	Robustness	Condition	Interaction	Connections	Materials
δIp_j [equation 3.1]	24%	30%	32%	40%	37%

5.4 Conclusions

Taking into account this preliminary diagnosis, more detailed structural analysis of the Church of Kuño Tambo will investigate the following main issues:

(i) The interaction between the buttresses and the longitudinal walls;

(ii) The connection of the tie beams to the walls, which should be also further investigated through experimental work;

(iii) The interaction of the main nave with the baptistery and sacristy; and

(iv) The interface between the base course and the adobe masonry. Tests should be performed in order to quantify the level of friction among the two materials.

Conversely, more detailed investigations and structural analysis of the Cathedral of Ica will investigate the following main issues:

(i) Sensitivity analysis should be conducted to identify and determine the influence of the most critical joints to the seismic performance of the timber frame;

(ii) The mechanical properties of the critical timber joints need to be characterized by means of experimental tests. The critical joints to be tested should be identified by means of sensitivity analysis;

(iii) The wooden species should be identified and characterized by means of experimental work;

(iv) The reason why the bay-edge arches failed;

(v) The reason why in many bays of the nave only the internal arches have collapsed and not the bay-edge arches; and

(vi) The hypothesis of the roof's cladding behaving as a rigid or flexible diaphragm should be investigated.

As far as the laws of mathematics refer to reality, they are not certain;
and as far as they are certain, they do not refer to reality.

Albert Einstein

CHAPTER 6

Quantitative analysis at the local level and knowledge-based uncertainty of historic adobe and timber churches

6.1 Introduction

The preliminary diagnosis of the Church of Kuño Tambo and Cathedral of Ica provided an initial understanding of the critical aspects that govern the structural response of historic churches in Peru on the basis of field observations and analyst's judgement. Those critical aspects are here analysed in more detail at a local level, while the uncertainties present in the assessment due to limited knowledge are also estimated. This work will inform more complex analyses conducted at the global level and provide a method of measuring uncertainties and propagating it up to the final diagnosis. The sequence and logic of this strategy follows the approach described in Chapter 3 and illustrated in Figure 3.1.

The term 'local level' is here used to denote structural analyses that are performed with portions of the structures (i.e. local models, LM). These analyses allow the simulation of local structural responses, the calibration of input parameters and the verification of alternative hypotheses regarding the behaviour and modelling of the structures. The local models are also used to quantify the uncertainty of the inputs and identify the critical variables.

The local analyses conducted in this chapter illustrate the distinct research questions and challenges posed to the analysis of adobe and timber churches in countries like Peru. The Church of Kuño Tambo represents historic churches built in high lands with a simple layout made of a material difficult to simulate - adobe. On the other hand, the structural behaviour of churches in low lands, such as the Cathedral of Ica, is governed by the response of a timber structure and masonry walls. In order to prove the validity of the methodology proposed in Chapter 3, the aim here is to test this methodology in the assessment of the timber structure only, since the masonry system in this type of church requires an investigation similar to the one conducted for the Church of Kuño Tambo. The timber structure of the Cathedral of Ica represents a construction with a complex geometry and hundreds of joints whose simulation has not been investigated in the past.

Having as reference the Church of Kuño Tambo and the Cathedral of Ica, an answer to the following research questions is pursued in the present chapter:

(a) *How detailed should the structural analysis of historic adobe and timber churches be to make a final meaningful diagnosis?*
(b) *What are the main uncertainties present in such structural analysis and what is their influence?*

The software package Autodesk Simulation Multiphysics 2013© is used to carry out the numerical analysis. This software has a good 3D graphic interface, allowing complex geometries to be simulated. It also includes a large suite of linear and nonlinear material models and finite elements which can be adapted to the purpose of the analysis. Moreover, it allows importing 3-D architectural models from AUTOCAD© and convert them into finite element models with relatively little operator input. There are several other software packages commercially available, which can be used by professionals in South America to conduct similar analyses. The modelling approach and the software used in this research were selected with the purpose of developing a procedure that can be applied by practitioners.

This chapter discusses relevant hypotheses for the structural analysis of historic adobe and timber churches at the local level. Investigation of these hypotheses helps to refine the local model of the churches, which is used in its final state in the analysis of the uncertainty of the input. In the case of the Cathedral of Ica, emphasis is here given to the modelling of

the planked arches, since the failure of the nailed joints of these arches was the most significant failure observed in many churches after the 2007 Pisco earthquake.

6.2 Analysis of a historic adobe church at the local level

The structural behaviour of adobe churches in high lands in Peru, such as the Church of Kuño Tambo, is governed by the response of thick walls and buttresses. In such cases, the following hypotheses require a detailed investigation:

(i) Relevance of transverse shear deformation;
(ii) Material model;
(iii) Distribution of shear stresses through the thickness of the walls;
(iv) Effect of boundary conditions; and
(v) Effect of the base course.

6.2.1 Material properties

At an initial phase of the assessment of a historic building or if experimental work can not be carried out, the material properties of the structure can be defined on the basis of information available in literature. Annex I presents a summary of results of tests performed on adobe and rubble stone masonry available in literature. Taking into account that the characterisation of the material properties of historic buildings by means of experimental tests is often not feasible or limited, the availability of information in literature can dictate the uncertainty of the analysis. The availability in literature of material properties of adobe, which is the principal structural material of earthen churches in Peru, is qualified in terms of low, medium and high based on an extensive literature review in Table 6.1. 'High' means that the property is easily available in literature and therefore a wide range of data can be compared. 'Medium' means that information about the property is available in literature up to a rather limited extent, which limits the representativeness of the data. Finally, 'low' means that information about the property is rare in literature and when available the representativeness is normally valid to a specific case study. Table 6.1 also shows the properties obtained by an experimental campaign conducted within the EAI-SRP with the purpose of characterizing the material behaviour of the Church of Kuño Tambo and Cathedral of Ica. The author participated in the planning of these tests, which were carried out by PUCP.

Table 6.1 Availability of information in literature to characterise the material behaviour of adobe

Property		Availability in literature reporting experimental work			PUCP experimental campaign
		Low	Medium	High	
Specific weight	w		X		X
Modulus of elasticity	E		X		X
Poisson ratio	υ	X			X
Cohesion	c	X			X
Internal friction angle	φ	X			X
Shear strength	fv		X		X
Compression strength	fc		X		X
Tension strength	f_t	X			X
Bond strength	f_b	X			X
Biaxial compression strength	bf_c	X			
Fracture energy	G_f	X			

In general, information about adobe is rare in literature compared to fired brick masonry for instance. The modulus of elasticity and the compression and shear strength are the most common properties obtained by experimental work conducted on adobe. This information is directly relevant to the Peruvian churches, and this can be explained by the fact that compression tests and diagonal compression tests are indicated in the Peruvian code for earthquake resistance (E.080, 2006) for the determination of the compression and shear strength used in the design of new adobe structures, being therefore a common practice in the country.

Based on the literature review of Annex I and provisions of standards and codes (e.g. E.020, 2006), the material properties of Table 6.2 were adopted in the local models and preliminary global models of the Church of Kuño Tambo. These material properties were revised and adjusted after the results of compression and shear tests carried out at PUCP with specimens made either of original materials or new materials reproducing the original ones were available. Details of these tests can be found in Torrealva and Vicente (2014). The final material properties used in the uncertainty analysis, final analysis at the global level and detailed diagnosis are also indicated in Table 6.2. This table also shows the material models that are characterized by the various variables. As will be discussed in the following, the structural analyses conducted at the local level showed that the Drucker-Prager is more appropriate to model adobe churches than concrete-based material models. From these

results, the experimental work at PUCP was planned such as to provide the necessary inputs to characterize the Drucker-Prager model. For this reason, no experimental inputs for the Modified HTC model were obtained.

Table 6.2 Material properties adopted in the local models of Kuño Tambo from information available in literature and experimental work conducted at PUCP

Material		Control Variables	Values from literature	Values from PUCP tests	Units
Adobe	Elastic properties	Modulus of elasticity	200000	140000	kPa
		Poisson ratio	0.15		m/m
	Drucker-Prager model	Cohesion	30	41	kPa
		Friction angle	0.47	0.55	rad
		Specific weight	19	16	$kN.m^{-3}$
		Tension cut-off	20	30	kPa
	Modified HTC model	Uniaxial tensile strength	50		kPa
		Uniaxial compressive strength	1000		kPa
		Biaxial compressive strength	1160		kPa
		Fracture energy/area	272.86		J/m^{-2}
Rubble stone masonry	Elastic properties	Modulus of elasticity	800000	870000	kPa
		Poisson ratio	0.20	0.20	m/m
	Drucker-Prager model	Cohesion	100	65	kPa
		Friction angle	0.37	0.42	rad
		Specific weight	19	19	$kN.m^{-3}$
		Tension cut-off	85	55	kPa

6.2.2 Local model of the Church of Kuño Tambo

The sacristy is modelled here for the analysis at the local level (Figure 6.1), since the modelling of this portion of the church is sufficient to investigate the aforementioned hypotheses. The sacristy is composed of three adobe walls with rubble stone masonry base course and two windows with timber lintels. The model is composed of volume elements and subjected to permanent loading, simulating the self-weight of the structural materials, distributed vertical loading, representing the self-weight of the roof, and distributed horizontal loading at the top of the walls, representing the roof's thrust. An equivalent acceleration is applied in both the X and Y global direction to represent earthquake action,

which is depicted in Figure 6.1 by a resultant vector. The term ‘equivalent’ is used here to denote a body force (mass*acceleration) that is a static equivalent to seismic excitation.

Taking into account the modest height of the building, the uniform mass distribution and prevalent shear behaviour, the acceleration is considered constant over the height of the model. The magnitude of the acceleration is increased monotonically from 0 to the value that determines the failure of the structure, hence performing a push over analysis.

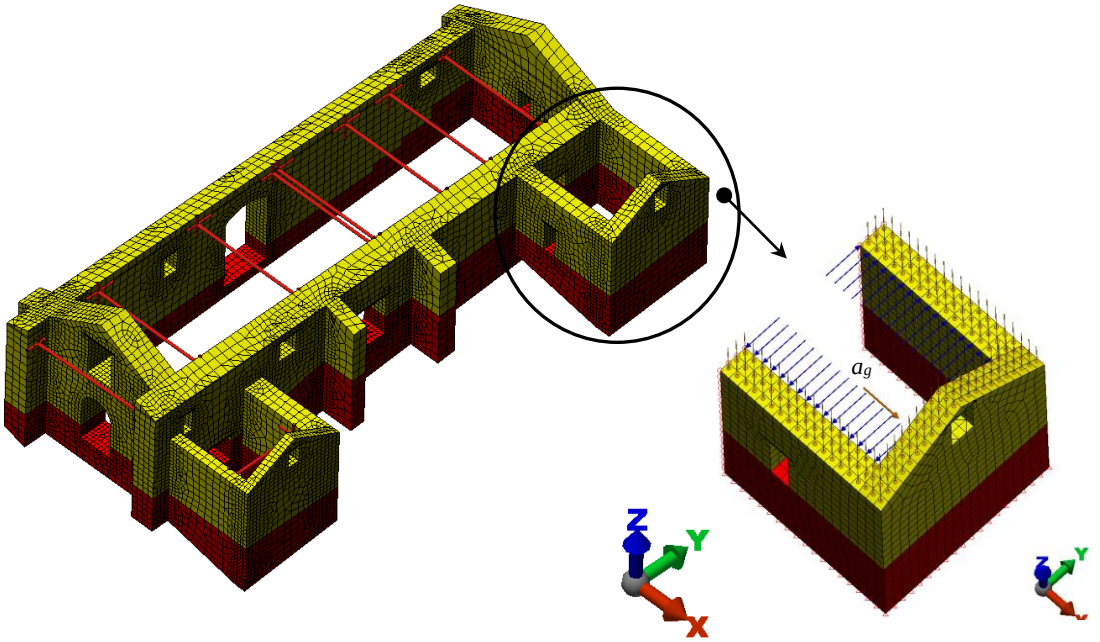

a) Global model b) Local model (sacristy)

Figure 6.1 Local and global models of the Church of Kuño Tambo

6.2.3 Relevance of transverse shear deformation

Most walls of the church are thick, with vertical slenderness ratios inferior to 6. Thus, it can be assumed that stresses are not constant through the thickness of the walls due to eccentricities of the vertical loads, and bending and shear caused by earthquake loading. Plate or shell elements are often used to simulate the structural response of masonry walls, since the meshing and handling of those elements are normally easier than volume elements. Investigations conducted with a local model of Kuño Tambo made of plate elements show that the distribution of maximum principal stresses and the deformation of the model are similar to the response obtained with the model with volume elements (Figure 6.2).

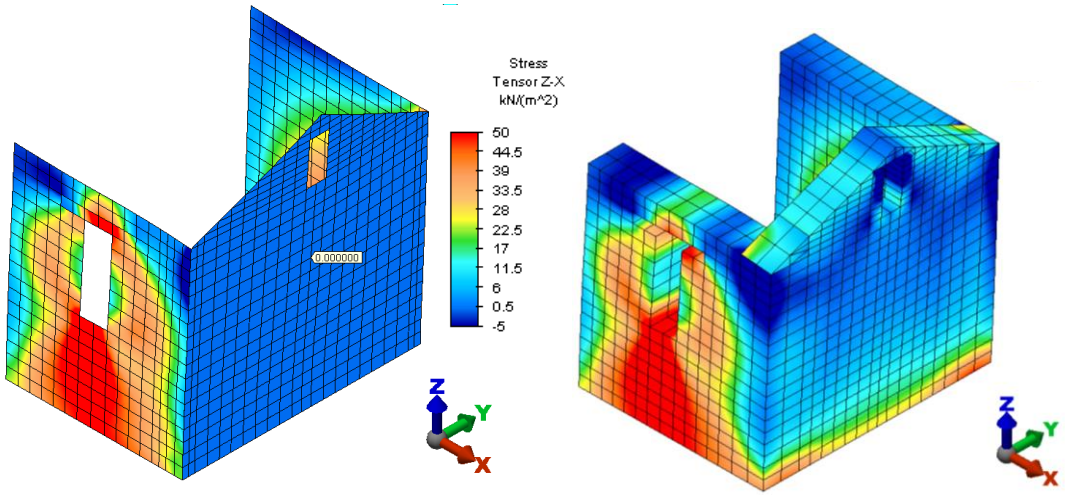

a) Model with plate elements based on the Kirchhoff-Love plate theory

b) Model with volume elements

Figure 6.2 Distribution of principal stresses in the local model with plate and volume elements

However, the volume element model presents shear stresses higher than 20kPa at lower levels of the façade for an equivalent acceleration of 0.3g in X-direction, which is within the order of magnitude of typical shear strength of adobe masonry as shown in Table I.1 of Annex I. Thus, out-of-plane shear stresses in the case of adobe churches cannot be overlooked. A direct conclusion of this simulation is that thin plates based on the Kirchhoff-Love plate theory (Love, 1888) should not be used in the assessment of this type of structure, since this type of plates are unable to represent out-of-plane (through depth) shear stresses (by hypothesis, $\tau_{Z\text{-}X}$ equal to zero in the façade of the sacristy when an equivalent acceleration is applied in the X-direction), as shown in Figure 6.2a. Moreover, thin plates do not provide a good representation of maximum principal stresses in parts where their orientation corresponds to the through depth shear stresses which accompany out-of-plane overturning mode of failure.

6.2.4 Material model

The most widely applied material models to the analysis of masonry structures, in particular adobe structures, are the Drucker-Prager and concrete-based models as discussed in Chapter 2. In the Drucker-Prager model (Drucker and Prager, 1952), failure is governed by cohesion *c* and internal friction angle θ, as shown by the yield function of equation 6.1:

$$F(t) = aI_1(t) + \sigma(t) - \beta \quad [6.1]$$

$$I_1(t) = \sigma_{11}(t) + \sigma_{22}(t) + \sigma_{33}(t) \quad [6.2]$$

$$\sigma(t) = \sqrt{\frac{1}{2}\sum_{i,j=1}^{3} S_{i,j}(t) S_{ij}(t)} \quad [6.3]$$

$$S_{ij}(t) = \sigma_{ij} - \frac{1}{3}\delta_{ij} I_1(t) \quad [6.4]$$

, where the parameters α and β are given by equation 6.5 and 6.6 respectively.

$$\alpha = \frac{2\sin\theta}{(3 - \sin\theta)\sqrt{3}} \quad [6.5]$$

$$\beta = \frac{6c\cos\theta}{(3 - \sin\theta)\sqrt{3}} \quad [6.6]$$

These equations show that both deviatoric (S_{ij}) and hydrostatic stresses, expressed in the form of the stress invariant I_1, govern the failure of the material. Failure in shear is therefore dependent on the state of hydrostatic stresses. Materials that follow this failure criterion are called non-conforming, as they do not comply with the associative rules of plasticity that state normality of strain vector at failure with respect to the failure surface.

In modelling procedures where units and joints are not discretised; cohesion and internal friction angle govern a failure that can occur in any direction depending on the loading. Experimental tests to characterize these variables are usually performed on masonry under shear parallel to the bed joints in presence of a normal load (see for instance the provisions of BSI, 2002) and values are taken from the cohesion and internal friction angle of the bed joint. Work by Calderini *et al.* (2010) discusses the use of diagonal compression tests to obtain values of cohesion and friction coefficient of mortar joints. This method could be particularly useful to obtain representative values of cohesion and friction angle for irregular

masonry arrangements. Moreover, diagonal compression tests are a common practice in Peru as discussed in section 6.2.1, and therefore a potential good source of information on material behaviour.

The software package ASM© has available a modified Drucker-Prager material model, which allows to define a tension cut-off region and a cap hardening region (Figure 6.3). The tension cut-off, T_{cut}, takes into account the fact that masonry has a low tensile strength, which is independent of the initial cohesion and friction angle as per the hypothesis of Mohr-Coulomb criterion. The tensile strength value is usually difficult to define in terms of laboratory testing. It can be obtained from diagonal compression tests or considered as the flexural bond strength of masonry obtained by the bond wrench method of testing (see for instance BSI, 2005). Zhou *et al.* (2008) performed series of tests on brickwork bonded with lime-based mortar and have achieved a good correlation between results of bond wrench tests and values of flexural strengths (with planes of failure parallel to the bed joints) obtained by means of tests performed in accordance with BSI (1999).

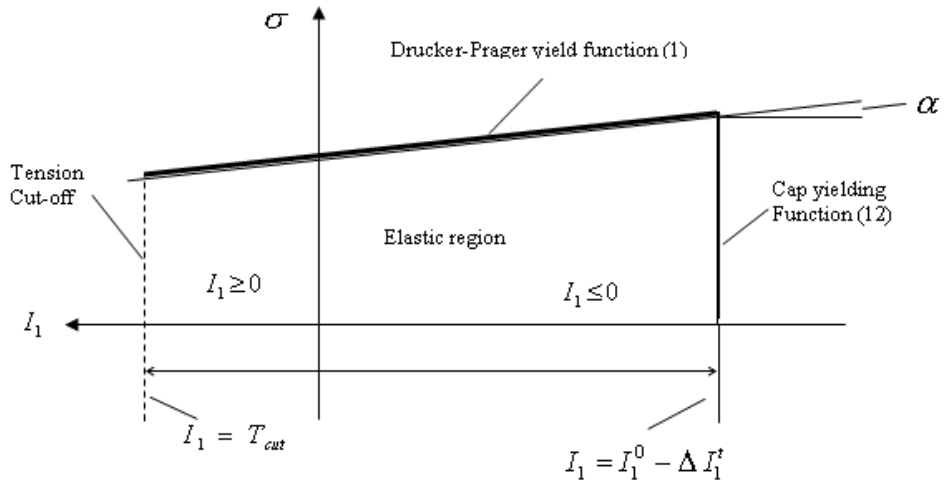

Figure 6.3 Modified Drucker-Prager yield function (User Guide of the Autodesk Simulation Multiphysics 2013©)

In Figure 6.3, ΔI_1^t is the increment of the cap position due to pressure hardening and it is a function of two cap hardening parameters, C_1 and C_2, the plastic volume strain and the initial cap position, I_1^0. The cap considers the fact that purely hydrostatic compression introduces plasticity. However, in seismic analysis of historic adobe churches with thick walls and light roofs, it is reasonable to assume that the peak compression strength is rarely achieved before the masonry fails in shear or tension, in real loading conditions.

The concrete-based material model available in ASM©, namely the Modified Hsieh-Ting-Chen (HTC) model, uses a failure function similar to the HTC four-parameter criterion (Chen and Han, 1998). However, the effect of the angle of Lode φ is introduced by means of the deviatoric radius r representation of Willam and Warnke (1975), as follows:

$$F = a_1\left(\frac{\rho r}{f_c'}\right) + a_2\left(\frac{\rho r}{f_c'}\right) + a_3\frac{\xi}{f_c'} - 1 = 0 \qquad [6.7]$$

$$r(\theta, e) = \frac{4\left(1-e^2\right)\cos^2\theta + (2e-1)^2}{2\left(1-e^2\right)\cos\theta + (2e-1)\sqrt{4\left(1-e^2\right)\cos^2\theta + 5e^2 - 4e}} \qquad [6.8]$$

$$e = 1 - 0.5\frac{\xi_0 - c_0 f_c'}{\xi - c_0 f_c'} \qquad [6.9]$$

,where e is the eccentricity as defined by Kang and William (1999), C_0 is a material constant that can be calibrated from experiments, ξ, ρ and φ are the Haigh-Westergaard coordinates, ξ_0 is the equi-triaxial tensile strength ($\xi_0 = \sqrt[3]{f_t'}$) and f_c' denotes the uniaxial compression strength.

The Modified HTC model has a failure surface similar to the Drucker-Prager surface, but the representation in the deviatoric plane varies, being a circle only when the failure is independent of the angle of Lode (Figure 6.4). In the case of Drucker-Prager, the failure surface is always represented by a circle in the deviatoric plane (Figure 6.4).

A constitutive law with compression hardening and linear softening in tension is defined for the Modified HTC model in the post elastic range. A shear retention coefficient can be introduced, in which a value of 1 indicates that the structure is able to completely transmit shear forces parallel to the plane of the crack, whereas a value equal to 0 indicates a perfectly smooth crack with no friction. In reality, the value of shear retention lies between 1 and 0; however a value of 0 is adopted here since it results in better solution convergence while being also the most unfavourable condition.

Nonlinear static (pushover) analyses conducted with the local model of the Church of Kuño Tambo using the material properties of Table 6.2 show that the Modified HTC model leads to a globally stiffer structure with a more brittle failure and unrealistic high values of shear stress. The Drucker-Prager model has higher relative tensile to shear strength in the out-of-plane wall. Such evidences can be seen in Figure 6.5, where the $\sigma_{z\text{-}z}$-$\tau_{z\text{-}x}$ stress state of both material models is compared with Mohr-Coulomb failure envelopes derived

independently with the same values of cohesion and friction angle. Thus, the Drucker-Prager model provides more realistic results for historic adobe masonry and it is therefore adopted here for the global analysis.

Principal stress space	Deviatoric plane
Drucker-Prager model	
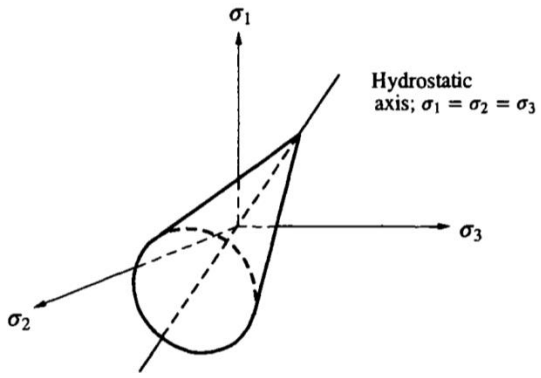	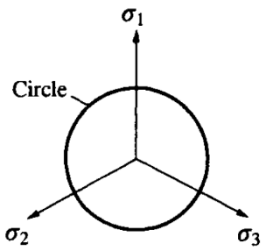
Modified HTC model	
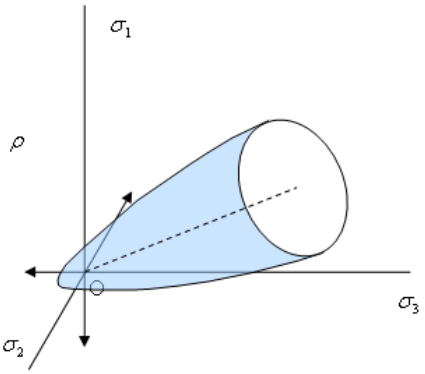	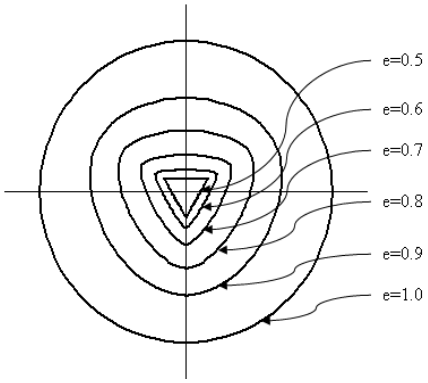

Figure 6.4 Drucker-Prager and Modified HTC surfaces (Ottosen and Ristinmaa, 2005; User Guide of the Autodesk Simulation Multiphysics 2013©)

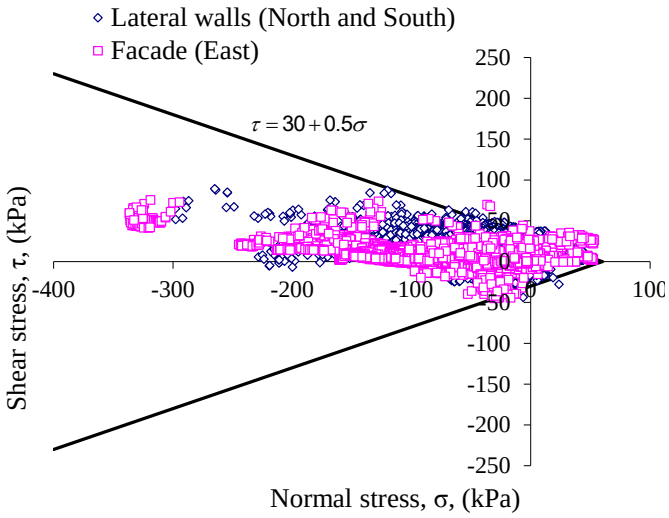

a) Drucker-Prager model

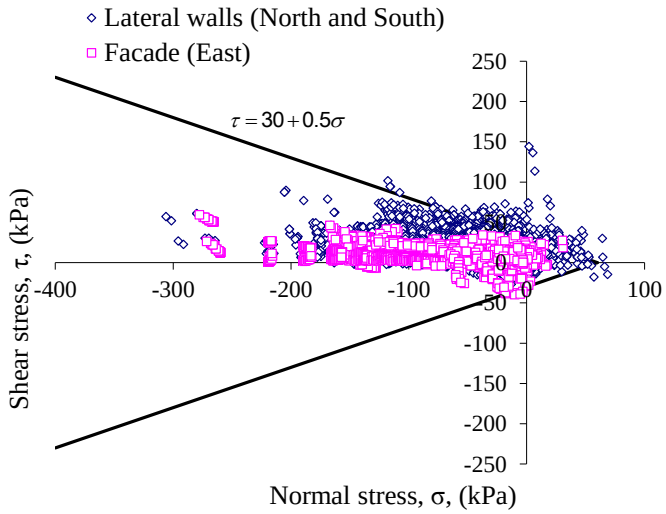

b) Modified HTC model

Figure 6.5 Comparison of the stress state of the local model of the Church of Kuño Tambo with the Mohr-Coulomb failure criterion

6.2.5 Distribution of shear stresses through the thickness of the walls

Constant strain elements are used to model the sacristy. A direct consequence of this modelling choice is the need to use more than one element through the thickness of the thick walls of the church in order to simulate the variation of strain. Nonlinear static (pushover) analyses are conducted with the local model of the church assuming a Drucker-Prager material model for the adobe walls. The analysis of alternative hypotheses of different number of elements spread across the thickness of the walls shows that models with less number of elements are slightly stiffer than models with more elements, as it would be

expected when dealing with constant strain elements. Figure 6.6 illustrates the difference between the distribution of out-of-plane shear stresses in a 2-elements and 3-elements model. It shows that the model with 3 volume elements simulates more accurately through-thickness shear stresses. However, to evaluate the implications of such differences, the results of both models in terms of $\sigma_{z\text{-}z}$-$\tau_{z\text{-}x}$ distributions are compared with Mohr-Coulomb failure envelopes. These comparisons show for instance that 1.3% of the elements of the out-of-plane façade fail in the 2-elements through thickness model whereas in the 3-elements model the same proportion is 1.2%. Since these differences are rather small and the use of 2 elements decreases the mesh complexity and the analysis runtime while providing results that are slightly conservative, a minimum of 2 elements through the thickness of the walls is the modelling choice taken forward for the global model. In the case of large masonry buildings, such as churches, the number of elements should be kept to a minimum necessary to provide reasonable results. Otherwise, the time necessary to handle the geometry and run the analyses would be impractical at a professional level. The aim of this type of local analyses is to identify the correct balance between the appropriateness of the model and the practicality of the analysis.

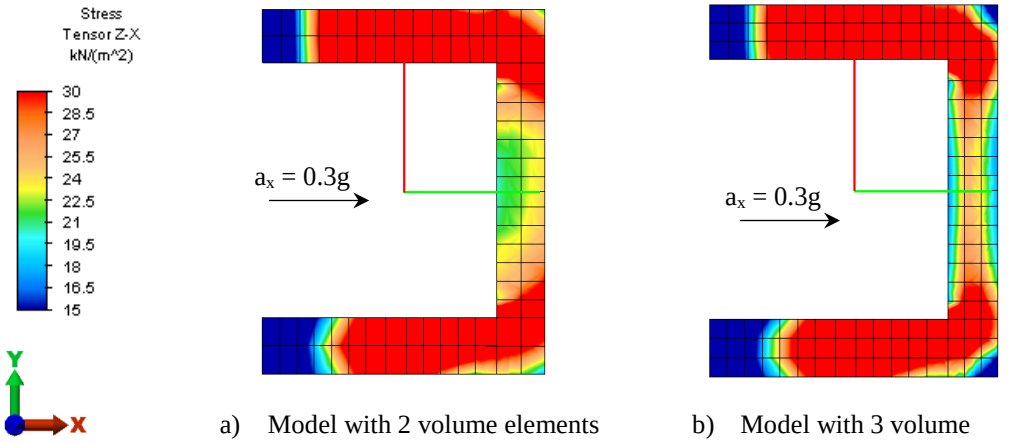

a) Model with 2 volume elements spread across the thickness of the walls

b) Model with 3 volume elements spread across the thickness of the walls

Figure 6.6 Shear stresses ($\tau_{z\text{-}x}$) distribution through the thickness of the walls of the sacristy

6.2.6 Effect of boundary conditions

During the field investigations, foundation failure was not observed in the Church of Kuño Tambo, and hence a detailed numerical modelling of the soil/foundation interaction is not required. However, the local model of the church has rigid constraints at the bottom of the walls, which causes concentration of stresses at the base due to the sharp variation of stiffness between the adobe masonry and the boundary. Springs are therefore used at the base to allow some deformation in the horizontal plane.

The $\sigma_{z\text{-}z}$-$\tau_{z\text{-}x}$ state of stress of the local model with springs at the bottom with 4E3kN/m stiffness after nonlinear static (pushover) analysis is compared with a Mohr-Coulomb failure envelop in Figure 6.7. Comparison of Figure 6.7 with Figure 6.5a highlights the fact that shear is more significant for points subjected to normal compression rather than normal tension in the model with elastic springs. This is a more realistic distribution of stresses in an adobe structure. The use of elastic foundations is therefore preferred for the global model.

However, the use of flexible constraints at the base should not significantly alter the global results of the model. Sensitivity analysis can be used to identify the appropriate value of stiffness. In terms of displacement, Figure 6.8 shows that the use of springs of 5E4kN/m stiffness yields global results that differ little from the infinite rigid ones, without causing spurious stress concentration.

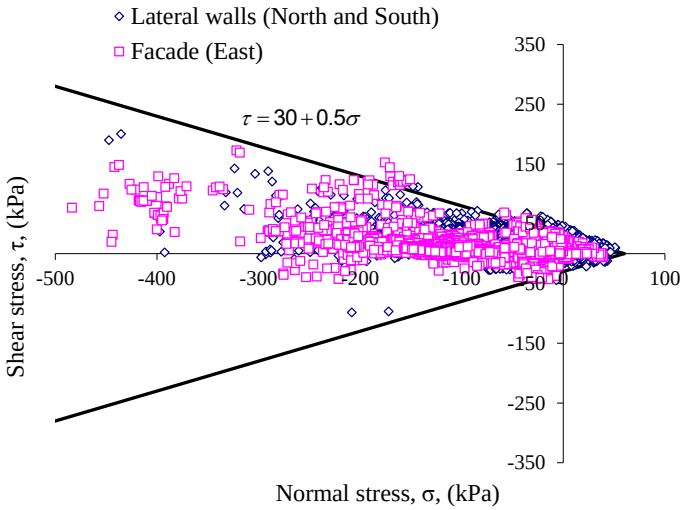

Figure 6.7 Comparison of the stress state of the local model of the Church of Kuño Tambo with flexible constraints at the base with the Mohr-Coulomb failure criterion

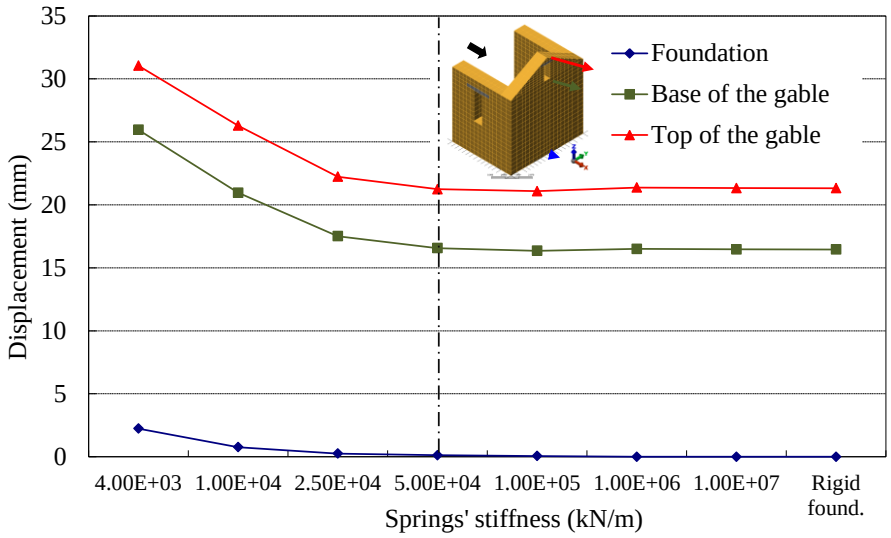

Figure 6.8 Maximum displacements of the local model of the Church of Kuño Tambo for different values of stiffness of the springs simulating elastic boundaries at the base

6.2.7 Discussion of results of the analyses at the local level

Alternative hypotheses provide different capacity curves and stress states. Figure 6.9 shows the capacity curves of the various hypotheses verified with the local model of the church. The Drucker-Prager model is more ductile and simulates well the early decrease of stiffness of adobe structures due to cracking at low values of loading. On the other hand, the Modified HTC model presents higher capacity and a more brittle failure. Although out-of-plane shear stresses are relevant to assess the lateral capacity of thick adobe masonry structures, the use of more than 2 elements through the thickness of the walls do not considerably change the results. The models of the sacristy discussed so far are only composed of adobe walls; however the walls of the historic churches of the Andean region have rubble stone base courses. A local model of the church with a rubble stone base course is also analysed and the respective results compared with the other models in Figure 6.9. The Drucker-Prager material model is assumed for both adobe and rubble stone masonry. The capacity curves show that the model with base course is stiffer and has higher capacity than the model without base course.

Figure 6.10 shows the $\sigma_{z\text{-}z}$-$\tau_{z\text{-}x}$ stress state at four critical locations both in the façade and lateral walls. Point 3 is located at mid-thickness of the façade.

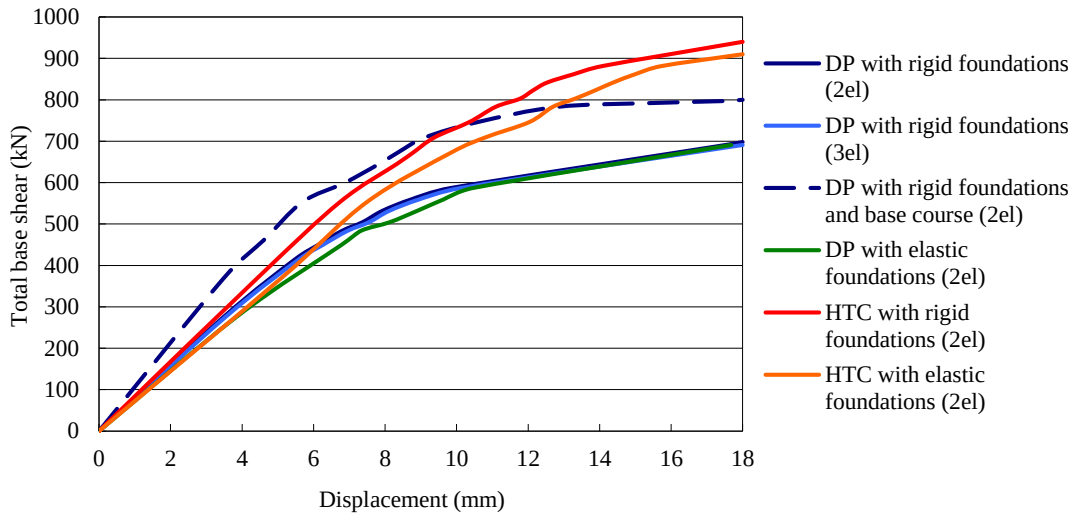

DP: Drucker-Prager
HTC: Modified Hsieh-Ting-Chen criterion

2el: 2 elements across the thickness of the walls
3el: 3 elements across the thickness of the walls

Figure 6.9 Capacity curves of the local model of the Church of Kuño Tambo for different hypotheses

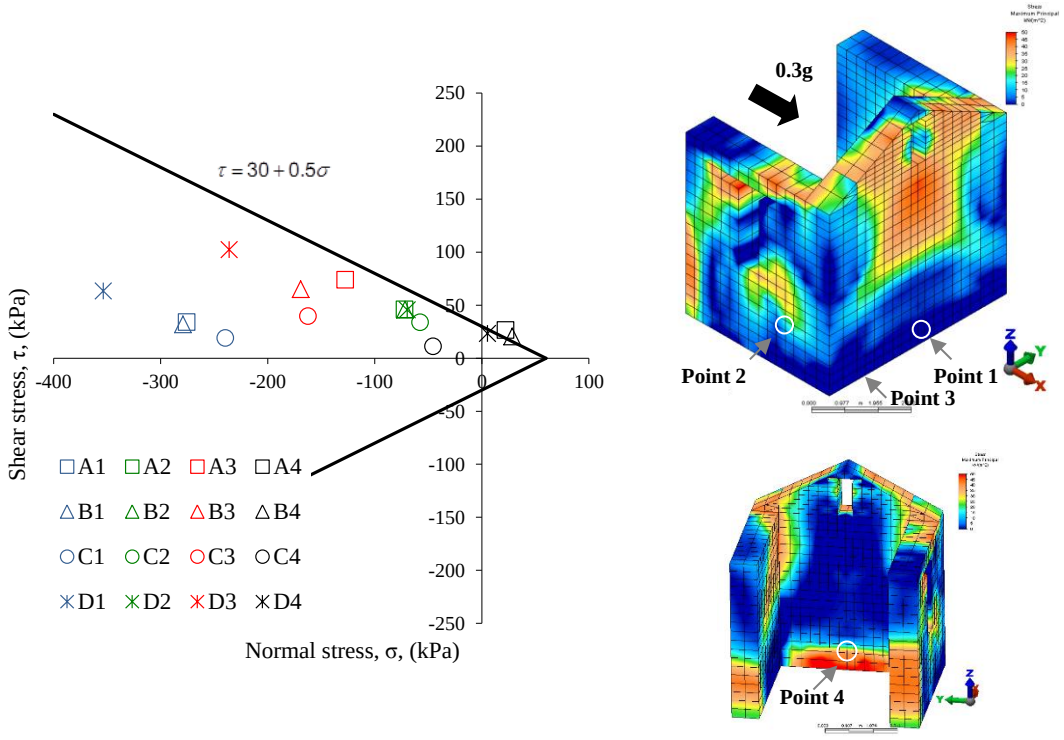

A: Drucker-Prager (DP) with rigid boundaries conditions (RBC) and 2 elements through the thickness of the walls (2el)

B: DP + RBC + 3el

C: HTC model + RBC + 2el

D: DP + Elastic boundary conditions + 2el

Figure 6.10 $\sigma_{z\text{-}z}$-$\tau_{z\text{-}x}$ stress state of four critical locations (Points 1, 2, 3 and 4) under different hypotheses (A, B, C and D)

The figure shows that the use of the Modified HTC model provides lower values of shear than the Drucker-Prager model. The elastic boundary conditions only substantially change the state of points located at the bottom of the walls (case of point 1 and point 3). Points located across the thickness of walls have different stress states for local models with 2 and 3 elements across the thickness of the walls; even though the global results are not substantial different as shown by the capacity curves.

6.3 Uncertainty of the input in the assessment of a historic adobe church

As indicated in Figure 3.1 and discussed in Section 3.5.2, the uncertainty of the input in the assessment of the Church of Kuño Tambo can be obtained by carrying out sensitivity analysis with the local model of the church (Figure 6.1b). In the following, reference will be made to relevant sections of Chapter 3, especially Section 3.4 and 3.5.2 for more clarity.

6.3.1 Control variables

The control variables with the respective plausible values and states are set out in Table 6.3 and Table 6.4, respectively, where δV_{Ki} is the range of variation of the control variables. No control variables of the "geometry" class are considered in this assessment, since it is assumed that the geometry of the model is precisely defined, based on the control data collected within the work performed by the EAI-SRP.

The material properties of adobe were obtained both from experimental work performed at PUCP within the EAI-SRP (Torrealva and Vicente, 2014) and specialised literature (Vargas *et al.*, 1983; Vargas *et al.*, 1986; E.020, 2006; Vecchi, 2009). When experimental results are available, the reference values are an approximation of the mean experimental results, and the minimum and maximum values the corresponding bounds of the tests. The range of variation for adobe reflects the fact that the tests were conducted both with original samples of another historic buildings and with new adobe.

The quality of the information for rubble stone masonry is poorer than for adobe since only a few results from experimental work are available for the specific type of rubble masonry found in the church. For this reason, most of the information was taken from literature (e.g. OPCM 3431, 2005).

Table 6.3 Control variables of the Church of Kuño Tambo characterised by values and respective intervals of plausibility [V_{kimn}, V_{kiref},V_{kimx}] and ranges of variation δV_{Ki}

Class		Control Variables		Units	V_{kimn}	V_{kiref}	V_{kimx}	$\delta V_{Ki} = 1 - \left(\frac{V_{Kimn}}{V_{Kimx}}\right)$ *[normalized]*
Materials	Adobe	V_{P1}	Modulus of elasticity	kPa	50000	140000	225000	0.78
		V_{P2}	Poisson ratio	m/m	0.15	0.15	0.2	0.25
		V_{P3}	Cohesion	kPa	38	41	44	0.14
		V_{P4}	Friction angle	rad	0.5	0.55	0.6	0.17
		V_{P5}	Specific weight	$kN.m^{-3}$	16	16	19	0.16
		V_{P6}	Tension cut-off	kPa	25	30	30	0.17
	Rubble stone masonry	V_{P7}	Modulus of elasticity	kPa	750	870	1050	0.29
		V_{P8}	Poisson ratio	m/m	0.15	0.20	0.20	0.25
		V_{P9}	Cohesion	kPa	55	65	65	0.15
		V_{P10}	Friction angle	rad	0.37	0.42	0.5	0.26
		V_{P11}	Specific weight	$kN.m^{-3}$	16	19	22	0.27
		V_{P12}	Tension cut-off	kPa	40	55	55	0.27
Actions		V_{A1}	Equivalent acceleration	g	0.130	0.234	0.312	0.58
Modelling		V_{M1}	Maximum mesh size	mm	100	400	1150	0.91

Table 6.4 Control variables of the church of Kuño Tambo characterised by plausible states

Class	Control variables		Plausible states	
			Reference	Alternative
Details	V_{D1}	Presence of effective tie-beams	No	Yes

As far as the cohesion of rubble stone masonry is concerned, since adobe and rubble stone have a similar type of mortar, a value of the same order of magnitude could be assumed for both materials. Nevertheless, triplet tests performed on the interface between new adobe and rubble stone masonry at PUCP (Torrealva and Vicente, 2014) show that the imbrication of the stones and their irregular geometry improves the cohesion of the material. The reference value and upper bound of the cohesion of rubble stone corresponds to the experimental result obtained by PUCP in the aforementioned triplet tests. According to both Senthivel and Lourenço (2009) and PUCP experimental work (Torrealva and Vicente, 2014),

the friction angle of rubble stone masonry is likely to be lower than the value associated to adobe and, hence the minimum plausible value for adobe is assumed here as the maximum for rubble stone. The reference value of the friction angle of rubble stone masonry is assumed from triplet tests performed by PUCP on new adobe block/rubble stone masonry. The values of tension cut-off were taken from literature and typical relations of cohesion and tensile strength.

In some intervals of plausibility, the lower or upper bound is equal to the reference value. In those cases, it is assumed that the most plausible value of the control variable corresponds to an extreme of the interval. Hence, the analyst is confident that the variable is not likely to have a value that is either above or below the reference value. Such decision can result from the analysis of the sensitivity of the SPIs to the variation of a specific variable. For instance, if the output does not significantly change when the reference value is varied either to the lower or upper bound of the interval, it is hence reasonable to reduce the size of the interval. This can be done by changing the lower bound or upper bound to a value equal to the reference value. Another possibility is to reduce the interval of plausibility to a single reference value, in which case the uncertainty is assumed as null.

The control variable V_{A1} is defined on the basis of literature and expert judgment. The reference equivalent acceleration, $V_{A1,}$ corresponds to a 10% probability of exceedance in 50 years considering soft foundation soil in zone 2, which includes the region of Cusco, according to the code for earthquake resistance in Peru (E.030, 2003). The maximum importance factor provided by the code is used due to the historic nature of the building and its use as a community space. The interval of plausibility reflects the uncertainty in the definition of the hazard zone and type of soil.

Taking into account that the survey carried out on the site did not allow reaching a firm conclusion on the effectiveness of the tie-beams to control out-of-plane movements of the longitudinal walls during an earthquake, the hypotheses of presence or lack of tie-beams was evaluated through the V_{D1} control variable. The lack of tie-beams is assumed as the reference state, since wooden anchors of different configurations were only observed at the end of a limited number of tie-beams (Figure 4.18). In the case of tie-beams that are not anchored to the walls, it is expected that lateral restraint is assured only by friction between timber and adobe.

As seen in sections 6.2.3 and 6.2.5 decisions on the mesh size (V_{M1}) are governed by the ability of the model to simulate through-thickness shear strains in out-of-plane walls supported by considerations on the number of failed points in shear assuming a

Coulomb-like failure criterion. The minimum plausible and reference values are selected taking into account the dimensions of the adobe units, whereas the maximum mesh size corresponds to the maximum thickness of the walls of the partial model. Thus, the latter corresponds to the hypothesis of one finite element simulating transverse shear deformation.

V_{M1} is the control variable with the highest range of variation (δV_{M1} equal to 0.91) since the most appropriate mesh size is usually unknown at priori and should be normally selected after a few analyses with the partial models. It is followed by V_{P1}, for which a broad range of possible values for adobe is available in literature and results from experimental work are either not directly applicable to the Church of Kuño Tambo or have a significant variability.

6.3.2 Level of influence of control variables and sensitivity of structural performance indicators

The structural performance indicators (SPIs) considered relevant to the seismic assessment of the Church of Kuño Tambo are indicated in Table 6.5.

Local sensitivity analyses are performed for each control variable assuming the reference analysis conditions and varying one by one the control variables from the minimum to the maximum plausible values or varying the state of the model. The range of variation of a control variable *Ki*, δV_{Ki}, is obtained by means of equation 3.4 and the sensitivity of a SPI *j* to the variation of the same variable, $\delta I_{j,Ki}$, by means of equation 3.5.

Table 6.5 Structural performance indicators of the assessment of the Church of Kuño Tambo

Structural performance indicator	Objective
SPI 1: Total base shear	To investigate the global lateral strength capacity.
SPI 2: Global drift	To investigate the ability of the structure to dissipate energy by elastic and plastic deformation. It is obtained by dividing the displacement in the direction of application of the acceleration by the height at a control point, usually the maximum height of the out-of-plane wall.
SPI 3: Percentage of failed points in the adobe walls	To investigate the stiffness degradation assuming an elastic-plastic Drucker-Prager failure criterion (Drucker and Prager, 1952), where the percentage of nodal points in either the walls or base course with a state of stress that is on the failure surface of the Drucker-Prager criterion is estimated.
SPI 4: Percentage of failed points in the rubble stone masonry base course	

When the control variables are defined by means of values, a comparison of the input variation, δV_{Ki}, with the output sensitivity, $\delta I_{j,Ki}$, can be established, as shown in Figure 6.11. For this purpose, the variation/sensitivity is considered relevant if δV_{Ki} or $\delta I_{j,Ki}$ are larger than the minimum reference knowledge-based uncertainty, m_{urmn}, assumed by the analyst (see Section 3.5.2.1 for further details). Four quadrants can be established where the control variables belonging to the first quadrant have the most unfavourable condition since they have high output sensitivity for low input variation (Figure 6.11). In the assessment of the Church of Kuño Tambo, it is assumed m_{urmn} equal to 0.05 and m_{urmx} equal to 0.35. The maximum reference threshold is based on the recommendations of CIB 335 (2010) for masonry buildings, whereas the minimum reference threshold is assumed half of the level suggested in the same publication. It is considered by the author that a lower minimum uncertainty should be assumed for historic buildings when the knowledge level is considered high in order to take into account the importance of empirical knowledge and on-site observations.

In the present assessment, no control variables belong to the 1st and 4th quadrants, meaning that all control variables have a high input variation, i.e. the variation is always higher than m_{urmn}. SPI 3 and SPI 4 are the most sensitive SPIs, since they have the highest percentage of control variables in the 2nd quadrant.

SPI 1 is especially influenced by the lateral acceleration and the specific weight of the materials, as would be expected. Although the input variation associated to the mesh size (V_{M1}) is high, the comparative sensitivity of the SPI 1 is reduced which signifies that the uncertainty is diminished.

The properties of the adobe walls have the most important influence on SPI 2, especially the modulus of elasticity (V_{P1}) with a linear correlation and the specific weight (V_{P5}), in which case the uncertainty is amplified since the sensitivity of the output is higher than the variation of V_{P5}.

The tension cut-off (V_{P6}), cohesion (V_{P3}) and the specific weight of adobe (V_{P5}) have the most important influence on SPI 3 since they govern the failure surface of the Drucker-Prager model and the capability of the material to resist shear due to normal loading. Especially in the case of tension cut-off and specific weight, there is an amplification of the uncertainty.

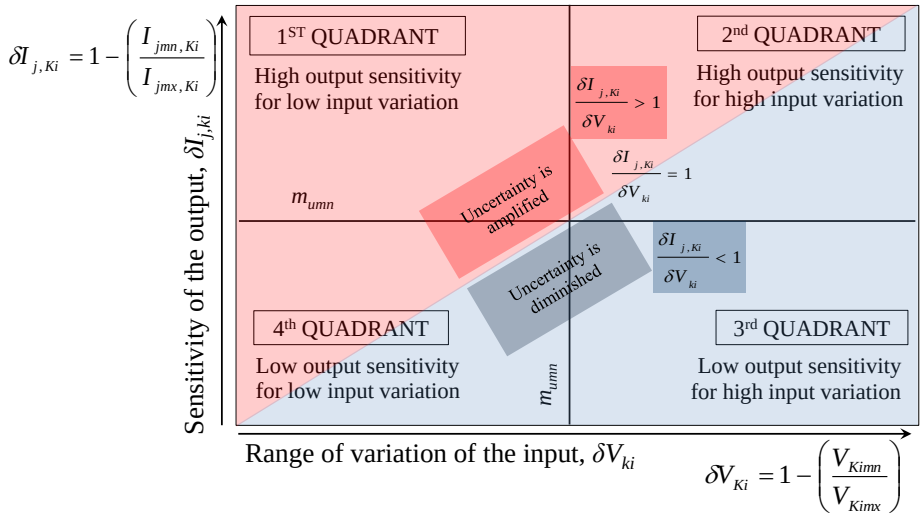

SPI 1: Total base shear

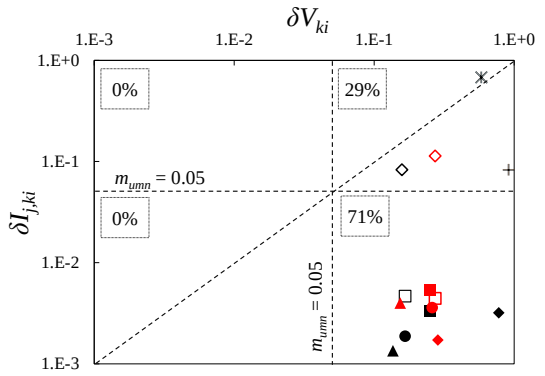

SPI 2: Global drift

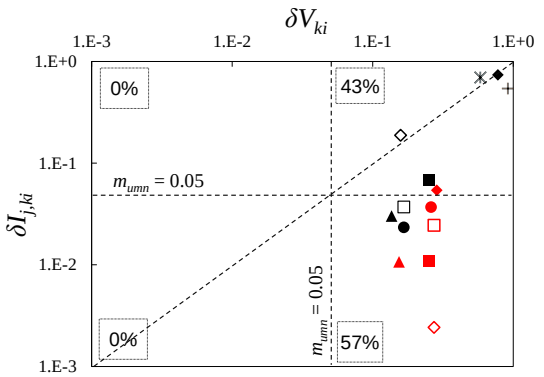

SPI 3: Failed points (adobe walls)

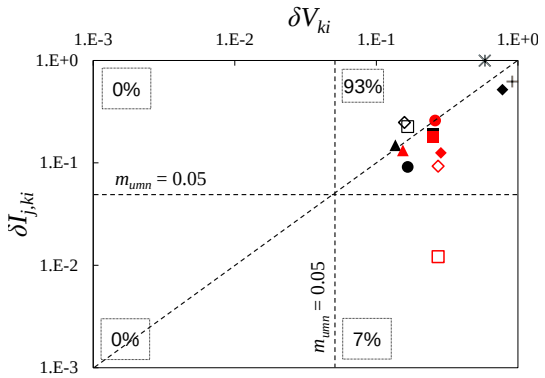

SPI 4: Failed points (rubble stone base course)

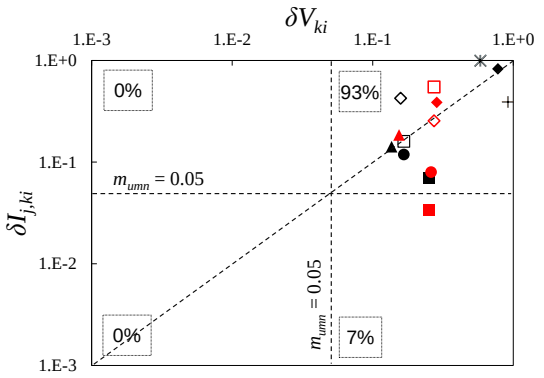

Modulus of elasticity (adobe)	◆ VP1	■ VP2	Poisson ratio (adobe)
Cohesion (adobe)	▲ VP3	● VP4	Friction angle (adobe)
Specific weight (adobe)	◇ VP5	□ VP6	Tension cut-off (adobe)
Modulus of elasticity (rubble stone)	◆ VP7	■ VP8	Poisson ratio (rubble stone)
Cohesion (rubble stone)	▲ VP9	● VP10	Friction angle (rubble stone)
Specific weight (rubble stone)	◇ VP11	□ VP12	Tension cut-off (rubble stone)
Equivalent acceleration	✳ VA1	+ VM1	Maximum mesh size

Figure 6.11 Propagation of uncertainties: comparison of input variation with output sensitivity

The behaviour of the interface between the adobe walls and the rubble stone masonry base course may explain some of the differences on the relative influence of the control variables associate to adobe or rubble stone on SPI 3 and SPI 4. This behaviour will be governed by the cohesion, tension cut-off and specific weight of adobe and by the friction angle of the rubble stone masonry. This is the reason why the variation of the friction angle of rubble stone (V_{P10}) has an important influence on SPI 3.

As far as SPI 4 is concerned, the specific weight of the adobe wall (V_{P5}) and the tension cut-off of rubble stone masonry (V_{P12}) influence the most the sensitivity of the structural performance indicator, leading to significant amplifications of the uncertainty. This is explained by the fact that these control variables govern the relative capacity of the base course to resist shear and tension.

Table 6.6 shows the sensitivity of the structural performance indicators to the variation of the control variables characterised by states, $\delta I_{j,Ki}$. Since the tie-beams are acting as constraints to the out-of-plane behaviour of the transversal walls of the model, the presence of the tie-beams reduces the drift (SPI 2) or deformation of these walls, leading to a reduction on the level of failed points (SPI 3 and SPI 4).

The overall sensitivity of a SPI j to the variation of all control variables, δI_j, can be obtained as an average over all values of $\delta I_{j,Ki}$, as per equation 3.6. The values of δI_j are shown in Table 6.7 for all SPIs.

In the present assessment, the response of the base course is most sensitive to the uncertainty of the input due to the greater range of variation of the properties that govern the failure of rubble stone masonry in shear and tension. The value of δI_4 is close to the maximum reference value of the uncertainty, m_{urmx}, assumed here as 0.35. The failure of the walls and the global drift is also highly sensitive with overall sensitivities significantly greater than the minimum reference value, m_{urmn}, assumed here as 0.05. Finally, the total base shear is the least sensitive SPI with sensitivity similar to the minimum reference value.

Table 6.6 Sensitivity of a SPI j to the variation of control variables characterised by states

Control variable	$\delta I_{1,D1}$	$\delta I_{2,D1}$	$\delta I_{3,D1}$	$\delta I_{4,D1}$
V_{D1} (presence of tie-beams)	0.001	0.057	0.129	0.221

Table 6.7 Overall sensitivity of the SPIs, δI_j

	δI_1 (SPI 1: Total base shear)	δI_2 (SPI 2: Global drift)	δI_3 (SPI 3: Failed points - adobe walls)	δI_4 (SPI 4: Failed points - rubble stone base course)
δI_j	0.07	0.17	0.27	0.32

In order to identify the critical variables of the seismic assessment of the Church of Kuño Tambo, the influence of each control variable is evaluated by means of the overall influence indexes α_{ki} obtained by means of equation 3.7. These indexes correspond to an average over all values of sensitivity associated to the four SPIs, $\delta I_{j,Ki}$, due to the variation of a specific control variable.

The indexes α_{ki} can be calculated assuming that all SPIs are equally important. In alternative, the α_{ki} indexes can be calculated as a weighted sum of the sensitivity indexes associated to the four SPIs, according to equation 3.8. The weight, w_j, can be selected such that SPIs that are more relevant to verify whether a structure complies with a specific performance level or not have higher weights. In the present assessment, the fours SPIs will be used in the analyses at a global level to verify whether the structure exceeds the damage states of 'near collapse', 'significant damage', and 'damage limitation' for different rehabilitation hypotheses; and hence all SPIs are equally important.

Nevertheless, the three procedures proposed in Section 3.5.2.1 to calculate the weight, w_j, on the basis of the actual sensitivity of the SPIs can be considered here. The results are shown in Table 6.8. The indexes α_{ki} for all control variables are shown in Table 6.9, according to the various procedures used to calculate α_{ki}. The control variables are ranked according to the corresponding influence indexes, α_{ki}, from the highest to the lowest index within each class. It can be seen that the ranking may vary according to the procedure used to combine the various $\delta I_{j,Ki}$ in the calculation of α_k. The ranking shown in Table 6.9 corresponds to the ranking provided by the majority of the procedures.

Procedure I underestimates the importance of SPIs that are significantly sensitive to the uncertainty of the input but which are not the most sensitive to the variation of any control variable. It provides the highest weight to SPI 4 since this is the most sensitive indicator for most control variables. On the other hand, this procedure may overestimate the relevance of SPIs that are more sensitive to control variables that have an overall modest influence on the outputs.

Table 6.8 Weights used in the combination of the sensitivity of all SPIs

Structural performance indicators		w_j			
		All SPIs equally relevant	Proc. I	Proc. II	Proc. III
SPI 1 (Total base shear)	w_1	0.25	0.00	0.10	0.07
SPI 2 (Global drift)	w_2	0.25	0.00	0.18	0.23
SPI 3 (Failed points - adobe walls)	w_3	0.25	0.47	0.36	0.23
SPI 4 (Failed points - rubble stone base course)	w_4	0.25	0.53	0.36	0.46

Table 6.9 Influence indexes of the control variables of the Church of Kuño Tambo

Class		Control Variables		α_{ki}			
				All SPIs equally relevant	Proc. I	Proc. II	Proc. III
Materials	Adobe	V_{P1}	Modulus of elasticity	0.52	0.68	0.62	0.67
		V_{P5}	Specific weight	0.24	0.34	0.28	0.30
		V_{P6}	Tension cut-off	0.11	0.19	0.15	0.14
		V_{P3}	Cohesion	0.08	0.15	0.11	0.11
		V_{P2}	Poisson ratio	0.08	0.13	0.11	0.09
		V_{P4}	Friction angle	0.06	0.11	0.08	0.08
	Rubble stone masonry	V_{P7}	Modulus of elasticity	0.14	0.26	0.19	0.22
		V_{P12}	Tension cut-off	0.15	0.30	0.21	0.26
		V_{P11}	Specific weight	0.12	0.18	0.14	0.15
		V_{P10}	Friction angle	0.10	0.16	0.13	0.11
		V_{P9}	Cohesion	0.08	0.16	0.12	0.12
		V_{P8}	Poisson ratio	0.06	0.10	0.08	0.06
Actions	V_{A1}	Equivalent acceleration		0.84	0.99	0.91	0.90
Modelling	V_{M1}	Maximum mesh size		0.41	0.50	0.47	0.46
Details	V_{D1}	Presence of effective tie-beams		0.10	0.18	0.14	0.15

Procedures II and III require the attribution of a sensitivity class to each SPI for all control variables based on the criterion of Table 3.6, considering m_{urmn} equal to 0.05 and m_{urmx} equal to 0.35. The fact that SPI 3 and SPI 4 are the most affected SPIs by the uncertainty of the inputs can be here seen by the fact that they have the highest number of control variables belonging to a ‘high’ and ‘medium’ sensitivity classes.

When a procedure such as II is applied instead of procedure III, looking in average terms to the influence of all control variables, higher weights are obtained to the SPIs that are influenced by a larger number of control variables. Thus, 'local' peaks of influence/sensitivity are not emphasised. Interesting to notice that SPI 2 and SPI 3 have the same weight as per procedure III, which means that these SPIs have the same percentage of control variables with 'High' sensitivity class.

As suggested in Section 3.5.2.1, the control variables are considered critical when their influence index, α_{ki}, is equal or higher than a minimum reference uncertainty assumed by the analyst, m_{urmn}, which is 0.05 in the present assessment. Following this criterion, all control variables are critical variables in the present assessment.

6.3.3 Level of knowledge associated to the critical variables

The level of knowledge provides a measure of the uncertainty with which the analyst defines the reference analysis conditions, the intervals of plausibility and the alternative states. An indicator of this uncertainty is given by the knowledge index λ_{ki} following the criteria of Table 3.8 and provisions of current codes and guidelines, as explained in Section 3.5.2.2. In the present assessment, the index associated to high knowledge is equal to m_{urmn}, since even the intervals defined on the basis of experimental work carried out for the purpose of this assessment were conducted with new materials or original samples collected in other sites. It is therefore reasonable to assume a marginal uncertainty in the present case. Moreover, the choice of a modelling strategy and the selection of the local model have also an inherent uncertainty that should be taken into account.

The knowledge indexes of all critical variables and the respective rationale for the assumption are indicated in Table 6.10. These knowledge indexes can be combined into a global knowledge index, λ, calculated as an average of all λ_{ki}, according to equation 3.10. The λ in the assessment of the Church of Kuño Tambo is equal to 0.16.

6.3.4 Knowledge-based uncertainty of the inputs

The uncertainty of the inputs associated to each SPI j, m_{uj}, is obtained by means of equation 3.11, considering both the overall sensitivity of the SPIs, δI_j, and the global knowledge index, λ. In the assessment of the Church of Kuño Tambo, the uncertainty m_{uj} is expressed in Table 6.11 for the four SPIs.

The m_{uj} can be combined in order to obtain an overall uncertainty measure of the inputs, m_u, according to equation 3.14. The m_u for the assessment of the Church of Kuño Tambo is indicated in Table 6.12 taking into account alternative procedures to combine the results of the various SPIs.

Table 6.10 Knowledge level and indexes of the assessment of the Church of Kuño Tambo

Critical variables				Level of knowledge	λ_{ki}	Rationale
Materials	Adobe	V_{P1}	Modulus of elasticity	HK	0.05	(a) Values taken from experimental work on specimens built with original materials from other sites and/or new materials.
		V_{P2}	Poisson ratio	HK	0.05	(b) Values taken from specialised literature
		V_{P3}	Cohesion	MK	0.2	(a)
		V_{P4}	Friction angle	MK	0.2	(a)
		V_{P5}	Specific weight	HK	0.05	(b)
		V_{P6}	Tension cut-off	MK	0.2	(a)
	Rubble stone masonry	V_{P7}	Modulus of elasticity	MK	0.2	(b)
		V_{P8}	Poisson ratio	HK	0.05	(b)
		V_{P9}	Cohesion	MK	0.2	(a)
		V_{P10}	Friction angle	MK	0.2	(a)
		V_{P11}	Specific weight	MK	0.2	(b)
		V_{P12}	Tension cut-off	LK	0.35	Values assumed from experimental work conducted with adobe samples.
Details		V_{D1}	Presence of effective tie-beams	MK	0.2	No detailed inspection of a representative sample of connections of the tie-beams to the walls was conducted.
Actions		V_{A1}	Equivalent acceleration	MK	0.2	(b)
Modelling		V_{M1}	Maximum mesh size	HK	0.05	Defined on the basis of expert judgement.
λ (according to Equation 3.10)					0.16	

Table 6.11 Knowledge-based uncertainty of each SPI in the assessment of the Church of Kuño Tambo

SPI 1 (Total base shear)	SPI 2 (Global drift)	SPI 3 (Failed points - adobe walls)	SPI 4 (Failed points - Rubble stone base course)
m_{u1}	m_{u2}	m_{u3}	m_{u4}
0.24	0.36	0.47	0.53

Table 6.12 Overall knowledge-based uncertainty of the assessment of the Church of Kuño Tambo

	All SPIs equally relevant	Proc. I	Proc. II	Proc. III
m_u	0.40	0.50	0.45	0.45

Procedure I can be seen as an upper bound of the uncertainty, whereas the value calculated as a mean of all indicators (i.e. all SPIs equally relevant) can be seen as a lower bound. Since in the present case, all indicators will be used in the detailed diagnosis and they are therefore all equally relevant for the present assessment, the lower bound of 0.4 is selected as the reference overall uncertainty of the inputs, m_u. This m_u value is equivalent of having a confidence factor of 1.4, which can be directly compared with the prescriptions of current codes, such as Eurocode 8 (CEN, 2005b). Although the prescriptions of Eurocode 8 for selection of confidence factors are not tailored to historic constructions and therefore do not take into account the value of heuristic knowledge, it can be concluded that according to Eurocode 8 a confidence factor of 1.2 would be assumed for the assessment of the Church of Kuño Tambo. This factor would be selected considering that a detailed in-situ inspection and "comprehensive" experimental campaign was conducted within the EAI-SRP for characterization of this structure. However, the prescriptions of the code do not take into account the limited reliability of experimental work conducted on materials like adobe and rubble stone, especially when the components have been subjected to years of weather demands and past earthquakes. Thus, the prescriptions of the code underestimate the uncertainties present in the assessment of historic constructions such as the Peruvian adobe churches.

6.4 Analysis of a historic timber structure at the local level

In the case of timber structures, the structural behaviour is governed by the joints connecting various elements of the system, and by the effect of the roof cladding. Hence, the following hypotheses require a detailed investigation at the local level:

(i) Overall relevance of modelling the timber joints in comparison to the assumption of a continuously connected timber structure;
(ii) Relative relevance of the different timber joints;
(iii) Mechanical characterization of planked timber arches; and
(iv) Hypothesis of a rigid vs flexible diaphragm.

As far as hypothesis (iii) is concerned, the numerical analyses at the local level were focused on the mechanical characterization of the nailed joints of the planked arches. These joints failed during the 2007 Pisco earthquake in two bays of the nave of the Cathedral of Ica (bay 1 and bay 2), and this was a common type of failure observed in many churches in Peru after the earthquake. Thus, the simulation of these joints requires a more in-depth investigation. The other joints of the cathedral were characterized by experimental work conducted at PUCP, as explained in the relevant sections.

The most important inputs in the case of adobe churches were associated to material properties of adobe and rubble stone. In the case of the timber structure of the Cathedral of Ica, mechanical parameters characterizing the timber joints appear to be at least as important as the material properties of the timber members. It will be seen in the following that the local models evolved from continuous models made of volume elements to more refined models consisting of beams and springs simulating the timber members and joints, respectively.

6.4.1 Local models of the Cathedral of Ica

As described in Chapter 4, the timber structure of the Cathedral of Ica is composed of five similar bays in the nave and the bay of the transept, which includes the central dome. Bay 1 is slightly different from the other bays of the nave since it accommodates the mezzanine. The bays of the nave underwent the most critical damage, resulting in the collapse of the bay-edge arches of bays 1 and 2 and the collapse of the internal arches of bays 3, 4 and 5. In

the bay of the transept, damage was more localised in the central dome. Moreover, all critical joints are present in the structure of the nave. Hence, conclusions made with a local model of the nave's bay can be extrapolated to simulate the whole structure in the global model. In this context, it is reasonable to consider one single bay of the nave of the cathedral as the local model used to test the aforementioned hypotheses (i) and (ii) (Figure 6.12).

In the case of hypothesis (iii), a smaller local model including only the vault of the representative nave's bay is used to calibrate the stiffness of the nailed joints of the planked arches (Figure 6.13).

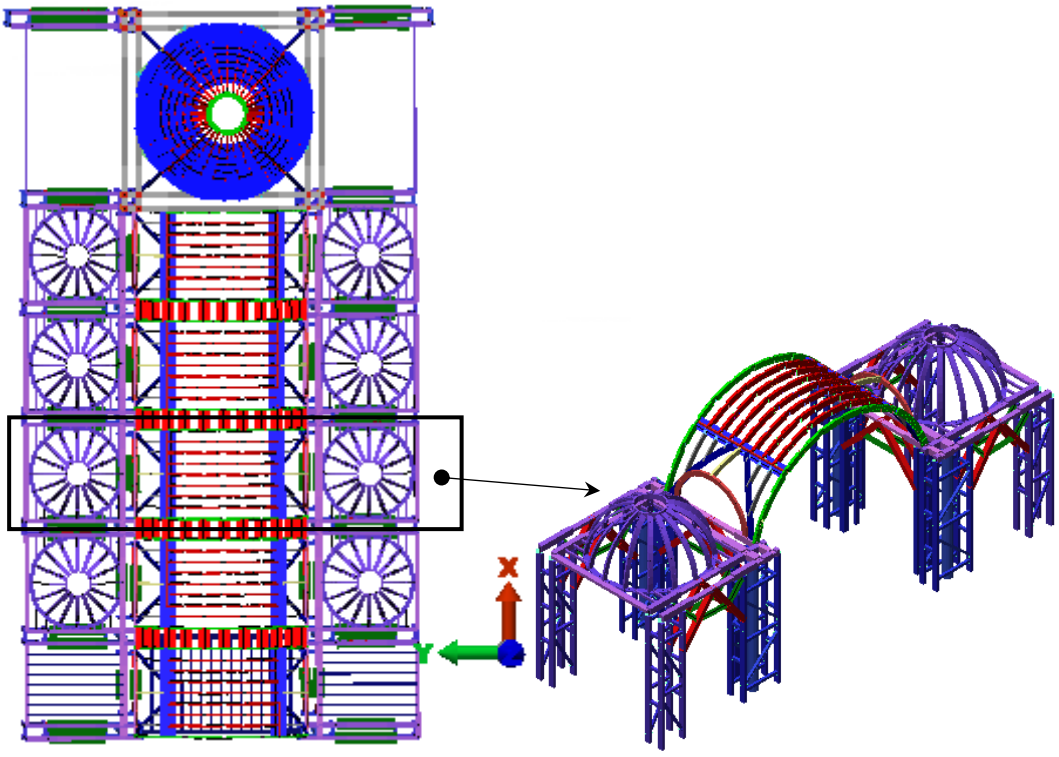

a) Global model b) Local model (nave's bay)

Figure 6.12 Local and global models of the timber structure of the Cathedral of Ica

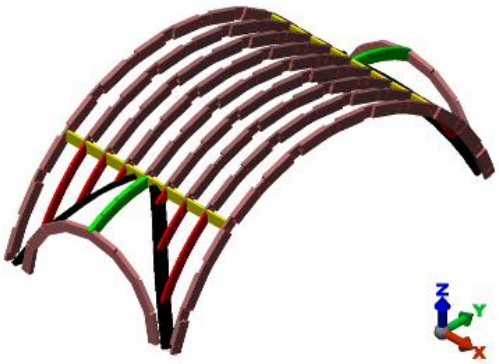

Figure 6.13 Local model of the vault of the nave' bay used in the calibration of the stiffness of the nailed joints of the planked arches

The material behaviour of timber is assumed isotropic linear elastic, which is a reasonable assumption taking into account that the timber joints are the principal sources of nonlinearity and unrecovered deformation. This assumption is supported both by literature and observations made on the site. The model is completely fixed at the base, since no deformation of the foundations was observed on the site.

6.4.2 Mechanical properties

Since the modelling of the timber framing of the nave's bay evolved from a continuous model made of volume elements to a more refined model of beams and springs, the type and variety of inputs required by the different models have also changed.

After the 1st data collection, which was based on observation and geometrical measurements, information about wooden species of the timber structure was not available, and therefore in the initial local model of the nave's bay, it was assumed that cedar was the species of all timber members, as it was quoted in literature as a common wooden species used in colonial churches in Peru. Table 6.13 shows the material properties of cedar as taken from literature.

After the 1st data collection, the identification and mechanical characterization of wooden species of the various timber elements was conducted by the Universidad La Molina in Peru (Chavesta Custodio *et al.*, 2012), and an extensive experimental campaign was carried out by PUCP in order to characterise the response of the main connections (Torrealva and Vicente, 2014). The initial local analyses conducted to investigate hypotheses (i) and (ii) above informed the planning of the experimental campaign carried out at PUCP.

In parallel with the work in Peru, the author collaborated with a research team at UPM in order to characterise the response of the nailed joints of the planked arches.

As a result of the extensive experimental work conducted in Peru and Madrid, the mechanical properties assumed in the refined beam and spring model of the nave's bay and in the global model of the timber structure of the cathedral are the ones indicated in Table 6.14 and Table 6.15.

Table 6.13 Input parameters of the model of the nave's bay with volume elements

Specie	Specific Weight, W ($kN.m^{-3}$)	Modulus of elasticity parallel to the grain, E (kPa)	Poisson's Ratio, υ
Cedar	3.2	8470000	0.3

Table 6.14 Input parameters of the numerical models for material characterization of timber members

Species	Specific weight, W ($kN.m^{-3}$)	Modulus of elasticity parallel to the grain, E (kPa)	Poisson's ratio, υ
Caoba Africana	4.1	10300000	0.3
Guarango	9.1	16900000	0.3
Cedar	3.3	9400000	0.3

Table 6.15 Translational and rotational stiffness of timber joints used in the global models

Joint	Translational stiffness	Rotational stiffness
	K_{trans} ($kN.m^{-1}$)	K_{rot} ($kN.m.rad^{-1}$)
Mortice and tenon	-	30 (parallel to grain) 30 (perpendicular to grain)
Pegged mortice and tenon	9800	-
Nailed connections of pillars' diagonals	-	20
Nailed connections of the arches	6600 (parallel to grain) 4500 (perpendicular)	5.4

6.4.3 Overall and relative relevance of the timber joints

The first local model of the nave's bay is totally composed of volume finite elements. This type of elements allows modelling the geometry of the structure in detail to properly include existing offsets between different members. The planked timber arches are modelled as continuous arches. This continuous model was developed at a time of the assessment process when the timber species of the cathedral were unknown, and the results of experimental work unavailable. Moreover, the existence of longitudinal bracing connecting the bay-edge arches in each bay (Figure 4.35b) was also unknown.

The material properties of cedar are assumed for all timber members, as shown in Table 6.13. The simulation of the timber joints as semi-rigid connections is conducted by changing the modulus of elasticity of cedar at the location of the joints. Figure 6.14 shows the model discretized into hexahedron and tetrahedron elements and the location of the principal connections. All possible translations are fixed at the base.

Although this local model is based on several simplifications of the real structural response of the bay in presence of limited information, such a study is relevant to evaluate the relative importance of the various joints to the global behaviour of the structure. This study was especially useful at an initial phase of the EAI-SRP in order to identify the most critical joints and to plan experimental work to characterise in more detail these joints.

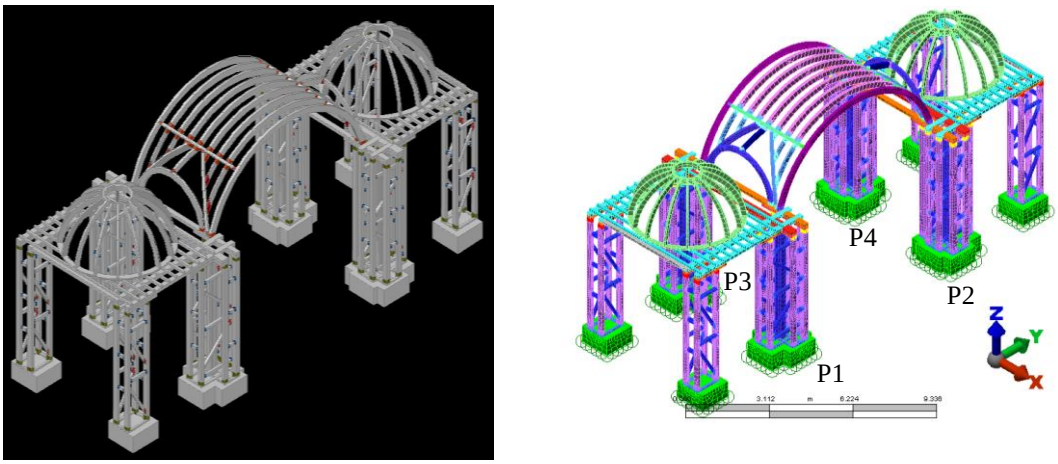

a) CAD model: location of the principal joints are shown with different colours

b) Finite element mesh

Figure 6.14 Local model of the nave's bay with volume elements

Modal analysis is carried out with four variations of the local model in order to investigate the effect and relevance of varying the stiffness of the model at the location of the joints, and to understand the relative behaviour of the frame and vault, taking into account that the vault and the frame have different stiffness.

Hence the 4 models represent (Table 6.16):

(i) an elastic continuum as base model;
(ii) a model with all joints with variable stiffness and lower than the members;
(iii) a model with the joints between the lunettes and arches with variable stiffness and lower than the members; and
(iv) a model with the joints connecting the bay-edge arches, lunettes' ribs and pillars to the longitudinal and transversal beams with variable stiffness and lower than the members.

Relevant modal shapes for the dynamic response of the nave's bay are shown in Table 6.17 for the continuum. Mode A and mode B have the most significant participating modal masses for the longitudinal and transversal direction, respectively. These modes are also the most important for the other three modelling options. The cumulative participating modal mass of a model without base courses is 79.16% in the X-direction (longitudinal) and 76.55% in the Y-direction (transversal) if 20 modes are calculated.

Figure 6.15 shows the effect of stiffness' variation on the natural periods of the bay, in which all joints undergo the same variation of stiffness ('All joints' model). The E_{joint}/E_{timber} ratio denotes the difference between the stiffness of the joint's material and the stiffness of the material constituting the timber member. The smaller the stiffness of the material at the location of the joint under analysis is, the more pronounced is the discontinuity. The figure also shows the modal shapes corresponding to the lowest E_{joint}/E_{timber} ratio.

According to the theory of structural dynamics, a structure vibrates with higher frequency, *f*, when the stiffness increases, if the mass of the structure is kept constant, as in the case of this parametric analysis. The effect of stiffness' variation on the period of the structure becomes critical when E_{Joint} is equal to $0.001E_{Timber}$. The natural period of mode A increases approximately 35 times from a decreasing ratio of 1 to 1E-5, whereas the period increases 20.5 and 18 times for modes B and C, respectively. The effect is therefore more pronounced for the longitudinal mode, whereas modes B and C have similar increasing rates. This can be explained by the fact that deformation is localised at the arches of the vault in mode A, with decreasing participation of the rest of the structure.

Table 6.16 Hypotheses for the local model of the nave's bay with volume elements

Model	Modelling of Joints	
All joints	All connections of the model are undergoing parametric analysis.	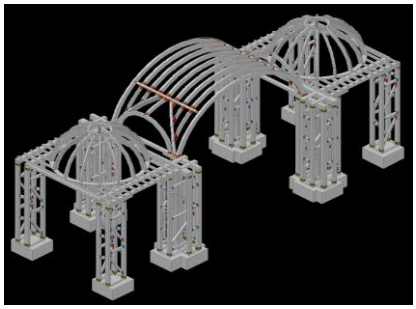
Continuous	The structure is continuous. No joint undergoes parametric analysis.	
Arc_L model	Connection of the internal arches to the lunette beam, of the lunette ribs and diagonals to the lunette beam and of the lunette beam to the bay-edge arches are undergoing parametric analysis. The rest of the structure is considered as with joints having the same stiffness as the elements they are connecting.	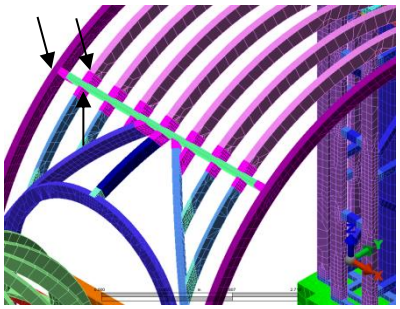
Parc_MT model	Connection of the lunette arch and ribs to the horizontal beams, of the bay-edge arches to the horizontal beams and of the central pillars to the horizontal beams are undergoing parametric analysis. The rest of the structure is considered as with joints having the same stiffness as the elements they are connecting.	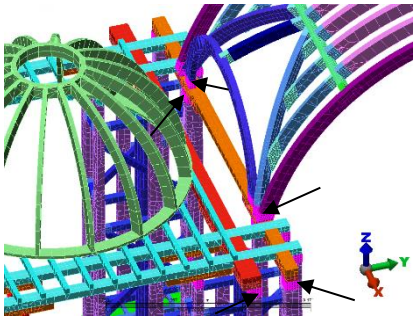

Table 6.17 Modal shapes of the nave's bay with volume elements continuously connected

	Modal shape	Description
Mode A	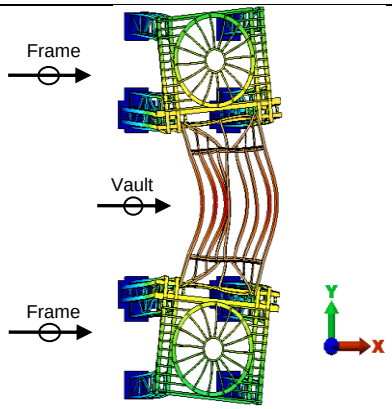	*T* = 0.123sec Longitudinal first order mode (X global direction of the model). The highest relative displacements are observed at the arches. The frames are also subjected to torsion.
Mode B	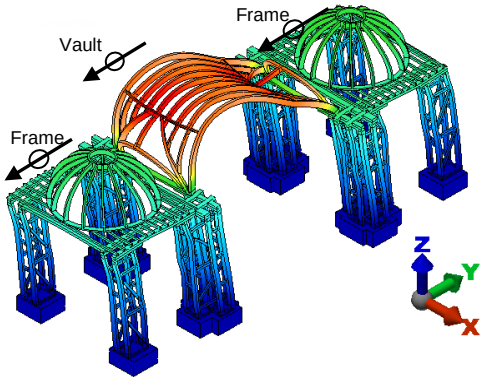	*T* = 0.088sec Transversal mode (Y global direction of the model). It is a unidirectional first order mode where the frames and the vaults are moving together in one direction. The highest relative displacements are observed at the arches.
Mode C	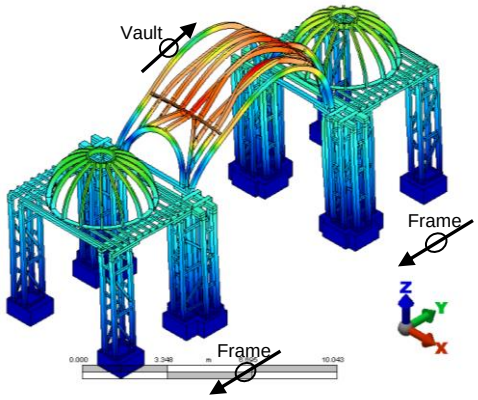	*T* = 0.053sec Transversal mode (Y global direction of the model). It is a unidirectional second order mode where the frames are moving in one direction and the vault in the opposite direction. The highest relative displacements are observed at the arches.

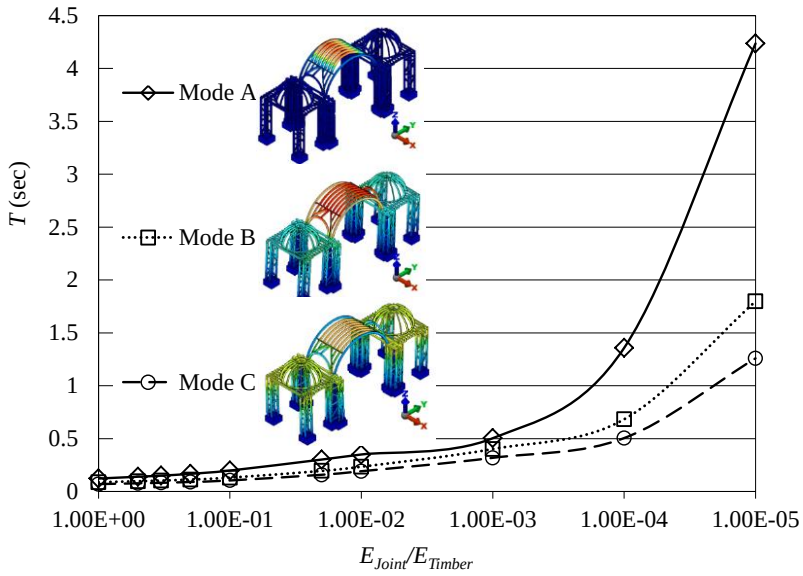

Figure 6.15 Effect of stiffness' variation on the period of the local model of the nave's bay with volume elements due to the presence of connections

The effect of stiffness' variation on the participating modal masses of modes A and B can be seen in Figure 6.16. The participating mass in the Y-direction of the transversal mode (mode B) slightly increases up to a E_{Joint}/E_{Timber} ratio of 1E-3 and then it decreases down to a value similar to the value of the continuous model. A different situation is observed for the longitudinal mode (mode A), where the participating mass in the X-direction substantially decreases from a E_{Joint}/E_{Timber} ratio equal to 1E-2 and then stabilises at a value of 1.6%. This value corresponds to the participation of the arches at the top of lunettes.

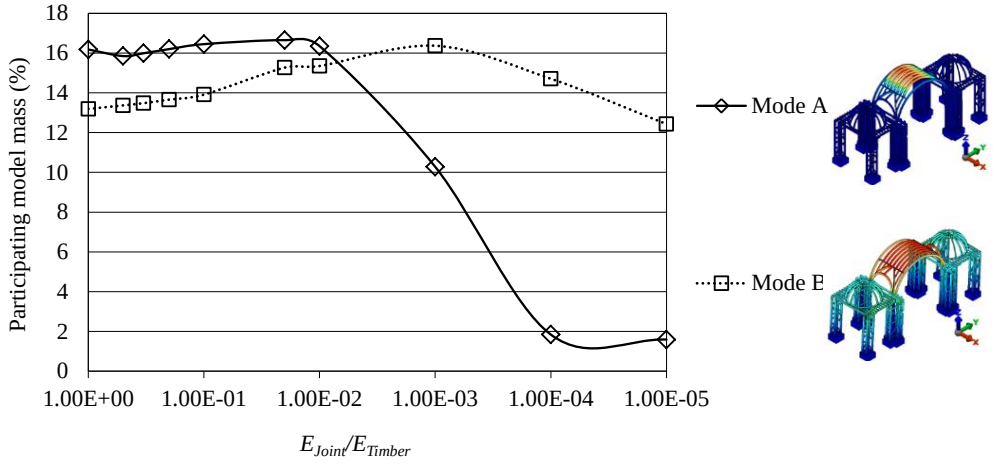

Figure 6.16 Effect of stiffness' variation due to the presence of timber joints on the participating modal masses of modes A and B

The same analysis is conducted with the other two models, as shown in Figure 6.17 and Figure 6.18. Mode A has the highest period and modal mass participation, in which the Arc_L model presents a dynamic response similar to the "All joints" model. This confirms the relevance of Arc_L connection for mode A. A different situation is observed for modes B and C (transversal modes), where the Parc_MT model shows a response more close to the "All joints" model, since the connection at the top of the frame governs the relative response of the vault and frame. In Arc_L model, mode C is just caught up to a value of E_{joint}/E_{timber} equal to 1e-3, since the modal shapes are related to local dynamic responses of the arches for ratios lower than this value. The reduction of stiffness of the Arc_L connection favours the occurrence of local modes affecting the arches as they will work more independently of the rest of the structure. This can be confirmed by the sharp drop of mass participation of Arc_L in modes A and B.

In the case of mode B, the participating modal masses of Arc_L and Parc_MT models decrease with the reduction of stiffness at the joints, whereas a different behaviour is observed for the "All joints" model. This could be explained by the reduction of rigidity of the aisles in the "All joints" model when the stiffness of the connections of the bracing to the posts is decreased. If the bracing is assumed continuously connected to the posts (case of Arc_L and Parc_MT), such reduction of rigidity of the frame does not occur. The reduction of stiffness of the joints of Arc_L and Parc_MT results in a more local response of the arches and vault, leading to a reduction in the participating modal masses.

These results also show that not only the joints simulated in Arc_L and Parc_MT but other joints, such as the ones connecting the bracing to the posts, also govern modes B and C.

Elastic response spectra recorded in Ica province during the 2007 Pisco Earthquake are shown in Figure 6.19. Modal superposition analyses are performed with the Arc_L, Parc_MT and the "Continuous" models using the spectrum corresponding to the North-South components of motion, which is the transversal (Y) direction of the local models.

Figure 6.20 shows the deformed shapes and displacements in the Y-direction of Arc_L, Parc_MT and of the "Continuous" local model after modal superposition analysis. The displacements in the Y-direction at the centre of the arches are depicted in Figure 6.21 for different stiffness values of the Arc_L and Parc_MT joints. The displacement significantly increases from a value of stiffness lower than 1/100 in the case of Parc_MT. The increment of displacement is much less pronounced in the case of Arc_L.

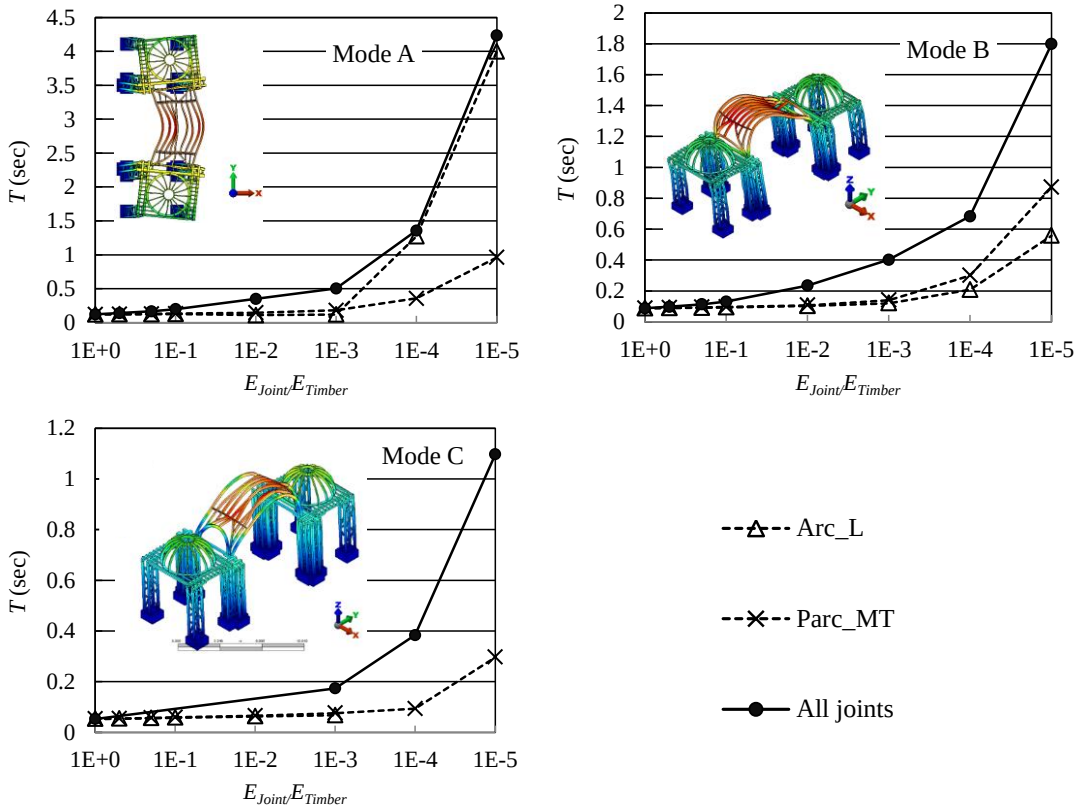

Figure 6.17 Natural periods of the nave's bay model with volume elements for various hypotheses of E_{Joint}/E_{Timber} ratio

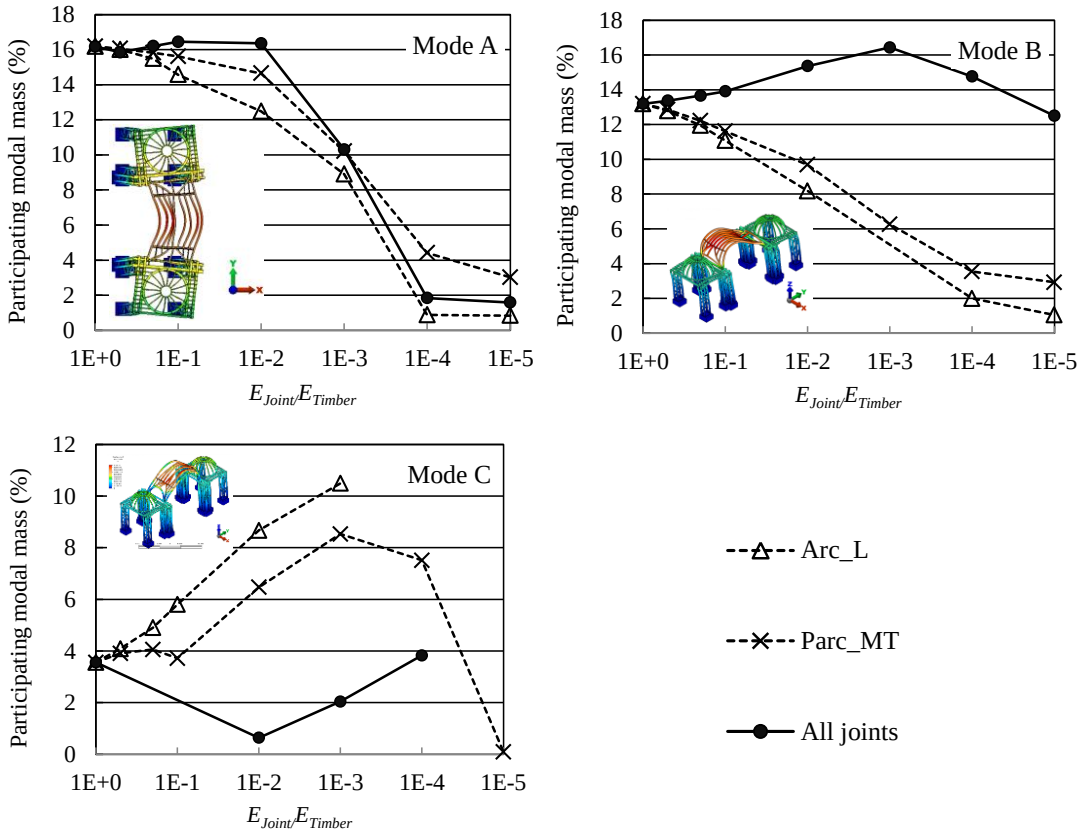

Figure 6.18 Participating modal masses of the model of the nave's bay with volume elements for various hypotheses of E_{Joint}/E_{Timber} ratio

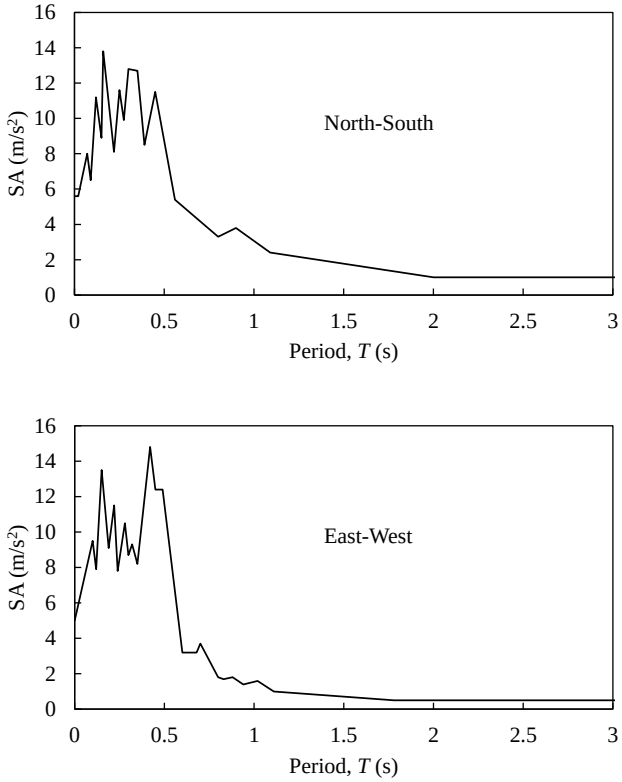

Figure 6.19 Response spectra recorded at the station of Parcona (PCN) during the 2007 Pisco Earthquake. (after Tavera *et al.*, 2009)

	E_{joint}/E_{timber} =1/100	E_{joint}/E_{timber} =1/10000
Arc_L model	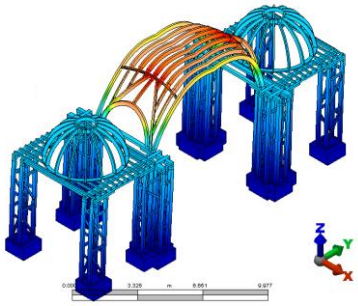	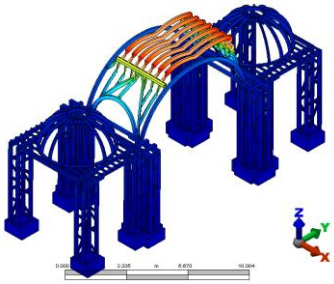
	Maximum displacement: 4mm	Maximum displacement: 13mm
Parc_MT model	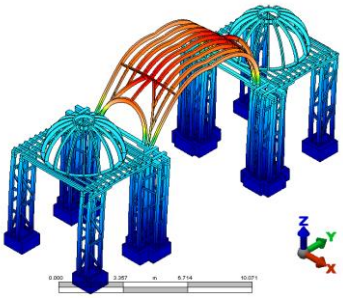	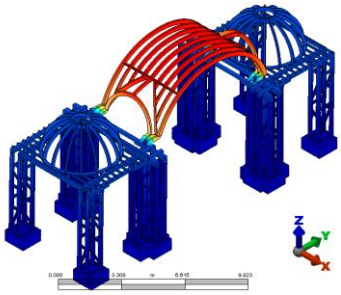
	Maximum displacement: 5mm	Maximum displacement: 33mm
	E_{joint}/E_{timber} =1/1	
"Continuous" model	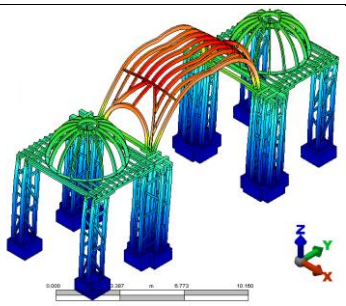	
	Maximum displacement: 2.5mm	

Figure 6.20 Deformed shapes of the models of the nave's bay with volume elements after modal superposition analysis (displacement in the Y-direction)

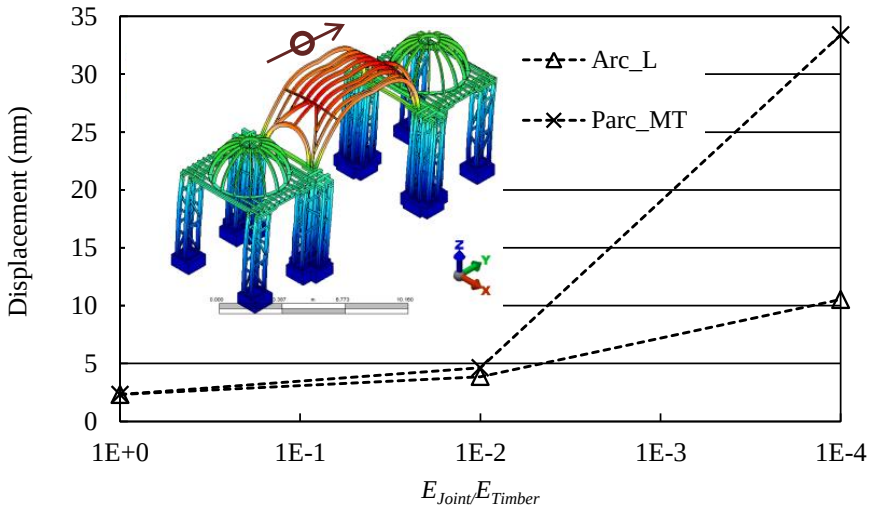

Figure 6.21 Displacement in the Y-direction at the top of the vault of the local model of the nave's bay with volume elements

The drift of the four pillars of the nave's bay (see location of the pillars in Figure 6.14b) is expressed in Figure 6.22 as the ratio of the value corresponding to each of the hypotheses considered to the drift in the "Continuous" model ($D_{continuous}$). This ratio increases in the case of Parc_MT local model, whereas the opposite occurs in the case of the Arc_L model. The simulation of Arc_L connection does not have influence on the lateral displacement of the pillars up to a stiffness of E_{joint}/E_{timber} = 1/100. Beyond this point, the drift decreases since the vault's arches, where the mass of the roof is applied, work independently of the rest of the structure. When the stiffness approaches zero, the Arc_L connection behaves as a hinge and the aisles remain very stiff due to the condition of continuity. Thus, the drift decreases to 30% of the drift of the "Continuous" model.

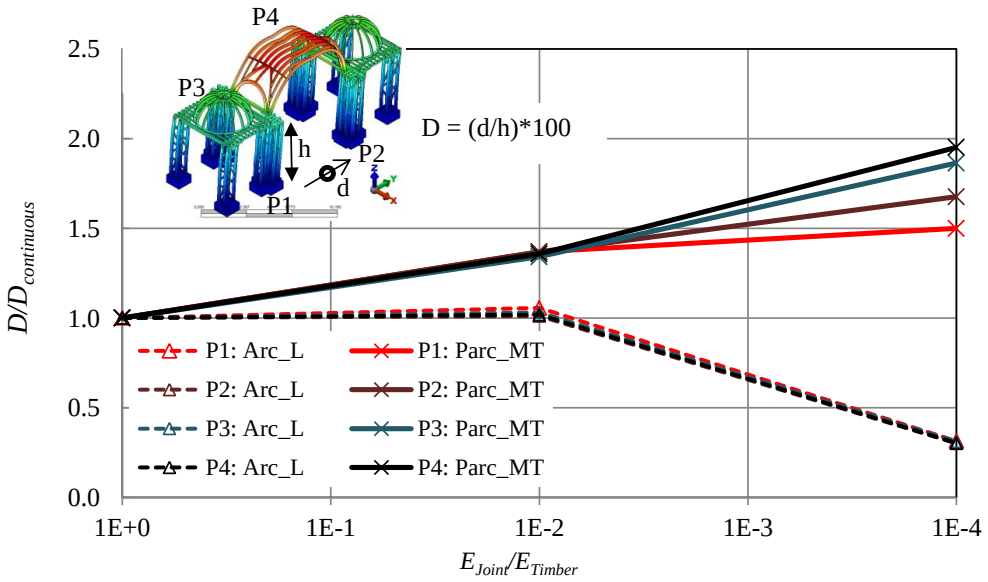

Figure 6.22 Drift in the Y-direction of the central pillars of the local models of the nave's bay with volume elements

6.4.4 Mechanical characterization of planked timber arches

Improved understanding of the structural behaviour of planked timber vaults did not follow the increasing application of the system in the 17th and 18th centuries. Hahmann (2006) reviewed German studies on planked arches developed at the end of the 18th century and beginning of the 19th century, concluding that until the mid-19th century engineers regarded the shape of masonry arches, mainly optimised for the transmission of compression forces, to be the best shape for planked timber arches. In the early 19th century, the architect David Gilly reported that the causes of the failure of several planked timber structures during heavy windstorms were their unfavourable shapes, insufficient longitudinal stiffening and poor carpentry skills (Hahmann, 2006). It was in the 19th century that experimental tests provided evidence that failure of the planked arches occurs at the joints (Hahmann, 2006, Figure 6.23); even though the theoretical formulations of the time were unable to describe the response of the joints in bending and shear.

However, to the author's knowledge, the first attempt to simulate a planked timber arch with realistic values of bending and shear stiffness of nailed joints was developed by Fernandez Cabo *et al.* (2012). The present research on planked timber vaults builds on this work as a result of a collaboration of the author with the research group at UPM led by Prof. Fernandez Cabo.

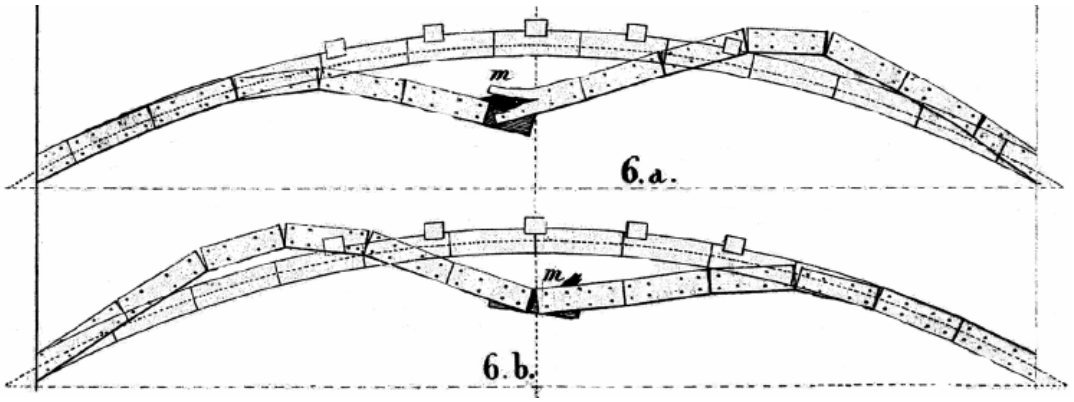

Figure 6.23 Failure of a planked timber arch during experimental tests performed by Zimmermann in 1830 under distributed vertical load, as reported by Hahmann (2006)

A representative planked timber arch is illustrated in Figure 6.24. The arch is composed of two parallel alignments of arc-shaped timber planks, designated as arch *i* and arch *j*, that are connected by means of pairs of nails. The loads are transmitted from plank 1 in arch *j*, for instance, to the adjacent planks 1 and 2 in arch *i* through the pairs of nails. Adjacent planks in either arch *i* or arch *j* (plank 1 and plank 2) may or may not be in contact depending on whether the construction gap usually present, may have closed due to relative rotation during its loading history.

The in-plane response of the arch is governed by constitutive laws describing the structural behaviour of the nailed joints under shear in the directions parallel and perpendicular to the grain and under bending moment around an axis normal to the plane of the arch. For instance, if a force F_y or F_z is applied to plank 2 of arch *i*, each nail will transfer the load to the connected planks of arch *j* through a local deformation of the timber, dependent upon its shear stiffness parallel to the grain, K_{par}, or perpendicular to the grain, K_{per}, respectively. Similarly, each pair of nails will resist a bending moment, M_x, proportional to the rotational stiffness, K_{rot}, of the connection. If the surfaces of arch *i* and *j* are in contact, reaction forces develop upon these surfaces when relative movement in a vertical plane occurs, dependent upon the timber friction coefficient and normal pressure exerted by the nailed connection. A similar phenomenon occurs when two planks of the same arch are in contact due to the deformation of the arch. These friction forces are not represented in Figure 6.24.

The out-of-plane response of the arch is similar to the response of a continuous arch of thickness equal to the sum of the thickness of arch *i* with arch *j*, since the nails are hooked at the end and therefore withdrawal of the nails and separation of the two alignments of planks are not expected (this can be seen in Figure 6.25 which shows representative nails of the Cathedral of Ica taken from collapsed elements by the author).

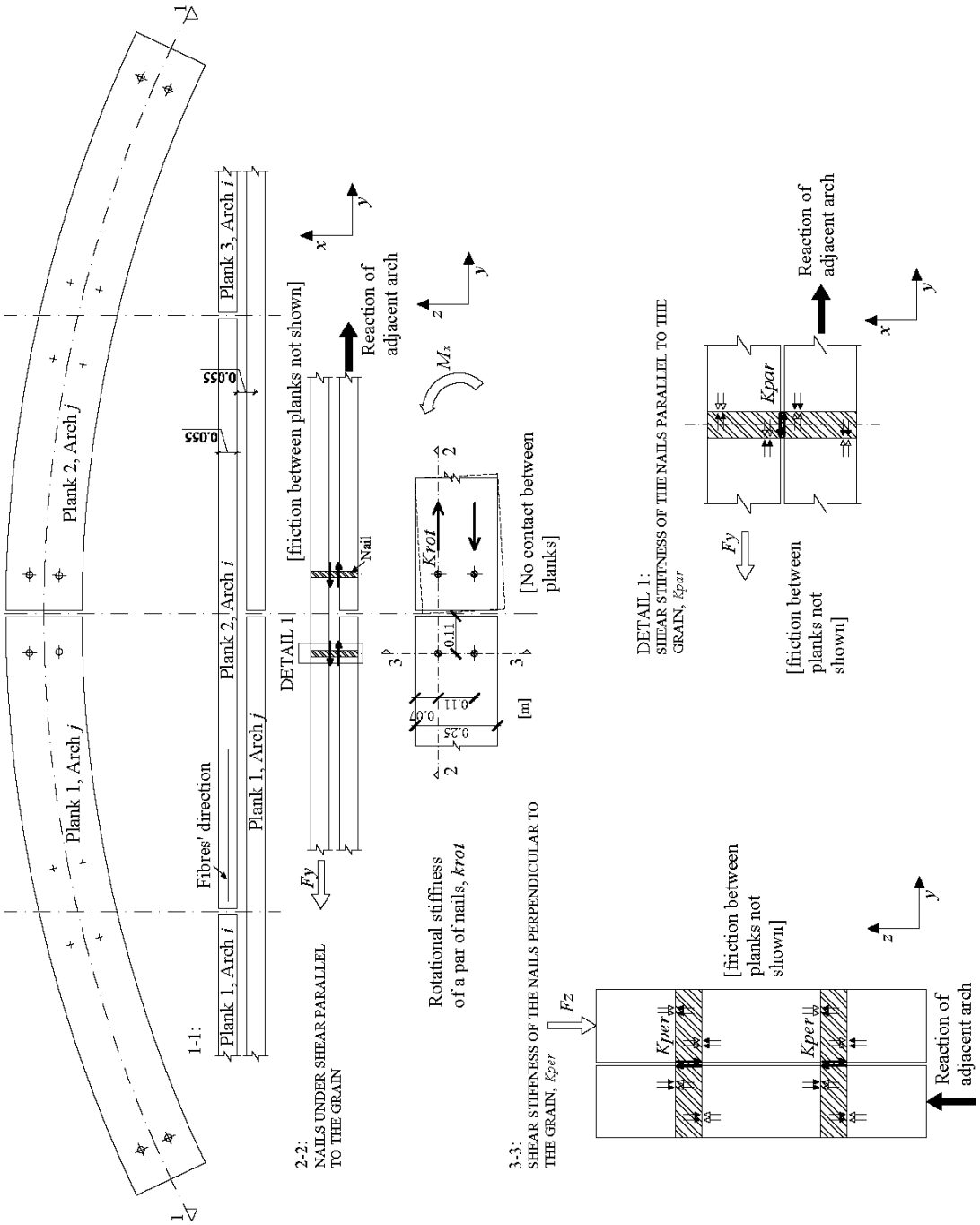

Figure 6.24 In-plane response and stiffness of the nailed joints of a representative planked timber arch

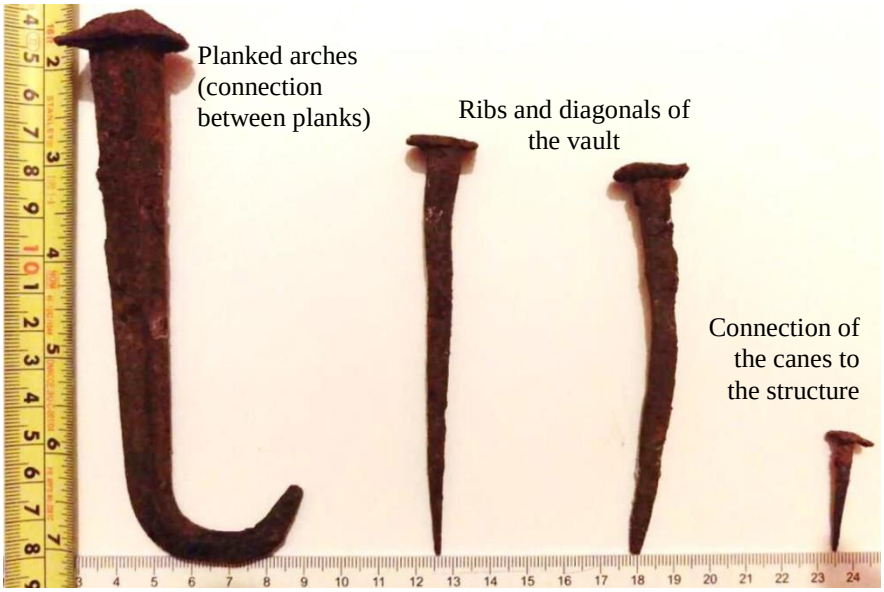

Figure 6.25 Representative nails of the cathedral of Ica

6.4.4.1 SIMULATION OF EXPERIMENTAL TESTS FOR VALIDATION OF NUMERICAL INPUTS

A representative arch, composed of linear planks, similar to historic arches of timber vaults in Spain, was tested under increasing monotonic in-plane vertical static load at Universidad Politécnica de Madrid (UPM) by Fernandez *Cabo et al.* (2012). The aims of the test were (1) to measure the natural frequencies and (2) to evaluate the displacements of the experimental model. Pine of Cuenca, Spain, (*Pinus nigra* Arnold) was used to build the experimental model, since it has material properties similar to *guarango* (*Prosopis pallida* L.) and Mexican cedar (*Cedrela odorata* L.), which are wooden species traditionally used in historic timber vaults in Latin America. Self-tapping screws were used instead of the traditional wrought iron nails due to difficulties in getting a sufficient number of similar original nails in good condition. The experimental model is composed of two similar arches connected to each other by means of a horizontal and diagonal bracing, which provides out-of-plane stability to the arches (Figure 6.26).

Mean and maximum experimental values of shear stiffness parallel and perpendicular to grain and rotational stiffness, *Kpar*, *Kper* and *Krot* respectively, of screwed joints replicating the joints of UPM's experimental model are indicated in Table 6.18, as obtained by shear and bending tests performed in accordance with the European standard EN 26891 (CEN, 1991, Fernandez Cabo *et al.*, 2012). Mean and maximum values of the modulus of elasticity of *Pinus nigra* Arnold (Table 6.19) were obtained by work of Fernández-Golfín

Seco *et al.* (2003), who tested 3312 pieces of wood in bending following the procedure of UNE EN 408 (2000). The experimental arch was simulated in the software package Autodesk Simulation Multiphysics 2013© (former ALGOR©), using the approach shown in Figure 6.27 to model the planks and nailed connections (Fonseca Ferreira *et al.*, 2013).

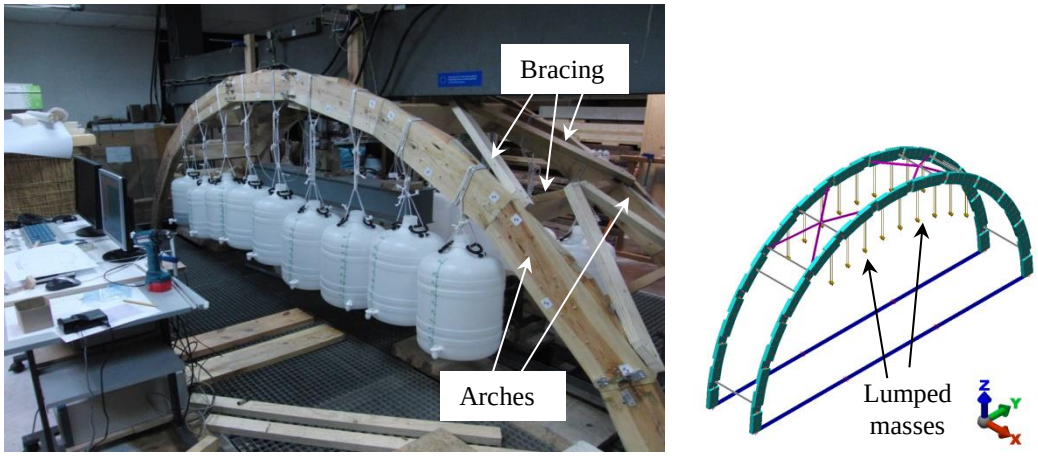

a) Experimental model after testing in UPM b) Author's numerical model

Figure 6.26 Arch test and numerical model

Table 6.18 Experimental shear and rotational stiffness of screwed joints, according to Fernandez Cabo *et al.* (2012)

	K_{par} (kN.m^{-1})		K_{per} (kN.m^{-1})		K_{rot} (kN.m.rad^{-1})
	Mean	Maximum	Mean	Maximum	
1 screw	2050	3300	1460	2250	-
2 screws	4100	6600	2920	4500	5.4
Value selected for the numerical models after sensitivity analysis					
1 screw	3300		2250		5.4
2 screws	6600		4500		5.4

Table 6.19 Experimental material properties of timber

Wooden specie	Density (kg/m^3)	Modulus of elasticity parallel to the grain, *MoE* (N/mm^2)		Poisson's ratio
		Mean	Maximum	
Pinus nigra Arnold	550	16525	38183	0.3
Value for *pinus nigra* selected for the numerical models after sensitivity analysis	550	38183		0.3
Cedar (material properties obtained through tests conducted at PUCP)	380	9400		0.3

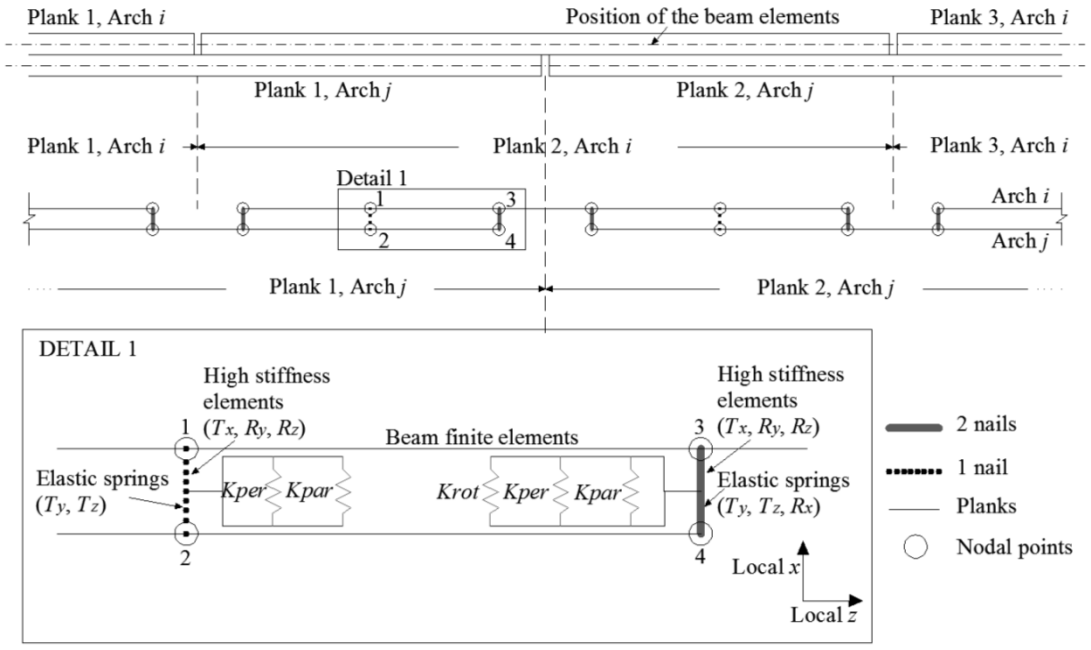

Figure 6.27 Approach for the three-dimensional numerical modelling of planked arches

The timber planks are modelled by means of beam elements which are located at the longitudinal axis of the real members. During the experimental work, only the in-plane behaviour of the experimental specimen was studied. Hence, only the in-plane response of the nailed joints is modelled. This is done by means of elastic springs that transmit the loads from arch *i* to arch *j* or vice-versa. Three springs are introduced at the location of the pair of nails, corresponding to K_{par}, K_{per} and K_{rot}, and 2 springs at the location of the 1-nail joint, which has negligible rotational stiffness. The springs K_{par} and K_{per} simulate the relative

translation of the planks in the plane of the arch by reproducing the behaviour in shear of the nailed joints in the direction parallel and perpendicular to the grain of the planks respectively. Moreover, the spring with K_{rot} simulates the relative rotation of the planks in the plane of the arch. Because most of the deformations occur between nails and timber, it is important to account for the different stiffness and strength in the direction parallel and perpendicular to the grain of the timber, when determining the characteristics of the springs.

The vertical load applied to the experimental specimen is simulated in the numerical model by means of lumped masses; beam elements connecting the spring points of the arches are introduced in the model to simulate steel ties used during the test to measure the lateral thrust (Figure 6.26b).

The stiffness of the joints, K_{par}, K_{per} and K_{rot} and the modulus of elasticity of the beam elements, *MoE*, are varied in the numerical model within the ranges shown in Table 6.18 and Table 6.19, in order to determine the best fit to the experimental response. This validation of the input parameters of the numerical model is based on the comparison of natural frequencies of the unloaded arch and displacement and rotations measured during the loading sequence. The first mode has an experimental natural frequency of 3.9Hz, compared to the 2.55Hz and 3.17Hz obtained with the mean and maximum spring values, respectively. For the second mode corresponding values are 11.7Hz, 8.08Hz and 10.17Hz, respectively. The first mode has a participating mass of 65% in the Y direction, while the second mode has a participating mass of 23% in the Z direction. Differences between the numerical and experimental values are within 15 to 20%.

Comparison of displacement and rotation of the planks at locations of four LVDTs are shown in Figure 6.28. Within the loading range applied, the behaviour remains essentially linear at all positions. The values of displacement are within 20% to 30% below the experimental ones when using the maximum values of the input range.

The results of both modal analysis and static stress analysis show that the experimental model is stiffer than the numerical models and therefore a reasonable agreement is achieved when the maximum values of the input parameters are used. This can be due to light pretensioning of the arch ties in the experimental setting, and/or stronger fastening of the screws connections which might have been tighter in the arch than in the connection tests leading to increased rotational stiffness. Moreover, further sensitivity analysis performed by Fernando Cabo *et al.* (2012) also show that the response of the arches is more sensitive to variation of the joints' stiffness than to variation of the material modulus of elasticity parallel to the grain.

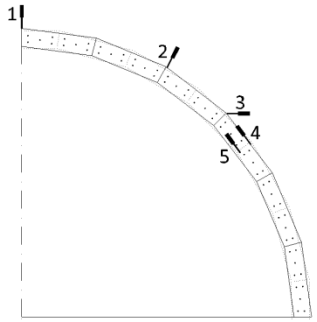

Location of the LVDTs
during the test performed at UPM

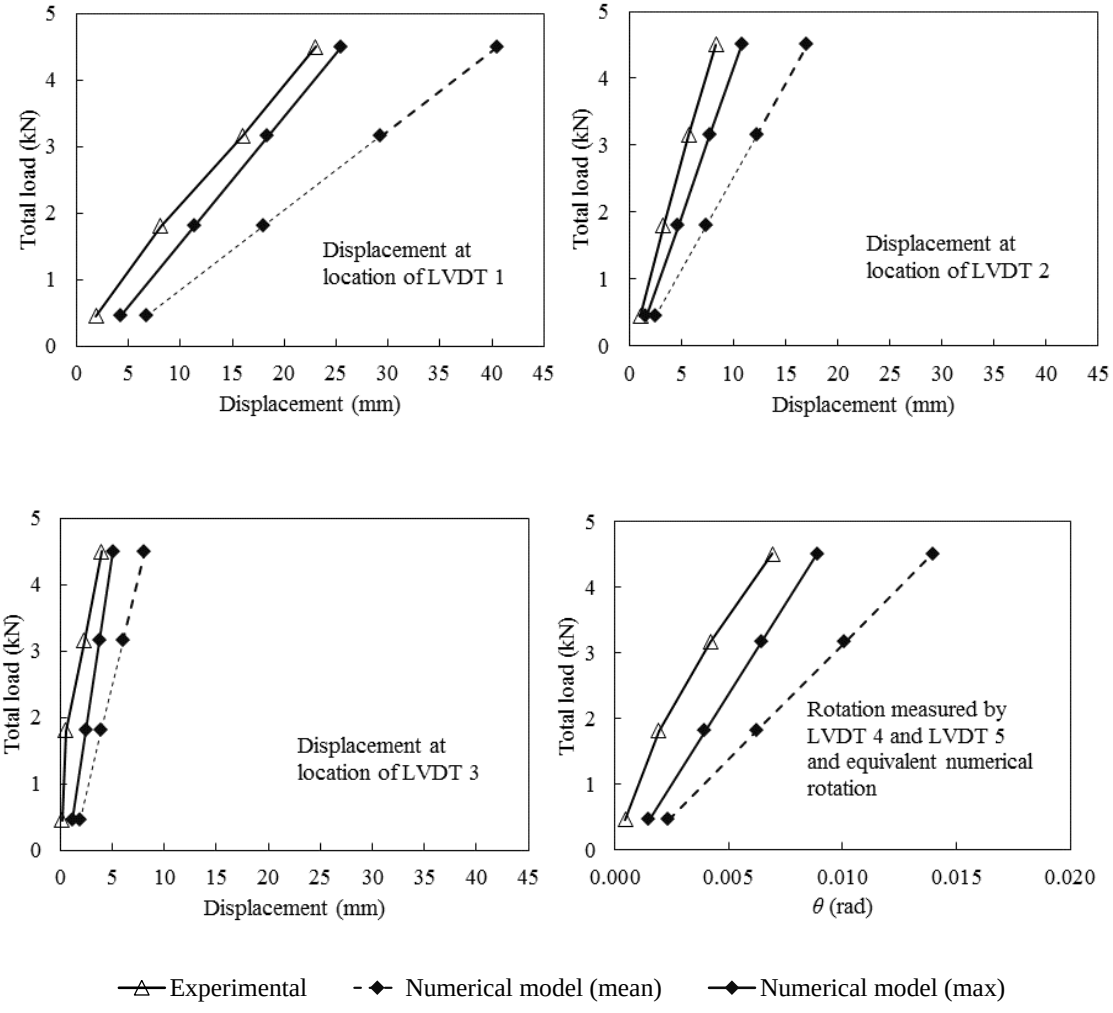

Figure 6.28 Comparison between experimental and numerical results of linear static analysis, considering both mean and maximum values for input parameters

6.4.4.2 LOCAL MODEL OF THE VAULT WITH REALISTIC SIMULATION OF TIMBER JOINTS

A representative bay of the vault of the central nave of the Cathedral of Ica is reproduced in the model of Figure 6.13, using the modelling approach shown in Figure 6.27, without considering however the 1-nail joints located at the centre of the planks. The maximum input values of Table 6.18 and Table 6.19 are used in this model to characterise the beam and spring elements. The results of this model, referred to as 'discontinuous model', are compared with the results of analyses performed with a 'continuum model', with the same geometry but composed of volume elements continuously connected (Fonseca Ferreira and D'Ayala, 2012).

Table 6.20 shows that the natural frequencies of the continuous vault associated to modes 1 and 2 are three times larger than the corresponding frequencies of the discontinuous vault, which is explained by the decrease of stiffness of the vault when realistic values of shear and rotational stiffness of the nailed joints are considered.

Table 6.20 Natural frequencies and modal participating masses of the discontinuous and continuous model of a representative bay of the vault of the Cathedral of Ica

	Mode 1		*Mode 2*	
	Frequency (Hz)	Participating mass (%)	Frequency (Hz)	Participating mass (%)
Discontinuous model (simulation of joints)	3.8	75.0 (Y direction)	9.1	16.6 (Z direction)
Continuous model (no simulation of joints)	13.1	67.0 (Y direction)	29.0	8.8 (Z direction)

Modal superposition analysis is also performed with both models using the North-South elastic response spectrum recorded at the station of Parcona in the province of Ica (Peru) during the 2007 Pisco earthquake (Tavera *et al.*, 2009), applied to the Y direction (in-plane) of the numerical models (Figure 6.19).

Although distribution of stresses and deformed shape are consistent in the two models, accurate analysis of the deformed shape of the central arch of the models (Figure 6.29) shows that the displacements of the continuous model are in the range of millimetres, one order of magnitude smaller than the displacements of the discontinuous model. The 2007 Pisco earthquake caused permanent relative deformations of the planked arches of the same

order of magnitude of the discontinuous numerical model. Hence, the modelling of the nailed joints seems to be fundamental to realistically simulate the deformation of the arches and the relative movement of the planks as it is evidenced by the difference between the deformed shape of arch *i* and arch *j* in the output of the discontinuous model.

Furthermore, this modelling approach provides a direct measure of the shear forces acting at each joint for a given seismic demand. This allows an expedite verification of the condition of the joints and ultimately of the safety of the vault, as discussed in Chapter 9.

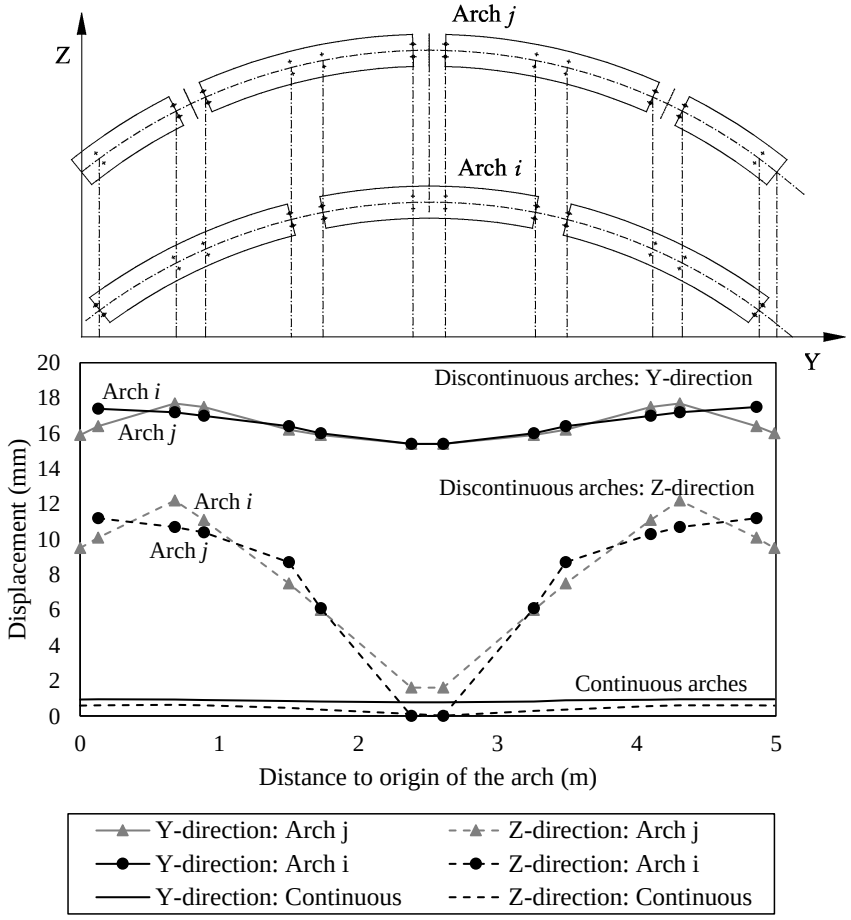

Figure 6.29 In-plane displacement of the discontinuous and continuous models after modal superposition analysis

6.4.5 Hypothesis of a rigid vs flexible diaphragm

A complementary qualitative analysis is conducted in the following in order to evaluate the structural role of the roof's covering of the Cathedral of Ica. The evaluation of the influence of the composite cane-gypsum-mud-cement-mortar layers to the structural behaviour of the roof, and possibility of its assumption as an in-plane rigid diaphragm requires the analysis of the following considerations:

(i) Condition of the building after the earthquake shows/does not show evidences of in-plane diaphragm action of the roofing;
(ii) Stiffness of the composite layers; and
(iii) Connection of the composite layers to the timber frame is/is not effective.

6.4.5.1 CONDITION OF THE BUILDING AFTER THE EARTHQUAKE SHOWS/DOES NOT SHOW EVIDENCES OF IN-PLANE DIAPHRAGM ACTION OF THE ROOFING

The hypothesis of a rigid diaphragm requires that the composite roofing (canes + plaster) behaves as a rigid body in its plane. This hypothesis implies that all bays of the central nave deform approximately the same amount in the longitudinal direction. Typical rigid diaphragm action is illustrated in Figure 6.30 and a typical flexible diaphragm action is illustrated in Figure 6.31, in a simplified way. A flexible composite cane-plaster layer would be overall cracked due to the presence of stresses within its plane caused by the relative deformation of the bays in relation to each other, and the relative deformation of the components within each bay. This cracking can be clearly seen in the cathedral, as shown in Figure 6.32.

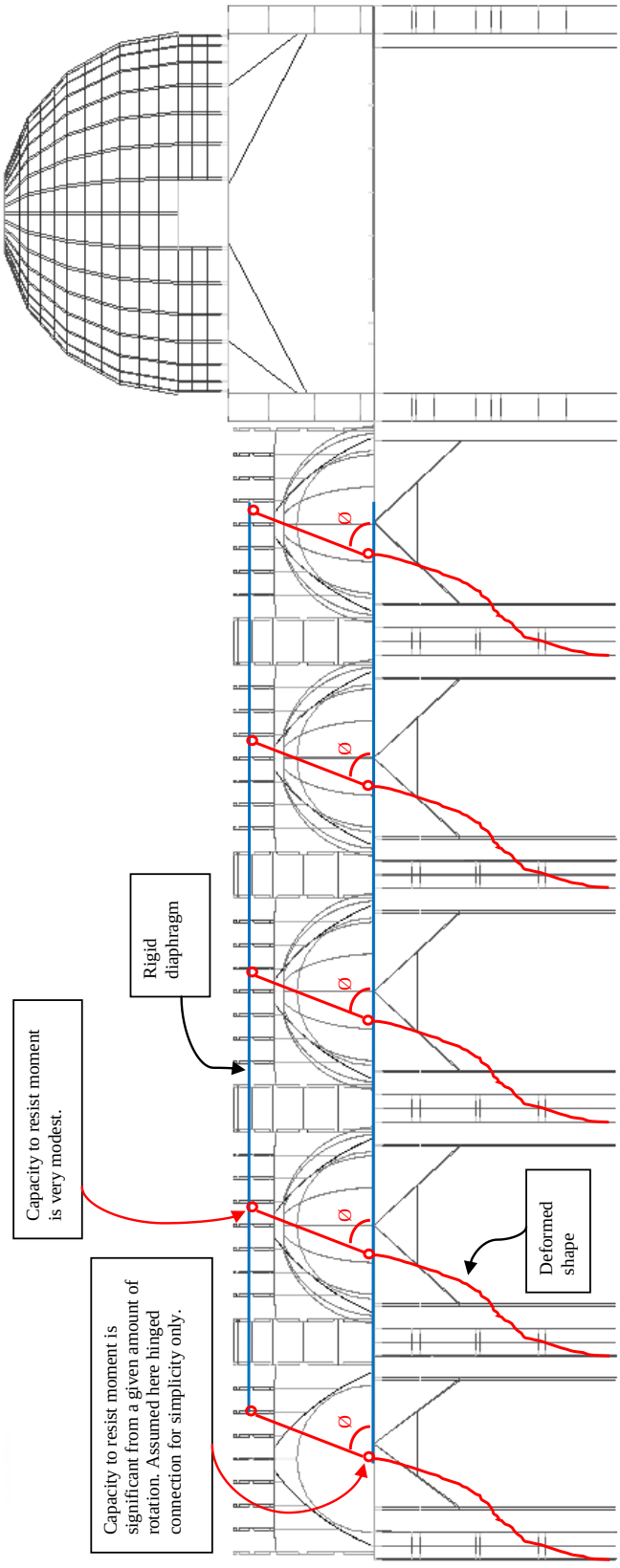

Figure 6.30 Hypothesis of rigid diaphragm action (simplified sketch) longitudinal direction

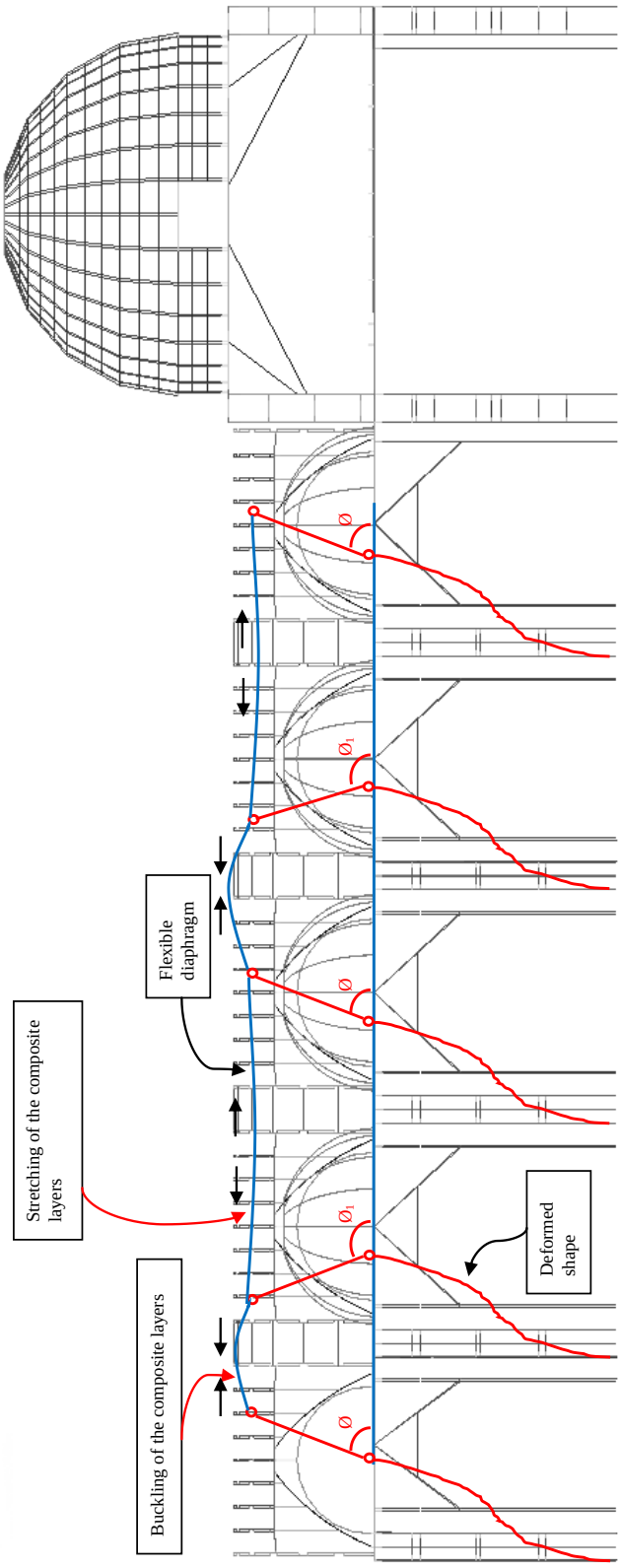

Figure 6.31 Hypothesis of flexible diaphragm action (simplified sketch with exaggerated deformations) in the longitudinal direction

Figure 6.32 Generalized cracking of the roof of the Cathedral of Ica (courtesy of Claudia Cancino)

In the transversal direction, a rigid composite cane-plaster layer would restrict the relative displacement of the bays and of the elements within each bay in relation to each other due to its high shear and bending stiffness, as illustrated in Figure 6.33. However, on-site measurements show that the pillars of bay 3 of the main nave have lateral permanent deformations of one order of magnitude greater than the deformation of the pillars of bays 1 and 5. This difference indicates the presence of a flexible diaphragm; as evidenced by many examples of this type of response available in literature, either when considering a timber composite roof (e.g. Proaño *et al.*, 2007; Betti and Vignoli, 2011; Gattulli *et al.* 2013) or when considering masonry vaults (e.g. Croci, 2001; Betti and Galano, 2012).

Moreover, the composite layers at the top of the cathedral's roof are more flexible than common solutions considered in literature as closer to a rigid diaphragm (e.g. Piazza and Turrini, 1983; Meda and Riva, 2001; Giuriani *et al.*, 2005; Giuriani and Marini, 2008). These solutions involve at least the existence of two layers of orthogonal wooden planks, as proposed by Benedetti (1981). However, the roof at the top of the vault does not have any layer of wooden planks. The roof of the aisles has only one layer, which is not continuous due to the presence of the domes. Thus, the cathedral's roof behaves as a flexible diaphragm with low stiffness, as it is further discussed in the following.

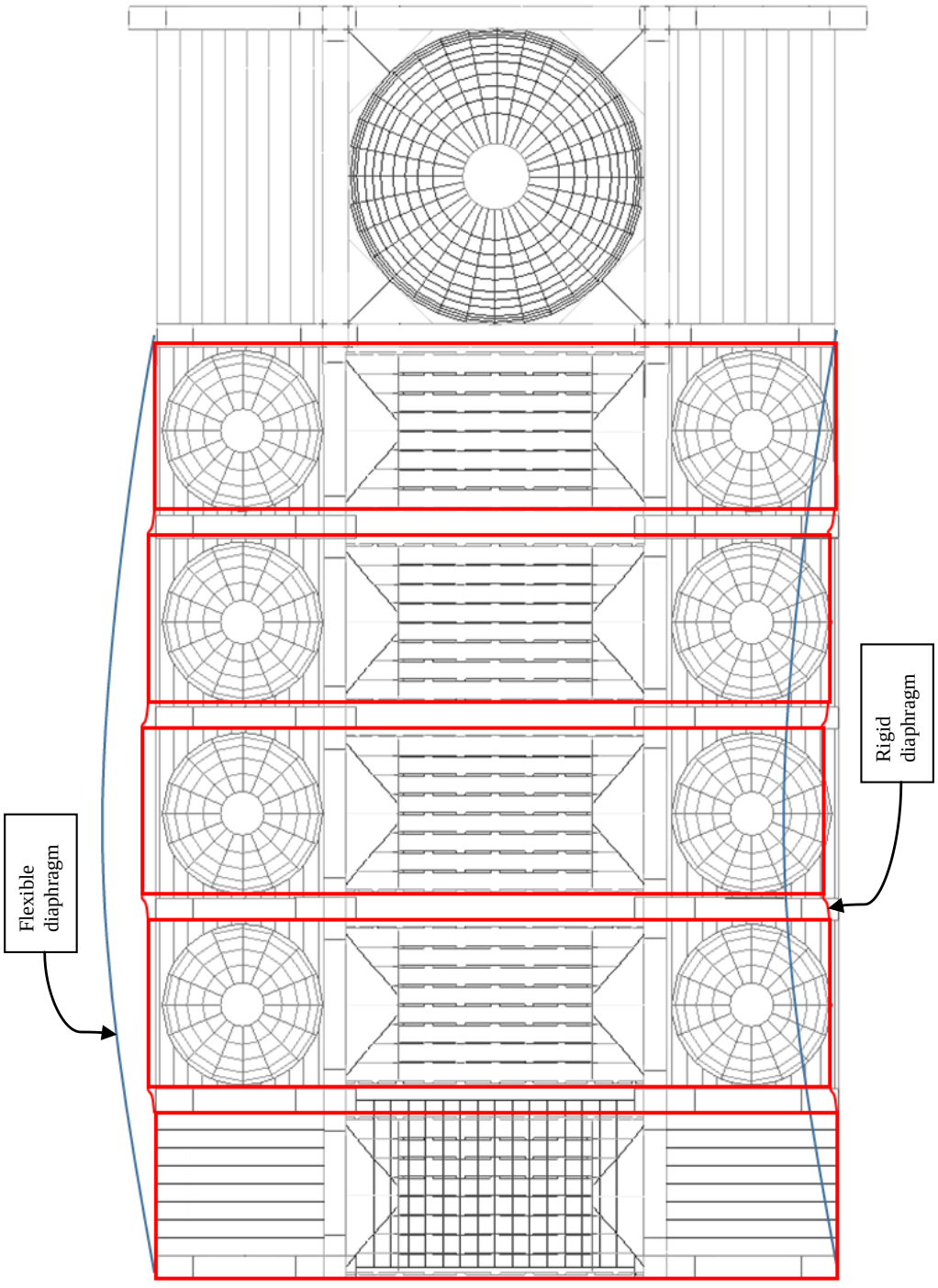

Figure 6.33 Transversal response of the nave for hypothesis of rigid/flexible diaphragm (simplified sketch)

6.4.5.2 STIFFNESS OF THE COMPOSITE LAYERS

Bariola *et al.* (1988) tested diverse modern *quincha* panels in compression, shear and bending. Results of these tests are summarized in Table 6.21, Table 6.22 and Table 6.23.

Table 6.21 Results of compression tests performed with modern quincha panels (after Bariola *et al.*, 1988)

Panel	Initial stiffness (kN/m)	Max. load (kN)	Vertical displ. at max. load (mm)	Buckling disl. at max. load (mm)	Obs.
With cane mat. No plaster.	14000	17	3.0	9.3	In-plane buckling
With cane mat. Plastered with cement mortar.	20000	27.8	4.0	18.0	Out-of-plane buckling
With cane mat. Plastered with 1 layer of mud with 10% straw (20mm) and 1 layer of sand-cement mortar (10mm).	7200	34.5	4.1	7.9	Out-of-plane buckling.

Table 6.22 Results of shear tests performed with modern quincha panels (after Bariola *et al.*, 1988)

Panel	Initial stiffness (kN/m)	Max. load (KN)	Displacement at maximum load (mm)	Observations
No cane. Frame only.	2.0	0.070	100	The contribution of the frame is very modest. It behaves like a mechanism.
With cane mat. No plaster.	18	0.230	93	Strength was very low. Damage was not observed. The panel can develop large deformations with no appreciable damage.
With cane mat. Plastered with 1 layer of mud with 20% straw (20mm) and 1 layer of soil-cement (10mm).	230	1.600	36	Failure type: base uplifting There were no cracks in the mortar except at the lower corner far from the load. The panel underwent a rigid body motion.

Table 6.23 Results of bending tests performed with modern quincha panels (after Bariola *et al.*, 1988)

Panel	Stiffness at 2mm disp. (kN/m)	Stiffness at 5mm disp. (kN/m)	Final stiffness (kN/m)	Load at 50mm displ. (kN)	Observations
Panels plastered with a 1st layer of mud (1soil:1sand) + 2nd layer of sand-cement	210	130	35	2.5	Failure type: cracking of the plastering.
Panels plastered with a 1st layer of mud (1soil:2sand) + 2nd layer of sand-cement	370	200	35	3.0	Failure type: cracking of the plastering. Results not reliable.
Panels plastered with a 1st layer of mud (1soil:3sand) + 2nd layer of sand-cement	310	200	45	3.5	Failure type: cracking of the plastering.

Some general conclusions about the effect of the composite layers can be made from the results of these tests; even though the mechanical properties measured are not directly applicable to the Cathedral of Ica due to the following issues:

(i) the cane system is composed of a woven cane mat placed on both sides of the timber frame, with canes running in two orthogonal directions and in both case strongly connected to the frame elements by timber plates nailed to the timber frame, preventing the cane's end from slipping or rotating. Thus, there is substantial in-plane shear stiffness due to the double weave. The cane mat and respective connection of the roof of the cathedral have lower stiffness (see Figure 6.34);
(ii) The plastering's layers are different from the ones observed in the Cathedral of Ica.

The stiffness of the composite layers of the cathedral can be assumed from the tests, as shown in Table 6.24; even though these values are far greater than the real stiffness due to the aforementioned issues. The axial stiffness is equal to the difference between the stiffness of the panel with canes and plaster and the stiffness of the frame alone (7000kN/m).

Figure 6.34 Cane system of the Cathedral of Ica's roof

Table 6.24 Stiffness of the composite layers (based on Bariola *et al.*, 1988)

Panel	Axial stiffness (kN/m)	Shear stiffness (kN/m)	Out-of-plane stiffness (bending tests) (kN/m)
Cane mat with plaster	200-7000 depending on testing condition	230	370

This overestimated stiffness of the Cathedral of Ica's roof is far from the stiffness of a typical rigid diaphragm, which would need to be substantially greater.

Moreover, for the roof to be considered as an in-plane rigid diaphragm, it has to be significantly stiffer than the timber framing. The in-plane and out-of-plane stiffness of each internal arch are shown in Table 6.25. These values were obtained from modal superposition analysis performed with the local model of the nave of the Cathedral of Ica, in which the joints' stiffness was realistically simulated.

Table 6.25 Stiffness of the internal arches of the Cathedral of Ica

Out-of-plane stiffness (stiffness of the arches in the X-direction of the models)	1400kN/m
In-plane stiffness (stiffness of the arches in the Y-direction of the models)	2000kN/m

The out-of-plane stiffness of each internal arch (1400kN/m) is either greater or at best five times smaller than the axial stiffness of the composite layer. Furthermore, the in-plane stiffness of the arches is one order of magnitude greater than the shear and out-of-plane stiffness of the composite layers. This leads to the conclusion that the covering is unable to restraint relative in-plane displacements between the arches.

As concluded in Bariola *et al.* (1988) and shown in Table 6.23, the contribution of the plaster for the stiffness of the system is only relevant for small deformations. As soon as the plaster cracks, the stiffness of the system depends almost entirely on the stiffness of the timber framing.

6.4.5.3 CONNECTION OF THE COMPOSITE LAYERS TO THE TIMBER FRAMING (IS/IS NOT) EFFECTIVE

For the composite layers to be effective in providing restraint to the internal arches, the canes have to be connected to these arches. Evidence of this would be nails and leather marks on each arch. Observation of the arches found on the floor of the Cathedral of Ica reveals that:

(i) Not all arches bear those marks;
(ii) The ones that bear the marks, usually only have it on one of the planks alignment, such that the restraint is asymmetric in relation to the middle plane of the arch, and hence not totally effective in preventing out-of-plane movement (see Figure 6.35).

Figure 6.35 Collapsed internal arches on the ground of the Cathedral of Ica, showing that the canes were fixed to only one alignment of planks in each arch

Further evidence that the canes are not connected to all internal arches can be deduced from the fact that the canes are longer than the span between two adjacent arches, and that where the arches have collapsed the canes have not followed (see Figure 6.36). Moreover, the canes are not continuous between adjacent bays and between the edge arches of each bay (Figure 6.36), leading to a non-uniform deformation of the bays, as per the graphics of Figure 6.31.

Figure 6.36 Failure of the composite layers after the 2007 Pisco Earthquake (courtesy of Erika Vicente)

At the top of the vault, the cathedral has *caña brava* (a Peruvian type of cane) which is attached to the arches by leather straps nailed to the timber members (Figure 6.34). The leather straps have lost the state of pre-compression over the years, and hence do not guarantee a tight connection anymore. This was observed throughout the cathedral. The composite layers therefore might be loose, especially if the nails are fixed to the leather straps and not to the canes; even though the canes do not detach from the timber framing. The connection canes/frame is a critical issue, since the failure will occur at this point rather than by failure of the canes. This was concluded in Bariola *et al.* (1988) after testing both the canes isolated and the connection under tension. The tension strength of the cane was found to be 250MPa and the strength of the connection was found to be 0.3MPa for a state of stress of 2.5MPa in the canes (much lower than the tensile strength). This was also clearly observed in the Cathedral of Ica.

The plaster is overall cracked, as shown in Figure 6.32. Cracking is likely to develop after construction due to shrinkage, which would decrease the stiffness of the roof, even if no further damage occurs. Moreover, the plaster has detached from the canes in most of the areas where the self-weight is not sufficient to keep the plaster in place (see for instance Figure 6.34). This indicates poor adherence of the plaster to the canes.

The aforementioned investigations show that the roof cladding of the Cathedral of Ica does not behave as a rigid diaphragm. Thus, at the ultimate limit state, the roof's cover should not be included in the global model if not as added weight. It should also be noted that the assumption of the timber roofs as added weight is a common modelling approach applied in literature (see for instance Betti and Galano, 2012).

6.5 Uncertainty of the input in the assessment of a historic timber structure

As indicated in Figure 3.1 and discussed in Section 3.5.2, the uncertainty of the input in the assessment of the Cathedral of Ica can be obtained by carrying out sensitivity analysis with the local model of the cathedral (Figure 6.12b). In the following, reference will be made to relevant sections of Chapter 3, especially Section 3.4 and 3.5.2 for more clarity.

6.5.1 Local model for uncertainty analysis

As a result of the analyses conducted at a local level and the experimental campaign carried out at PUCP, the local model of the nave's bay evolved from a continuous model made of volume elements to the refined beam and spring model shown in Figure 6.37. Beam elements are used to simulate the timber members, and springs are used to simulate the following timber joints:

(i) nailed joints of the arches;
(ii) mortice and tenon without pegs;
(iii) pegged mortice and tenon;
(iv) nailed joints of the diagonal bracing of the pillars.

The modelling of the in-plane response of the planked arches was already discussed in Section 6.4.4.1. However, the out-of-plane response has not been discussed yet. In this regard, elements of very high stiffness are used to transmit the out-of-plane translation (along X), and rotation around both Y and Z between parallel planks in the arch. Hence, in

the out-of-plane direction, the two alignments of planks of the arches respond together as continuous arches made of one curved timber member of thickness double of the thickness of a plank, and no relative out-of-plane separation between these alignments is admitted.

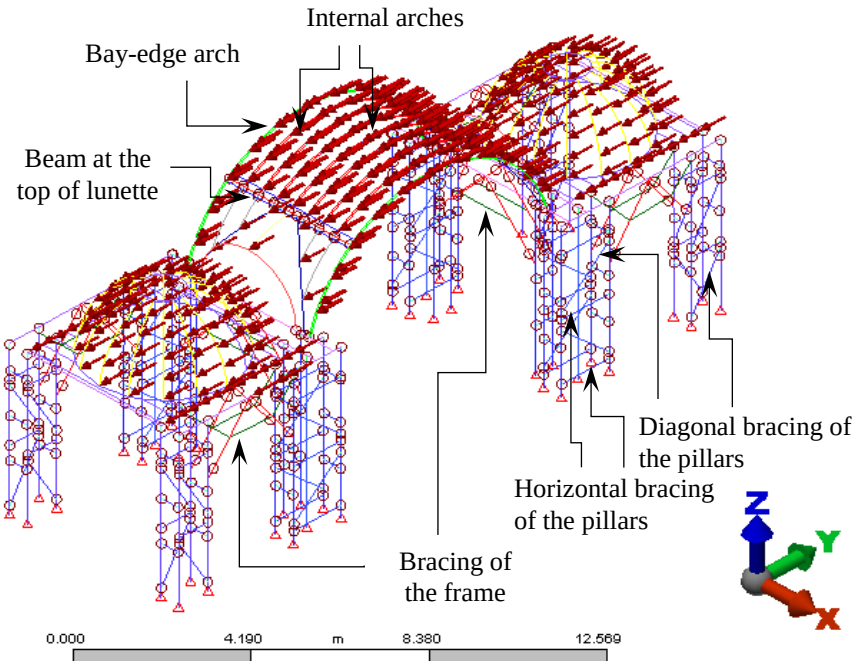

Figure 6.37 Final local beam and spring model of the nave's bay

This is a valid assumption since the nails are hooked at the end. The timber members are simulated by means of beam elements with isotropic and linear material models. The wooden species of the structural elements are indicated in Table 6.26 and the respective material properties in Table 6.14.

Caoba Africana was used to build long elements of the structure, such as the posts and beams of the frame and vault. Cedar was used to build the various members of the vault, except the beam at the top of lunettes, and *guarango* was used to build the diagonals and the central post of the pillars.

Mortice and tenon joints are simulated by releasing the degrees-of-freedom (DOF) corresponding to the rotation of the tenon around an axis parallel and perpendicular to the grain of the morticed beam. Two elastic springs are introduced between the timber members, one with a rotational stiffness of the joint parallel to grain and the other with a rotational stiffness of the joint perpendicular to grain, using the values of Table 6.15.

Pegged mortice and tenon joints are simulated by releasing the translation of the ends of the elements in the direction of the centreline of the horizontal bracing and introducing a spring with the stiffness indicated in Table 6.15.

Table 6.26 Wooden species of the structural members of the nave of the Cathedral of Ica

Wooden species	Structural elements
Caoba Africana	1. Beam at the top of lunettes; 2. Longitudinal beams and corresponding supports at the ends; 3. Longitudinal beams of the aisles; 4. Transversal beams and corresponding supports; 5. Aisles' joists; 6. Top and bottom rings, meridians and parallels of the aisles' domes; 7. Posts of lateral pillars; 8. Horizontal bracing of lateral pillars; 9. Posts of central pillars; 10. Horizontal bracing of central pillars; 11. Choir loft's transversal beams and joists.
Guarango	12. Diagonals of lateral and central pillars; 13. Central post of central pillars.
Cedar	14. Bay-edge arches' planks; 15. Internal arches' planks; 16. Lunette's ribs; 17. Lunette's diagonals; 18. Lunette's central rib; 19. Lunette's arch.

The nailed connections of the diagonals are simulated by releasing the in-plane rotation of the diagonal corresponding to the opening of the connection, as shown in detail 9 of Figure 4.36, and introducing a spring with the stiffness indicated in Table 6.15.

The modelling approach of the most relevant timber joints of the structure of the nave are summarized in Table 6.27.

Table 6.27 Modelling approach of the principal timber joints of the nave

Type of joint	Structural elements connected	Modelling approach
Nailed joints of the arches	1. Planks of the bay-edge arches; 2. Planks of the internal arches.	Figure 6.27
Mortice and tenon	Connections within the vault: 3. Internal arches / Beam at the top of lunettes; 4. Beam at the top of lunettes / Bay-edge arches; 5. Lunettes' ribs / Beam at the top of lunettes; 6. Lunettes' diagonals / Beam at the top of lunettes; 7. Lunettes' central rib / Beam at the top of lunettes. Connection of the vault to the frame: 8. Bay-edge arches / Longitudinal beams; 9. Lunettes' diagonals / Longitudinal beam; 10. Lunettes' arch / Longitudinal beam. Connections within the frame: 11. Posts of lateral pillars / Transversal beams; 12. Posts of central pillars / Transversal beams; 13. Posts of central pillars / Longitudinal beams; 14. Central post of central pillars / Transversal beams.	Rotations around an axis parallel and perpendicular to the grain of the beam are released. 1 elastic spring with experimental stiffness is introduced to govern each released DOF.
Pegged mortice and tenon	15. Horizontal bracing of central pillars / Posts of central pillars; 16. Horizontal bracing of lateral pillars / Posts of lateral pillars.	Translation in the direction of the centre line of the horizontal bracing is released. 1 elastic spring with experimental stiffness is introduced to govern this DOF.
Nailed connections (diagonals)	17. Diagonals of lateral pillars / Posts of lateral pillars; 18. Diagonals of central pillars / Posts of central pillars.	Rotation around an axis perpendicular to the grain of the posts is released. 1 elastic spring with experimental stiffness is introduced to govern this DOF.
No joint simulation (continuous connections)	19. Lunettes' ribs / Lunettes' diagonals; 20. Transversal beams / Longitudinal beams; 21. Aisles' joists / Transversal beams; 22. Connections among elements of the aisles' domes.	Elements continuously connected.

6.5.2 Control variables

The control variables with the respective plausible values and states are set out in Table 6.28 and Table 6.29, respectively, where δV_{Ki} is the range of variation of the control variables. In the case of historic timber structures that are hidden by plaster, control variables associated to the geometry and structural details are an important source of uncertainty. If original drawings are not available, removal of plaster or advanced laser scanning techniques may be normally required to identify the geometry of the structure and details of the joints.

In the case of the Cathedral of Ica, recording and measuring of the geometry of the vault, frame and central dome were conducted in detail to an extent due to the partial collapse of bay 1, vault and central dome. A complementary survey of representative lateral and central pillars of the nave and central and lateral domes, with removal of plaster was conducted within the EAI-SRP. This allowed having a detailed record of the geometry of the whole timber structure.

Likewise, an identification of the wooden species and characterization of material properties of samples collected on the site was conducted by Universidad La Molina (Chavesta Custodio *et al.*, 2012). The principal timber joints were tested in the laboratory at PUCP (Torrealva and Vicente, 2014) for mechanical characterization, as mentioned before.

However, a detailed survey is not sufficient to assure a high level of knowledge due to the following two principal reasons:

(i) Geometry and structural details may vary throughout the structure due to poor quality assurance; and
(ii) Level of deterioration might be sufficiently high to significantly change the structural behaviour of the joints and members of the structure. The level of deterioration is difficult to evaluate on this type of structures, since deterioration is normally not localized at a few points but generalized and not uniform throughout the structure.

Deterioration is difficult to identify, since a thorough identification would require a large operation of removal of plaster. This operation would compromise the cultural value of the building, because the original plaster is an intrinsic part of this value. Moreover, even if deterioration is concentrated at a few locations, the impact of deterioration on the structural response of the building is normally evaluated with a high level of uncertainty.

Table 6.28 Control variables of the Cathedral of Ica characterised by values and respective intervals of plausibility [V_{kimn}, V_{kiref},V_{kimx}] and ranges of variation δV_{Ki}

Class	Control Variables			Units	V_{kimn}	V_{kiref}	V_{kimx}	$\delta V_{Ki} = 1 - \left(\frac{V_{Kimn}}{V_{Kimx}}\right)$ *[normalized]*
Materials	V_{P1}	Modulus of elasticity of *Caoba Africana*		MPa	7500	10300	15000	0.50
	V_{P2}	Modulus of elasticity of *Guarango*		MPa	9500	16900	18600	0.49
	V_{P3}	Modulus of elasticity of Cedar		MPa	7500	9400	14800	0.49
Structural details	V_{D1}	Stiffness of the nailed joints of the arches	K_{par}	kN/m	2050	6600	6600	0.69
			K_{per}	kN/m	1400	4500	4500	0.69
			K_{rot}	kNm/ rad		5.4		
	V_{D2}	Stiffness of the mortice and tenon joints at the top of lunette	K_{rot_par}	kNm/ rad	0	30	30	1.00
			K_{rot_per}	kNm/ rad	0	30	30	1.00
	V_{D3}	Stiffness of the mortice and tenon joints at the top of frame	K_{rot_par}	kNm/ rad	0	30	30	1.00
			K_{rot_per}	kNm/ rad	0	30	30	1.00
	V_{D4}	Stiffness of the nailed joint connecting the diagonal bracing to the posts	K_{rot}	kNm/ rad	0	20	20	1.00
	V_{D5}	Stiffness of the pegged mortice and tenon joint connecting the horizontal bracing to the posts	K_{rot}	kN/m	4900	9800	9800	0.50
Actions	V_{A1}	Roof's weight	Aisles	kN/m^2	1.25	2.50	2.50	0.50
			Vault	kN/m^2	0.85	1.70	1.70	0.50

Table 6.29 Control variables of the Cathedral of Ica characterised by plausible states

Class	Control variables		Plausible states	
			Reference	Alternative
Geometry	V_{G1}	Presence of longitudinal bracing between the bay-edge arches within each bay	Yes	No
	V_{G2}	Presence of the central guarango trunk	Yes	No
	V_{G3}	Presence of diagonal bracing between the posts of the pillars	Yes	No
	V_{G4}	Presence of horizontal bracing between the posts of the pillar	Yes	No
	V_{G5}	Presence of bracing between pillars (bracing of the frame)	Yes	No

Since destructive tests are normally not viable, the properties of the deteriorated material can only be taken from results of semi or non-destructive tests. This step adds another layer of uncertainty to the assessment, which depends on the reliability of existing correlations between results of semi or non-destructive tests, and mechanical properties of the materials.

Following the division into classes of Table 3.4, the control variables belonging to the 'Materials' class regard the modulus of elasticity of the wooden species. The reference value was taken from results of tests conducted at Universidad La Molina with original samples from the Cathedral (Chavesta Custodio *et al.*, 2012). Since the representativeness of these samples is limited, upper and lower thresholds are also defined from information available in literature (Chavesta Custodio *et al.*, 2012).

The uncertainty associated to deterioration is taken into account by considering a large range of variation of the stiffness of the principal joints. The reference thresholds of the mortice and tenon joints and diagonals to posts nailed joints, which are also assumed as maximum thresholds, are results of tests conducted at PUCP (Torrealva and Vicente, 2014) with experimental specimens that reproduce the typical geometry and layout of the joints of the cathedral. These experimental specimens were built with new undamaged/non-deteriorated members arranged such as the joint is tight. However, in historic buildings, even if the joint is not damaged or deteriorated, it might be no longer tight due to shrinkage of the timber. The effect of shrinkage, damage and deterioration on the stiffness of the joints can only be evaluated in depth by testing representative joints under the various conditions identified in the cathedral. However, this is not feasible at a practical

level. A simplified but informative way of taking into account this effect is considering a minimum possible stiffness equal to zero. In the case of mortice and tenon joints, this is equivalent of assuming hinged connections.

As far as the nailed joints of the planked arches are concerned, the interval of plausibility is defined from tests conducted at UPM and reported in Section 6.4.4.1. In this case, deterioration does not have a major role since the timber planks made of cedar are in overall fair condition.

The weight of the roof was estimated from the layout and composition of the various covering layers observed in inspections conducted at specific locations of the cathedral. The interval of plausibility of this control variable takes into account the possibility of the weight of the roof to vary throughout the structure. Moreover, the influence of the roof's weight on the outputs will clarify whether the weight of the roof could have played a major role on the failure of the timber vaulted system.

Alternative states related to the 'Geometry' class are also taken into account in this uncertainty analysis. The relative influence of a specific timber member on the outputs is evaluated by assuming a model of the nave's bay with and without the timber member. All timber members evaluated in variables V_{G1} to V_{G5} were observed and measured in detail in the Cathedral of Ica by the author at specific locations of the structure. For instance, the central *guarango* tunk and the diagonal and horizontal bracing of the pillars were observed and recorded in a few central and lateral pillars. Although it is likely that the rest of the structure has a similar layout, the surveys conducted within the EAI-SRP did not allow concluding on the condition of a large portion of the timber structure. In reality, if this condition is poor the structural capacity of the timber members can be significantly reduced. By including this central trunk as a control variable, this type of uncertainty associated to the geometry of the building can be taken into account.

The presence of the *guarango* trunk is an interesting and peculiar characteristic of this structure. To the author's knowledge, the survey conducted by the EAI-SRP revealed for the first time the existence of this type of element in this type of church. This central trunk is not present in the pillars of the Cathedral of Lima, for instance. Investigations conducted by Proaño *et al.* (2007) revealed that the pillars in Lima are composed by timber posts braced by horizontal and diagonal members, without any central trunk.

6.5.3 Level of influence of control variables and sensitivity of structural performance indicators

The structural performance indicators (SPIs) considered relevant to the seismic assessment of the timber structure of the Cathedral of Ica are indicated in Table 6.30.

Table 6.30 Structural performance indicators of the assessment of the Cathedral of Ica

Structural performance indicator	Objective
SPI 1: Maximum shear force acting in the nailed joints of the arches	To investigate the demand produced by the 2007 Pisco earthquake in the arches.
SPI 2: Maximum tensile force acting in the mortices of the beam at the top of lunettes	To investigate the demand produced by the 2007 Pisco earthquake in the beam at the top of lunettes;
SPI 3: Displacement of the frame	To investigate the overall deformation of the frame caused by the earthquake. It corresponds to the maximum displacement, measured at the top of the frame.
SPI 4: Displacement of the vault	To investigate the overall deformation of the vault caused by the earthquake. It corresponds to the maximum displacement, measured at the top of lunette or at the top of the internal arches depending on whether the spectrum is applied in the transversal or longitudinal directions, respectively.

Local sensitivity analyses are conducted for each control variable assuming the reference analysis conditions, and varying one by one the control variables from the minimum to the maximum plausible values or varying the state of the model. All analyses are conducted in the transversal direction (Y-direction) of the model, except in the case of V_{G1}, in which case the longitudinal direction (X-direction) corresponds to the most unfavourable situation.

The range of variation of a control variable *Ki*, δV_{Ki}, is obtained by means of equation 3.4 and the sensitivity of a SPI *j* to the variation of the same variable, $\delta I_{j,Ki}$, by means of equation 3.5.

A comparison of the input variation, δV_{Ki}, with the output sensitivity, $\delta I_{j,Ki}$, is shown in Figure 6.38. The variation/sensitivity is considered relevant if δV_{Ki} or $\delta I_{j,Ki}$ are larger than the minimum reference knowledge-based uncertainty, m_{urmn}, assumed by the analyst (see Section 3.5.2.1 for further details).

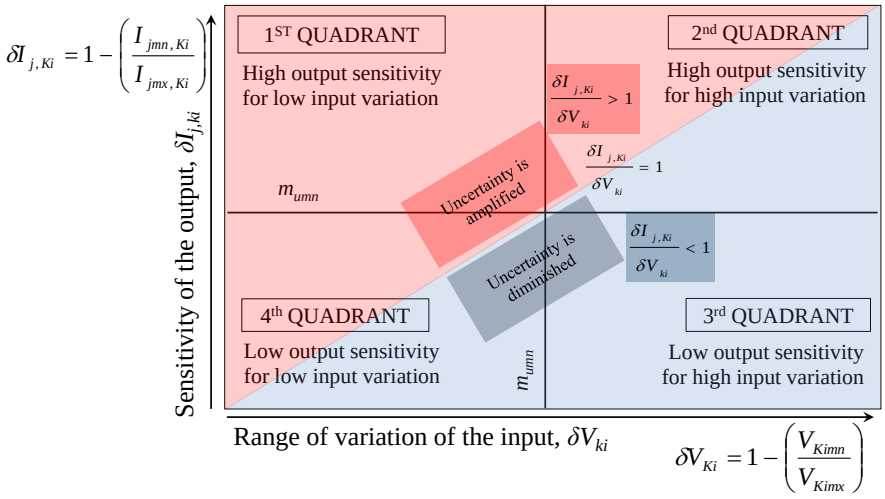

SPI 1: Maximum shear force in the arches

SPI 2: Maximum tensile force in the beam at the top of lunettes

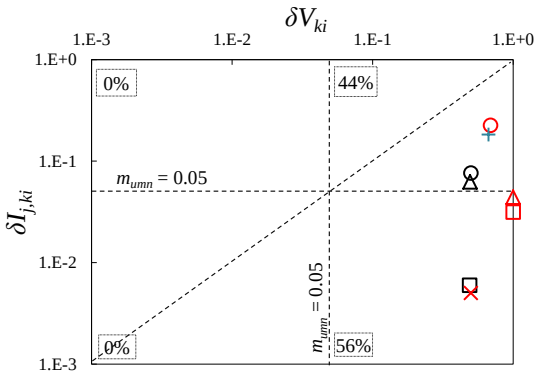

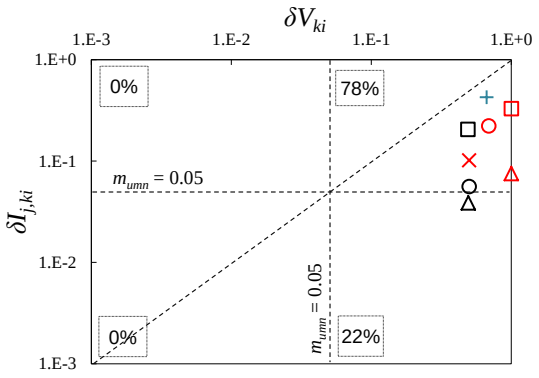

SPI 3: Displacement of the frame

SPI 4: Displacement of the vault

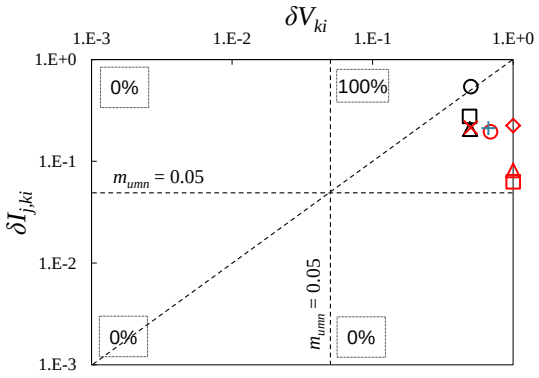

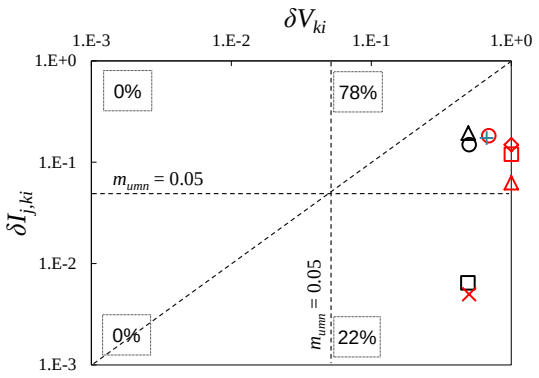

E (*caoba Africana*)	○VP1	□VP2	*E* (*guarango*)
E (cedar)	△VP3	○VD1	Stiffness of the nailed joints of the arches
Stiffness of the mortice and tenon joints at the top of lunette	□VD2	△VD3	Stiffness of the mortice and tenon joints at the top of frame
Stiffness of the nailed joint connecting the diagonal bracing to the posts	◇VD4	×VD5	Stiffness of the the pegged mortice and tenon joint connecting the horizontal bracing to the posts
Roof's weight	+VA1		

Figure 6.38 Propagation of uncertainties: comparison of input variation with output sensitivity

In the assessment of the Cathedral of Ica, m_{urmn} is assumed equal to 0.05 and m_{urmx} equal to 0.35, as in the case of the Church of Kuño Tambo. Four quadrants can be established where the control variables belonging to the first quadrant have the most unfavourable condition, since they have high output sensitivity for low input variation (Figure 6.38).

Table 6.31 shows the sensitivity of the SPIs to the variation of the control variables characterised by states, $\delta I_{j,Ki}$.

Table 6.31 Sensitivity of a SPI *j* to the variation of control variables characterised by states

Control variable	$\delta I_{1,ki}$	$\delta I_{2,ki}$	$\delta I_{3,ki}$	$\delta I_{4,ki}$
V_{G1} (longitudinal bracing between bay-edge arches)	0.02	0.02	0.02	0.02
V_{G2} (*guarango* trunk)	0.004	0.02	0.05	0.001
V_{G3} (diagonal bracing)	0.12	0.25	0.75	0.16
V_{G4} (horizontal bracing)	0.08	0.18	0.60	0.10
V_{G5} (bracing of the frame)	0.05	0.27	0.47	0.09

The overall sensitivity of a SPI *j* to the variation of all control variables, δI_j, can be obtained as an average over all values of $\delta I_{j,Ki}$, as per equation 3.6. The values of δI_j are shown in Table 6.32 for the fours SPIs.

Table 6.32 Overall sensitivity of the SPIs, δI_j

	δI_1 (SPI 1: Maximum shear force in the arches)	δI_2 (SPI 2: Maximum tensile force in the beam at the top of lunettes)	δI_3 (SPI 3: displacement of the frame)	δI_4 (SPI 4: displacement of the vault)
δI_j	0.07	0.16	0.28	0.10

These results show that the displacement of the frame (SPI 3) is the most sensitive structural performance indicator for all control variables, except V_{G1} and V_{G2}, having an influence above the minimum reference value, m_{urmn}, of 0.05. The second most sensitive indicator is the tensile force acting in the beam at the top of lunettes (SPI 2). Uncertainties on the properties of wood are especially reflected on the displacement of the frame. This is most

relevant for the modulus of elasticity of *caoba Africana* (V_{P1}), whose uncertainty is amplified in the case of SPI 3 (i.e. $\delta I_{3,P1} > \delta V_{P1}$).

Uncertainties on the stiffness of the mortice and tenon joints at the top of lunettes have a relevant influence on the uncertainty of the SPI 2, as would be expected since these joints govern the connection of the internal arches to the beam at the top of lunettes. The assumption of hinged connections at the top of lunettes would lead to a tensile force approximately 33% lower than the force transmitted by the springs simulating the mortice and tenon joints. This is a significant difference on the outputs that can lead to an erroneous diagnosis.

The bracing of the pillars and the bracing of the frame, especially the diagonal bracing, has a significant influence not only on the displacement of the frame but also on the tensile force acting on the beam at the top of lunettes, as shown for instance by the high values of $\delta I_{2,G3}$ and $\delta I_{3,G3}$ (Table 6.31). This conclusion is also evident by the high sensitivity of SPI 2 and SPI 3 to the variation of the modulus of elasticity of *guarango* (i.e. $\delta I_{2,P2}$ and $\delta I_{3,P2}$), which is the wooden specie of the diagonals. On the other hand, the *guarango* trunk appears to have a modest relevance to the structural behaviour of the nave.

Variations on the roof's weight (δV_{A1}) have an important influence over all structural performance indicators. This influence is as important as the stiffness of the nailed joints of the arches (V_{D1}) in the case of the maximum shear forces acting on the arches (SPI 1). The uncertainty on V_{A1} has also the highest influence on the uncertainty of the maximum tensile force acting in the beam at the top of lunettes (SPI 2). A 67% reduction on the roof's weight leads to a reduction of 43% on the tensile force acting on the beam at the top of lunette.

The shear forces acting on the arches (SPI 1) are mostly sensitive to the variation of inputs that directly characterise the elements of the vault - V_{D1}, V_{A1}, V_{P1} and V_{P3}. The sensitivity of SPI 1 to the variation of stiffness of the mortice and tenon joints at the top of the frame, V_{D3}, is close to a minimum reference uncertainty, m_{urmn}, of 0.05. This means that the connections of the bay-edge arches to the frame might not have had a relevant role in the failure of these arches during the 2007 Pisco earthquake.

In order to identify the critical variables for the seismic assessment of the Cathedral of Ica, the influence of each control variable is evaluated by means of the overall influence indexes α_{ki} obtained by means of equation 3.7. These indexes correspond to an average over all values of sensitivity associated to the four SPIs, $\delta I_{j,Ki}$, due to the variation of a specific control variable. The indexes α_{ki} can be calculated assuming that all SPIs are equally important. In alternative, the α_{ki} indexes can be calculated as a weighted sum of the

sensitivity indexes associated to the four SPIs, according to equation 3.8. The weights obtained from the three alternative procedures proposed in Section 3.5.2.1 are shown in Table 6.33. The indexes α_{ki} for all control variables are shown in Table 6.34, according to the various procedures used to calculate α_{ki}. The control variables are ranked according to the corresponding influence indexes, α_{ki}, from the highest to the lowest index within each class. It can be seen that the ranking may vary according to the procedure used to combine the various $\delta I_{j,Ki}$ in the calculation of α_k. The ranking shown in Table 6.34 corresponds to the ranking provided by the majority of the procedures.

Procedure I underestimates the importance of SPIs that are significantly sensitive to the uncertainty of the input but which are not the most sensitive to the variation of any control variable, as in the case of SPI 4. Procedure III underestimates the relevance of both SPI 1 and SPI 4, since the sensitivity of these performance indicators is below the maximum reference uncertainty, m_{urmx}, equal to 0.35 for all control variables.

The results show that most control variables are critical, except V_{G1} and V_{G2}. Although the results of the model show that the longitudinal bracing between the bay-edge arches (V_{G1}) has a modest contribution to the longitudinal response of the structure, in practice such contribution appears to be relevant to keep the arches in place in terms of out-of-plane stability. Apart from this bracing, only the canes of the roof's cladding and the friction developed at the mortice and tenon connection of the beam at the top of lunettes to the bay-edge arches keep the out-of-plane stability of the arches (detail 1 of Figure 4.36). Even if it is assumed that the tenon is nailed to the mortice, as observed at other locations of the structure, the longitudinal bracing is still relevant for the out-of-plane stability of the arches.

Table 6.33 Weights used in the combination of the sensitivity of all SPIs

Structural performance indicators		w_j			
		All SPIs equally relevant	Proc. I	Proc. II	Proc. III
SPI 1 (shear force - arches)	w_1	0.25	0.14	0.16	0.00
SPI 2 (tensile force – top of lunete)	w_2	0.25	0.14	0.26	0.20
SPI 3 (displacement - frame)	w_3	0.25	0.71	0.32	0.80
SPI 4 (displacement - vault)	w_4	0.25	0.00	0.26	0.00

Table 6.34 Influence indexes of the control variables of the Cathedral of Ica

Class		Control Variables	α_{ki}			
			All SPIs equally relevant	Proc. I	Proc. II	Proc. III
Materials	V_{P1}	Modulus of elasticity of *Caoba Africana*	0.21	0.41	0.24	0.45
	V_{P2}	Modulus of elasticity of *Guarango*	0.12	0.23	0.14	0.26
	V_{P3}	Modulus of elasticity of Cedar	0.13	0.16	0.14	0.17
Structural details	V_{D1}	Stiffness of the nailed joints of the arches	0.21	0.20	0.20	0.20
	V_{D2}	Stiffness of the mortice and tenon joints at the top of lunette	0.14	0.10	0.14	0.12
	V_{D5}	Stiffness of the pegged mortice and tenon joint connecting the horizontal bracing to the posts	0.08	0.17	0.10	0.19
	V_{D4}	Stiffness of the nailed joint connecting the diagonal bracing to the posts	0.09	0.16	0.11	0.18
	V_{D3}	Stiffness of the mortice and tenon joints at the top of frame	0.07	0.08	0.07	0.08
Actions	V_{A1}	Roof's weight	0.25	0.24	0.25	0.26
Geometry	V_{G3}	Presence of diagonal bracing between the posts of the pillars	0.32	0.59	0.36	0.65
	V_{G4}	Presence of horizontal bracing between the posts of the pillar	0.24	0.47	0.28	0.52
	V_{G5}	Presence of bracing between pillars (bracing of the frame)	0.22	0.38	0.25	0.43
	V_{G2}	Presence of the central guarango trunk	0.02	0.04	0.02	0.04
	V_{G1}	Presence of longitudinal bracing between the bay-edge arches within each bay	0.02	0.02	0.02	0.02

This contribution of the longitudinal bracing is not captured by the numerical model, since the possibility of the tenon to slide along the mortice is not simulated; and hence the beam cannot separate from the arches in the model. This assumption is reasonable since sliding is not likely to occur in the joint due to the longitudinal bracing. The only possibility for the tenon to slide is due to the deformation of the beam. In summary, in terms of modelling strategy, it is reasonable to infer that if this bracing is present, the sliding of the tenon does not need to be simulated.

However, it should be noted that the inclusion of bracing in the model is not critical, since the modelling of the mortice and tenon without the possibility of sliding of the tenon will *per se* restrain the deformation of the arches in the longitudinal direction in a similar way as the effect of the bracing.

6.5.4 Level of knowledge associated to the critical variables

The level of knowledge provides a measure of the confidence with which the analyst defines the reference analysis conditions, the intervals of plausibility and the alternative states. An indicator of this uncertainty is given by the knowledge index λ_{ki} following the criteria of Table 3.8 and provisions of current codes and guidelines, as explained in Section 3.5.2.2.

In the assessment of the Cathedral of Ica, the index associated to high knowledge is equal to the minimum reference value, m_{urmn}, of 0.05. This minimum level of uncertainty takes into account the fact that the choice of the variables on itself and the modelling strategy applied to this assessment have an inherent uncertainty that is not otherwise included.

The knowledge indexes of all critical variables and the respective rationale for the assumption are shown in Table 6.35. These knowledge indexes can be combined into a global knowledge index, λ, calculated as an average of all λ_{ki}, according to equation 3.10.

A λ in the assessment of the Cathedral of Ica is equal to 0.058. This value is near the minimum reference of 0.05, showing that the knowledge level in this assessment is very high due to the large amount of experimental work and detailed inspections conducted for characterization of the timber structure.

6.5.5 Knowledge-based uncertainty of the inputs

The uncertainty of the inputs associated to each SPI j, m_{uj}, is obtained by means of equation 3.11, considering both the overall sensitivity of the SPIs, δI_j, and the global knowledge index, λ. In the assessment of the Cathedral of Ica, the uncertainty m_{uj} is expressed in Table 6.36 for the four SPIs.

The m_{uj} can be combined in order to obtain an overall uncertainty measure of the inputs, m_u, according to equation 3.14. The m_u for the assessment of the Cathedral of Ica is indicated in Table 6.37 taking into account alternative procedures to combine the results of the various SPIs.

Table 6.35 Knowledge level and indexes of the assessment of the Cathedral of Ica

Critical variables			Level of knowledge	λ_{ki}	Rationale
Materials	V_{P1}	Modulus of elasticity of *Caoba Africana*	MK	0.20	Experimental work conducted with original healthy samples. However, this wooden specie is the most affected by deterioration.
	V_{P2}	Modulus of elasticity of *Guarango*	HK	0.05	Experimental work conducted with original healthy samples.
	V_{P3}	Modulus of elasticity of Cedar	HK	0.05	
Structural details	V_{D1}	Stiffness of the nailed joints of the arches	HK	0.05	
	V_{D2}	Stiffness of the mortice and tenon joints at the top of lunette	HK	0.05	
	V_{D3}	Stiffness of the mortice and tenon joints at the top of frame	HK	0.05	Experimental work conducted with representative experimental specimens.
	V_{D4}	Stiffness of the nailed joint connecting the diagonal bracing to the posts	HK	0.05	
	V_{D5}	Stiffness of the pegged mortice and tenon joint connecting the horizontal bracing to the posts	HK	0.05	
Action	V_{A1}	Roof's weight	HK	0.05	Information taken from detailed inspection of some representative locations of the structure.
Geometry	V_{G1}	Presence of longitudinal bracing between the bay-edge arches within each bay	MK	0.20	Bracing could only be observed within one of the bays of the nave.
	V_{G2}	Presence of the central guarango trunk	MK	0.20	Presence of the *guarango* trunk could only be checked in two central pillars.
	V_{G3}	Presence of diagonal bracing between the posts of the pillars	HK	0.05	Observed in only a few representative central and lateral pillars. However, the presence of these elements in the structure could also be observed in other similar structures. The presence of these elements is more likely to be uniformly present throughout the structure than V_{G1} and V_{G2}.
	V_{G4}	Presence of horizontal bracing between the posts of the pillar	HK	0.05	
	V_{G5}	Presence of bracing between pillars (bracing of the frame)	HK	0.05	

Table 6.36 Knowledge-based uncertainty of each SPI in the assessment of the Cathedral of Ica

SPI 1 (Shear - arches)	SPI 2 (Tensile force – top of lunette)	SPI 3 (Displacement - frame)	SPI 4 (Displacement - vault)
m_{u1}	m_{u2}	m_{u3}	m_{u4}
0.14	0.25	0.40	0.18

Table 6.37 Overall knowledge-based uncertainty of the assessment of the Cathedral of Ica

	All SPIs equally relevant	Proc. I	Proc. II	Proc. III
m_u	0.24	0.34	0.26	0.37

Procedure III can be seen as an upper bound of the uncertainty, whereas the value calculated as a mean of all indicators (i.e. all SPIs equally relevant) can be seen as a lower bound.

The procedure that considers all SPIs equally relevant is here selected as the reference for the detailed diagnosis due to two main reasons: (1) the SPI 1, consisting of the shear forces acting on the arches, is the less relevant SPI in terms of uncertainty (as per Table 6.36); however it should not be overlooked since it is a key output to explain the reason why the timber planked arches failed during the 2007 Pisco earthquake; and (2) the SPI 4, consisting of the displacement of the vault, whose relevance is also modest as per Table 6.36, is an important indicator of the relative deformation of the vault and frame, and ultimately of the demand on the connections of the vault to the frame, and therefore should not be overlooked also.

Thus, it is considered here that the uncertainty of the input, m_u, is equal to 0.24 in the assessment of the Cathedral of Ica. This m_u value is equivalent of having a confidence factor of 1.24, which can be directly compared with the prescriptions of current codes, such as Eurocode 8 (CEN, 2005b).

The prescriptions of Eurocode 8 (CEN, 2005b) are vague and the minimum requirements for different levels of inspection and testing extremely high to be feasible for application to historic buildings. For instance, the code recommends that a medium (or normal) level of knowledge should be considered only if 50% of the structural details are checked by *in situ*

inspection. This entails checking 50% of the joints of the cathedral, which is not feasible from a practical, economic and conservation viewpoints. If the procedure of the code is strictly applied, a confidence factor of 1.35, corresponding to a low (or limited) level of knowledge, should be selected. This factor would be much higher than the factor 1.24 obtained through the approach proposed here.

6.6 Conclusions

At the beginning of this chapter, two research questions were posed:

(a) How detailed should the structural analysis of historic adobe and timber churches be to make a final meaningful diagnosis?

(b) What are the main uncertainties present in such structural analysis and what is their influence?

In the case of adobe churches, such as the Church of Kuño Tambo, the principal findings of this chapter that give an answer to these questions are:

(i) The principal aspects that govern the structural response of adobe churches are related to the material behaviour of walls and buttresses, and to structural details associated to the connectivity of elements, such as tie-beams, that restrain the deformation of the walls;

(ii) The analysis must be able to simulate the non-linear material behaviour of thick walls and buttresses made of adobe, since cracking occurs for low values of earthquake action due to the low tensile and shear strength of adobe. Large levels of permanent deformation occur, which cannot be captured by linear analyses;

(iii) Adobe behaves as a soil-like material typically reinforced with organic agents such as straw or crushed bone, that went through a process of compaction and drying in order to develop a given cohesion. The Drucker-Prager material model was formulated for soil-like materials responding mainly in shear. It is appropriate to simulate the almost null tensile strength of adobe, with a brittle response, by means of an area on the failure surface delimited by a tension cut-off. The model simulates well the equivalent structural ductility and

the early reduction of stiffness of thick adobe walls due to cracking. The alternative use of a concrete model, governed by the behaviour of the material in uniaxial compression, tension and biaxial compression simulates a material that is stiffer than adobe and rubble stone masonry, being unable to simulate the early reduction of stiffness under modest actions;

(iv) Material properties such as the specific weight, modulus of elasticity, tension cut-off, cohesion, and friction angle are key properties of both walls and base course, which require a detailed characterization in order to reduce the level of uncertainty;

(v) However, reference values of these properties for adobe and rubble stone masonry are difficult to find in literature, if not for specific sites. Since these materials are made with local resources and technology, the properties normally vary from site to site. Moreover, representative original samples of these materials are difficult to collect and test due to lack of representativeness of the samples and restrictions related to conservation of the assets. The lack of representativeness of the samples is especially relevant in the case of rubble stone masonry due to its high heterogeneity. As a result, inputs related to material properties typically have a large range of variation;

(vi) The mesh size in FEM analysis is also another critical source of uncertainty, which must be selected such as to properly represent transversal (through depth) shear. Between 2 and 3 volume elements through the thickness of the walls with a maximum mesh size of 0.40m is recommended as a reference to simulate the response of adobe churches with thick and long walls of similar size to the Andean churches. This provides a reasonable balance between the accuracy of the results and the practicality of the model within a practitioner environment and timeframe;

(vii) The existence of a base course at the bottom of an adobe wall creates a discontinuity in the vertical system. The interface adobe/rubble stone masonry, characterized by a value of cohesion lower than the most cohesive material (rubble stone), and an angle of friction lower than the highest angle of friction of both materials (associated to adobe), acts as a preferred plan of weakness;

(viii) To obtain more realistic distributions of stresses and strains, elastic springs can be used to avoid spurious stress concentrations caused by the assumption of rigid constraints at the base of the models, which could lead to an unrealistic failure of the wall at the foundation level; and

(ix) The overall uncertainty of the inputs, m_u, shows that confidence factors recommended by existing codes and guidelines, normally used in the assessment of heritage constructions, underestimate the uncertainty present in the analysis of constructions made of traditional materials and local construction technologies. The lack of reference values of critical variables from literature, and the limitations of carrying out tests to measure these critical variables, results in levels of uncertainty larger than the typical uncertainty of the assessment of existing buildings made of modern materials. Moreover, existing codes and guidelines for assessment of existing constructions ignore the fact evidenced here that decisions made by the analyst during the analysis and definition of actions contribute to the overall uncertainty as much as other aspects, such as the geometry, materials and structural details of the historic building.

In the case of historic timber structures, such as the one of the Cathedral of Ica, the principal findings that give an answer to the aforementioned questions are:

(i) The response of the bay of the nave is most critical in the transversal direction. The deformation in the longitudinal direction of the bay-edge arches is restrained by the longitudinal bracing. In the case of the internal arches, this deformation is restrained by the canes of the roof's cladding. Although the physical modelling of the bracing of the bay-edge arches is not critical; the presence of this bracing must be investigated in order to conclude on whether the sliding of the tenon of the beam at the top of lunette along the mortice of the bay-edge arch must be allowed or not in the simulation of the joint;

(ii) The bay-edge arches and the beam at the top of lunette are the most critical points of the timber structure of the nave. The largest demand occurs at these points of the structure. Nevertheless, this rather local behaviour of the vault is highly influenced by the response of the frame. Hence, a high level of detail

must be pursued in the modelling of the whole timber structure, even though some members and joints are more critical than others;

(iii) The geometry of the timber structure must be characterised in detail. It has been found that aspects such as the bracing of the posts and the bracing of the frame are critical control variables of the structural response of the structure. It is interesting to notice that the diagonals of the pillars, which are critical to the performance of the structure, are made of the strongest timber specie – *guarango* – with good resistance to deterioration. If these elements were made of *caoba Africana* for instance, such as the horizontal bracing, a more global failure of the structure could potentially occur;

(iv) It has been found that the nailed joints of the arches and the mortice and tenon joints connecting the arches to the beam at the top of lunettes are critical control variables of the analysis, which must be investigated in detail in the assessment of this type of structures. Uncertainties on the stiffness of these joints have a significant effect on the outputs;

(v) The modelling of the planked arches as continuous timber members would lead to global results in terms of deformations that are one order of magnitude lower than the deformations of timber planked arches. The modelling of the planks and nailed joints is critical to investigate the structural performance of the vault and to explain the failure of the arches during the 2007 Pisco earthquake. Likewise, this detailed model is needed to test possible retrofitting solutions for this type of structures if retrofitting is deemed necessary;

(vi) The weight of the roof has a significant influence on both the tensile forces acting on the beam at the top of lunette and shear forces acting on the nailed joints of the arches; hence the weight of the roof must be further investigated by global analysis in order to determine whether the weight of the roof could have had a major role on the failure of the planked arches during the 2007 Pisco earthquake;

(vii) An important source of uncertainty is also associated to material characterization of *caoba Africana*, which was used to build the longest elements of the structure, such as the posts and beams. This is a key issue of the assessment, since this wooden specie is the most affected by deterioration. It is

therefore expected that members or joints made of this specie may have properties that are significantly different from the reference values; and

(viii) It has been found that the *guarango* trunk does not have a primary structural role under lateral loads, being more important to the response under vertical loads.

From the local analyses conducted in this chapter, a complete modelling approach for the global models of the Church of Kuño Tambo and Cathedral of Ica can be devised. The global analyses are discussed in Chapter 7 with the purpose of informing the detailed diagnosis of these churches. The overall uncertainty of the inputs, m_u, calculated in this chapter will be used in the detailed diagnosis to verify whether this uncertainty can lead or not to diverse and contradictory diagnoses.

What is there to study about wood structures?

Ricardo O. Foschi's father[3]

[3] Ricardo O. Foschi (1989). What we do and what we need to do in timber engineering. *Wood Science and Technology*, 23, p.289-293

CHAPTER 7

Quantitative analysis at the global level and detailed diagnosis of historic adobe and timber churches

7.1 Introduction

The final step of the assessment, as per the framework of Figure 3.1, regards the detailed diagnosis of a historic construction. In the case of the Church of Kuño Tambo, the objective is to identify the performance level that the church will sustain under a hazard level corresponding to 10% probability of exceedance in 50 years as per the code for earthquake resistance in Peru (E.030, 2003). Pushover analyses are used for this purpose since they allow simulating the non-linear response of adobe structures while avoiding the complexity of more detailed non-linear dynamic methods. As emphasized in Chapter 1, the accuracy of the results will increase only if the increased sophistication of the analysis method is accompanied by an increased level of confidence in the value of the additional parameters required to conduct those refined analysis. In the particular case of adobe churches in high lands, lack of knowledge on the additional parameters needed to conduct non-linear time history analyses would increase the uncertainty of the results, and thus compromise any additional benefit in terms of final diagnosis.

With regards to the Cathedral of Ica, the assessment of which is conducted in a post-earthquake context, the objective is to explain the cause of the damage that the structure sustained after the 2007 Pisco earthquake. Modal superposition analyses are used to investigate initiation of damage when the capacity of the components is exceeded. More detailed non-linear dynamic analyses are not conducted since these would require a significant additional amount of experimental work to characterise the non-linear response of several historic timber joints. Such amount of work is normally not feasible in practice.

The uncertainty of the input, m_u, calculated in Chapter 6 is used here to change the values of the structural performance indicators and evaluate the respective effect of uncertainty on the detailed diagnosis. While conducting global structural analyses and making detailed diagnoses, this chapter will answer one of the main research questions of this thesis:

> *What is the structural concept and seismic performance of historic Peruvian earthen and timber churches?*

7.2 Analysis at the global level of a historic adobe church

Global finite element models of the Church of Kuño Tambo are developed with the purpose of analysing the global response of the building to inform the detailed diagnosis (Figure 7.1a). Although two additional buttresses are still standing on the East side of the church, next to buttresses B10 and B12, they are completely detached from the nave and therefore they are not included in the model. Similarly, the church had four buttresses on the West side, from which two buttresses are known to have been connected to the nave by interlocking of adobe units (Cancino *et al.*, 2012). The present state of the church is marked by the collapse of buttresses B4 and B6. Figure 7.1b shows the state of the church if these collapsed buttresses are reinstated.

There is evidence of the existence of only a few timber anchors in the nave and one in the baptistery. Thus, the connection of some tie-beams of the main nave to the walls relies only on the friction developed between the tie and the wall. In the model, the tie-beams are anchored to the walls by means of a connection that allows bending moments to be transmitted, which is simulated by a group of three or four beams connected each other to two volume elements of the wall.

Global analyses are performed to evaluate the benefit of restoring the church to its initial condition and improving some of the most important interactions. This allows evaluating the original conceptual design of the church. The analyses allow comparing the relative benefit of each improvement also.

The hypotheses under investigation are:

H_1. Present state structure without tie-beams;

H_2. Present state structure with tie-beams;

H_3. Rehabilitated structure without tie-beams;

H_4. Rehabilitated structure with tie-beams.

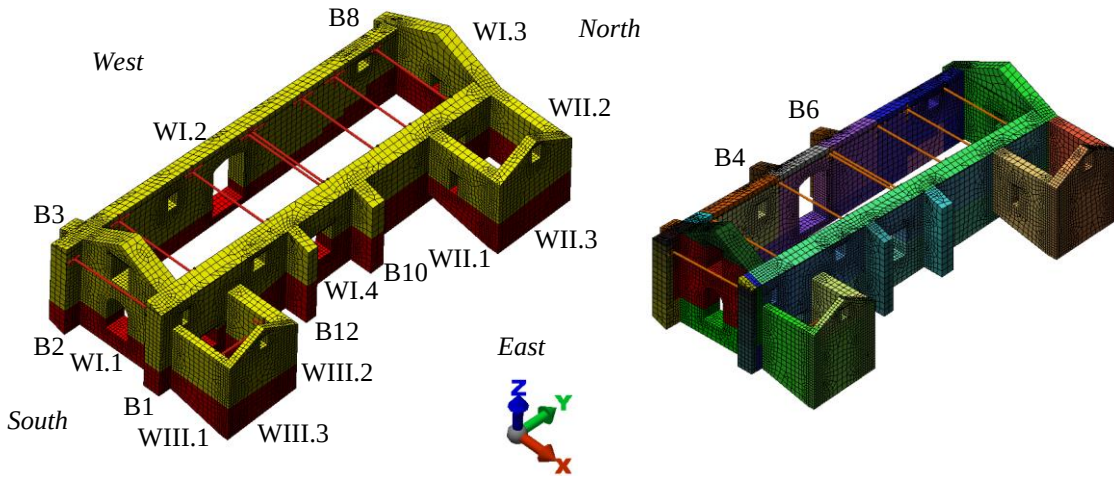

a) Present state

b) State after reinstatement of buttresses B4 and B6

Figure 7.1 Global models of the Church of Kuño Tambo used in the detailed diagnosis

Although H_2 is called "present state structure", it corresponds in reality to a retrofitted model of the church where all tie-beams are perfectly connected to the adobe walls by means of traditional timber anchors; and hence the global structure is able to work as a unity. Hypotheses 3 and 4 are called "rehabilitated" since the models assume the rebuilding of buttresses B4 and B6 (see Figure 7.1b). The walls are assumed continuously connected in all models, which correspond also to an improvement of the interaction among the walls of the main nave, baptistery and sacristy, and between the main nave and the baptistery/sacristy.

7.2.1 Modal analysis

Figure 7.2 shows the modal shapes of the 1st mode for the four hypotheses described above. The fundamental mode of H_1 excites the West wall of the main nave (detail 1), which is only restrained by buttresses B3 and B8. If all tie-beams are included in the structure (hypothesis H_2), both the West and East walls are mobilised together (detail 2). The inclusion of the

collapsed buttresses stiffens the West wall so that the participation of the North and South walls of the main church become more relevant in the 1st mode (detail 3).

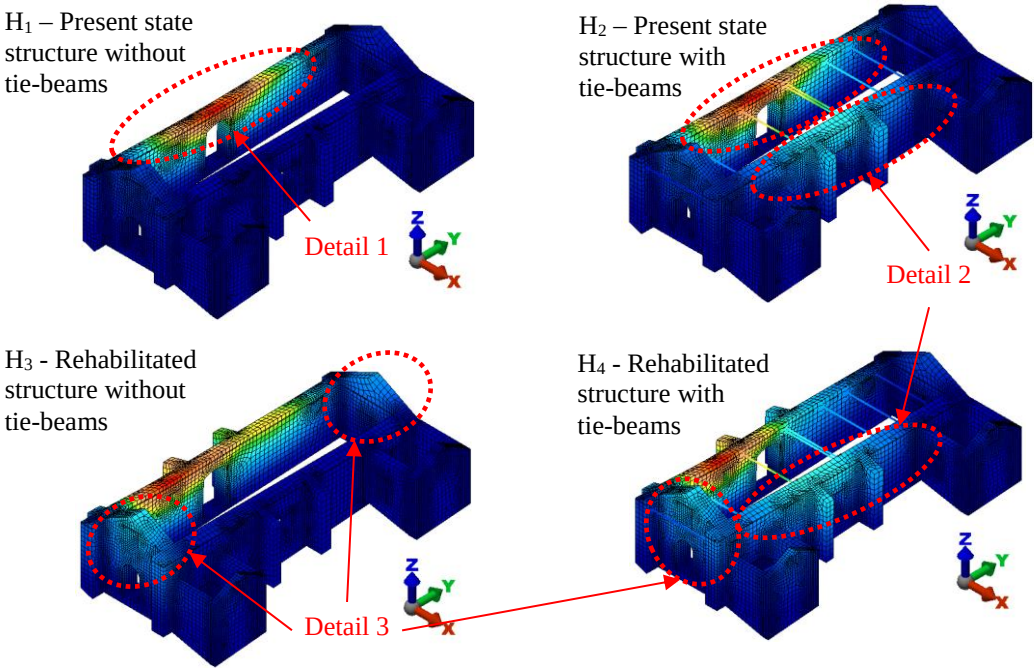

Figure 7.2 First modal shape of hypotheses $H_{i,\ i = 1\text{-}4}$

The natural periods of the first 40 modes for hypotheses $H_{i,\ i = 1\text{-}4,}$ and the modal shapes from mode 2 to 7 are shown in Figure 7.3. The cumulative modal effective masses in the X and Y direction are shown in Figure 7.4. If 100 modes are calculated, the cumulative masses are approximately equal to 73.5% and 72.5%, in the X and Y direction, respectively. The dynamic response of the church is characterized by the existence of several local modes, in which different portions of the structure vibrate. This is a typical response of a structure without a stiff diaphragm and with walls of different slenderness, hence different frequency.

The most relevant differences on the natural periods of the various hypotheses occur at the first 10 modes, which are predominantly transversal modes (X-direction). This can be explained by the fact that most tie-beams and collapsed buttresses are effective in this direction. The tie-beams diminish the occurrence of local modes, favouring a more global participation, as evidenced by mode 5. The introduction of connections of the facades of the baptistery and sacristy to the nave could therefore avoid other local modes such as mode 7.

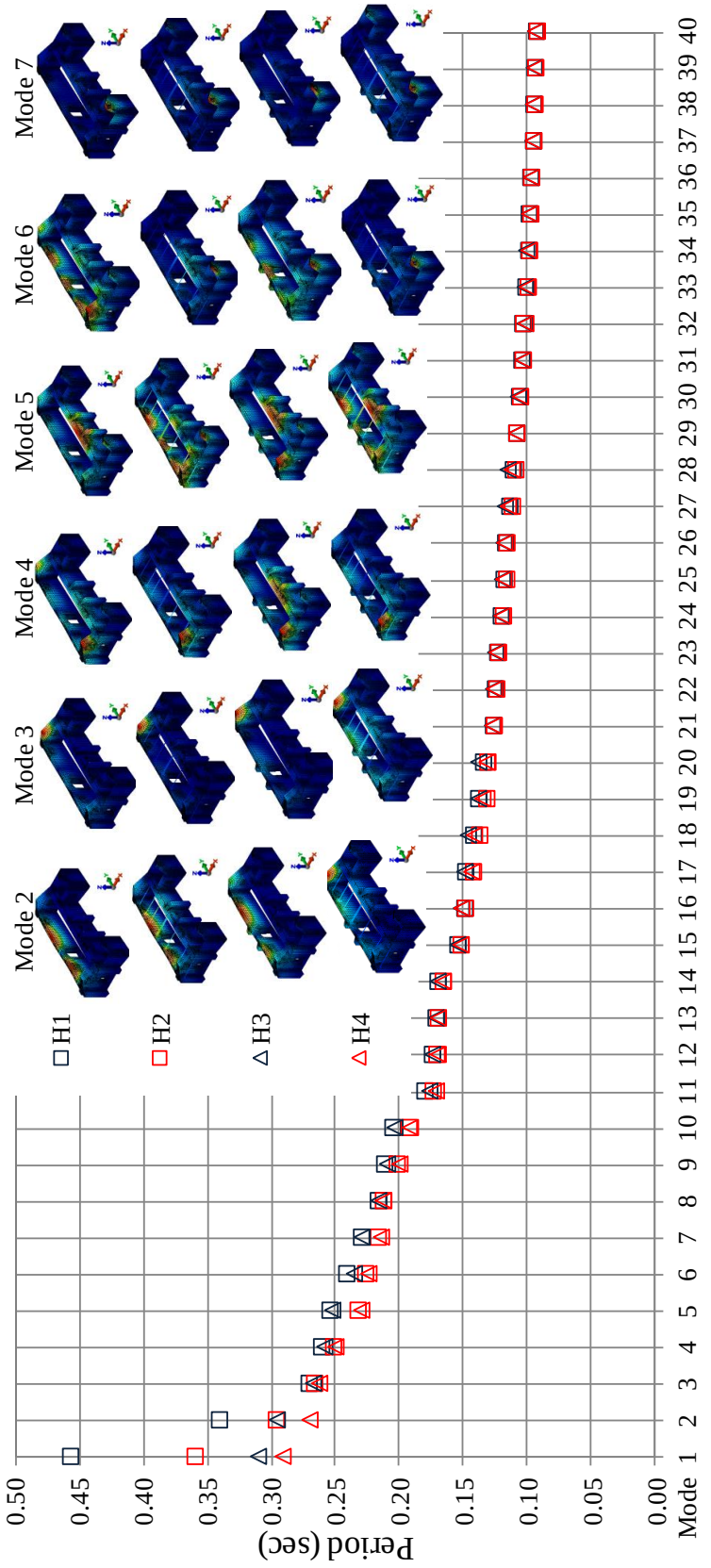

Figure 7.3 Natural periods of the first 40 modes of hypotheses $H_{i,\,i\,=\,1\text{-}4}$

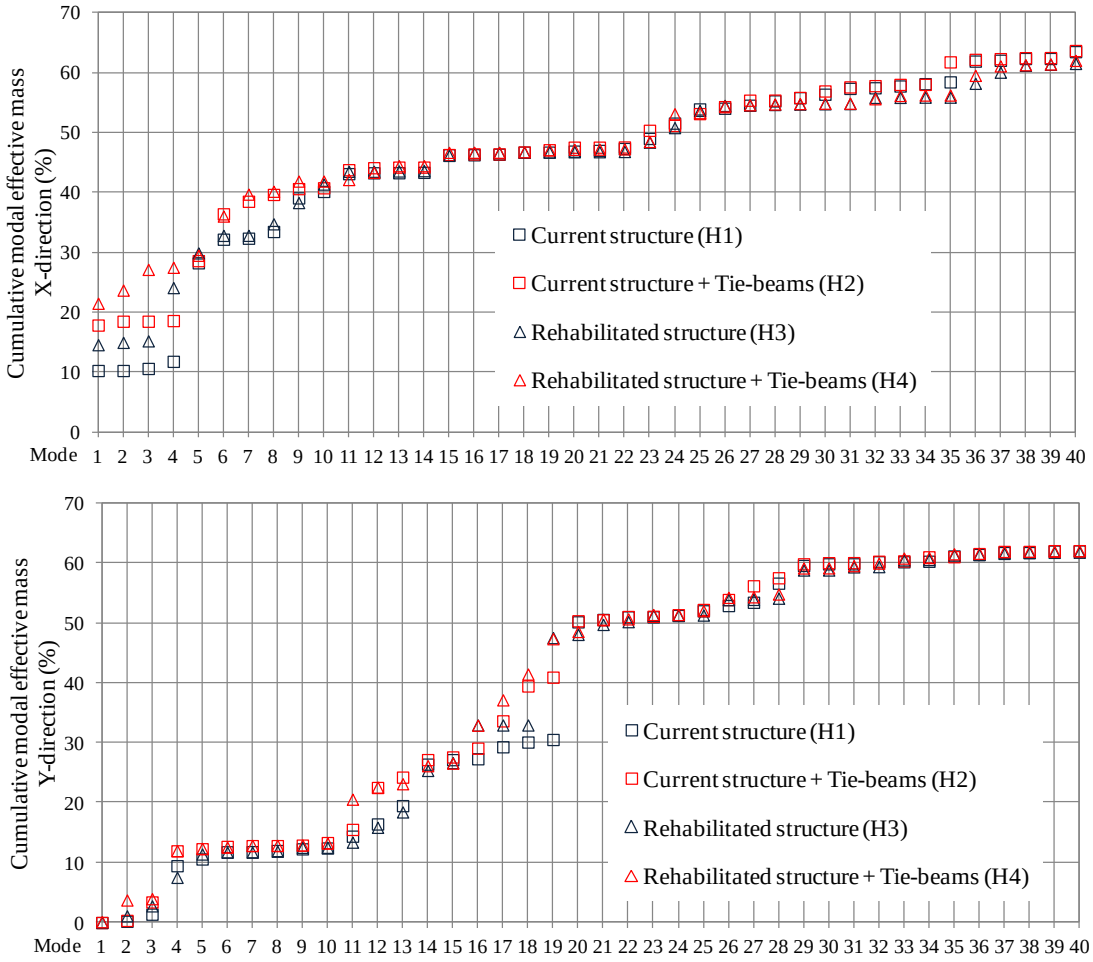

Figure 7.4 Cumulative modal effective mass (X and Y direction) of the first 40 modes of hypotheses $H_{i,\ i = 1\text{-}4}$

7.2.2 Nonlinear static (pushover) analysis under simulated earthquake loading

Nonlinear static (pushover) analyses are performed with the four hypotheses described above. A uniform lateral load, corresponding to an equivalent static load for acceleration equal to 0.15g is applied in the global X-direction. For the purpose of comparison of alternative hypotheses, the value of lateral acceleration (or hazard level) is not important; if not that it should be sufficiently high for the structure to behave in the non-linear range. The roof action is accounted for both as vertical load on the top of the walls and horizontal load produced by its horizontal thrust action. Its diaphragm action is neglected, as neither its original or current state would be able to effectively redistribute the inertia forces and confine the deformation of the walls.

The distribution of maximum principal stresses of the four hypotheses is shown in Figure 7.5. The most relevant effect of the tie-beams and collapsed buttresses is the reduction of the deformation of the West wall of the main nave. However, the buttresses alone appear to improve the response better than the tie-beams alone, providing the buttresses are fully connected to the walls. Moreover, the tie-beams create concentration of stresses in the anchoring region, which can lead to local failures. Another relevant concentration of stresses occurs at the top of the base course and at the intersection between the walls and walls/buttresses.

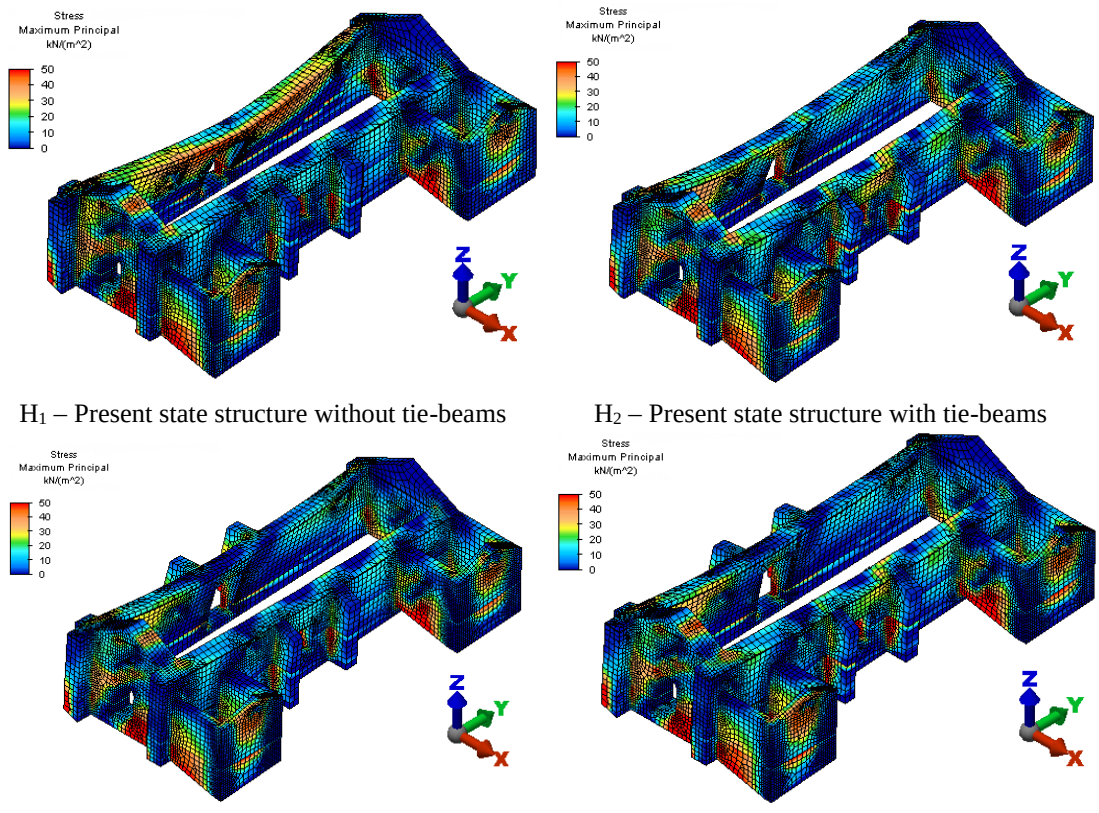

H_1 – Present state structure without tie-beams

H_2 – Present state structure with tie-beams

H_3 - Rehabilitated structure without tie-beams

H_4 - Rehabilitated structure with tie-beams

Figure 7.5 Maximum principal stresses distribution for hypotheses $H_{i,\ i = 1\text{-}4}$

The rebuilding of the collapsed buttresses and the improvement of the connection of the tie-beams to the adobe walls by means of anchors would result in a significant reduction of the displacement of the longitudinal walls of the nave, as evidenced by the capacity curves of

Figure 7.6. In these capacity curves, the pushover analyses are curtailed at the same level of lateral acceleration that produces the failure of the weakest model. Although the structural capacity (maximum total base shear) is similar in the four hypotheses, the model without collapsed buttresses and tie-beams (H1) presents 0.04m as maximum displacement at the top of the West wall, whereas the model with reinstatement of collapsed buttresses and tie-beams (H4) presents 0.012m. The loss of stiffness in the model due to the elements that fail, interpreted as cracking, is therefore limited by the presence of well-connected tie-beams and well distributed buttresses. By controlling the cracking, and therefore the existence of large offsets, the possibility of the adobe walls to lose stability during a large earthquake is reduced.

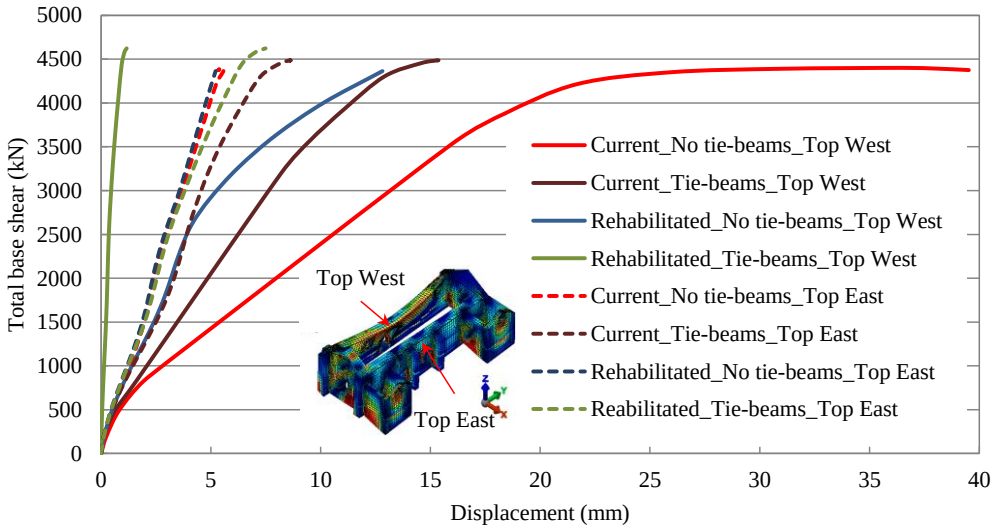

Figure 7.6 Capacity curves of hypotheses $H_{i,\ i\ =\ 1\text{-}4}$ after pushover analysis

The absolute values of displacement shown in Figure 7.6 appear to be rather low for adobe structures and they can be justified by the fact that the walls are continuously connected in the model. The level of connection among walls is difficult to assess on site. If there is a good interlocking of adobe blocks, the hypothesis of walls continuously connected in the model is reasonable. However, in reality the extent to which the walls are well connected depends on the quality of construction and may vary from intersection to intersection. Thus, any attempt to simulate a poor connection among walls would have a high level of uncertainty. Whether this uncertainty lies on the conservative or non-conservative side would also be unknown. For the purpose of conducting a detailed diagnosis, the simulation of the walls of the Church of Kuño Tambo as continuously

connected does not compromise the validity of the comparison and conclusions made in terms of the relative benefit of tie-beams and buttresses to the lateral response of the church.

In the following section, an alternative procedure will be applied to the analysis of this church with the principal objective of evaluating the effect of assuming the walls continuously connected on the detailed diagnosis.

7.2.3 Application of alternative approaches

Taking into account that the finite element models assume the walls of the Church of Kuño Tambo continuously connected, a limit analysis based approach, known as FaMIVE (D'Ayala and Speranza, 2003), is applied to analyse the effect of this assumption on the failure of the building. FaMIVE identifies load factors associated to failure mechanisms for masonry structures subdivided in macroelements. A lateral load factor for each failure mechanism is calculated in the form of a percentage of the weight of the macroelement (acceleration/gravity). The failure mechanism with the lowest load factor is the first to occur for a given macroelement. The load factors associated to the most important in-plane and out-of-plane failure mechanisms of the Church of Kuño Tambo are shown in Figure 7.7. Each wall is considered as a different macroelement and the symbol used here to denote each macroelement can be seen in Figure 7.1a. The load factors of the vertical arch failure mechanism are calculated for WI.2 and WI.4 considering the presence of tie-beams and assuming that only the portions between tie-beams and buttresses participate in the mechanism.

The results show that the walls of the church are vulnerable to partial and total out-of-plane overturning if the orthogonal walls do not participate in the mechanism. On the other hand, a substantial increase of the load factor is verified when the orthogonal walls participate, which emphasises the importance of good connection between walls.

The participation or non-participation of the orthogonal walls in the out-of-plane overturning can be seen as alternative states and the load factor as a structural performance indicator. In this context, the various macroelements can be seen as control variables. The sensitivity of the load factor (a/g) to the variation of the state of the mechanical model (participation and non-participation of the orthogonal walls), $\delta I_{j,Ki}$, as obtained by means of equation 3.5, is indicated in Table 7.1 for each macroelement.

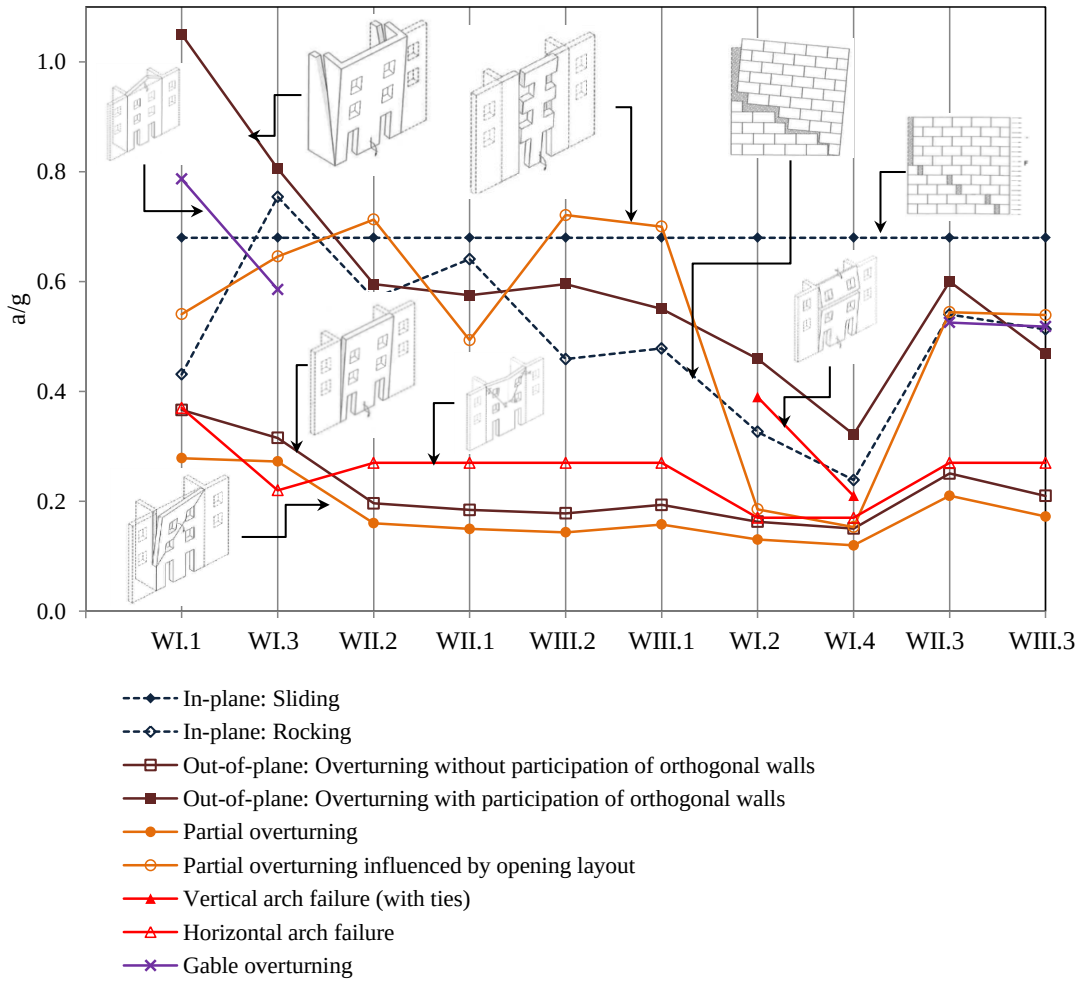

Figure 7.7 Seismic vulnerability of the Church of Kuño Tambo according to the FaMIVE procedure

Table 7.1 Sensitivity of the load factor obtained by FaMIVE to the variation of the state of the model (overturning of the walls with and without participation of the orthogonal walls)

	WI.1	WI.3	WII.2	WII.1	WIII.2	WIII.1	WI.2	WI.4	WII.3	WIII.3
$\delta I_{j,Ki}$	0.651	0.609	0.670	0.679	0.701	0.648	0.645	0.532	0.582	0.552

The overall sensitivity of the load factor, δI_j, can be obtained as an average of the sensitivity associated to each macroelement according to equation 3.6. In this case, this overall sensitivity, δI_j, is equal to 0.68. This value is above the uncertainty, m_u, calculated to

the Church of Kuño Tambo by any of the alternative procedures shown in Table 6.12. It is reasonable to assume that in reality the state of the church lies within the aforementioned alternative states of participation and non-participation of the orthogonal walls. The interlocking of blocks observed between some of the walls shows that the friction developed at the common interfaces might avoid the triggering of an out-of-plane failure mechanism with no participation of orthogonal walls. On the other hand, an out-of-plane failure mechanism may happen for load factors lower than the ones corresponding to overturning with participation of orthogonal walls. This discussion can lead to the conclusion that the uncertainty calculated for Kuño Tambo, which is within the interval 0.40, is reasonable to reflect the uncertainty associated to the assumption of continuous walls.

This simplified analysis of the vulnerability of the walls of the church by means of the FaMIVE procedure confirms the conclusions of the preliminary diagnosis (Chapter 5). The robustness of the macroelements, namely the presence of several openings, and the interaction between macroelements substantially affects the vulnerability of the church. A substantial reduction of this vulnerability to out-of-plane overturning could be achieved by improving the level of connection between the macroelements. These results also confirm empirical evidence collected by Tolles *et al.* (2002) on basic failure modes of unrestrained and restrained adobe walls.

7.3 Detailed diagnosis of a historic adobe church

The detailed diagnosis of the Church of Kuño Tambo is based on pushover analyses conducted with the present state global model of the church (Figure 7.1a). This model corresponds to an interpretation of the present state of the building.

The global model is subjected to permanent loading simulating the self-weight of the structural materials, a distributed vertical loading, representing the self-weight of the roof, and distributed horizontal loading at the top of the walls, representing the roof's thrust. An equivalent acceleration of 0.3g corresponding to 10% probability of exceedance in 50 years (E.030, 2003) is applied in the four global directions to represent earthquake action. This acceleration is slightly higher than the value recommended to Acomayo by the Peruvian adobe code (E.080, 2006), which recommends 0.234g for the worst foundation conditions.

The detailed diagnosis is conducted assuming no deterioration of the materials for the 'Robustness', 'Interaction', 'Connections' and 'Materials' attributes. The influence of material decay is then discussed within the 'Condition' attribute. The diagnosis is conducted

following the procedure described in Chapter 3 and bringing together information from various sources, namely:

(i) results of structural analyses conducted with the global models;
(ii) results of tests conducted at PUCP (Torrealva and Vicente, 2014) and interpretation of these results;
(iii) interpretation of results of tests from other sources;
(iv) *in-situ* observations; and
(v) reference literature.

A matrix summarizing the detailed diagnosis of the Church of Kuño Tambo concludes this chapter.

7.3.1 Robustness of the church

The robustness of the church is evaluated by considering the geometry, regularity and performance in terms of drift of the masonry structure. A relationship is established between performance and damage states on the basis of literature. A discussion on each of these aspects is presented in the following.

7.3.1.1 SLENDERNESS OF MASONRY WALLS

If only the height of the adobe wall is considered in the calculation of the vertical slenderness of the walls, all walls of the church are considered thick except WIII.3, which contains the staircase, as discussed in the preliminary diagnosis (Chapter 5). Such assumption in the calculation of vertical slenderness is reasonable since there is a plane of discontinuity at the interface adobe/base course. Moreover, the base course is normally built as a foundation with good interlocking at the corners, as per traditional practices (see for instance INC, 2008).

7.3.1.2 REGULARITY IN ELEVATION

The vertical resisting system of the church does not have significant misalignments or interruptions, as recommended by the Peruvian Building Code (E.030, 2003). The existence of an adobe wall on the top of a high rubble stone base course causes a non-negligible

variation of lateral stiffness in elevation within the resisting system; even though the thickness of the base course is similar to the thickness of the adobe wall. According to Eurocode 8 (CEN, 2004), the existence of substantial differences on the lateral stiffness of the components in elevation should be avoided.

The total height of the walls and the relative heights of the base course and adobe wall over the total height of the walls vary since the building follows the natural topography of the place. These variations have however some advantages. The height of the base course varies less than the total height of the walls, being always more than 2m high, in order to protect the adobe walls from raising water. For instance, the total height of WI.3 is lower than the total height of WI.1, whereas the base course has a similar height in both cases. This is a favourable state of the structure, since the presence of water significantly reduces the strength of adobe.

The existence of the base course creates a plane of discontinuity at the interface adobe/rubble stone masonry, which can lead to sliding of the adobe wall on the top of the base course if the stress state at this interface overcomes the shear strength, corresponding to the combined effect of cohesion and friction of the interface and the weight of the adobe wall as per a Coulomb-type friction law. Due to typical material properties of rubble stone masonry assumed in the model, the base course of the church is stiffer than the adobe walls. The base course can therefore act as an amplifier of seismic action, whereas the interface rubble stone/adobe can act as a damper. This interaction between base course and adobe walls is further analysed in the 'Interaction' attribute.

7.3.1.3 Regularity in plan

The evaluation of the regularity in plan of the church considers the symmetry in plan with respect to two orthogonal axes and the presence of torsional effects due to eccentricities between the centre of mass and the centre of stiffness. For instance, Eurocode 8 (CEN, 2004) specifies that the structure shall be approximately symmetrical in plan with respect to two orthogonal axes as far as both lateral stiffness and mass distribution are concerned.

The presence of the sacristy and baptistery creates asymmetry with respect to the longitudinal direction of the church (Y-direction of Figure 7.1), even if the collapsed buttresses B4 and B6 are reinstated. As far as the transversal direction is concerned (X-direction of Figure 7.1), the church is also asymmetric due to the progressive reduction of the height of the walls from South to North, as the church is located on a hill. This makes the building asymmetric in terms of both mass and stiffness with respect to two orthogonal

directions. In the Y-direction, there is more mass and stiffness on the East side if the sacristy and the baptistery are fully connected to WI.4. In the X-direction, the South part of the church has more mass, since the façade has higher thickness and height.

7.3.1.4 IN-PLANE AND OUT-OF-PLANE DRIFT

The in-plane and out-of-plane drift of the walls of the church, considering the most unfavourable direction of earthquake motion (positive or negative in-plane directions) for each wall, are compared with reference values for unreinforced masonry walls available in literature. Table 7.2 shows reference drift ranges for in-plane and out-of-plane behaviour for several damage states (DS) obtained by experimental campaigns and by the FaMIVE procedure for masonry buildings in Nepal, Italy and Turkey, according to D'Ayala (2013).

In the case of the Church of Kuño Tambo, the hypothesis of a good connection of the walls by interlocking of units at intersections and by the presence of tie-beams is investigated. Failure modes involving more than one wall are likely to develop (combined behaviour) under this hypothesis, as discussed in Section 7.2.3. This type of failure mode has greater stiffness than in-plane and out-of-plane modes and hence it is characterised by lower values of drift (D'Ayala, 2013). Table 7.3 shows drift ranges for combined behaviour obtained from the FaMIVE procedure for buildings in Nepal, Italy and Turkey (D'Ayala, 2013). Reference limits can also be obtained from the provisions of Eurocode 8 (CEN, 2005b) for the 'significant damage' and 'near collapse' damage states, as shown in Table 7.4. The provisions are based on the slenderness of the structural elements and the limit drift is calculated in a similar way as in-plane rocking.

Table 7.2 Drift ranges for in-plane and out-of-plane response of masonry walls (after D'Ayala, 2013)

Source	In-plane drift (%)			Out-of-plane drift (%)		
	DS of Damage Limitation	DS of Significant Damage	DS of Near Collapse	DS of Damage Limitation	DS of Significant Damage	DS of Near Collapse
Experimental	0.18-0.23	0.65-0.90	1.23-1.92	0.33	0.88	2.3
FaMIVE procedure	0.023-0.226	0.069-0.679	0.790-1.579	0.263-0.691	0.84-1.580	1.266-1.969

Table 7.3 Drift ranges for combined response of masonry walls (after D'Ayala, 2013)

Source	Drift for combined behaviour (%)		
	DS of Damage Limitation	DS of Significant Damage	DS of Near Collapse
FaMIVE procedure	0.030-0.168	0.099-0.582	0.198-1.401

Table 7.4 Drift limits for KT according to the provisions of Eurocode 8 (EN 1998-3, 2005b)

Walls of KT	In-plane drift (%)			Out-of-plane drift (%)		
	DS of Damage Limitation	DS of Significant Damage	DS of Near Collapse	DS of Damage Limitation	DS of Significant Damage	DS of Near Collapse
WI.1		0.4	0.53		0.36	0.48
WI.2		0.4	0.53		0.25	0.33
WI.3		0.4	0.53		0.37	0.49
WI.4		0.4	0.53		0.25	0.34
WII.1		0.4	0.53		0.28	0.37
WII.2		0.4	0.53		0.24	0.33
WII.3		0.4	0.53		0.45	0.60
WIII.1		0.4	0.53		0.44	0.58
WIII.2		0.4	0.53		0.23	0.31
WIII.3		0.4	0.53		0.74	0.98

The in-plane capacity curves of all walls and the out-of-plane capacity curves of the most vulnerable walls of the church are shown in Figure 7.8, in terms of lateral acceleration and drift. The drift is the ratio of the lateral displacement at the top of the wall to the height of the adobe wall. Taking into account that there is a surface of discontinuity between the adobe wall and the base course, and the base course is a continuous element stiffer than the walls, the height of the base course is not included in the analysis of drift.

As far as the in-plane capacity curves are concerned, the most vulnerable walls are WIII.2 and WII.1. In order to make a judgment on the performance of these critical walls, the uncertainty, m_u, calculated in Section 6.3.4 must be considered. As specified in equation 3.9, the 'real' or exact value of drift, I_j, lies within an interval defined by the uncertainty m_u. As explained in Chapter 6, since all SPIs are considered equally relevant, m_u is equal to 0.40 (see Table 6.12). Hence, it is reasonable to consider that the exact value of drift lies within an interval defined by the upper and lower bounds indicated in Table 7.5.

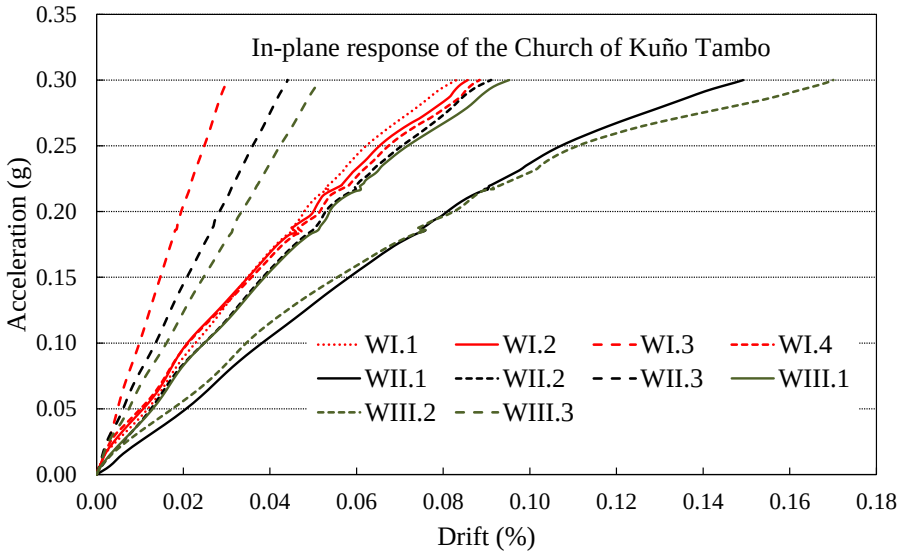

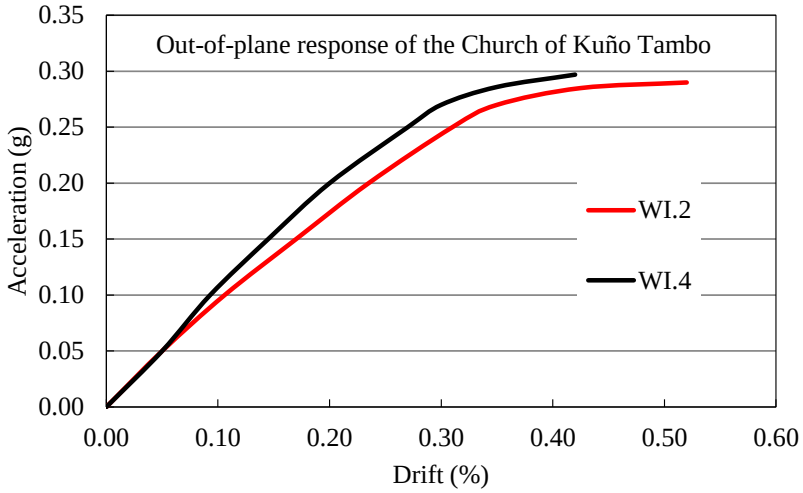

Figure 7.8 Capacity curves of the Church of Kuño Tambo described in terms of acceleration and drift

Table 7.5 In-plane drift of critical walls of the Church of Kuño Tambo considering the knowledge-based uncertainty of the diagnosis

In-plane drift (%)		WIII.2	WII.1
Most plausible value, calculated under the reference analysis conditions		0.17	0.15
Interval of plausibility of in-plane drift after taking into account the overall uncertainty of the diagnosis	$\frac{I_j}{1+m_u}$	0.12	0.11
	$I_j \times (1+m_u)$	0.24	0.21

Assuming the values of literature for combined response as a reference, the drift of WIII.2 and WII.1 exceed the damage state (DS) of significant damage even if the lower bounds of Table 7.5 are taken into account. On the other hand, the upper bounds of drift, greater than 0.2, indicate that the walls can exceed the DS of near collapse. These walls are subjected to large in-plane inertial forces transmitted by the out-of-plane movement of the longitudinal walls of the nave.

The most vulnerable walls have a nonlinear response from approximately 0.055% drift onwards, which indicates that an important reduction of stiffness initiates for an acceleration between 0.2g and 0.25g. Thus, 0.055% drift appears to be a lower bound for the DS of damage limitation for the walls of the Church of Kuño Tambo. The exceedance of this limit state should be avoided since the church has valuable interior wall paintings. Although the walls seem unlikely to fail in-plane under 0.3g, an adobe wall might become instable for small values of drift when large diagonal cracking occurs. Hence, further investigations in terms of reduction of integrity are required in order to evaluate the response from 0.2g onwards.

The Eurocode 8 reference drifts indicated in Table 7.4 seem to be excessively large for traditional adobe walls. According to this document, a limit state of damage limitation is characterised by negligible permanent drifts lower than 0.4, where the structural elements retain their strength and stiffness properties (see e.g. CEN, 2005b). However, according to the results shown in Figure 7.8 and Table 7.5, such value of drift should lead to a state of significant damage or near collapse. In terms of out-of-plane response, the longitudinal WI.2 and WI.4 walls are the most critical. The limits of drift under 0.3g of these critical walls are shown in Table 7.6 taking into account the uncertainty, m_u, equal to 0.4.

Table 7.6 Out-of-plane drift of critical walls of the Church of Kuño Tambo considering the knowledge-based uncertainty of the diagnosis

Out-of-plane drift (%)		WI.2	WI.4	WI.3
Most plausible value, calculated under the reference analysis conditions		0.46	0.40	0.25
Interval of plausibility of in-plane drift after taking into account the overall uncertainty of the diagnosis	$\frac{I_j}{1+m_u}$	0.33	0.29	0.18
	$I_j \times (1+m_u)$	0.64	0.56	0.35

The uncertainty m_u has a significant impact on the conclusions that can be made in terms of out-of-plane structural performance of the most critical walls. However, any choice of reference drift thresholds from literature (Table 7.2 and Table 7.3) to check whether the church exceeds a certain damage state is made with high level of uncertainty. This reflects the fact that properties of traditional materials are normally representative of a specific construction technology used in a small geographical area. The properties of similar materials are therefore likely to significantly vary from place to place.

Notwithstanding these uncertainties, a first general conclusion can be made: the critical walls WI.2 and WI.4 are likely to present significant damage for an acceleration of 0.3g. Moreover, if the upper bounds of the interval of plausibility of drift are considered, these walls are likely to be at a state of near collapse. The uncertainty in this case does not change the diagnosis, since for an historic construction that is used as a place of assembly with high cultural significance; the DS of significant damage should not be reached.

WI.2 and WI.4 present an important nonlinear plastic response from 0.24% and 0.20% drift onwards, respectively, which corresponds to an acceleration of 0.2g in both cases.

It is therefore reasonable to conclude that the existing lateral restraints of WI.2 and WI.4 are insufficient to avoid significant damage and even the collapse of these walls for accelerations larger than 0.25g.

Finally, in order to make a final judgement of the robustness of the original undamaged state it is necessary to check whether the lateral response of the longitudinal walls is considerably improved with the reconstruction of buttresses B4 and B6. The out-of-plane drift of these walls is therefore shown in Figure 7.9 for the following hypotheses of the model:

(i) tie-beams modelled and not modelled; and
(ii) buttresses B4 and B6 modelled and not modelled.

Hypothesis (i) informs on the structural relevance of the tie-beams and hypothesis (ii) informs on the structural relevance of the collapsed buttresses.

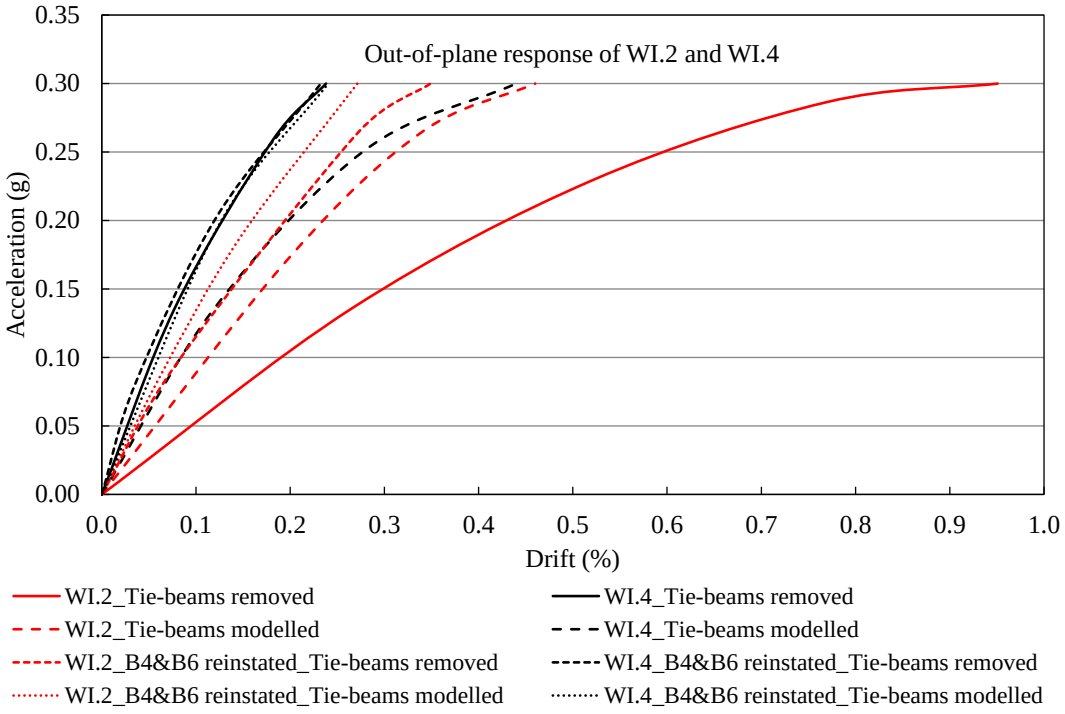

Figure 7.9 Out-of-plane capacity curves of WI.2 and WI.4 for various hypotheses

The results show that the benefit of reconstructing the buttresses is more significant than the benefit of improving the connection of the tie-beams to the walls. The response of WI.4 when the tie-beams are effective and buttresses B4 and B6 are reinstated is similar to its response without tie-beams.

The limits of drift under 0.3g of the most critical wall, WI.2, are shown in Table 7.7, taking into account the uncertainty, m_u, equal to 0.4. If the buttresses B4 and B6 are reinstated as originally designed, this wall is not likely to exceed the DS of significant damage even if the upper bound of the interval of plausibility is considered. However, it may exceed the DS of damage limitation. A direct conclusion of this outcome is that buttresses B4 and B6 should be rebuilt with a better design than the original collapsed buttresses in order to protect the interior wall paintings from damage. This intervention should be accompanied by the retrofitting or enlargement of buttresses B10 and B12. The insufficient capacity of original buttresses to avoid damage to the walls might have been understood in the past by local masons, who attempted to improve the structural response of the church by building buttresses B5, B7, B11 and B9 (see Figure 4.8).

Table 7.7 Out-of-plane drift of the most critical wall, WI.2, of the Church of Kuño Tambo considering the knowledge-based uncertainty of the diagnosis

Hypotheses	Reference drift (under the reference analysis conditions)	Interval of plausibility of out-of-plane drift after taking into account the overall uncertainty of the diagnosis	
		$\frac{I_j}{1+m_u}$	$I_j \times (1+m_u)$
Tie-beams removed [No tie-beams, No buttresses]	0.950	0.680	1.328
Tie-beams modelled [Tie-beams, No buttresses]	0.460	0.329	0.643
B4&B6 reinstated – Tie-beams removed [No tie-beams, Buttresses]	0.350	0.250	0.489
B4&B6 reinstated – Tie-beams modelled [Tie-beams, Buttresses]	0.270	0.193	0.377

7.3.1.5 POST-ELASTIC RESPONSE AND REDUCTION OF STRUCTURAL INTEGRITY

The extent and evolution of cracking are indicators of the post-elastic response of the walls. Walls that develop large cracks shortly after the component enters the post-elastic phase will lose structural integrity and fail at an early stage and abruptly. A simplified way of evaluating the post-elastic behaviour through finite element modelling is by computing the percentage of finite elements that enter the post-elastic phase at several stages of loading. This evaluation method is useful to check in a simplified way whether the extent of in-plane cracking can be sufficient to create large offsets that compromise the stability of the walls. In the case of the Church of Kuño Tambo, the Drucker-Prager failure criterion (Drucker-Prager, 1952) with a tension cut-off is used to evaluate the state of finite elements loaded in-plane.

The capacity curves discussed in the previous section indicate that the post-elastic response of the church is significant from an acceleration of 0.2g onwards. The percentage of failed elements of the most vulnerable walls is indicated in Figure 7.10 for an in-plane acceleration increasing from 0.2g to 0.3g. The elements tend to fail in tension before the shear strength of the material is reached, which indicates that the interfaces between walls are critical points, as most of the failed elements are located at these interfaces. A rapid

reduction of integrity of WII.1 and WIII.2 can occur from 0.25g onwards, since when loaded in-plane, these walls are subjected to large out-of-plane loads transmitted by WI.4. These results further support the conclusion that the buttresses on the East side of the wall must be reinforced.

Observations made during the field campaign showed that walls WII.1 and WIII.2 are among the most damaged and deteriorated due to their position within the structural system and interaction with longitudinal wall WI.4 as will be further discussion in the next section (see Figure 7.11).

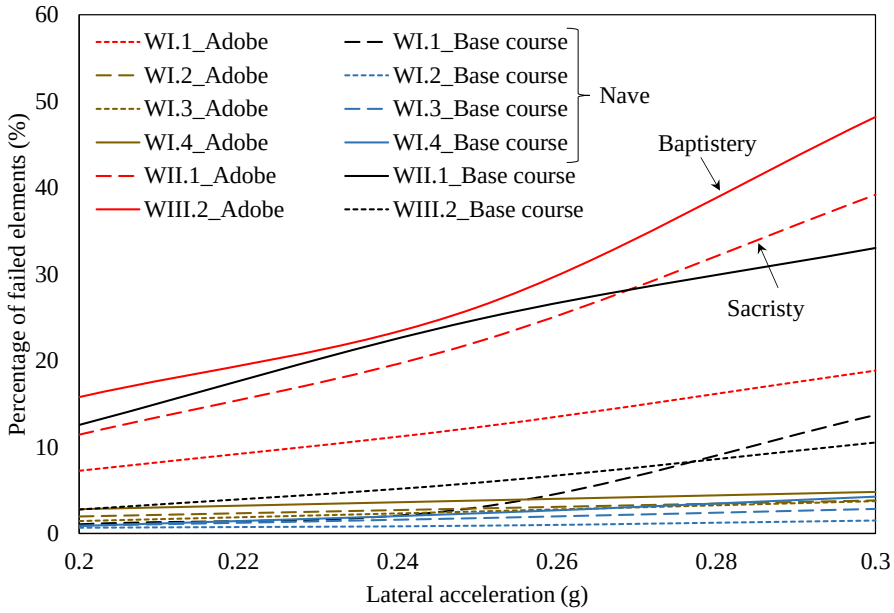

Figure 7.10 Evolution of the percentage of failed points in the most vulnerable walls

a) Cracking in WII.1 b) Cracking in WIII.2

Figure 7.11 Cracks caused by poor interaction of the walls of the nave with the sacristy and baptistery and by poor interaction of the roof with the walls

7.3.2 Condition

The most important change to the original condition of the church regards the collapse of buttresses B4 and B6. Regarding material decay, adobe is poorly protected of weather demands except in the case of WI.1. Two situations can explain this fact:

- All walls were initially plastered but weather demands caused the detachment of the plaster. In this case, WI.1 presents a better condition since (i) it has beneficiated from better maintenance, or (ii) it is better isolated of weather demands due to the presence of buttresses B1 and B2, and due to the extension of the roof's eaves along these buttresses. In this case, the poor state of the walls was only triggered by deterioration and poor maintenance; or
- The walls of the church have never had the same quality of the façade (WI.1). In this case, the quality of the masonry is poor. This option is related to the 'Materials' attribute.

On-site observations, as shown in Figure 7.12, indicate that it is likely that all walls of the church have been covered with plaster after the original construction. The plaster might have deteriorated and fall down due to lack of maintenance.

Figure 7.12 Deteriorated plaster in WI.3

7.3.3 Interaction of macroelements

The macroelements have structural interfaces that govern their interaction. The following interactions are relevant to the diagnosis of the Church of Kuño Tambo:

(i) Interaction between the walls of the nave;
(ii) Interaction between the walls of the baptistery/sacristy;
(iii) Interaction of the walls of the nave with the walls of the baptistery/sacristy;
(iv) Interaction of the walls with the buttresses;
(v) Interaction of the base course with the adobe walls;
(vi) Interaction of the tie-beams with the walls; and
(vii) Interaction of the roof's structure with the walls.

Interlocking of adobe units between the sacristy and the nave and between the walls of the nave and buttresses B10 and B12 was observed *in-situ*, as shown in Figure 7.13. This indicates that there is a positive connection between these macroelements. On the other hand,

in-situ observations also allowed concluding that the baptistery does not have the same level of interlocking, which might suggest a poor interaction of the baptistery with the nave.

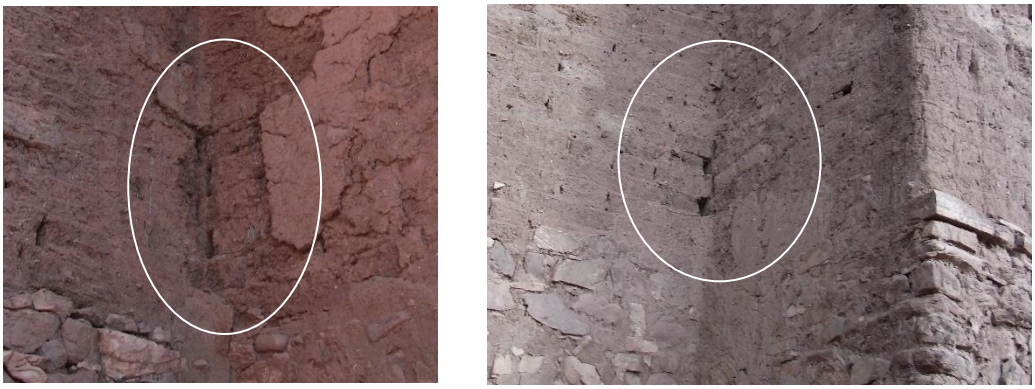

a) Interlocking between WI.4 and WII.1 b) Interlocking between WI.4 and B12

Figure 7.13 Interaction between KT macroelements

The interaction between adobe components (walls and buttresses) at corners is governed by the friction developed at the interlocking of blocks of orthogonal components. If this interlocking is present, as observed between many macroelements during field work, the assumption of continuity between adobe components in the models is realistic. In this case, the Drucker-Prager failure criterion (Drucker-Prager, 1952) with a tension cut-off can be used to evaluate whether the interfaces are likely to fail under a certain lateral load.

The percentage of failed elements at the interfaces between the adobe components and base course in the most unfavourable directions of application of the equivalent acceleration of 0.3g is shown in Table 7.8. Both the values obtained under the reference analysis conditions and the interval of plausibility taking into account the uncertainty, m_u, equal to 0.4 are indicated.

The interfaces tend to fail in tension rather than in shear due to the predominant out-of-plane bending response of the walls. The poorest interaction between the walls of the nave occur between WI.3 and the longitudinal walls WI.2 and WI.4, which can cause the overturning of the back wall WI.3 of the church. The interfaces of WI.1 with the longitudinal walls of the nave (WI.2 and WI.4) are also likely to be cracked; even though the damage is not expected to be as severe as in the previous case due to the presence of the longitudinal walls' extensions B1 and B2 (see Figure 4.8). Nevertheless, these interfaces have cracks even in the absence of earthquake damage (Figure 7.14), which indicates that their capacity is overcome by the roof thrust or past earthquakes.

Table 7.8 Percentage of failed elements at the interfaces between adobe components and the base course

Interfaces		% of failed elements		
		Reference analysis conditions	$\frac{I_j}{1+m_u}$	$I_j \times (1+m_u)$
Walls of the nave	WI.1 / WI.2	23	16	32
	WI.1 / WI.4	17	12	24
	WI.2 / WI.3	37	26	52
	WI.3 / WI.4	51	36	71
Walls of the sacristy	WII.1 / WII.3	19	14	27
	WII.2 / WII.3	30	21	42
Walls of the baptistery	WIII.1 / WIII.3	32	23	45
	WIII.2 / WIII.3	31	22	43
Nave and sacristy	WI.4 / WII.1	76	54	100
	WI.4 / WII.2	17	12	24
Nave and baptistery	WI.4 / WIII.1	34	24	48
	WI.4 / WIII.2	75	54	100
Walls and buttresses	WI.2 / B3	3	2	4
	WI.4 / B10	27	19	38
	WI.4 / B12	36	26	50
Adobe walls with base course		20	14	28

Figure 7.14 Crack at the interface WI.1/WI.4

The interfaces of the gable walls of the sacristy and baptistery (WII.3 and WIII.3) with the transversal walls also concentrate a significant amount of stresses leading to the failure of approximately 30% of the interfaces.

The interfaces between the nave and the sacristy and baptistery, in particular WI.4/WII.1 and WI.4/WIII.2, have the highest concentration of stresses and percentage of failed elements. The demand is greater at these interfaces than at WI.4/WIII.1 and WI.4/WII.2, due to the presence of the in-plane WI.1 and WI.3 walls, which are almost in the same alignment of WIII.1 and WII.2, respectively. This conclusion is supported by observations made during the field campaign which show severe cracks in walls WII.1 and WIII.2 (Figure 7.11).

For the evaluation of the interaction of the walls with the buttresses; B1, B2 and B8 are considered extensions of walls WI.4, WI.2 and WI.3, respectively. The most critical wall/buttress interaction occurs at interface WI.4/B12, since it does not beneficiates as WI.4/B10 of the existence of two tie-beams closed spaced near the interface. These tie-beams restrain to an extent the out-of-plane deformation of WI.4.

In the adobe/base course interface, 20% of the elements are likely to fail under 0.3g. Although this interface does not appear to be critical as per the results of Table 7.8, it becomes increasingly important to maintain the stability of the walls after the interaction between walls and walls/buttresses fail and the components behave independently of each other.

The interaction of tie-beams with the walls is evaluated by means of the criteria shown in Figure 7.15.

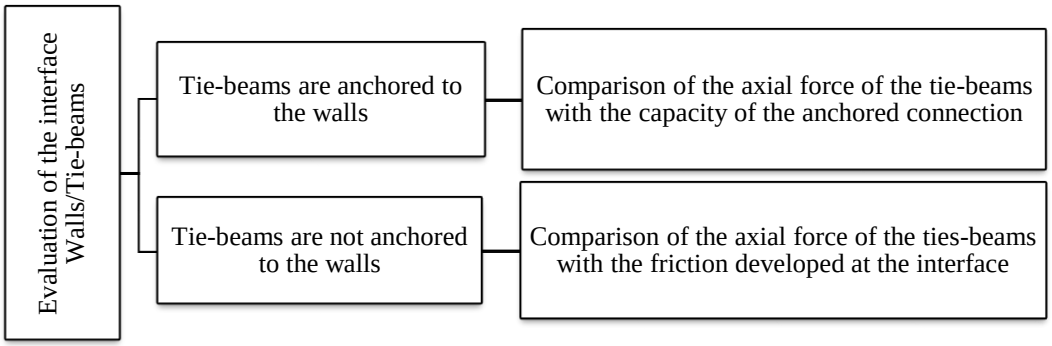

Figure 7.15 Criteria for evaluation of the interaction between walls and tie-beams

The tie-beams of the Church of Kuño Tambo are connected to the walls either by approximately 0.6m embedment in the adobe wall or by means of timber anchors. The axial stress of the tie-beams numbered from 1 to 9 is shown in Figure 7.16. It can be seen that T3 is subjected to the highest level of load, followed by T7. T4 and T5 benefit from the fact of being closely spaced.

The capacity of the tie-beams that are not anchored to the walls, F_{su}, is governed by a Coulomb-type friction law, according to Equation 7.1.

$$F_{su} = \mu_{su} N \quad [7.1]$$

, where μ_{su} is the static coefficient of friction between adobe and timber and N is the normal force acting on the connection. The normal force is equal to the weight of the adobe wall on the top of the tie-beam plus the vertical overload provided by the roof. Considering a coefficient of friction of 0.3 (NZSEE, 2011a and 2011b), the capacity of the connection, F_{su}, is equal to 4.8kN. This can be considered a lower bound of the capacity of the connection.

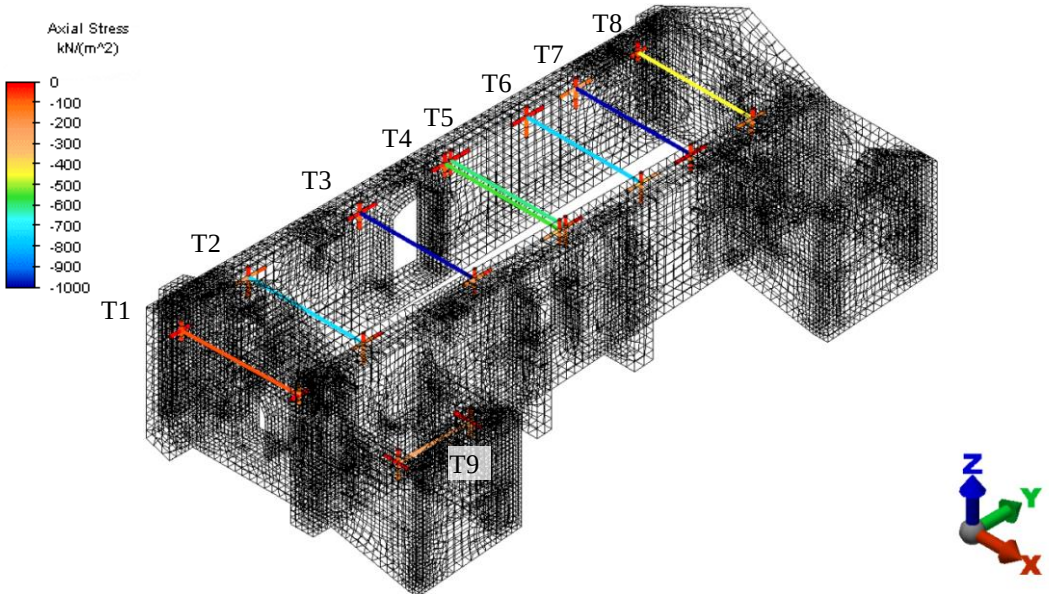

Figure 7.16 Axial stresses in the tie-beams after pushover analysis performed with an equivalent acceleration of 0.3g in the positive X direction

In the case of connections with timber anchors, the axial force acting on the tie-beams is compared to the capacity of the connection, F_m, obtained by PUCP through pull-out tests (Torrealva and Vicente, 2014). The capacity of the connections is obtained by linear interpolation of the maximum force measured during these tests on walls of 0.26m, 0.54m and 0.83m thickness taking into account the thickness of the longitudinal walls of the nave and baptistery (Table 7.9). The anchorages failed in a combination of shear and tension with the formation of a failure cone during PUCP's pull-out tests. This type of failure normally

occurs when there is a good connection among the components of the anchors and a good connection of the anchor to the wall. This failure mode has normally the highest capacity; and therefore these results obtained by PUCP can be considered as an upper bound of the capacity of the anchorages of the Church of Kuño Tambo.

Table 7.9 Capacity of anchored connections of tie-beams to adobe walls after results of pull-out tests conducted by PUCP (Torrealva and Vicente, 2014)

Thickness of the wall (m)	Tie-beams	Capacity of the connection, F_m (kN)
1.60	T1 to T8	90
0.75	T9	44

The capacity of the anchored connections is substantially greater than the capacity of the connection when the tie-beams are simply embedded in the walls, especially because the tie-beams are located almost at the top of the adobe walls, so a relatively modest vertical load is present. The intervals of plausibility of the ratio of axial force to capacity of the connection are shown in Table 7.10 considering an uncertainty m_u equal to 0.4. These intervals of plausibility are defined by considering the reference value of the axial load, N_e, and the upper and lower bounds defined according to equation 3.9.

If the connection is not anchored, all tie-beams are likely to slide for an acceleration of 0.3g, even if the lower bounds of the interval of plausibility of N_e are considered. On the other hand, the connections are not likely to fail if the tie-beams are properly anchored to the walls. Finally, it should also be noted that the quality of adobe at the top of the wall is poor due to moisture. Hence, this condition could trigger the failure of the anchored connection by a cone pull-out type for a lower value of force than the maximum capacity considered here.

Finally, as far as the interaction of the roof's structure with the walls is concerned, it should be noted that the wall-plates of the nave are not continuous and therefore they do not work as an element that distributes the load evenly among the adobe walls. This configuration of the wall-plates enables the load provided from the roof weight to be distributed along the top of the walls; however, it does not promote a re-distribution of the inertial forces uniformly among the walls. In the case of the sacristy and baptistery, there are no wall-plates, and therefore the rafters are sitting directly on the walls.

Table 7.10 Intervals of plausibility of the ratio of demand to capacity of the anchorages for an acceleration of 0.3g

Tie-beams	Axial load, N_e, (kN)	N_e/F_m	N_e/F_{su}
T1	[6, 8, 11]	[0.06, 0.09, 0.12]	[1.19, 1.65, 2.33]
T2	[17, 24, 34]	[0.19, 0.27, 0.37]	[3.58, 5.06, 6.99]
T3	[36, 50, 70]	[0.40, 0.56, 0.78]	[7.45, 10.44, 14.56]
T4	[17, 24, 34]	[0.19, 0.27, 0.37]	[3.58, 5.08, 6.99]
T5	[19, 27, 38]	[0.22, 0.30, 0.42]	[4.02, 5.65, 7.86]
T6	[24, 33, 46]	[0.26, 0.37, 0.51]	[4.92, 6.85, 9.61]
T7	[34, 47, 66]	[0.37, 0.52, 0.73]	[7.00, 9.71, 13.69]
T8	[11, 16, 22]	[0.13, 0.18, 0.25]	[2.38, 3.35, 4.66]
T9	[9, 12, 17]	[0.20, 0.28, 0.38]	[1.79, 2.52, 3.50]

This interaction creates excessive concentration of stresses around the rafters, which may also contributed to the development of existing cracks in walls WII.1, WIII.1 and WIII.2 (see Figure 7.11).

7.3.4 Connections within macroelements

In the case of the Church of Kuño Tambo, the following connections are the most relevant for the diagnosis:

(i) Connections within the timber roof; and
(ii) Connection of the wooden tie-beams to the timber anchors.

The rafters of the nave are sitting on wall-plates with a modest scarf, as shown in Figure 7.17. Each pair of rafters is connected together by means of leather straps with scarfs and, in some cases, wrought iron nails, as shown in Figure 7.18. The same type of connection is used to connect the collar beam to the rafters. These joints are very flexible and the elements slender, so the roof has a modest in-plane and out-of-plane stiffness.

Figure 7.17 Detail of connection of rafter to wall-plate in the nave

Figure 7.18 Connection between rafters and connection of collar beams to rafters

There are three different types of timber anchors in the church, as shown in Figure 7.19. In all cases, the anchors have a configuration that is unable to distribute the stresses in a way that local failure of the adobe wall does not occur, especially when there is no horizontal timber element, such as in the cases of ties T2 and T9. The layout and construction technology of these anchors show that they were built without proper design at different periods of time. The current timber anchors are unable to provide an effective lateral restraint to the out-of-plane deformation of the walls.

a) Wall I.2, Tie T2 b) Wall I.2, Tie T1 c) Wall III.2, Tie T9

Figure 7.19 Layout of the timber anchors of the Church of Kuño Tambo

7.3.5 Materials

A typical adobe brick measures 0.70m long x 0.35m wide x 0.20m high (Cancino *et al.*, 2012). The shape ratios of the units are 1:2 width/length and 1:3.5 height/length. The adobe units are set in an English bond pattern (Figure 4.11); even though the pattern is not clearly identifiable in some areas of the walls due to deterioration of adobe. The fabric is characterised by an overlapping length of 0.35m, corresponding to ½ of an adobe unit, on face and through thickness of the wall. Head and bed joints are completely filled with fairly homogeneous mud mortar mixed with straw. These aspects are typical of fabrics of good quality.

However, the thickness of both head and bed joints shows some variability, within a range of 3-15cm. Moreover, the mud plaster detached almost completely from most of the adobe walls and buttresses, except from WI.1 which seems to have been done with a better quality cover, and therefore the adobe is unprotected from weather demands.

The rubble stone masonry of the base course (Figure 7.20) is made of heterogeneous stones with joints of thickness ranging within 2-6cm. The joints are filled with mud mortar, even though some parts of the masonry have completely lost the mortar. These aspects are typical of irregular and poor quality masonry. The base course is not plastered; and therefore the mortar is exposed to weather demands, which might have caused the loss of infill mortar.

Figure 7.20 Rubble stone masonry of the base course of the Church of Kuño Tambo

7.3.6 Matrix of the detailed diagnosis of the Church of Kuño Tambo

The detailed diagnosis of the adobe church is summarized in the matrix of Table 7.11. Since the diagnosis do not contradict the available information, especially the observations made on the site, it is reasonable to assume that the level of uncertainty of the output is acceptable. Hence, the reference analysis conditions and the intervals of plausibility do not need to be revised. Otherwise, other iteration would be needed to improve the quality of the analysis.

Table 7.11 Detailed diagnosis of the Church of Kuño Tambo

1.ROBUSTNESS	+ Regular structure that complies with the life safety performance level. However it is likely to exceed the damage limitation state, and therefore to damage the wall paintings. Generalized cracking occurs for an acceleration between 0.2g and 0.25g. The structure is robust in terms of conceptual design; however the poor quality in terms of other attributes compromises its structural performance.				**Robustness negative**
2.CONDITION	+	- Two buttresses collapsed and materials are decayed.			
3.INTERACTIONS	+ | -	+ Positive interaction of the rubble stone with the adobe wall.		- Excessive concentration of stresses occurs at most interfaces. Tie-beams are not properly anchored to the walls, and they are likely to slide for an acceleration of 0.3g.	
4.CONNECTIONS	+ | - | + | -	+	- Modest in-plane and out-of-plan stiffness of the roof with flexible joints.	+ | - Modest in-plane and out-of-plan stiffness of the roof with flexible joints.	
5.MATERIALS	+ | - | + | - | + | - | + | - | + | -	+ Adobe's fabric regular, but requiring protection for weather demands.	- Rubble stone's fabric irregular and requiring protection for weather's demands.	+ | - | + Adobe's fabric regular, but requiring protection for weather demands. | - Rubble stone's fabric irregular and requiring protection for weather's demands.	

7.4 Analysis at a global level of a historic timber structure

7.4.1 Global model of the timber framing of the Cathedral of Ica

The global model of the timber framing of the cathedral is developed by replicating multiple times the local model of the nave's bay developed and refined in Chapter 6, and merging it with a model of the transept and crossing bay and with a model of the choir loft's bay. The latter model is a modification of the nave's bay, in which the joists of the choir loft and lateral aisles are assumed continuously connected to the transversal and longitudinal beams.

The timber elements of the bay of the transept and crossing (Figure 7.21), which has the central dome, are framed with joints similar to the joints of the nave, whose characteristics and modelling approach have been already discussed in Chapter 6. The weight of the roof cover is considered as lumped masses on the top of the vault and dome. The timber members are simulated by means of beam elements with isotropic and linear material models. The wooden species of the structural elements are indicated in

Table 7.12 and the respective material properties in Table 7.2. The modelling approach of the timber joints of the transept and crossing is summarised in Table 7.13, and the stiffness of the joints is indicated in Table 7.3.

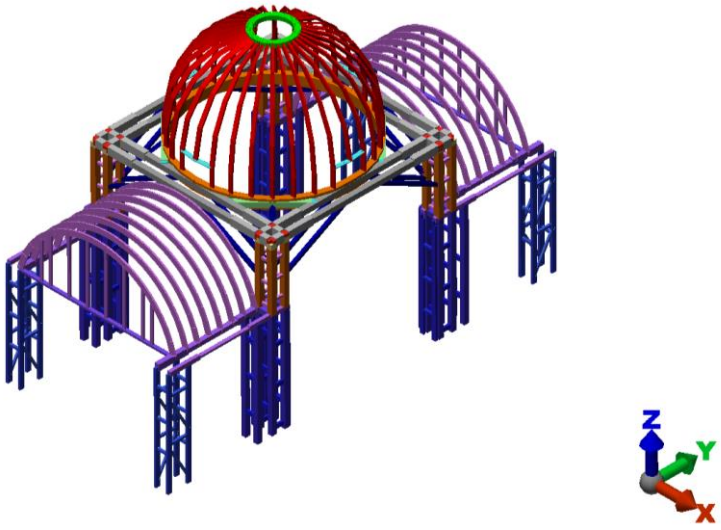

Figure 7.21 Beam and spring model of the Cathedral of Ica's transept and crossing

Table 7.12 Wooden species of the structural members of the bay of the transept and crossing

Wooden species	Structural elements
Caoba Africana	20. Central dome's top and bottom ring; 21. Central dome's meridians and parallels; 22. Central dome's lintels; 23. Transversal and longitudinal beams supporting the dome; 24. Pendentives' members; 25. Upper part of central pillars' posts; 26. Horizontal bracing of upper part of central pillars' posts; 27. Transversal and longitudinal beams; 28. External posts of central pillars; 29. Horizontal bracing of central pillars; 30. Posts of lateral pillars.
Guarango	31. Horizontal bracing of central pillars; 32. Internal posts of central pillars; 33. Diagonal bracing of lateral pillars.
Cedar	34. Arches of the aisles; 35. Vertical bracing of the end arches of the aisles.

Table 7.13 Modelling approach of the principal timber joints of the transept and crossing

Type of joint	Structural elements connected	Modelling approach
Mortice and tenon	Connections within the crossing: 23. Top of upper part of central pillars' posts / Beams supporting the central dome; 24. Bottom of upper part of central pillars' posts / Beams of the aisles; 25. Central pillars' posts / Longitudinal and transversal beams; Connections within the transept: 26. Lateral pillars' posts / Longitudinal and transversal beams.	Rotations around an axis parallel and perpendicular to the grain of the beam are released. 1 elastic spring with stiffness obtained from experiments is introduced to govern each DOF released.
Pegged mortice and tenon	Connections within the crossing: 27. Horizontal bracing of upper part of central pillars / Posts of upper part of central pillars; 28. Horizontal bracing of central pillars / Posts of central pillars; Connections within the transept: 29. Horizontal bracing of lateral pillars / Posts of lateral pillars.	Translation in the direction of the centre line of the horizontal bracing is released. 1 elastic spring with a realistic stiffness is introduced to govern this DOF.
Nailed connections (diagonals)	Connections within the transept: 30. Lateral pillars' diagonals / Lateral pillars' posts.	Rotation around an axis perpendicular to the grain of the posts is released. 1 elastic spring with experimental stiffness is introduced to govern this DOF.
No joint characterisation available	Connections within the crossing: 31. Central dome's top ring / Central dome's ribs; 32. Central dome's ribs / Central dome's bottom ring; 33. Connection among the planks of each central dome's ribs; 34. Central dome's ribs / Lintels; 35. Central dome's ribs / Concentric bracing; 36. Connections among transversal and longitudinal beams; Connections within the transept: 37. Arches of the aisles / Transversal beams; 38. Bracing of the transept arches / Transept arches; 39. Bracing of the transept arches / Longitudinal beams.	Elements continuously connected.

The bracing of the frames between bays (Figure 4.35a) and the bracing between bay-edge arches (Figure 4.35b) is simulated by means of trusses. It is assumed that these connections effectively contributed to an increase in stiffness in both the longitudinal direction and a coupling of the local vault swaying modes in the transversal direction during the earthquake, since no evidence of the failure of this bracing was observed

The timber structure is cladded in a layer made of canes and mud, nailed to the timber by leather straps. However, it has been concluded in Chapter 6 that the stiffening effect of this cladding system is negligible, and hence this element is not directly simulated in the global models, if not in terms of added weight. The weight of the roof is 1.7kN/m^2 on the top of the vault and domes, and 2.5kN/m^2 on the top of the aisles. The weight on the aisles is larger due to the existence of a layer of bricks, which is not present on the top of the vault.

Circumferential ribs connecting the meridians of the central dome are also included in the global model. They are shaped so as to connect two adjacent ribs. They stabilise the dome against torsional effects.

7.4.2 Hypothesis on the failure of the timber structure of the Cathedral of Ica due to the 2007 Pisco earthquake

As explained in Section 4.4.3, the almost complete collapse of the vault of bay 1, observable in Figure 4.40a, was due to the failure of the nailed connections of the bay-edge arches, as shown in Figure 4.40b. The mortice and tenon connections of the internal arches and lunette's elements with the beam at the top of lunette failed in bays 2, 3 and 4 due to the failure of the beam in shear, as shown in Figure 4.41. This failure could be identified in bay 2 after the earthquake by the visible settlement of the top of the vault (Figure 4.40a); however the internal arches did not collapse immediately due to the existence of a layer of canes connected to the bay-edge arches. In bays 3 and 4, the internal arches collapsed on the ground of the cathedral. The whole weight of the roof at the top of bay 2 was therefore completely supported by the bay-edge arches. Several nailed joints of the East bay-edge arch of bay 2 failed in shear and in tension perpendicular to the grain, which shows that these connections were not capable of supporting the forces produced by the masses being supported by the arches. Subsequent minor shakes in 2010 caused the collapse of this edge arch in a similar way as in the case of bay 1 (Figure 4.42 and Figure 4.43). It is therefore reasonable to assume a similar but quicker progress of damage in bay 1 during or immediately after the earthquake.

Taking into account these observations and interpretation of data made after the earthquake, it is necessary to verify whether the redistribution of loads that occurred after the failure of the beam at the top of lunettes in bays 2, 3 and 4, led to the failure of the bay-edge arches of bays 1 and 2.

For this purpose, modal analyses and modal superposition analyses are performed, aimed at verifying the different state and response of the church before and after the earthquake in order to better understand the collapse dynamics. Two alternative global models of the timber framing of the Cathedral of Ica, shown in Figure 7.22, are considered:

Model 1. Hypothetical state of the structure before the 2007 Pisco Earthquake: (a) all elements and joints are modelled; and (b) the roof-weight is fully applied and uniformly distributed among all arches; and

Model 2. Hypothetical state of the structure during or immediately after the 2007 Pisco earthquake: (a) bay 5 is fully modelled and weight is redistributed on the arches; (b) internal arches and lunettes not modelled in bays 1 and 2, and weight is fully applied on the bay-edge arches; (c) internal arches and lunettes not modelled in bays 3 and 4, and only the weight of the lunettes is considered, in which case it is supported by the corresponding bay-edge arches; and (d) the longitudinal beams are in place.

The natural frequencies, modal shapes and participating masses of the modes predominantly affecting the vault and global modes of Model 1 and Model 2 are shown in Figure 7.23 and Table 7.14.

The structure is characterised by many local modes with close frequencies due to the lack of a rigid diaphragm and the differences in stiffness and distribution of masses of the various parts of the timber framing. The bay of the principal dome and bay 1 of the nave, which has the mezzanine, have a strong influence on the response of the adjacent bays.

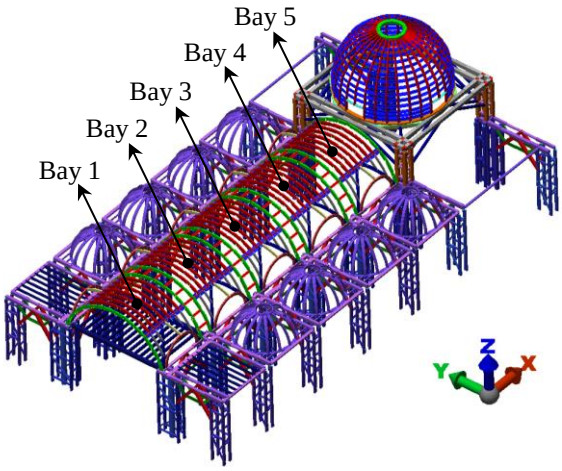

b) Model 1 – Before the earthquake

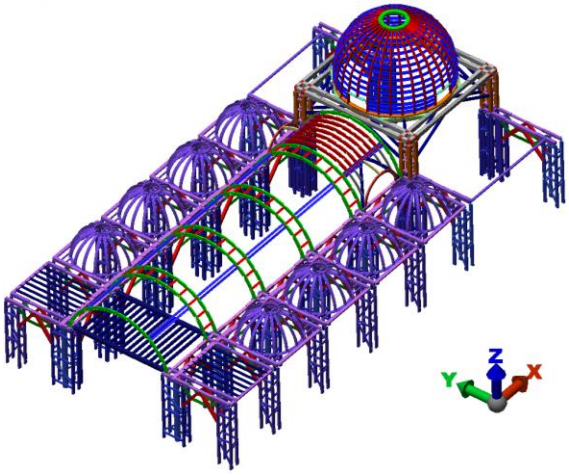

b) Model 2 – During or imediately after the earthquake

Figure 7.22 Numerical models of the global timber framing of the Cathedral of Ica assuming hypothetical states of the structure before and after the 2007 Pisco earthquake

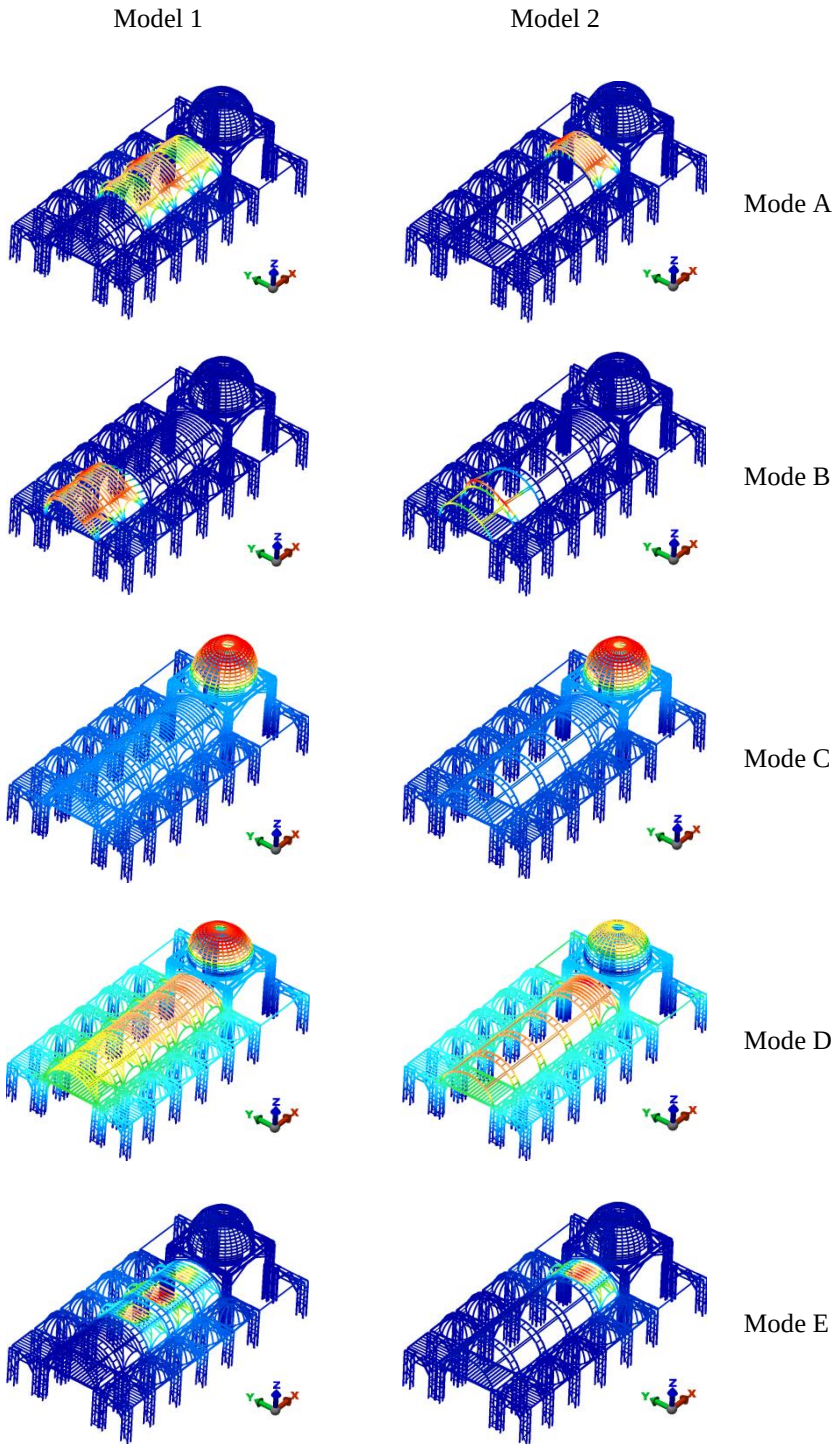

Figure 7.23 Modal shapes of model 1 and model 2 of the timber framing of the Cathedral of Ica

Table 7.14 Frequencies and modal participating masses of the global model of the timber framing of the Cathedral of Ica

	Modes	Period, *T* (s)		Modal participating masses (%)					
				X direction		Y direction		Z direction	
		Model 1	Model 2	Model 1	Model 2	Model 1	Model 2	Model 1	Model 2
A	Lateral symmetrical vibration of Bay 5, Bay 4 and Bay 3.	1.348	1.342	0.00	0.00	27.95	11.60	0.00	0.00
B	Lateral symmetrical vibration of Bay 2 and Bay 1.	0.787	0.950	0.00	0.00	7.27	7.74	0.00	0.00
C	Longitudinal vibration, in which the nave and the principal dome's bay vibrate in the same direction.	0.597	0.590	41.49	32.71	0.00	0.00	0.00	0.00
D	Longitudinal vibration, in which the nave and the principal dome's bay vibrate in the opposite direction.	0.479	0.436	44.12	49.86	0.00	0.00	0.00	0.07
E	Lateral anti-symmetrical vibration of Bay 5, Bay 4 and Bay 3.	0.456	0.448	0.01	0.18	0.00	0.00	17.47	7.03

The frequency of the mode related to the lateral symmetrical vibration of bays 1 and 2 (mode B of Figure 7.23) is equal to 1.27Hz in Model 1 and 1.053Hz in Model 2, which means it is around 17% lower in the case of model 2 with around 6% more participating mass than the corresponding total mass of the model. This is due to redistribution of loads following the mainshock, in which case more percentage of total mass is concentrated in the first 2 bays. This alteration of the dynamic response of the church due to progressive damage of the structure might have therefore increased the demand on bays 1 and 2, as would be expected. Mode D has a natural frequency characterised by greater amplification than mode C if the North-South (Y-direction of the models) response spectrum of the 2007 Pisco earthquake is taken into account (Figure 6.19). This observation is more important in the case of Model 2, where mode D has more participating mass than mode C and it is furthermore subjected to even greater amplification, according to the same response spectrum, due to the 9% increase in the natural frequency. This explains the damage caused by the pounding phenomena that occurred between the nave and the bay of the principal dome. The fact that the natural frequency of mode E is associated to greater amplification than the frequency of mode A, according to the North-South response spectrum, indicates that mode E might be more critical than mode A; even though it has lower participating mass.

Modal superposition analyses are performed with Model 1 and Model 2 using the North-South (Y-direction of the models, transversal to the nave, which is the most critical direction of motion for the arches) natural spectrum recorded at the station of Parcona in the province of Ica (Peru) during the 2007 Pisco earthquake (see Figure 6.19). The deformed shape and displacement in the Y-direction of Model 1 and Model 2 are shown in Figure 7.24. It can be seen that bay 4 is the most critical bay of Model 1, followed by bay 3 and bay 5. The highest demands occur in the beam at the top of lunettes, which depending on the capacity of the mortice and tenon joints that connect the internal arches and lunette's elements to the beams, might indicate that the internal arches of bays 3 and 4 would collapse first, which is confirmed by observations made after the earthquake and shown in Figure 4.40a. The connections at the top of lunettes of bay 5 did not fail, since they are subjected to more modest demands. According to this interpretation, the mortice and tenon connections at the top of lunettes of bays 1 and 2 should not have failed also. However, Figure 4.40a shows evidence that these connections failed in bay 2 during the earthquake, since the structure at the top of the vault was subjected to a visible settlement.

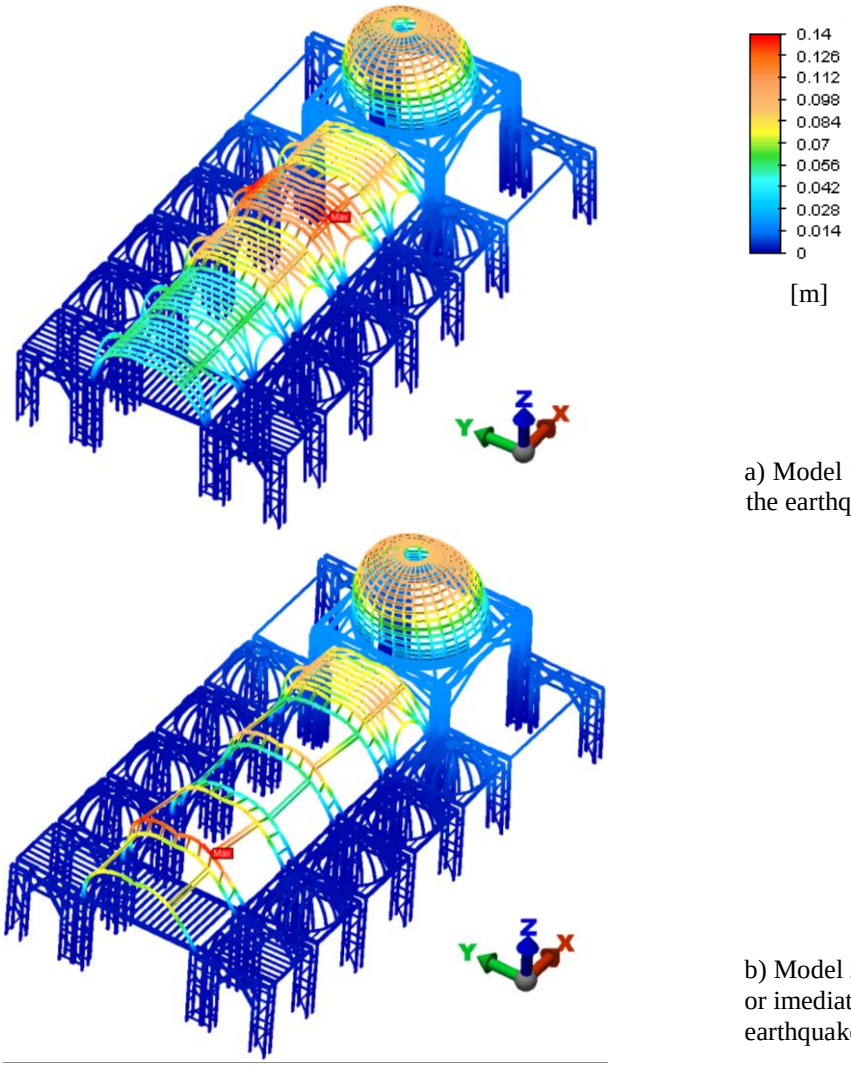

a) Model 1 – Before the earthquake

b) Model 2 – During or imediately after the earthquake

Figure 7.24 Displacements in Y-direction (in meters) in the timber framing of the Cathedral of Ica after modal superposition analysis with the North-South spectrum of the 2007 Pisco earthquake applied in the Y-direction

This might be explained by considering the deterioration of the beams at the top of lunette, since it is possible that the beams of bays 1 and 2 were more deteriorated than the beams of bay 5. If it is assumed that the demand in bays 1 and 2 was not great enough for the canes to disconnect from the arches, the weight of the internal arches and roof was therefore totally supported by the edge arches of bays 1 and 2, as modelled in Model 2. Indeed, the results of Model 2 show that bays 1 and 2 are the most critical for this state of the structure.

During the earthquake, the bay-edge arches were subjected to different demands throughout the cathedral. The arch at the Eastern edge of bay 4 is the most critical in Model 1, and the arch at the Eastern edge of bay 2 is the most critical in Model 2. The deformed shapes with colour shading corresponding to lateral displacement and the shear force resultant in these most critical arches of Model 1 and Model 2 are shown in Figure 7.25 and Figure 7.26. Each point in these graphs represents the shear resultant acting on the springs which simulate each nailed joint. The springs subjected to the greatest shear forces of the models occur at the joints that failed due to the 2007 Pisco earthquake and subsequent tremors. For instance, it can be seen that the maximum shear forces in the arch at the Eastern edge of bay 2 occur in Model 2 at the nailed joints located next to the connections at the top of lunette. Figure 4.40b and Figure 4.43a show that those connections completely failed due to the earthquake. The nailed connections at mid-span of the edge arches also failed in bays 1 and 2. Figure 7.25 and Figure 7.26 show that these connections are subjected to important shear forces; even though their complete failure could be a consequence of the failure of the connections near the top of lunette. Figure 7.25 also shows that the shear demand on the arch at the Eastern edge of bay 4 considerably decreases from Model 1 to Model 2. The opposite occurs for the arch at the Eastern edge of bay 2, the deformation of which dramatically increases from Model 1 to Model 2. This might explain the fact that the edge arches of bays 1 and 2 were the most severely affected by the earthquake.

The nailed joints of the bay-edge arches of Model 1 are subjected to shear forces, with a maximum of 20.4kN, greater than the maximum shear forces acting on the internal arches, 5.15kN. In Model 2, the maximum shear force acting on the bay-edge and internal arches are 24kN and 5.23, respectively. These results for the internal arches are confirmed by observations made on the site after the 2007 Pisco earthquake, since no important damage was observed then.

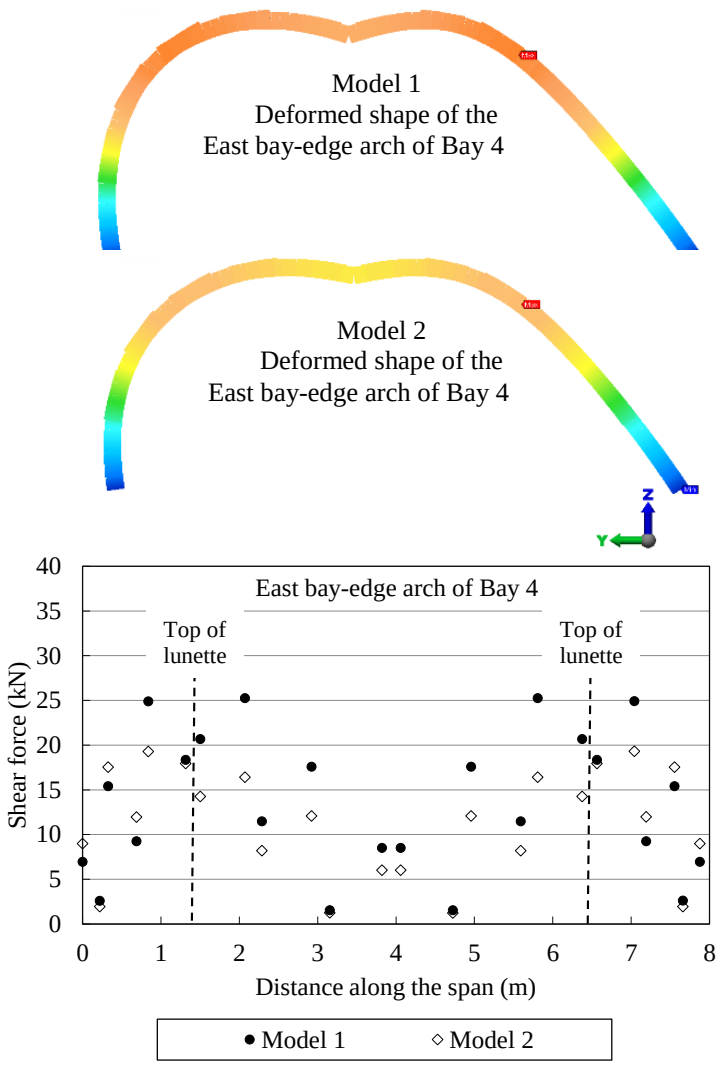

Figure 7.25 Shear forces acting on the Eastern bay-edge arch of Bay 4 of the Cathedral of Ica due to the 2007 Pisco earthquake

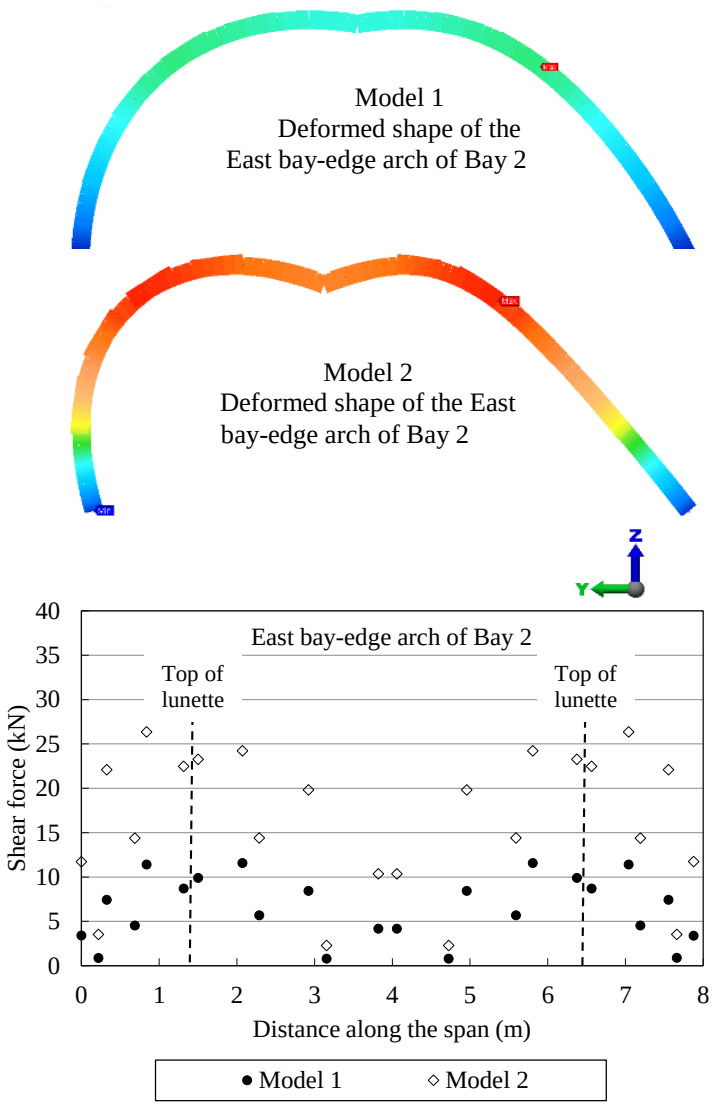

Figure 7.26 Shear forces acting on the Eastern bay-edge arch of Bay 2 of the Cathedral of Ica due to the 2007 Pisco earthquake

7.4.3 Structural analysis of the masonry walls and towers of the Cathedral of Ica

As discussed in Chapter 4, the timber framing behaves to a large extent independently of the masonry walls and towers. However, interaction between the timber framing and masonry walls created damage in the walls, as shown in Figure 4.45, and might have created further demands to the timber framing. The purpose of presenting the model of the walls and towers here is to investigate how possible hammering phenomena occurring between the timber and masonry systems can contribute to the damage observed in the cathedral.

The timber part of the towers is modelled assuming the hypothesis of full connection between all timber members, since no evidence of failure of the tower's timber connections was observed during the field work.

A modal analysis is initially performed in order to calculate the natural periods of the structure, as shown in Figure 7.27 and Table 7.15. The first mode corresponds to the transversal vibration of the North adobe wall with a period of 0.528s. The South adobe wall vibrates with a lower period of 0.419s due to the presence of adobe columns, which provide lateral restraint to this wall. These periods are smaller than the period of vibration for the transversal mode of the transept's bay of the timber structure, which is equal to 0.909s, as per modal analysis conducted with the global model of the timber framing. The brickwork façade vibrates with a period of 0.271s and the towers with a period of approximately 0.35s, whereas the timber frame vibrates in the longitudinal direction with a higher period of 0.597s and 0.479s (modes C and D of Table 7.14). These results indicate that it is plausible to assume that during the 2007 Pisco earthquake, the stiffer masonry walls and towers interacted with the more flexible timber framing resulting in additional localised demands at the points of interaction.

Pushover analyses are performed using a Drucker-Prager material model for both adobe and brickwork. An equivalent acceleration of 0.3g, corresponding to 10% probability of exceedance in 50 years according to the code for earthquake resistance in Peru (E.030, 2003) is applied both in the Y and X directions. The distribution of maximum principal stresses is shown in Figure 7.28. Major cracking of the walls is due to out-of-plane bending rather than in-plane shear, which is to be expected in long unrestrained adobe walls. Tension stresses are greater than the tension strength of the material at the following locations, which are marked in Figure 7.28: (i) connection of the base of the towers with the longitudinal walls; (ii) lower part of the longitudinal walls, near the interface of adobe with brickwork; (iii) top corners of the façade; and (iv) connection of the pediment with the façade. These results well agree

with the damage observed in the cathedral after the 2007 Pisco Earthquake, which is shown in Figure 4.45.

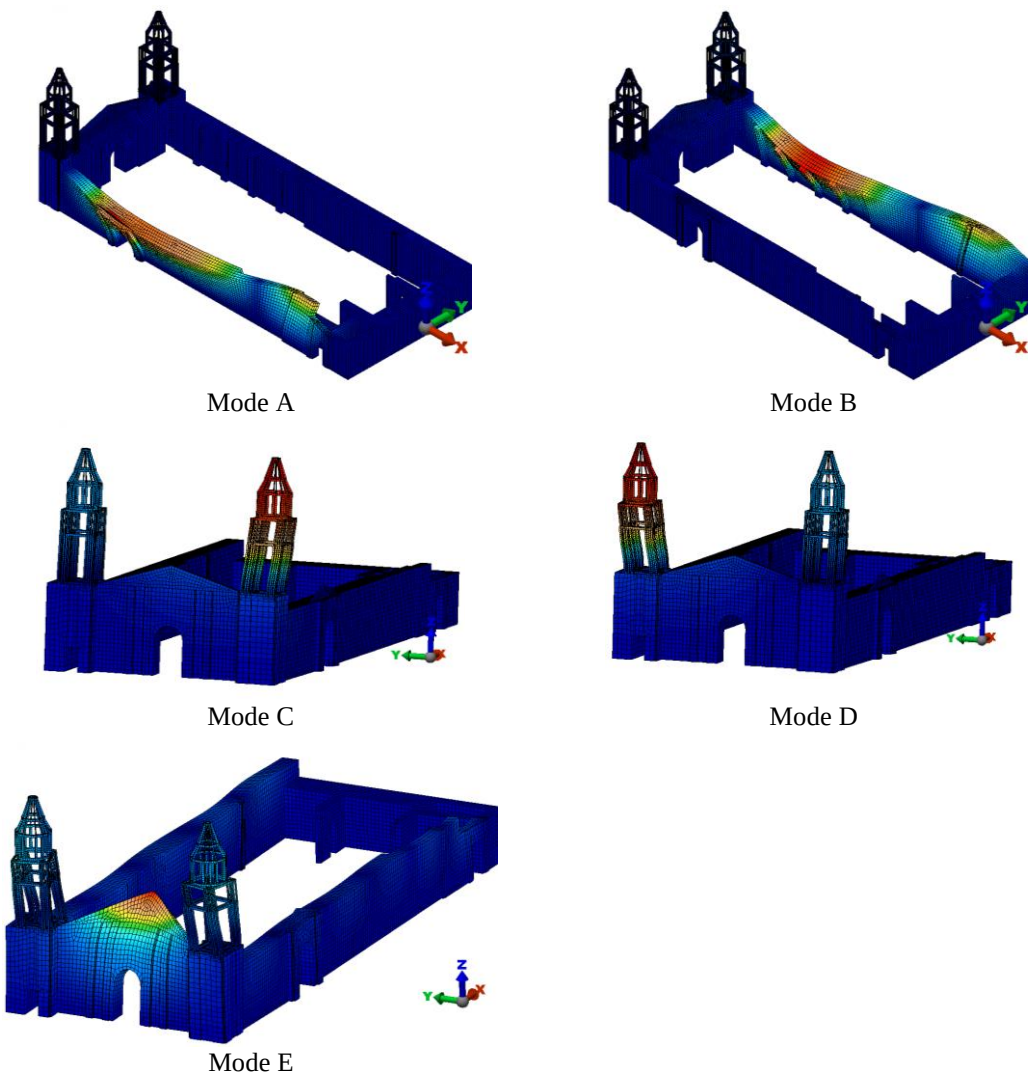

Figure 7.27 Modal shapes and natural frequencies and periods of the global model of the masonry walls and towers

Table 7.15 Periods of the global model of the masonry walls and towers of the Cathedral of Ica

Modes		Period, *T* (s)
A	Transversal vibration of the North wall	0.528
B	Transversal vibration of the South wall	0.419
C	Longitudinal vibration of the North tower	0.355
D	Longitudinal vibration of the South tower	0.350
E	Longitudinal vibration of the façade	0.271

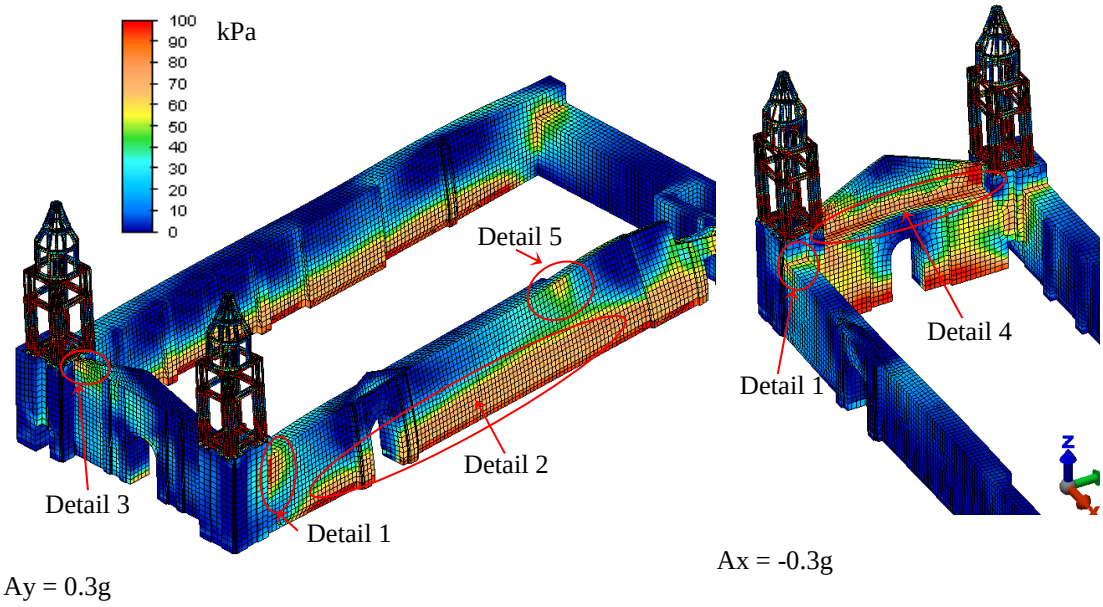

Figure 7.28 Maximum principal stresses (in kPa) distribution in the walls and towers of the Cathedral of Ica after pushover analysis

7.5 Detailed diagnosis of a historic timber structure

The structural response of the timber structure of the Cathedral of Ica is governed by the performance of the carpentry joints; even though deterioration may have triggered the early failure of the mortice and tenon joints at the top of lunettes. Hence, the attributes 'Connections' and 'Deterioration' are more relevant here than in the case of adobe churches in the Andes. Although the geometry and layout of the framing influence to a large extent the behaviour of the structure, these assumptions are related to a qualitative assessment of the

attribute ‘Robustness’. The main contribution of the global analyses and present detailed diagnosis regard the evaluation of the ‘Connections’ attribute, which require refined structural analysis. Moreover, results of the analysis of the timber joints may also contribute to the analysis of the other attributes. For this reason, the detailed diagnosis begins with the assessment of the connections.

7.5.1 Connections

There are four main types of carpentry joints in the timber structure of the Cathedral of Ica:

(i) Nailed joints of the planked arches;
(ii) Mortice and tenon;
(iii) Pegged mortice and tenon; and
(iv) Nailed joints of the diagonal bracing.

7.5.1.1 NAILED JOINTS OF THE PLANKED ARCHES

When the timber vault is subjected to lateral loading, the capacity of the nailed joints is governed by the resistance perpendicular to the grain and the shear strength parallel to the grain of the wood due to the embedding of the nail in those respective directions. The greatest forces are approximately acting in the direction perpendicular to the grain, which is illustrated in a simplified way in Figure 7.29 by the length and direction of the arrows. This takes into account the fact that shear in the Z direction is critical at the top of the arches and shear in the Y direction is critical from the top of lunette to the spring points of the arches. Yielding of the nails in bending can also occur since wrought iron is characterised by a low yielding stress of about 200MPa; and the nails of the Cathedral of Ica have a square tapering cross section of 10mm near the head of the nail, i.e. in the headside member, and about 5mm in the pointside member (Figure 6.25).

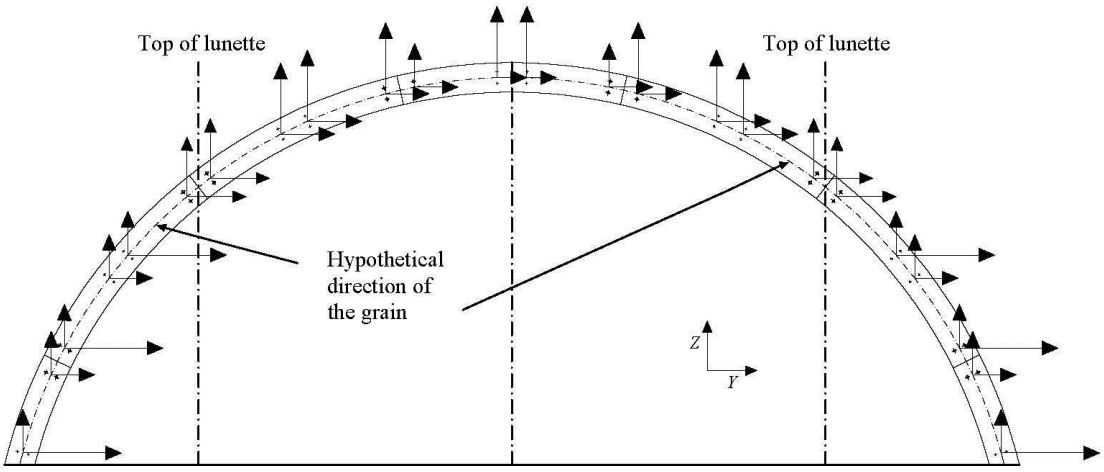

Figure 7.29 Direction of shear forces acting in planked arches laterally loaded in relation to the direction of the grain of wood

The nailed joints of the planked arches are assessed on the basis of the following models:

- Johansen's model (1949) for determining the load-carrying capacity of a nail in single shear, formulated on the basis of plasticity theory;
- van der Put and Leijten model (2000) for determining the splitting capacity of the planks loaded perpendicular to the grain, formulated on the basis of fracture mechanics.

The Johansen's mathematical model was adopted by Eurocode 5 (CEN, 2004b) to derive the design equations of lateral load-carrying nailed joints. According to Eurocode 5 (CEN, 2004b), the load-carrying capacity of a nail in single shear per shear plane, $F_{v,Rk}$, should be taken as the minimum value found from the expressions of equation 7.2. These expressions correspond to the modes of failure illustrated in Figure 7.30.

$$F_{v,Rk} = \min \begin{cases} f_{h,1,k}\, t_1\, d & (a) \\ f_{h,2,k}\, t_2\, d & (b) \\ \dfrac{f_{h,1,k}\, t_1\, d}{1+\beta}\left[\sqrt{\beta + 2\beta^2\left[1+\dfrac{t_2}{t_1}+\left(\dfrac{t_2}{t_1}\right)^2\right]+\beta^3\left(\dfrac{t_2}{t_1}\right)^2}-\beta\left(1+\dfrac{t_2}{t_1}\right)\right]+\dfrac{F_{ax,Rk}}{4} & (c) \\ 1.05\,\dfrac{f_{h,1,k}\, t_1\, d}{2+\beta}\left[\sqrt{2\beta(1+\beta)+\dfrac{4\beta(2+\beta)M_{y,Rk}}{f_{h,1,k}\, d\, t_1^2}}-\beta\right]+\dfrac{F_{ax,Rk}}{4} & (d) \\ 1.05\,\dfrac{f_{h,1,k}\, t_2\, d}{1+2\beta}\left[\sqrt{2\beta^2(1+\beta)+\dfrac{4\beta(1+2\beta)M_{y,Rk}}{f_{h,1,k}\, d\, t_2^2}}-\beta\right]+\dfrac{F_{ax,Rk}}{4} & (e) \\ 1.15\sqrt{\dfrac{2\beta}{1+\beta}}\sqrt{2M_{y,Rk}\, f_{h,1,k}\, d}+\dfrac{F_{ax,Rk}}{4} & (f) \end{cases} \quad [7.2]$$

where:

t_i is the timber or board thickness or penetration depth, with i either 1 or 2, corresponding to the pair of timber members connected;

$f_{h,i,k}$ is the embedment strength in timber member i;

d is the nail diameter;

$M_{y,Rk}$ is the characteristic nail yield moment;

β $\dfrac{f_{h,2,k}}{f_{h,1,k}}$;

$F_{ax,Rk}$ is the axial withdrawal capacity of the nail.

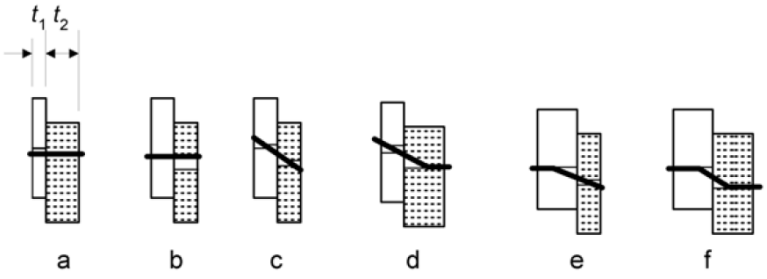

Figure 7.30 Failure modes of nailed joints in single shear according to Eurocode 5 (CEN, 2004b)

Taking into account the provisions of Eurocode 5 (CEN, 2004b) and assuming that the capacity of a nailed joint with two nails is equal to the double of the capacity of a joint with a single nail, the load-carrying capacity, $F_{v,Rk}$, of a representative nailed connection of the arches of the Cathedral of Ica for failure models (a) to (f) are shown in Table 7.16. These

results consider a nail's diameter of 10mm in the headside member and a nail's diameter of 5mm in the pointside member. Mode D is the most critical failure mode and it entails the yielding of the nail in the pointside member and the crushing of the fibres due to the bearing of the nails in the hole's wall. It does not correspond however to the failure of the joint, as the joint has some capacity to redistribute the loads. It is followed by Mode C, which corresponds to the crushing of the fibres in both the alignments of planks without yielding of the nails.

Table 7.16 Load-carrying capacity of the nailed connections of the bay-edge arches

Model		Capacity (kN)
Johansen's model (1949), $F_{v,Rk}$	Mode a	14.9
	Mode b	9.2
	Mode c	7.7
	Mode d	4.3
	Mode e	8.2
	Mode f	8.1
van der Put and Leijten model (2000), $F_{90,Rk}$		20.0

Eurocode 5 (CEN, 2004b) adopted the van der Put and Leijten model (2000) based on fracture mechanics for determining the splitting capacity of timber members made of softwoods loaded perpendicular to the grain. Although this equation was formulated for a connection at the middle of a beam and not for a connection near the end of a plank, it is applied here for comparison with the capacity provided by the Johansen's model, which was formulated on the basis of plasticity theory. Taking into account that the process of driving the nails into the timber causes the crushing of the timber around the hole and it can also create small cracks, the failure of the timber planks is more a problem of fracture mechanics than a problem of plasticity theory. Hence, considering equation 7.3 of Eurocode 5,

$$F_{90,Rk} = 14\, bw \sqrt{\frac{h_e}{\left(1 - \frac{h_e}{h}\right)}} \qquad [7.3]$$

where:

b is the member thickness;

w is a modification factor equal to 1 in the case of nails;

h_e is the loaded edge distance to the centre of the most distant nail;

h is the timber member height.

the splitting capacity, $F_{90,Rk}$, of a representative nailed connection of the arches of the cathedral of Ica is equal to 20kN, as shown in Table 7.16.

The ratio of maximum shear forces, V, to the capacities $F_{v,Rk}$ and $F_{90,Rk}$ of the most critical bay-edge arches and internal arches are shown in Table 7.17. It can be seen that the embedment capacities of modes (a) to (f) are reached at several locations of the critical arches both in Model 1 and Model 2. As far as mode (d) is concerned, these results show that the most critical nailed joints of the internal arches are also likely to fail if the mortice and tenon joints at the top of lunette do not fail. It seems therefore that the application of the Johansen's model to this type of structure underestimates the real capacity of the joints.

On the other hand, the splitting capacity, $F_{90,Rk}$, is reached only at the most critical joints of the critical bay-edge arches, especially in the arch at the Eastern end of bay 2 in Model 2, which are joints that failed due to the 2007 Pisco earthquake (Figure 4.43a). This can be seen in Figure 7.26. The failure of the most critical nailed joints of the bay-edge arches of bay 4 could not be checked on-site; however the severity of any hypothetical failure was not sufficient to cause the collapse of the arch.

This seems to agree with the results of the van der Put and Leijten model if it is assumed that the maximum shear forces acting in the arches of bay 4 in Model 1 were never reached, as the arch might have had a state similar to the one shown in Model 2 before the building was subjected to the most severe ground motion.

Table 7.17 Ratio demand/capacity of the most critical nailed connections of the arches of the Cathedral of Ica

Model	Location of the nailed joints	$V/F_{v,Rk}$						$V/F_{90,Rk}$
		Mode a	*Mode b*	*Mode c*	*Mode d*	*Mode e*	*Mode f*	
1	East bay-edge arch of bay 4	1.70	2.75	3.29	5.88	3.09	3.12	1.27
	East bay-edge arch of bay 2	0.78	1.26	1.51	2.70	1.42	1.43	0.58
	Internal arches	0.34	0.55	0.66	1.19	0.62	0.63	0.26
2	East bay-edge arch of bay 4	1.30	2.10	2.51	4.49	2.35	2.38	0.97
	East bay-edge arch of bay 2	1.77	2.86	3.42	6.12	3.21	3.25	1.32
	Internal arches	0.35	0.57	0.68	1.22	0.64	0.65	0.26

Since these numerical and analytical results do not contradict the observations made during the field work, it is reasonable to conclude that the reference analysis conditions assumed in the global analyses are acceptable. Nevertheless, it is important to check the results when the uncertainty of the input, m_u, calculated in Chapter 6, is taken into account. Since all SPIs used in the calculation of m_u are considered equally relevant, m_u is equal to 0.24. The results of demand vs capacity considering this uncertainty m_u and taking into account the most critical mode of the Johansen's model and the van der Put and Leijten model are shown in Table 7.18.

The lower bounds of the demand/capacity ratio, corresponding to the lower bounds of the maximum shear force, *V*, acting in the bay-edge arches, do not contradict the damage observed in the cathedral after the earthquake. In the case of the van der Put and Leijten model, the conclusions made for the reference results of Table 7.17 still hold valid when the lower bounds of Table 7.18 are taken into account. These lower bounds yield results that agree better with *in-situ* observations than the reference results in the case of the Johansen's model since no failure of the nailed joints of the internal arches is predicted.

Table 7.18 Ratio demand/capacity of the most critical nailed connections of the arches of the Cathedral of Ica taking into account the knowledge-based uncertainty

Model	Location of the nailed joints	$V/F_{v,Rk}$ [Mode D]		$V/F_{90,Rk}$	
		$\frac{I_j}{1+m_u}$	$I_j \times (1+m_u)$	$\frac{I_j}{1+m_u}$	$I_j \times (1+m_u)$
1	East bay-edge arch of bay 4	4.74	7.29	1.02	1.57
	East bay-edge arch of bay 2	2.18	3.35	0.47	0.72
	Internal arches	0.96	1.48	0.21	0.32
2	East bay-edge arch of bay 4	3.62	5.57	0.78	1.20
	East bay-edge arch of bay 2	4.94	7.59	1.06	1.63
	Internal arches	0.98	1.51	0.21	0.33

7.5.1.2 MORTICE AND TENON JOINTS

Mortice and tenon joints are connecting timber members at the following two main locations:

(i) Top of lunettes: where the internal arches and lunettes' members are connected to longitudinal beams; and

(ii) Top of frame: where the vault and the pillars are connected to longitudinal beams.

At the top of lunettes, splitting of the beams caused the collapse of the internal arches, as shown in Figure 7.31. According to *in-situ* observations, crushing of the tenons did not occur, so this mode of failure is not investigated here.

Figure 7.31 Splitting of the beam at the top of lunettes

The splitting capacity of the morticed beams loaded perpendicular to the grain can be estimated through the fracture mechanics model of van der Put and Leijten (2000) for joints loaded perpendicular to the grain, as illustrated in Figure 7.32.

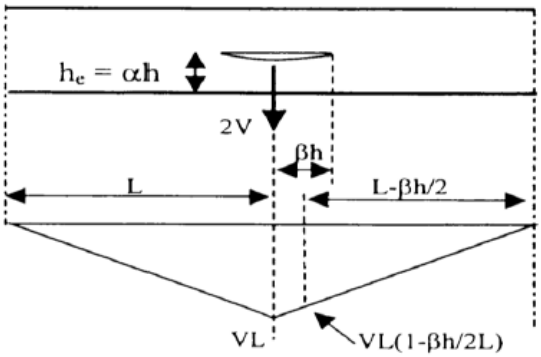

Figure 7.32 Beam with crack caused by the shear force of a joint and respective bending moment (van der Put, 2011)

This model is used in Eurocode 5 (CEN, 2004b) for design of members made of softwood. The splitting capacity or maximum shear force at fracture is given by equation 7.3, where *h* is the beam's cross section depth, *b* its width and h_e is the loaded edge distance.

A representative top of lunette beam is shown in Figure 7.33. The mortices at mid-span are typically larger than the mortices shown in this figure, since the tenons of the diagonals, central rib and internal arches are connected to the same mortice. The average splitting capacity $F_{90,Rk}$ of a representative top of lunette beam taking into account an average mortice size is indicated in Table 7.19.

.

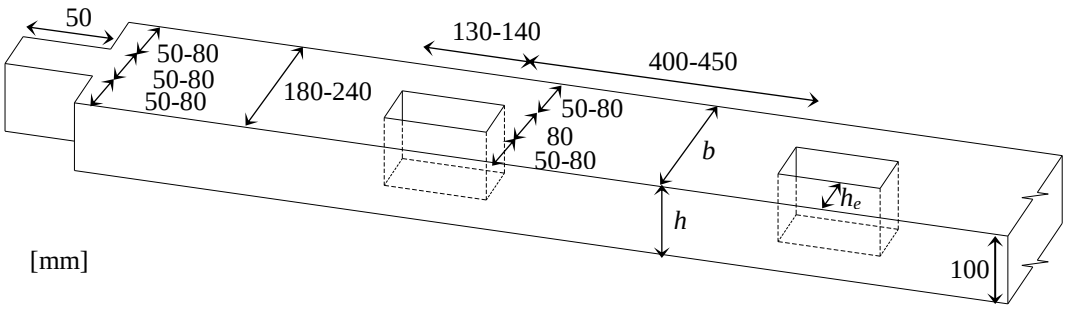

Figure 7.33 Representative geometry of the beam at the top of lunettes

Table 7.19 Splitting capacity of the morticed beam at the top of lunette

Morticed member	Splitting capacity, $F_{90,Rk}$ (kN)
Beam at the top of lunette	10

Modal superposition analyses conducted with Model 1 (Figure 7.22) and the North-South and East-West spectra of the 2007 Pisco earthquake indicate that the maximum shear force acting on the beams at the top of lunettes are produced in bays 3, 4 and 5, being in these bays greater than 10kN, which is the capacity of the beam. These results show that the beams of these bays are expected to split for the level of shear forces produced by the 2007 Pisco earthquake; even if the wood is in good condition. The maximum values of shear are produced at mid-span of the beams, showing that failure is expected to start at the mortice located at mid-span. This is also shown by observations made on site (Figure 7.31).

The shear force at the top of lunette was considered as SPI 2 in Chapter 6. In the present chapter, the same nomenclature is used. The shear force at the top of lunette is therefore assumed as I_2, being the reference, maximum and minimum values equal to $I_{2,ref}$, $I_{2,mx}$, $I_{2,mn}$, respectively. The interval of plausibility is calculated on the basis of an uncertainty m_u equal to 0.24. The maximum shear force produced at mid-span of the lunette's beams of bays 4 and 2 and the respective demand to splitting capacity ratio, are shown in Table 7.20 for the case of Model 1. As concluded before, these results show that the mortice and tenon joints at the top of Bay 4 are subjected to greater demands than in Bay 2, and therefore they are likely to fail first, leading to the collapse of the internal arches. However, since the top of lunette's beams are deteriorated, the capacity $F_{90,Rk}$ indicated in Table 7.19 is likely to be an overestimation of the capacity of the beam. This would explain the reason why the mortice and tenon connections at the lunette's beams in Bay 1 and Bay 2 also failed.

Table 7.20 Maximum shear demand/capacity ratio produced by the internal arches at the mortice and tenon joints of the vault due to the 2007 Pisco earthquake

Model	Bays	Reference value of shear force, $I_{2,ref}$ (kN)	$I_{2,mn}/ F_{90,Rk}$	$I_{2,ref}/ F_{90,Rk}$	$I_{2,mx}/ F_{90,Rk}$
1	Bay 4	18.1	1.46	1.81	2.24
	Bay 2	7.2	0.58	0.72	0.90

The ratio demand/capacity in Bay 4 is greater in Table 7.20 than in Table 7.18 when the capacity $F_{90,Rk}$ of the van der Put and Leijten model is taken into account. This means that the mortice and tenon joints are likely to fail before the failure of the nailed joints of the bay-edge arches. This further explains why the internal arches collapsed in bays 4 and 3 leading to a state similar to the one reproduced in Model 2 (Figure 7.24).

Regarding the mortice and tenon joints connecting the vault to the supporting frame, made of pillars and beams, a similar analysis can be conducted. These joints are likely to fail by splitting of the beams running in the longitudinal and transversal directions due to shear forces acting perpendicular to the grain. Other failure modes associated to the failure of the tenons are not as critical as the splitting of the beam, since the edge distances of the mortices are small and the largest shear forces are acting in the direction perpendicular to the grain of the beams. The van der Put and Leijten model is also used here to calculate the splitting capacity of the beams, according to equation 7.3. The bay-edge arches, lunettes' diagonals and lunettes' arches are connected to the longitudinal beams of the nave. The reference, minimum and maximum shear force produced by these elements at the top of the frame are indicated in Table 7.21 assuming an uncertainty m_u equal to 0.24. The values for the lunettes' diagonals and lunettes' arches are not shown for Model 2 because the collapse of the top of the vault reduced these forces to almost null values.

Table 7.21 Splitting capacity and demand at the mortice and tenon joints connecting the vault to the frame during the 2007 Pisco earthquake

Model	Critical bay	Element connected to the longitudinal beam	$F_{90,Rk}$ (kN)	$I_{2,mn}/ F_{90,Rk}$	$I_{2,ref}/ F_{90,Rk}$	$I_{2,mx}/ F_{90,Rk}$
1	Bay 4	Bay-edge pillars	24	2.05	2.54	3.15
		Lunettes' diagonals	24	2.02	2.50	3.10
		Lunettes' arches	24	4.20	5.21	6.46
2	Bay 2	Bay-edge arches	24	0.39	0.48	0.60

In Model 1, the most critical shear demands are produced in bay 4 leading to the splitting of the frame beam. However, as discussed before, the structure might have not been subjected to such high demands due to the failure of the joints at the top of lunette and subsequent collapse of the internal arches. This new state reproduced by Model 2 produces the highest demands in Bay 2 with values that are lower than the splitting capacity of the longitudinal beam. However, as shown in Figure 7.34, the mortice and tenon connection of the arch at the Eastern end to the beam failed due to extreme deterioration of the beam. Thus, it is reasonable to conclude that the poor performance of these mortice and tenon connections also contributed to the collapse of the arches of bay 2.

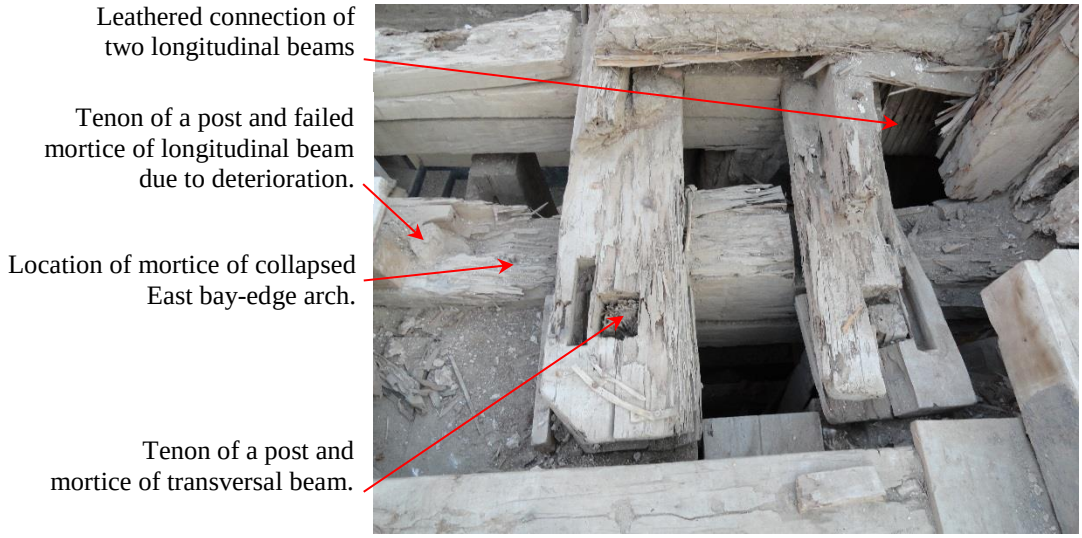

Figure 7.34 Representative connection of the central pillars of the nave to longitudinal and transversal beams in Bay 2 (courtesy of Erika Vicente, PUCP)

Mortice and tenon joints are also connecting the pillars to transversal and longitudinal beams of the frame, as shown in Figure 7.34. The capacity of these connections $F_{90,Rk}$ can also be calculated using the van der Put and Leijten model, as in the previous case. This capacity depends on the cross-section of the beams and location of the mortices. The reference cross-section of the beams is indicated in Figure 7.35, and the splitting capacity of the joints is shown in Table 7.22 for the various cases of Figure 7.36. It is assumed that the mortices are in the centre of the beams.

Cases 1 to 4 correspond to mortice and tenon joints that are connecting the central pillars to the frame beams. The connection of the *guarango* trunk to the longitudinal beam is similar

to Case 2; and it is therefore called Case 2.1. In cases 1, 2, 3, 9, 10 and 11 the tenons go all the way through the beam made of two elements connected to each other by leather (see Figure 7.34). In cases 6, 7, 8 and 12, the tenons go through notched joints that allow the intersections of the beams to lie all in the same horizontal plan. Finally, in cases 4 and 5, only one piece of timber has the mortice, as shown in Figure 7.36.

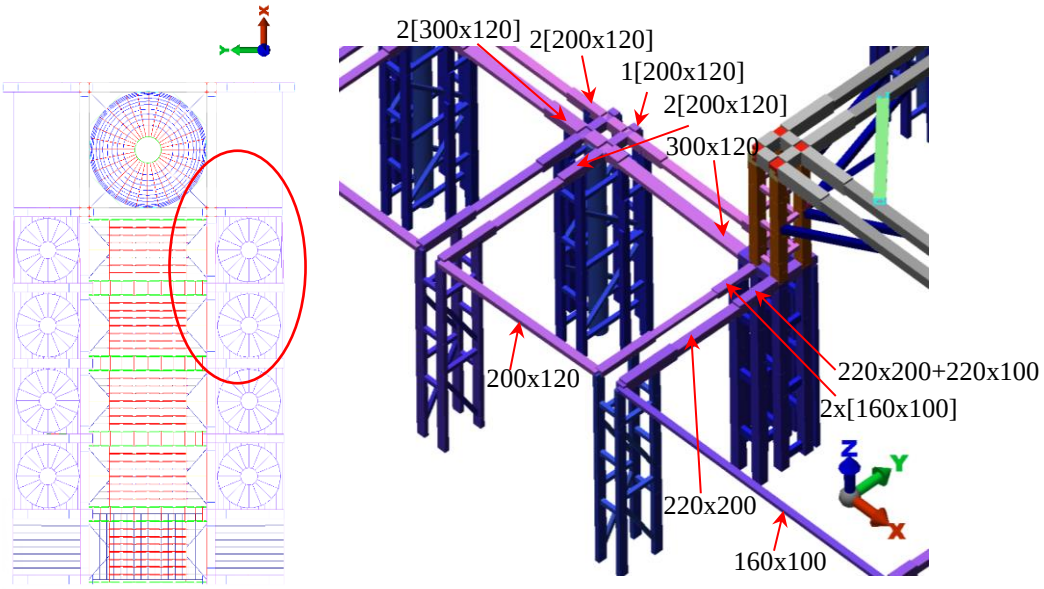

Figure 7.35 Reference cross-section of the longitudinal and transversal beams (in mm). For instance, 2[200x120] means that there are two beams placed on the top of each other, of 200x120 cross-section each, which are typically connected by leather straps

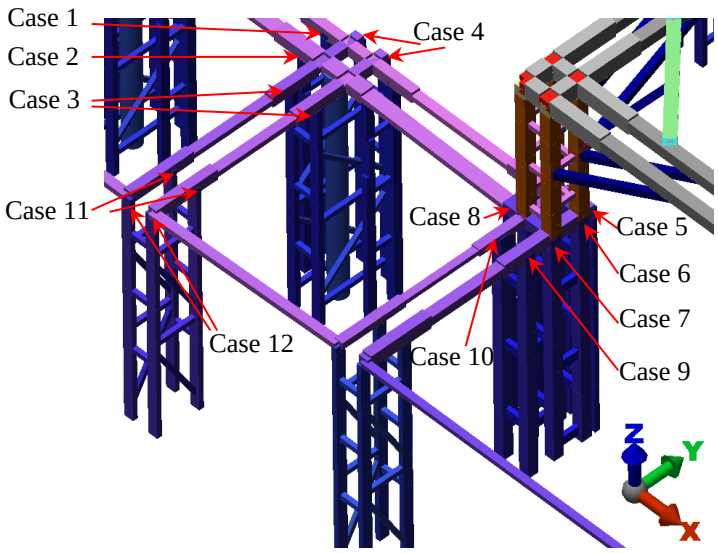

Figure 7.36 Different cases of mortice and tenon joints at the top of the frame corresponding to different splitting capacity of the beams

Table 7.22 Splitting capacity and demand at the location of the mortice and tenon connections of the pillars with the beams for an earthquake similar to the 2007 Pisco earthquake

	Case	$F_{90,Rk}$ (kN)	$I_{2,mn}/ F_{90,Rk}$	$I_{2,ref}/ F_{90,Rk}$	$I_{2,mx}/ F_{90,Rk}$
Central pillars of the nave	1	24	0.06	0.07	0.09
	2	23	0.06	0.07	0.09
	2.1	24	0.51	0.63	0.78
	3	24	0.22	0.28	0.34
	4	11	0.48	0.60	0.74
Central pillars of the central dome's bay	5	10	0.30	0.37	0.46
	6	25	0.52	0.64	0.79
	7	30	0.43	0.53	0.66
	8	30	0.10	0.12	0.15
	9	30	0.43	0.53	0.66
	10	16	0.16	0.20	0.25
Lateral pillars	11	24	0.37	0.46	0.57
	12	24	0.37	0.46	0.57

The results of Table 7.22 indicate that the mortice and tenon connections at the top of the frame are not likely to fail when subjected to the 2007 Pisco earthquake. These results confirm the observations made on site after the earthquake. However, local failures of the beam may have occurred due to extreme levels of deterioration of the beams at the location of the joints (see for instance Figure 7.34).

7.5.1.3 PEGGED MORTICE AND TENON JOINTS

The posts forming the central pillars are linked by horizontal bracings; being the connection formed by pegged mortice and tenon joints. A representative layout of such joints is shown in Figure 7.37. This representative joint was tested by PUCP (Torrealva and Vicente, 2014) in order to measure its stiffness and ultimate capacity. The forces acting on the joint are shown in Figure 7.38 by means of a sketch developed by Yeomans (2003).

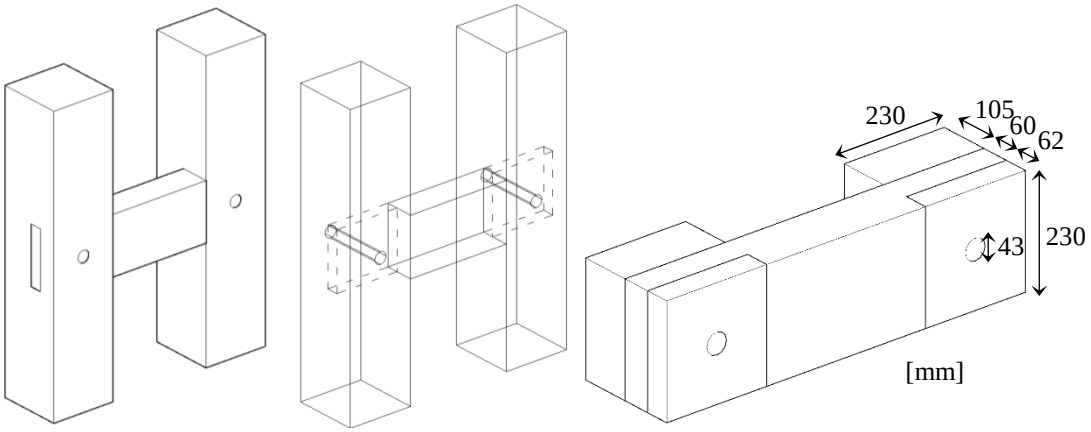

Figure 7.37 Representative pegged mortice and tenon joint of the Cathedral of Ica

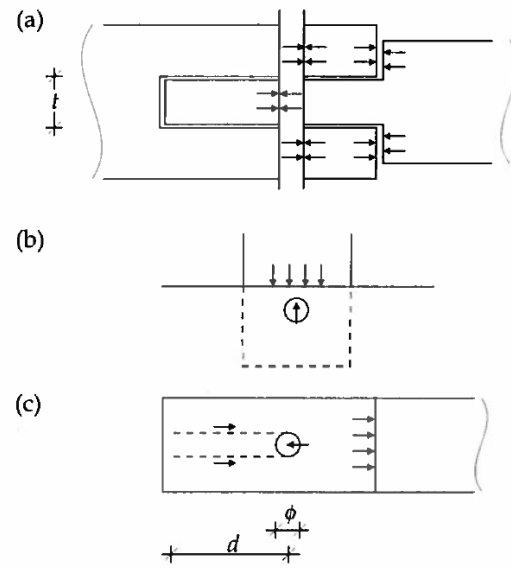

Figure 7.38 Forces in a pegged mortice and tenon joint (after Yeomans, 2003): a) pressure of the peg on the tenon and mortice; b) pressure of the peg on the timber located between the mortice's hole and the mortice's shoulder; and c) shear forces on the tenon

To assess these joints, two alternative procedures are here applied:

(i) Analytical response of a typical pegged mortice and tenon joint; and

(ii) Comparison of numerical results with tests conducted at PUCP.

Basic modes of failure of pegged mortice and tenon joints are summarized in the flowchart of Figure 7.39 and illustrated in Figure 7.40. A more comprehensive description of failure modes of timber pegged connections can be found in Shanks *et al.* (2008). Splitting of the morticed member by tension perpendicular to grain occurs due to insufficient edge distance on the morticed member, when the joint is no longer tight due to shrinkage or deterioration of the timber or due to past loading history. On-site observations of pegged mortice and tenon joints in the cathedral show that it is reasonable to assume that the joints are no longer tight. According to Yeomans (2003), the length from the tenon's hole to the end of the timber needs to be equal to or greater than the diameter of the peg for crushing of the peg to occur before shear failure of the tenon. It can be seen from Figure 7.37 that this length is 60% greater than the diameter of the peg. Thus, failure of the peg is expected to occur before shear failure of the tenon in the joints of the cathedral.

The capacity of the joint associated to various failure modes is:

- Splitting of the morticed member:

  Equation 7.3 (van der Put model, 2011)

- Crushing of the peg:

$$F_{cp} = f_1 t_1 \phi \qquad [7.4]$$

- Shear failure of the peg:

$$F_{sp} = 2 f_2 \frac{\pi \phi^2}{4} 0.75 \qquad [7.5]$$

- Shear failure of the tenon:

$$F_{st} = 2 f_2 l_1 t_1 \qquad [7.6]$$

, where t_1 is the thickness of the tenon, ϕ is the diameter of the peg, l_1 is the end distance of the tenon, f_1 is the compression strength perpendicular to the grain of guarango and f_2 is the shear strength of guarango.

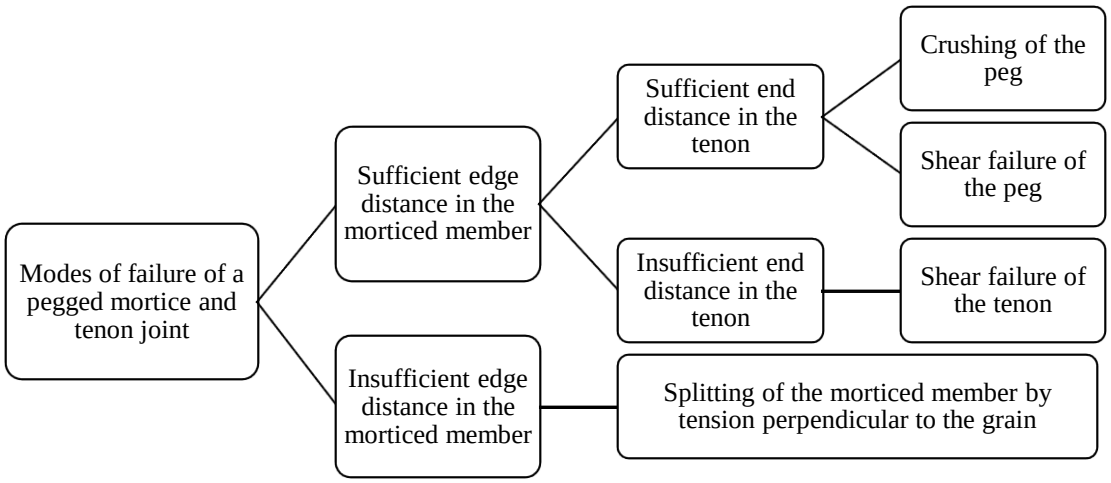

Figure 7.39 Typical modes of failure of pegged mortice and tenon joints

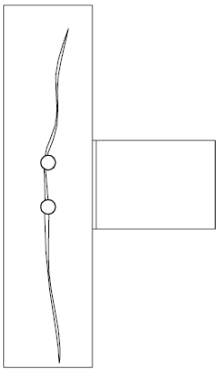

Splitting of the morticed member

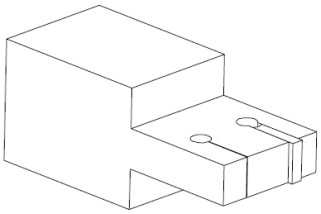

Shear failure of the tenon

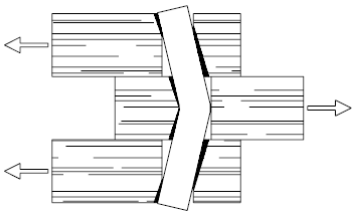

Crushing of the peg

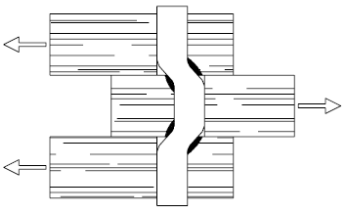

Shear failure of the peg

Figure 7.40 Illustration of the modes of failure of typical pegged mortice and tenon joints (after Miller and Schmidt, 2004)

According to the geometry of the joint and the mechanical properties of *guarango*, the maximum axial load for each failure mode is shown in Table 7.23. Splitting of the morticed posts is the most critical failure mode.

Table 7.23 Analytical capacity of a representative pegged mortice and tenon joint

Failure mode	Maximum axial force (kN)
Splitting of the morticed member, $F_{90,Rk}$	8
Crushing of the peg, F_{cp}	58
Shear failure of the peg, F_{sp}	45
Shear failure of the tenon, F_{st}	250

The maximum axial loads in the springs simulating the pegged mortice and tenon joints in Model 1 during the 2007 Pisco earthquake are shown in Table 7.24. These values correspond to the most unfavourable direction of motion. The ratio of these forces to the capacity of the critical failure mode is also shown in Table 7.24. The interval of plausibility of the maximum axial force is calculated taking into account an uncertainty m_u equal to 0.24.

Table 7.24 Maximum axial force in the pegged mortice and tenon joints of the Cathedral of Ica after modal superposition analysis performed with spectra of the 2007 Pisco Earthquake

Location of the joint	Maximum axial force, $F_{a,ref}$ (kN)	$1/2I_{Fa,mn}/F_{90,Rk}$	$1/2I_{Fa,ref}/F_{90,Rk}$	$1/2I_{Fa,mx}/F_{90,Rk}$
Connection of the horizontal bracing of the crossing pillars to the pillars' posts.	0.7	0.04	0.04	0.05
Connection of the horizontal bracing of the pillars that support the principal dome to the pillars' posts.	8.9	0.45	0.56	0.69
Connection of the horizontal bracing of the lateral pillars of the crossing's bay to the pillars' posts.	28	1.41	1.75	2.17
Connection of the horizontal bracing of the central pillars of the nave to the pillars' posts.	3.4	0.17	0.21	0.26
Connection of the horizontal bracing of the lateral pillars of the nave to the pillars' posts.	11	0.55	0.69	0.85

The numerical results show that the bracing of the lateral pillars of the crossing bay are subjected to the highest demands. These values of load are produced when the 2007 Pisco earthquake spectrum is applied in the transversal direction of the model. It could not be observed on site the condition of these connections. Nevertheless, this bay underwent significant transversal permanent deformations, which might have been also caused by failure of some components of the bracing. The horizontal bracing of other pillars of the cathedral are subjected to demands that are much lower than the capacity of the joint. Observations made on site confirm these results, since no significant deformations were observed in these joints.

The tests performed at PUCP considered that the pegged mortice and tenon joint is not tight, i.e. there is a gap between the shoulder of the morticed member and the shoulder of the tenon. Any of the modes of failure shown in Figure 7.39 can therefore occur. In the experimental work, the joint failed by shear failure of the pegs. This might be explained by the fact that the force was applied in a way that the forces were perpendicular to the grain in the member with the tenon and parallel to the grain in the morticed members. The experimental force-displacement curves are shown in Figure 7.41, where the maximum force acting in the pegged mortice and tenon joints of the cathedral during the 2007 Pisco earthquake is also shown. These results are in line with the analytical results, showing that under the conditions of the test, the joint would perform in the elastic range.

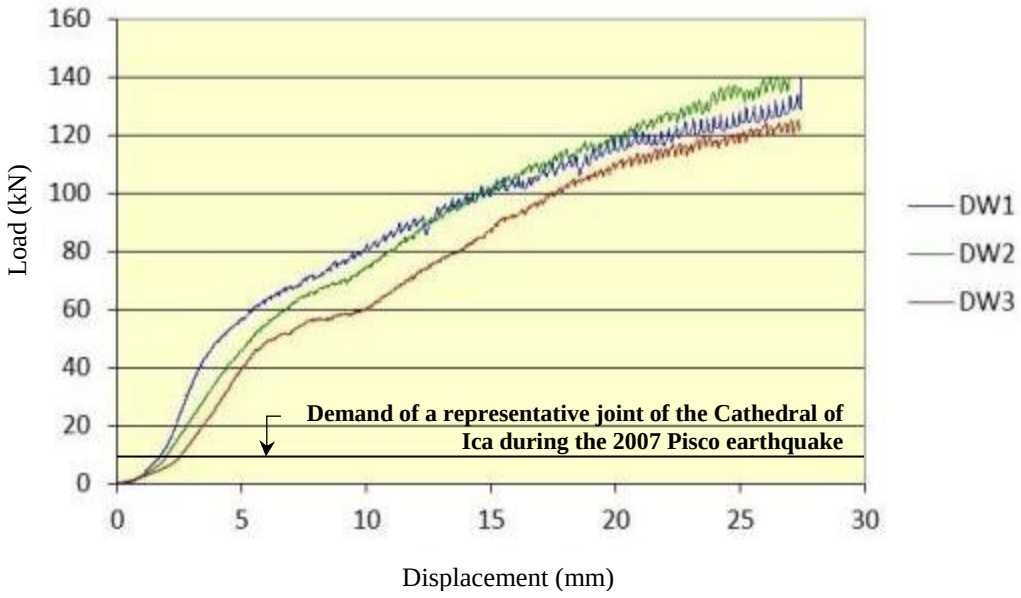

Figure 7.41 Force-displacement curves of three pull-out test conducted at PUCP on pegged mortice and tenon joints (Torrealva and Vicente, 2014)

7.5.1.4 NAILED JOINTS

Nailed joints are connecting the diagonal bracing of the pillars to the posts. A representative layout and geometry of the nailed joints of the Cathedral of Ica is shown in Figure 7.42. This representative joint was also tested at PUCP (Torrealva and Vicente, 2014).

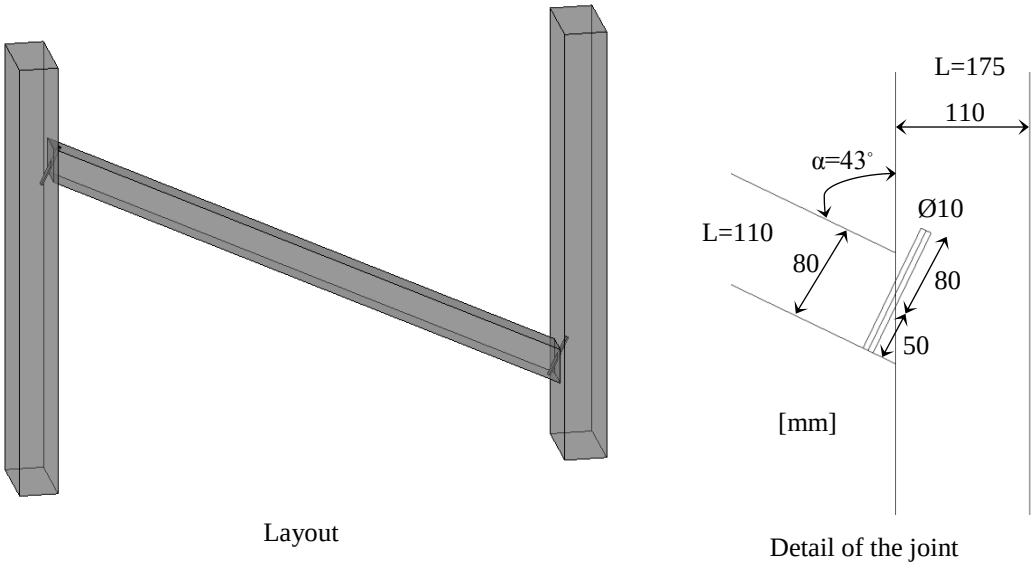

Figure 7.42 Representative nailed joint of the diagonal bracing of the Cathedral of Ica

According to Eurocode 5 (CEN, 2004b), the pointside penetration length of smooth nails should be at least 8*d*, where *d* is the nail diameter (CEN, 2008). Considering that the connection tested by PUCP and shown in Figure 7.42 corresponds to a close representation of the nailed connections of the cathedral, the penetration length is at least 80mm, which is the lowest limit given by Eurocode 5 for a nail of 10mm diameter.

Three modes of failure might occur:

(i) Splitting of the posts caused by the tension force component perpendicular to the grain;

(ii) Withdrawal of the nails; and

(iii) Yield of the nails in bending.

The forces acting in the connection for a negative moment M_x are shown in Figure 7.43.

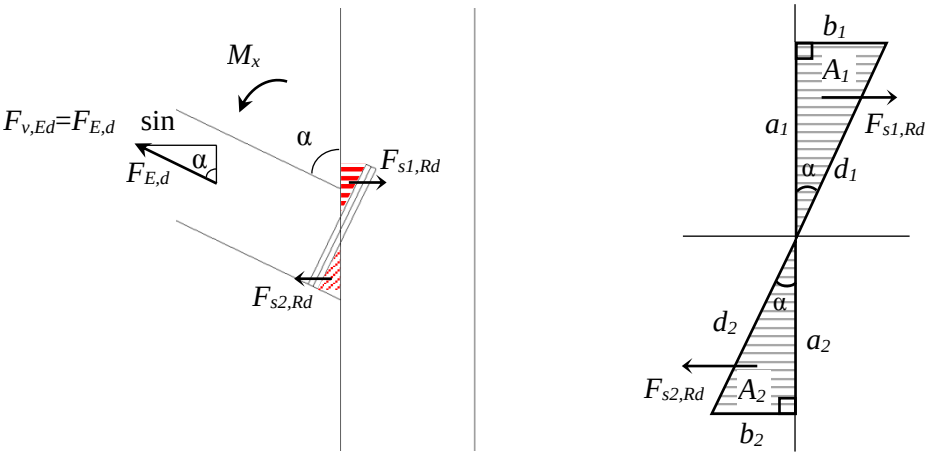

Figure 7.43 Forces in the nailed joints of the Cathedral of Ica for a negative moment M_x

According to Eurocode 5 (CEN, 2004b), in order to take into account of the possibility of splitting in either the post or the diagonal, the following should be satisfied:

$$\frac{F_{v,Ed}}{F_{s1,Rd}} \leq 1 \quad \text{or} \quad \frac{F_{v,Ed}}{F_{s2,Rd}} \leq 1 \qquad [7.7]$$

, where $F_{s,Rd}$ is the splitting capacity and $F_{v,Ed}$ is the horizontal component of the axial force acting in the diagonals. $F_{s,Rd}$ corresponds to the smallest value of $F_{s1,Rd}$ or $F_{s2,Rd}$, which are given by the following expressions:

$$F_{s1,Rd} = f_{s,ca} \times A_1 \qquad [7.8]$$

$$F_{s2,Rd} = f_{s,g} \times A_2 \qquad [7.9]$$

, where $f_{s,ca}$ and $f_{s,g}$ are the shear strength of *caoba Africana* and *guarango*, respectively, and A_1 and A_2 are indicated in Figure 7.43. Taking into account the representative joint of Figure 7.42, and considering $f_{s,ca}$ equal to 7MPa and $f_{s,g}$ equal to 20MPa:

$F_{s1,Rd}$ = 11.2kN

$F_{s2,Rd}$ = 12.5kN

It should also be noted that the diameter of the nails is not constant along the length. It is greater near the head and progressively decreases along the pointside of the nail. This means that the shear stresses near the head are distributed along a surface rather than concentrated in a line, which increases the capacity $F_{s2,Rd}$.

The maximum axial force, F_{Ed}, on the diagonals of the cathedral after modal superposition analysis is performed with the response spectra of the 2007 Pisco earthquake is shown in Table 7.25. The shear force is equal to F_{Ed} sin α, where α is the angle of the diagonal with the post and it is equal to 43 degrees, as shown in Figure 7.42 and Figure 7.43. The ratio $F_{v,Ed}/F_{s1,Rd}$ of the most vulnerable nailed connections of the cathedral is shown in Table 7.25. This table also shows the ratio taking into account the interval of plausibility of the shear force, composed of the minimum, reference and maximum values ($IF_{v,Edmn}$, $IF_{v,Edref}$, $IF_{v,Edmx}$, respectively) considering an uncertainty m_u equal to 0.24.

Table 7.25 Maximum axial force acting on the diagonals of the Cathedral of Ica and ratio demand/splitting capacity

Location of the joint	F_{Ed} sinα ($I_{v,Edref}$) (kN)	$IF_{v,Edmn}$ / $F_{s1,Rd}$	$IF_{v,Edref}$ / $F_{s1,Rd}$	$IF_{v,Edmx}$ / $F_{s1,Rd}$
Connection of the diagonal bracing of the lateral pillars of the nave to the posts.	5.5	0.40	0.49	0.61
Connection of the diagonal bracing of the central pillars of the nave to the posts.	5.4	0.39	0.48	0.60
Connection of the diagonal bracing of the lateral pillars of the transept to the posts.	8.0	0.58	0.71	0.89

According to these results, the nailed connections of the lateral pillars of the central dome's bay are not likely to fail. However, it should be emphasised that the splitting capacity of the connection depends on the areas A_1 and A_2 (Figure 7.43), so a good construction quality is essential. Moreover, these analyses consider the shear strength of timber in good condition. Although the capacity of the connection is substantially affected by decay of the timber, on-site observations showed that the diagonals and posts of the pillars are in overall fair condition.

The nails of the Cathedral of Ica do not have a constant square cross-section along their entire length and therefore they are not smooth nails, as per the definition of CEN (2008). According to Eurocode 5 (CEN, 2004b), the characteristic withdrawal capacity of nails other

than smooth nails, $F_{ax,Rk}$, for nailing perpendicular to the grain should be taken as the smaller of the following values:

$$F_{ax,Rk} = \left\{ \begin{matrix} f_{ax,k} \; d \; t_{pen} \\ f_{head,k} \; d_h^2 \end{matrix} \right\} \quad [7.10]$$

Where $f_{ax,k}$ is the pointside withdrawal strength, $f_{head,k}$ is the headside pull-through strength, d is the length of a side of the nail , t_{pen} is the pointside penetration length and d_h is the nail head diameter. CEN (2004b) recommends the following expressions for smooth nails:

$$\begin{aligned} f_{ax,k} &= 20 \times 10^{-6} \rho_k^2 \\ f_{head,k} &= 70 \times 10^{-6} \rho_k^2 \end{aligned} \quad [7.11]$$

, where ρ_k is the characteristic timber density in kg/m^3.

If it is assumed that the nails in the cathedral have a constant square cross section with a side of 5mm and nailing is perpendicular to the grain, the pointside withdrawal strength and the headside pull-through strength are:

$f_{ax,k}$ = 3.4MPa
$f_{head,k}$ = 58.0MPa

The withdrawal capacity of the connection is therefore equal to:

$F_{ax,Rk}$ = 2.2kN

The ratio $F_{v,Ed}/F_{ax,Rk}$ of the most vulnerable nailed connections of the cathedral is shown in Table 7.26. This table also shows the ratio taking into account the interval of plausibility of the shear force, composed of the minimum, reference and maximum values ($IF_{v,Edmn}$, $IF_{v,Edref}$, $IF_{v,Edmx}$, respectively) considering an uncertainty m_u equal to 0.24.

Table 7.26 Maximum axial force on the diagonals of the Cathedral of Ica and ratio demand/withdrawal capacity

Location of the joint	F_{Ed} sinα ($I_{v,Edref}$) (kN)	$I_{v,Edmn}$ / $F_{ax,Rk}$	$I_{v,Edref}$ / $F_{ax,Rk}$	$I_{v,Edmx}$ / $F_{ax,Rk}$
Connection of the diagonal bracing of the lateral pillars of the nave to the posts.	5.5	2.02	2.50	3.10
Connection of the diagonal bracing of the central pillars of the nave to the posts.	5.4	1.98	2.45	3.04
Connection of the diagonal bracing of the lateral pillars of the transept to the posts.	8.0	2.93	3.64	4.51

According to these results, the connections of the cathedral might fail by withdrawal of the nails, since the forces that push the nails out, indicated in Table 7.26, are greater than the withdrawal capacity. Headside pull-through is unlikely to occur, since the parameter $f_{head,k}\, d_h^2$ is equal to 13kN, which is greater than those pushing out forces.

As far as the yield of the nails in bending is concerned, if it is assumed that the yield stress, σ_y, of wrought iron is 200MPa, the yield moment of a square nail is:

$$M_y = \frac{\sigma_y \times I}{y} \qquad [7.12]$$

with $I = \frac{d^4}{12}, \qquad y = \frac{d}{2}$

, where I is the moment of inertia of the section and y is the distance from neutral axis to outer surface where maximum stress occurs. The yield moment is equal to 4.2N.m for a square nail of a side of 5mm. The maximum moment in the structure and respective ratio demand/yield moment for the various nailed connections of the cathedral's diagonals are shown in Table 7.27. These results show that the nailed joints of the diagonals of the cathedral are likely to yield. This table also shows the ratio taking into account the interval of plausibility of the moment, composed of the minimum, reference and maximum values ($M_{x,mn}$, $M_{x,ref}$, $M_{x,mx}$, respectively) considering an uncertainty m_u equal to 0.24.

Table 7.27 Maximum moment at the nailed connections of the diagonals of the Cathedral of Ica and ratio demand/yield moment

Location of the joint	Maximum moment, M_x (N.m)	$M_{x,mn}$ / M_y	$M_{x,ref}$ / M_y	$M_{x,mx}$ / M_y
Lateral pillars of the nave	4.6	0.88	1.10	1.36
Central pillars of the nave	5.9	1.13	1.40	1.74
Lateral pillars of the principal dome's bay	13.0	2.50	3.10	3.84

Thus, the nailed joints of the diagonals are likely to fail by withdrawal of the nails before splitting occurs either in the posts or diagonals. This is in accordance with on-site observations, as shown in Figure 7.44. The yield moment of these nails made of wrought iron is also very low, so yielding is likely to occur, as also observed in the cathedral after the 2007 Pisco earthquake (Figure 7.45).

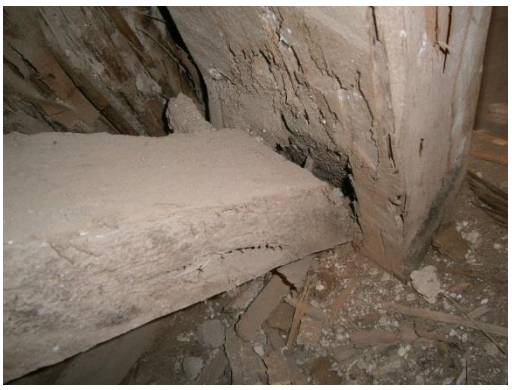

Figure 7.44 Withdrawal of a nail in the Cathedral of Ica without splitting of the timber members (courtesy of Erika Vicente, PUCP)

Figure 7.45 Yielding of the nail of a connection of the Cathedral of Ica (courtesy of Erika Vicente, PUCP)

7.5.2 Robustness

The following global criteria are applied to the diagnosis of the timber framing:

(i) Regularity and overall structural layout;
(ii) General arrangement of the carpentry joints;
(iii) Quality of the construction.

7.5.2.1 REGULARITY AND OVERALL STRUCTURAL LAYOUT

The structural scheme of the vault repeats from bay to bay and therefore the structure can be considered regular from an overall viewpoint. The structure of the bay-edge arches and internal arches is a robust system of arc-shaped planks connected together by means of nailed connections. The lunettes can be interpreted as a discontinuity of the vault's structural system; even though they are important elements for the natural lighting of the nave. A hypothetical structure without lunettes, composed of only bay-edge arches would have greater in-plane stiffness in the church transversal direction. However given the presence of the bending stiffness of the mortice and tenon joints at the top of lunettes, and the diagonal arrangements of the arches forming the lunettes, these actually provide a beneficial bracing effect in the longitudinal direction.

The existence of several types of carpentry joints, say mortice and tenon and nailed joints, which vary in the number of tenons and therefore on the size of the mortices and on the number of nails, also causes a non-uniform deformation of the vault. For instance, the connection of the shortest ribs of the lunettes to the diagonals has a negligible bending moment capacity, since only one nail is used, whereas the connections of the other ribs are made of pairs of nails with non-negligible bending moment capacity.

As far as the timber frame defining the aisle and supporting the vaults is concerned, the bays of the nave were similarly built with the exception of bay 1. The pillars are regularly spaced both longitudinally and transversally. The timber framing of each pillar is composed of a regular system of vertical posts braced by horizontal and diagonal elements. Buckling of the posts is therefore avoided, provided that the connections of the posts with the bracing do not fail. Bay 1, has an additional system of transversal and longitudinal joists that make the mezzanine and the corresponding lateral aisles. This system of joists was added to a primary structure similar to the structure of the other nave's bays.

The structural analysis results show that the deformation of the timber frame is considerably smaller than the deformation of the vault. The fact that the frame is stiffer than the vault is explained by the robust system used to brace the pillars and elements within each pillar.

In the bay of the central dome, the posts of the pillars are closely spaced and braced by horizontal elements. Buckling of these posts is also not likely to occur, since it has been concluded that the pegged mortice and tenon joints of the horizontal bracing are not likely to fail.

7.5.2.2 General arrangement of the carpentry joints

In the vault, the most vulnerable arrangement of joints occurs at the connection of the arches and lunettes' ribs to the longitudinal beams at the top of lunettes. According to the analyses conducted for the 'Connections' attribute, these joints are likely to fail first. The beams at the top of lunettes have many mortices closely spaced with modest edge distances. The mortices are very large in some cases in order to accommodate two or three tenons. Since the depth of the beams is modest, the proportion of solid cross section around the mortices is also modest and subsequently the shear capacity of the beams tends to be modest. Moreover, since the mortices are closely spaced, splitting of the beam at mid-cross section, where the shear stresses are the greatest, can simultaneously cause the failure of adjacent joints that would otherwise be subjected to safe level of demands before a brittle failure triggered force redistribution. This is a typical condition of a structure with poor robustness.

In the case of the frame, the original structural concept in terms of general arrangement of the carpentry joints is good except in the case of the connections of the vault to the timber frame. These connections are made of mortice and tenon joints, whose mortices are closely spaced in the longitudinal beams. Although, these joints are not likely to fail for an earthquake like the one in 2007 in Pisco, according to the analysis conducted for the 'Connections' attribute, the tenons of the ribs and arches of the vault are very close to the tenons of the pillars, requiring the existence of large mortices with limited edge distances. Furthermore, this arrangement of joints triggers the occurrence of several poor quality construction details in addition to deterioration.

7.5.2.3 QUALITY OF THE CONSTRUCTION

From a general viewpoint, the quality of the construction of the vault is good, since no major defects were observed.

In the case of the frame, the quality of the construction is poor at some specific locations of the cathedral. According to on-site observations, one of the lunette's arches of bay 2 is 'glued' to the longitudinal beam by lime plaster instead of being connected to the beam by a mortice and tenon joint, as shown in Figure 7.46. This solution was implemented during the construction by the carpenters who realised that the tenon of the lunette's arch was in the same alignment of the tenon of the post of the pillar and therefore there was no space for both tenons. Another evidence of poor construction quality was also observed in the other lunette of the same bay. One of the lunette's diagonals was nailed to the principal arch due to lack of space in the beam for a mortice and tenon joint, as shown in Figure 7.47. This bay has these errors since it is slightly shorter than the other bays of the nave; fact that in itself indicates poor construction quality.

Figure 7.46 Poor construction quality: connection of a lunette's arch to a longitudinal beam in bay 2 (courtesy of Erika Vicente, PUCP)

Figure 7.47 Poor construction quality: connection of a diagonal to a bay-edge arch in bay 2 (courtesy of Erika Vicente, PUCP)

7.5.3 Interaction

The following interactions are here analyzed:

(i) Interaction of the bays of the vault;
(ii) Interaction of bay 5 with the bay of the central dome; and
(iii) Interaction of the bays of the frame.

The vault does not interact with the brick masonry façade since there is a space of approximately 1.8m between the last arch of the vault and the pediment.

7.5.3.1 INTERACTION OF THE BAYS OF THE VAULT

The bays are connected in the longitudinal direction by means of the timber members shown in Figure 7.48. This longitudinal bracing is connected to secondary arches that are connected to the bay-edge arches. These secondary arches are mostly decorative; and therefore they were not included in the numerical models. If it is assumed that the nailed connections of the secondary arches to the bay-edge arches and the nailed connections of the secondary arches to the longitudinal bracing are in good condition, it is reasonable to consider that the behaviour is similar to a system in which the longitudinal bracing is directly connected to the

bay-edge arches. This is the assumption made in the numerical model. The nails of the connection arches/longitudinal bracing are working predominantly in shear parallel to the grain in the bracing member and shear perpendicular to the grain in the arch. These longitudinal elements might also provide some restraint to the relative lateral displacement of the bays, in which case each single nail is working in shear perpendicular to grain in the bracing member and shear parallel to the grain in the arch member. However, this lateral restraint is expected to be modest due to the low bending moment capacity of the joint composed of a single nail.

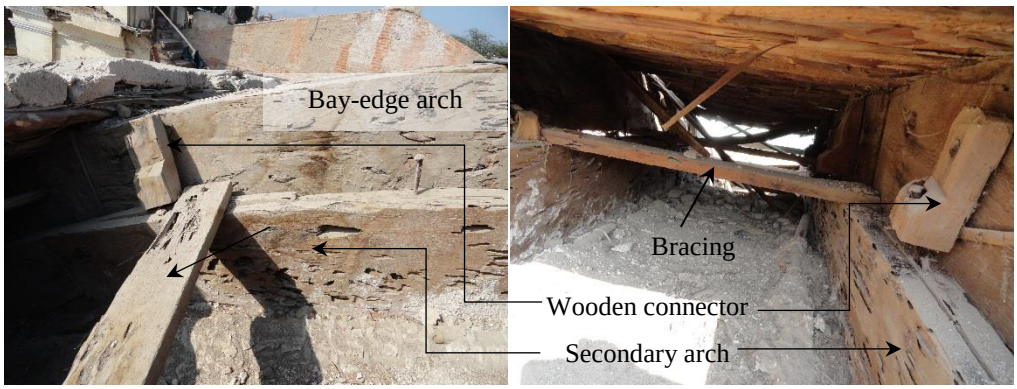

Figure 7.48 Longitudinal bracing connecting adjacent bays of the vault of the Cathedral of Ica

The maximum axial force in the longitudinal bracing when the East-West response spectrum of the 2007 Pisco earthquake is applied in the longitudinal direction of the global model of the Cathedral of Ica is 13kN. This value is produced between bay 2 and bay 3 on bracing located at the top of lunettes. If the values of Table 7.16 related to the Johansen's model are used as a reference, it can be concluded that the bracing is likely to fail in mode D at the most critical point (Figure 7.30). However, the other elements of the bracing connecting the same bays 2 and 3 are subjected to axial forces much lower than the capacity of the joints; and hence it is expected that the bracing was effective during the 2007 Pisco earthquake. This statement is further supported by observations made on site (see for instance Figure 7.48).

7.5.3.2 INTERACTION OF BAY 5 WITH THE BAY OF THE CENTRAL DOME

There was a hammering effect between bay 5 of the nave and the bay of the central dome during the 2007 Pisco earthquake, as shown in Figure 7.49. However, the damage caused by this interaction is non-structural as it caused only the loss of plaster and canes.

Figure 7.49 Damage caused by the interaction of bay 5 with the central dome's bay during the 2007 Pisco earthquake

7.5.3.3 INTERACTION OF THE BAYS OF THE FRAME

The various bays of the timber framing interact with each other by means of the longitudinal beams that are composed of several segments connected by leathered connections. If these connections are in good condition, the beams can be considered as continuously connected. It could be observed on site that no significant longitudinal slip of the longitudinal beams occurred during the 2007 Pisco earthquake; even though the leather is not in good condition in most of the connections between superimposed beams.

7.5.4 Condition

The beams at the top of lunettes are significantly deteriorated, as shown in Figure 7.50, up to a level that the strength of the beam is largely reduced. The meridians of the small domes of the aisles are also affected by deterioration, as shown in Figure 7.51. A similar situation was also observed in some lunettes' ribs. The secondary arches, which are connected to the bay-edge arches, and respective connectors are also deteriorated in many cases, as shown in Figure 7.52. On the other hand, the bay-edge and internal arches made of cedar are better preserved than the other members made of *caoba Africana*.

Figure 7.50 Deteriorated portion of top of lunette's beam

Figure 7.51 Deterioration of the lateral domes' meridians

Figure 7.52 Deteriorated secondary arch (Credits: GCI)

The longitudinal and transversal beams are severely affected by deterioration, as shown in Figure 7.46 and Figure 7.47. On the contrary, the pillars and corresponding bracing are in overall fair condition. However, where inspected the base of the pillars show advanced deterioration where it was imbedded in the brickwork of the base.

7.5.5 Materials

This attribute is evaluated on the basis of the quality of wooden species. In the Cathedral of Ica, there are three principal wooden species:

(i) *Caoba Africana*
(ii) *Guarango*; and
(iii) Cedar.

On-site observations showed that *caoba Africana* is the wooden specie most affected by deterioration. This specie was primarily used in long structural elements, such as beams and posts. This specie was used in the beams at the top of lunettes, which are very important elements to the structural response of the vault. Moreover, it was also used in the longitudinal and transversal beams of the nave, whose performance also influence the behaviour of the mortice and tenon joints that connect the vault to the timber frame. It is therefore reasonable to conclude that these elements should have been built with wooden species more resistant to deterioration; even though a good maintenance program would prevent deterioration.

Guarango is the most resistant to deterioration, and was used in the inner core of the pillars and bracing. For example, it was used to make the diagonal bracing of the pillars, the central post of the central pillars of the nave and the internal posts and horizontal bracing of the central pillars of the central dome's bay.

7.5.6 Matrix of the diagnosis of the timber structure of the Cathedral of Ica

The detailed diagnosis of timber structure of the Cathedral of Ica is summarized in the matrix of Table 7.28. Since the diagnosis do not contradict the available information, especially the observations made on the site, it is reasonable to assume that the level of uncertainty of the output is acceptable. Hence, the reference analysis conditions and the intervals of plausibility do not need to be revised. Otherwise, other iteration would be needed to improve the quality of the analysis.

Table 7.28 Detailed diagnosis of the timber structure of the Cathedral of Ica

<table>
<tr><td>1.ROBUSTNESS</td><td colspan="16">+
• Timber frame is overall robust, but with a few weak points.</td><td colspan="16">-
• Structural arrangement at the top of lunette is not robust
• Structural arrangement of the interaction vault/frame is not robust
• Roof is heavy
• Quality of construction poor at a few locations</td></tr>
<tr><td>2.CONNECTIONS</td><td colspan="8">+
• Arches made of planks connected together by means of nailed joints is sound but dependent on roof weight and connections with other elements
• Mortice and tenon connections of horizontal bracing to posts in central pillars
• Mortice and tenon connections of horizontal bracing to posts of lateral pillars of the nave</td><td colspan="8">-
• Mortice and tenon connections at top of lunette
• Mortice and tenon connections of vault to frame
• Pegged mortice and tenon connections of lateral pillars of transept's bay
• Nailed joints of diagonal bracing to posts</td><td colspan="8">+
• Arches made of planks connected together by means of nailed joints is sound but dependent on roof weight and connections with other elements
• Mortice and tenon connections of horizontal bracing to posts in central pillars
• Mortice and tenon connections of horizontal bracing to posts of lateral pillars of the nave</td><td colspan="8">-
• Mortice and tenon connections at top of lunette
• Mortice and tenon connections of vault to frame
• Pegged mortice and tenon connections of lateral pillars of transept's bay
• Nailed joints of diagonal bracing to posts</td></tr>
<tr><td>3.INTERACTIONS</td><td colspan="4">+
All satisfactory</td><td colspan="4">-</td><td colspan="4">+
All satisfactory</td><td colspan="4">-</td><td colspan="4">+
All satisfactory</td><td colspan="4">-</td><td colspan="4">+
All satisfactory</td><td colspan="4">-</td></tr>
<tr><td>4.CONDITION</td><td colspan="2">+</td><td colspan="2">-
Poor</td><td colspan="2">+</td><td colspan="2">-</td><td colspan="2">+</td><td colspan="2">-
Poor</td><td colspan="2">+</td><td colspan="2">-</td><td colspan="2">+</td><td colspan="2">-
Poor</td><td colspan="2">+</td><td colspan="2">-</td><td colspan="2">+</td><td colspan="2">-
Poor</td><td colspan="2">+</td><td colspan="2">-</td></tr>
<tr><td>5.MATERIALS</td><td>+</td><td>-</td><td>+</td><td>-
Caoba A</td><td>+</td><td>-</td><td>+</td><td>-</td><td>+</td><td>-</td><td>+</td><td>-
Caoba A</td><td>+</td><td>-</td><td>+</td><td>-</td><td>+</td><td>-</td><td>+</td><td>-
Caoba A</td><td>+</td><td>-</td><td>+</td><td>-</td><td>+</td><td>-</td><td>+</td><td>-
Caoba A</td><td>+</td><td>-</td><td>+</td><td>-</td></tr>
</table>

7.6 Conclusions

At the beginning of this chapter, the following research question was posed:

Are the structural concept and the seismic performance of historic earthen and timber churches acceptable in seismic prone countries?

The following main conclusions for the Church of Kuño Tambo provide an answer to this research question:

(i) A detailed diagnosis based on quantitative analysis is important to reach conclusions not only in terms of the current structural performance of the church, but also in terms of possibilities for improving this structural performance;

(ii) The Church of Kuño Tambo provides a representative example of circumstances that make the structural concept of adobe churches in high lands an unsafe structural system. Structural analyses discussed in this chapter show that existing buttresses and tie-beams are insufficient to avoid the collapse of the longitudinal walls for accelerations larger than 0.25g. There are three main reasons for this unsafe state: (1^{st}) buttresses providing lateral restraint to the West longitudinal wall collapsed; (2^{nd}) original buttresses were under-designed, which resulted in the construction of additional buttresses at a later stage in order to compensate this structural problem; however these buttresses are not connected to the walls and therefore are not effective buttressing elements; (3^{rd}) tie-beams added to the church in order to provide further lateral restraint are not properly anchored to the walls, and therefore are likely to fail under modest lateral loads. These circumstances are a result of poor local construction practices, in a context where the local community built the church more than three hundred years ago and keeps being the responsible for its maintenance; and

(iii) Although there is a clear lack of maintenance of the Church of Kuño Tambo, evident by the deterioration of the walls, the most critical aspect is the lack of quality in the construction of key components such as the buttresses and tie-beams. The original structural concept is viable both from a conservation and seismic engineering viewpoint, and hence it should be preserved. However, the following key structural details should be improved while keeping in place a regular maintenance program:

(1^{st}) buttresses must be well-designed and properly connected to the walls; (2^{nd}) walls must be well connected in order to avoid concentration of loads in specific elements; (3^{rd}) the gables are restrained by the roof and the roof is well connected to continuous wall-plates; and (4^{th}) tie-beams must be properly anchored to the walls in order to avoid local failures.

With regards to the Cathedral of Ica, the following main conclusions provide an answer to the aforementioned research question:

(i) Although the provisions of Eurocode 5 regarding the evaluation of nailed joints in shear and tension perpendicular to the grain provide a valuable first estimation of the capacity of historic timber joints of planked arches, more research is required in order to more accurately quantify this capacity. The Johansen's model provides a lower bound estimate of the real capacity of these joints, as, if it was realistic, a much more extensive failure of the principal arches of each bay would have occurred. On the other hand, the van der Put and Leijten model seems to provide results broadly in agreement with on-site observations and numerical simulations; even though it does not take into account the typical boundary conditions of nailed joints of planked arches;

(ii) The 2007 Pisco earthquake caused the collapse of the internal arches of the most critical bays, releasing the corresponding edge arches of their tributary loads. After this release, the shear forces acting on these critical arches reduced to demands lower than the capacity of the nailed joints of the arches. On the other hand, the edge arches of bays where the roof did not collapse, but the mortice and tenon joints of the internal arches failed, underwent a significant increase of loads caused by the fact that the full weight of the roof was then completely supported by those arches. The nailed joints of these arches were then subjected to shear forces larger than the capacity of the joints;

(iii) From an overall viewpoint, the vault is the critical element of the structure, which undergoes large permanent deformations compared to the stiffer frame with a robust bracing system which supports the vault. The lunettes reduce the

in-plane stiffness of the vault in the transversal direction, as compared to a hypothetical structure composed of only bay-edge arches. On the other hand, given the presence of the bending stiffness of the mortice and tenon joints at the top of lunettes, and the diagonal arrangements of the arches forming the lunettes, the lunettes provide a beneficial bracing effect in the longitudinal direction. The longitudinal behaviour is further improved by the longitudinal bracing of the arches within each bay and the bracing of the edge arches between bays. This shows that the overall concept of the structure was well conceived. However, the structure has the following critical points where the capacity is exceeded for an event like the 2007 Pisco earthquake even in the case of a healthy condition of the structure: (1st) nailed joints of the edge arches at the top of lunettes; (2nd) mortice and tenon connections at the top of lunettes; and (3rd) connections of the bracing of the lateral pillars of the bay of the central dome;

(iv) In the case of the Cathedral of Ica, deterioration of the timber framing, mostly concentrated in beams made of *caoba Africana* had a critical role in the partial collapse of the structure. Although the capacity of critical joints was likely to be exceeded, it is reasonable to conclude that perhaps collapse could have been avoided if the structure had a healthier condition. However, the fact that other primary structural components of the structure were made of wooden species more resistant to deterioration avoided a more global failure mechanism of the structure. This is a typical behaviour of a robust structure; and

(v) The original structural concept is viable both from a conservation and seismic engineering viewpoint, and hence it should be preserved. However, the structure has some vulnerable points that must be addressed. From an earthquake engineering viewpoint, in churches with healthy timber structures with lunettes, the connections at the top of lunettes should be reinforced. Moreover, to avoid excessive transversal deformation of the transept bay, which can cause damage to the longitudinal adobe walls, the lateral pillars in such bay must be stiffened and strengthened. The analyses conducted in this thesis also showed that a heavy roof can cause the collapse of the structure during an earthquake. However, the diagnosis in this type of structures is less clear that in the case of adobe churches, due to the dramatic level of deterioration of historic timber structures

in countries like Peru. The lack of maintenance is a critical aspect that may have contributed to the failure of many historic timber structures to an extent that is still unknown.

CHAPTER 8

Conclusions

8.1 Primary contribution

At the beginning of this thesis, the following research questions were posed:

(a) How can the seismic performance of heritage constructions be assessed in the presence of many uncertainties, and uncertainties be measured?

(b) What is the structural concept and seismic response of historic Peruvian earthen and timber churches?

While seeking an answer to each of these research questions, this thesis primarily contributes to knowledge in the following:

(i) *A new methodology for systematic structural assessment of heritage constructions that evaluates the uncertainty of the analysis at various phases of the assessment is proposed*: This methodology: (1^{st}) is tailored to heritage constructions, taking into account all important sources of knowledge and uncertainty; (2^{nd}) it is applicable to different form of heritage construction; (3^{rd}) it is applicable to both qualitative and quantitative methods; (4^{th}) it is a logic sequence of phases with increasing level of complexity, so that results of previous phases inform in a consistent way the planning of the next activities; (5^{th}) measures the uncertainty of the analysis's output by directly evaluating the

sensitivity of the results to variations in inputs and the analysts' level of confidence while conducting such analysis; and (6th) allows to determine the impact of uncertainty on the evaluation of multiple structural performance indicators, which inform the diagnosis. A major element of novelty is the ability of the proposed methodology to identify whether the level of uncertainty can or cannot ultimately lead to alternative diagnoses and whether this is acceptable or not. Moreover, while identifying a 'best' and 'worst' performance of the structure and evaluating whether the 'worst' leads to an acceptable structural performance, this methodology helps the analyst to avoid the planning of remedial measures that can compromise the cultural significance of the constructions.

(ii) *A detailed seismic assessment of historic Peruvian earthen and timber churches is conducted for the first time, in which a quantitative method to evaluate planked timber arches is proposed*: This assessment: (1st) provides a detailed diagnosis of adobe and timber churches, highlighting the major vulnerabilities and strengths of these two historic structural systems, not comprehensively studied before; (2nd) it models for the first time an historic planked timber structure, taking into account realistic values of stiffness of multiple timber joints, and providing a quantitative method to evaluate the joints; and (3rd) it formulates an hypothesis for the failure of the planked timber arches of the Cathedral of Ica.

8.2 Main conclusions

Currently, the assessment of heritage constructions still faces important challenges. The lack or shortage of knowledge and the inability to accurately estimate the structural response are key factors that limit the capacity of professionals to make a diagnosis with confidence.

From a methodological viewpoint, this research reached the following main conclusions:

- *Advances in structural analysis vs engineering practice*: While structural analysis methods have significantly evolved in the past decades from a mathematical and computational viewpoint, the capability of analysing the performance of a structural system in practice has followed a much slower trend. There are two main reasons for this: (1st) the most advanced methods for

structural analysis cannot be used to analyse large and complex structures, if not in the presence of many assumptions and simplifications; and (2nd) only a few researchers and professionals in the world have proper ability to use and access advanced structural analysis methods, since state-of-the-art engineering knowledge and tools have not yet become accessible to the wide engineering community, especially in developing countries.

- *The key challenge of heritage constructions*: Heritage constructions pose the largest challenges to the engineering community. The main reasons are: (1st) the limited knowledge on the 'real' structure and the difficulty to improve the knowledge without compromising the preservation of the assets; and (2nd) the limited knowledge on the behaviour of traditional construction methods, especially ones that have very regional connotations whose performance is highly dependent on local workmanship, such as adobe or carpentry framed timber.

- *Experimental work as the most viable source of information for adobe constructions and timber structures vs lack of tradition of conducting such tests*: Although experimental work is the most expensive and intrusive method to gather information about a heritage construction, at present it is still the most viable method to characterize the behaviour of traditional materials, such as adobe, or components. This reflects the lack of representative datasets for traditional materials like adobe and components such as timber members and their joints. Information available in literature for mechanical characterization of traditional materials like adobe is normally representative of a specific region and local construction technology. Moreover, in countries like Peru with an important heritage built in timber, there is no tradition of conducting experimental tests on timber joints or members, which are essential to analyse the structural performance of the buildings. To the author's knowledge, the first experimental campaign for mechanical characterization of Peruvian historic timber joints was conducted by PUCP for the Cathedral of Ica within the framework of the EAI-SRP.

- *Finite element based approaches as the most viable solution for the analysis in the practice of conservation at present*: FEM based approaches are almost worldwide known by the engineering community. Commercial FEM software is the most disseminated advanced tools for structural analysis. They allow three-dimensional analysis to be performed with large and complex structures, simulating multiple interactions among components. The principal limitation regards the availability of constitutive models appropriate to model simultaneously different behaviour in tension, shear and compression of traditional materials.

- *The tracking of uncertainties during the assessment as a principle to control the accuracy of the diagnosis*: Several uncertainties, especially of an epistemic nature, are present in the assessment process, from the initial data collection to the final diagnosis. The tracking of these uncertainties at various phases of the assessment should be pursued, such as to: (1st) plan the next phases of the assessment by identifying the needs for more data collection and use of alternative analysis methods; (2nd) evaluate the main sources of uncertainty, how uncertainties propagate and hence how they can be reduced; and (3rd) evaluate the impact of the uncertainties in the final diagnosis, to answer the question: 'Would the diagnosis change if the level of uncertainty is lower?'; if so, the uncertainty should be reduced up to a point that it does not affect compromise the conclusions of the diagnosis.

The challenges in the assessment of heritage constructions become increasingly critical in seismic prone developing countries, such as Peru. The 2007 Pisco earthquake put in evidence a vast heritage of colonial earthen and timber churches that is at risk. While validating the methodology for assessment of heritage constructions proposed in this thesis, the analysis and diagnosis of representative churches of Peruvian heritage earthen and timber construction allowed concluding on the soundness of the historic structural systems.

From the analysis and diagnosis of the Church of Kuño Tambo, which is representative of adobe churches built in high lands in Peru, the following main conclusions can be summarized:

- *Analysis of the mechanical behaviour of adobe and rubble stone masonry components as the main challenge*: The most critical aspect of the modelling is the ability to properly simulate the post-elastic response of adobe and rubble stone masonry by appropriate constitutive model. Under earthquake loading, thick walls and buttresses respond mainly in shear, with a low tensile strength and brittle response. The Drucker-Prager model is able to simulate this behaviour by using appropriate values of cohesion and friction angle and by means of an area on the failure surface delimited by the tension cut-off. The alternative use of concrete-based models, governed by the behaviour of the material in uniaxial compression, tension and biaxial compression simulates a material that is stiffer than adobe and rubble stone masonry, being unable to simulate the early reduction of stiffness under modest actions. In adobe churches with thick walls and light roofs, the compression strength is not a critical control variable, since the peak compression strength is rarely achieved before the masonry fails in shear or tension, in real loading conditions.

- *Critical variables of the analysis of historic adobe churches*: The sensitivity analysis conducted in this research generated results that show in a quantitative way that the material properties of both adobe and the rubble stone base course, specifically the specific weight, modulus of elasticity, tension cut-off, cohesion and friction angle are critical inputs of the assessment, and hence require reliable values. The mesh size in FEM analysis is also another critical source of uncertainty, which must be selected such as to properly represent transversal (through depth) shear. Between 2 and 3 volume elements through the thickness of the walls with a maximum mesh size of 0.40m is recommended as a reference to simulate the response of adobe churches with thick and long walls of similar size to the Andean churches. This provides a reasonable balance between the accuracy of the results and the practicality of the model within a practitioner environment and timeframe.

- *Provisions of existing codes inadequate to capture the uncertainty of the analysis of historic adobe churches*: The knowledge-based uncertainty factor obtained in this research shows that confidence factors recommended by existing codes and guidelines, normally used in the assessment of heritage constructions,

underestimate the uncertainty present in the analysis of constructions made of traditional materials and local construction technologies. The lack of reference values of critical variables from literature, and the limitations of carrying out tests to measure these critical variables, results in levels of uncertainty larger than the typical uncertainty of the assessment of existing buildings made of modern materials. Moreover, existing codes and guidelines for assessment of existing constructions ignore the fact evidenced in this thesis that decisions made by the analyst during the analysis and definition of actions contribute to the overall uncertainty as much as other aspects, such as the geometry, materials and structural details of the heritage construction.

- *Pushover analysis as a viable tool for assessment of historic adobe churches by practitioners*: Nonlinear static (pushover) analysis is recommended to evaluate the post-elastic response of historic adobe churches. The results of selected structural performance indicators of the post-elastic behaviour of the walls can be directly compared to a given performance level. More advanced nonlinear dynamic analysis would incorporate additional uncertainties in the assessment, which ultimately could compromise the benefit of applying a more refined analysis. Moreover, nonlinear dynamic analysis is still not comprehensively understood and widely applied by the engineering community of practitioners. This lack of experience of the practitioners would be an additional source of uncertainty of the assessment.

- *The structural concept of adobe churches in high lands*: The simple concept of four thick adobe walls on top of a rubble stone base course in a rectangular arrangement, with a sacristy and baptistery attached to the main longitudinal walls has 'survived' almost five hundred years of weather demands and earthquakes. The lateral buttresses are key elements to provide the lateral restraint needed to avoid excessive deformation and overturning of the longitudinal walls. Sensitivity analyses described in this thesis showed that the buttresses are more effective in providing lateral restraint than the wooden tie-beams, provided that the buttresses have sufficient resistance to support the large out-of-plane forces transmitted by the longitudinal walls. The simple but ingenious idea of extending the longitudinal walls beyond the main façade and

this one laterally beyond the side walls, has improved the out-of-plane response of the façade by providing some lateral restraint in a similar way as buttressing elements, provided that there is a good connection of the façade to the longitudinal walls. The back wall does not benefit from such extension of the longitudinal walls, and it is therefore vulnerable to out-of-plane failure if not properly connected to the other walls. In some Andean churches the risk of overturning of the back wall was reduced by constructing buttresses adjacent to this wall (see for instance the Church of Virgen Asunción de Choquekancha in Figure 4.3b).

- *Local construction technology and quality*: The Church of Kuño Tambo provides a representative example of circumstances that make the structural concept of adobe churches in high lands an unsafe structural system. Structural analyses discussed in this thesis show that existing buttresses and tie-beams are insufficient to avoid the collapse of the longitudinal walls for accelerations larger than 0.25g. There are three main reasons for this unsafe state: (1st) buttresses providing lateral restraint to the West longitudinal wall collapsed; (2nd) original buttresses were under-designed, which resulted in the construction of additional buttresses at a later stage in order to compensate this structural problem; however these buttresses are not connected to the walls and therefore are not effective buttressing elements; (3rd) tie-beams added to the church in order to provide further lateral restraint are not properly anchored to the walls, and therefore are likely to fail under modest lateral loads. These circumstances are a result of poor local construction practices, in a context where the local community built the church more than three hundred years ago and keeps being the responsible for its maintenance.

- *The structural role of the rubble stone base course*: The existence of a base course at the bottom of an adobe wall creates a discontinuity in the vertical system. The interface adobe/rubble stone masonry, characterized by a value of cohesion lower than the most cohesive material (rubble stone), and an angle of friction lower than the highest angle of friction of both materials (associated to adobe), acts as a preferred plan of weakness. The adobe wall of lower

slenderness than a wall of the same height without base course is more stable to out-of-plane loads but tend to rock and slide along the plane of the interface. However, results of pushover analysis indicate that the stress state at this interface overcomes the shear strength, corresponding to the combined effect of the cohesion and friction of the interface and the weight of the adobe wall as per a Coulomb-type friction law, in a relatively modest portion of the interface, especially if the walls are well restrained by buttresses.

- *A perspective for conservation*: Although there is a clear lack of maintenance of the Church of Kuño Tambo, evident by the deterioration of the walls, the most critical aspect is the lack of quality in the construction of key components such as the buttresses and tie-beams. The original structural concept is viable both from a conservation and seismic engineering viewpoint, and hence it should be preserved. However, the following key structural details should be improved while keeping in place a regular maintenance program: (1st) buttresses must be well-designed and properly connected to the walls; (2nd) walls must be well connected in order to avoid concentration of loads in specific elements; (3rd) the gables are restrained by the roof and the roof is well connected to continuous wall-plates; and (4th) tie-beams must be properly anchored to the walls in order to avoid the local failures. This form of construction is common to much wider parts of the world, from California to Bolivia, and hence such results are generalizable to a much wider context than just the Andean Peruvian community.

Finally, from the analysis and diagnosis of the timber structure of the Cathedral of Ica, which is representative of churches built in low lands in Peru, the following main conclusions can be summarized:

- *The modelling of the timber joints with realistic stiffness in elastic models and the verification of the capacity vs demand of the joints by simple analytical methods as the recommended approach to assess historic timber systems in practice*: A practical and powerful approach to assess historic timber systems consists of modelling the timber joints by means of springs with realistic

stiffness, and the timber members with beams characterized by a simple elastic and isotropic model. This approach can be realistically applied by the engineering community, provided that more detailed research on the mechanical characterisation of the timber joints is conducted by the academia and disseminated. Such approach is reasonable taking into account the evidence that failure of timber structures normally occurs at the joints. The sensitivity analysis conducted in this thesis further confirms that the stiffness of the joints is a critical indicator of the performance of the system, which must be characterised with a high level of knowledge. Modal superposition analysis is appropriate to measure the demands at the joints by taking into account the important dynamic effects acting in the system due to the existence of several parts of different relative stiffness and a non-uniform distribution of masses. Using simple analytical methods that can be used by professionals, the demands can be directly compared with the capacity of the joints to evaluate the need or not for reinforcement of the system.

- *The structural concept of historic planked timber structures*: From an overall viewpoint, the vault is the critical element of the structure, which undergoes large permanent deformations compared to the stiffer frame with a robust bracing system which supports the vault. The lunettes reduce the in-plane stiffness of the vault in the transversal direction, as compared to a hypothetical structure composed of only bay-edge arches. On the other hand, given the presence of the bending stiffness of the mortice and tenon joints at the top of lunettes, and the diagonal arrangements of the arches forming the lunettes, the lunettes provide a beneficial bracing effect in the longitudinal direction. The longitudinal behaviour is further improved by the longitudinal bracing of the arches within each bay and the bracing of the edge arches between bays. This shows that the overall concept of the structure was well conceived. However, the structure has the following critical points where the capacity is exceeded for an event like the 2007 Pisco earthquake even in the case of a healthy condition of the structure: (1^{st}) nailed joints of the edge arches at the top of lunettes; (2^{nd}) mortice and tenon connections at the top of lunettes; and (3^{rd}) connections of the bracing of the lateral pillars of the bay of the central dome.

- *A hypothesis for the failure of the timber vault of the Cathedral of Ica*: The 2007 Pisco earthquake caused the collapse of the internal arches of the most critical bays, releasing the corresponding edge arches of their tributary loads. After this release, the shear forces acting on these critical arches reduced to demands lower than the capacity of the nailed joints of the arches. On the other hand, the edge arches of bays where the roof did not collapse, but the mortice and tenon joints of the internal arches failed, underwent a significant increase of loads caused by the fact that the full weight of the roof was then completely supported by those arches. The nailed joints of these arches were then subjected to shear forces larger than the capacity of the joints.

- *The critical maintenance issue*: In the case of the Cathedral of Ica, deterioration of the timber framing, mostly concentrated in beams made of *caoba Africana* had a critical role in the partial collapse of the structure. Although the capacity of critical joints was likely to be exceeded, it is reasonable to conclude that perhaps collapse could have been avoided if the structure had a healthier condition. However, the fact that other primary structural components of the structure were made of wooden species more resistant to deterioration avoided a more global failure mechanism of the structure. This is a typical behaviour of a robust structure.

- *A perspective for conservation*: The original structural concept is viable both from a conservation and seismic engineering viewpoint, and hence it should be preserved. However, the structure has some vulnerable points that must be addressed. From an earthquake engineering viewpoint, in churches with healthy timber structures with lunettes, the connections at the top of lunettes should be reinforced. Moreover, to avoid excessive transversal deformation of the transept bay, which can cause damage to the longitudinal adobe walls, the lateral pillars in such bay must be stiffened and strengthened. The analyses conducted in this thesis also showed that a heavy roof can cause the collapse of the structure during an earthquake. However, the diagnosis in this type of structures is not as objective as in the case of adobe churches, due to the dramatic level of deterioration of historic timber structures in countries like Peru. The lack of

maintenance is a critical aspect that may have contributed to the failure of many historic timber structures to an extent that is still unknown.

8.3 Future research

This research with the Church of Kuño Tambo and the Cathedral of Ica should continue towards the identification of best construction practices for adobe churches in high lands (e.g. appropriate designs for buttresses and solutions locally sustainable for anchorage of the tie-beams), and the testing of strengthening solutions for critical joints of Peruvian historic timber structures through the structural models.

Moreover, at an academic level, research on the non-linear response of the timber joints should progress towards the optimization of strengthening solutions for historic timber joints that improve the structural performance without compromising the cultural significance of the original structural concept and construction.

Research should also progress towards the formulation and dissemination within the engineering community of more representative constitutive models of traditional materials, which still lags behind the rapid evolution and dissemination of computational engineering tools. Moreover, there is still much to advance in timber engineering in order to formulate appropriate failure models for historic timber joints. In this regard, the evolution of fracture mechanics models appears to be a promising solution to refine the assessment of historic timber structures and contribute to their preservation in the future.

A last key note: the author believes this search for more information about ecclesiastical buildings in seismic prone developing countries should continue towards an in-depth understanding of the risk and cultural significance of the churches. The immediate next step will be to print a three-dimensional model of the Cathedral of Ica to teach the students of Engineering and Architecture in Peru, who do not know this structural system. Research should seek next the analysis of other elements of the structures, such as the towers, and other systems, such as the churches with timber vaults sitting on the adobe walls.

Knowledge was always in the centre of this research, and only knowledge will protect the significance of this important heritage, and the occupants' life in the future.

References

Aguilar, V. & Farfan, E. (2002). *Estadística de daños ocasionados por el terremoto de Arequipa del 23-06-2001 en iglesias coloniales, monumentos históricos y calles de la ciudad de Arequipa y sus provincias*. In: Tavera, H. (ed.), El terremoto de la región sur de Perú del 23 de Junio de 2001, Instituto Geofisico del Perú, Lima, Perú

Alberti L.B. (1988). *On the art of building in ten books*. MIT Press, Cambridge MA

Anthoine A. (1995). Derivation of the in-plane elastic characteristics of masonry through homogenization theory. *International Journal of Solids and Structures*, 32(2), p.137-163

Apostolakis G. (1993). *A commentary on model uncertainty*. In: Proceedings of Workshop I in Advanced Topics in Risk and Reliability Analysis, Model Uncertainty: Its characterisation and quantification (Annapolis, MD), NUREG/CP-0138, U.S. Nuclear Regulatory Commission, p.13-22

Argyris J.H. & Kelsey S. (1955). Energy theorems and structural analysis. *Aircraft Engineering*, Vols. 26 and 27, October 1954 to May 1955. Part I by J.H. Argyris and Part II by J.H. Argyris and S. Kelsey

ASCE/SEI 41-06 (2007). *Seismic rehabilitation of existing buildings*. American Society of Civil Engineers – ASCE

Azevedo J., Sincraian G. & Lemos J.V. (2000). Seismic behavior of blocky masonry structures. *Earthquake Spectra*, 16(2)

Bariola J., Gonzales D., Tinman M., Vargas J. & Yañez V. (1988). *Quincha Construction*, Vol. II, Pontificia Universidad Católica del Perú, Departamento de Ingenieria

Bayraktar A., Sahin A., Ozcan D.M. & Yildirim F. (2010). Numerical damage assessment of Haghia Sophia bell tower by nonlinear FE modelling. *Applied Mathematical Modelling*, 34, p.92-121

Beckmann P. & Bowles R. (2004). *Structural aspects of building conservation*. Elsevier Butterworth-Heinemann, 2nd edition, Oxford, UK

Benedetti D. (1981). *Riparazione e consolidamento degli edifici in muratura*. In: AA.VV. Costruzioni in zona sismica, Cap.11, Edizioni Masson, Italy

Berto L., Saetta A., Scotta R. & Vitaliani R. (2002). An orthotropic damage model for masonry structures. *International Journal for Numerical Methods in Engineering*, 55(22), p.127-157

Betti M. & Vignoli A. (2011). Numerical assessment of the static and seismic behaviour of the basilica of Santa Maria all'Impruneta (Italy). *Construction and Building Materials*, 25(12), p.4308-4324

Betti M., Galano L. (2012). *Seismic analysis of historic masonry buildings: the Vicarious Palace in Pescia (Italy)*. Buildings, 2, p.63-82

Birolini A. (2004). *Reliability engineering: theory and practice*. Springer, 4th edition, New York

Block P., Ciblac T. & Ochsendorf J. (2006). Real-time limit analysis of vaulted masonry buildings. *Computers and Structures*, 84, p.1841-1852

Bontempi F., Giuliani L. & Gkoumas K. (2007). Handling the exceptions: robustness assessment of a complex structural system. *Structural Engineering, Mechanics and Computation*, 01/2007, 3, p.1747-1752

BSI (2005). *Methods of test for masonry, Part 5 – Determination of bond strength by the bond wrench method*. BS EN 1052-5, British Standard Institution (BSI), London

BSI (2002). *Methods of test for masonry, Part 3 – Determination of initial shear strength*. BS EN 1052-3, British Standard Institution (BSI), London

BSI (1999). *Methods of test for masonry, Part 2 – Determination of flexural strength*. BS EN 1052-2, British Standard Institution, London

Calderini C., Cattari S. & Lagomarsino S. (2010). The use of the diagonal compression test to identify the shear mechanical parameters of masonry. *Construction and Building Materials*, 24, p.677-685

Callerio A. & Papa E. (1998). *An elastic-plastic model with damage for cyclic analysis of masonry panels*. In: Computer Methods in Structural Masonry, 4, E&FN Spon, UK

Campolongo F., Saltelli A. & Cariboni J. (2011). From screening to quantitative sensitivity analysis. A unified approach. *Computer Physics Communications*, 182, p.978-988

Cancino C., Farneth S., Garnier P., Neumann J.V. & Webster, F. (2009). *Damage Assessment of historic earthen buildings after the August 15, 2007 Pisco Earthquake, Peru.* The Getty Conservation Institute, Los Angeles

Cancino C., Lardinois S., D'Ayala D., Fonseca Ferreira F., Torrealva D., Vicente E. & Villacorta Santamato L. (2012). *Seismic Retrofitting Project: assessment of prototype buildings. Vol. 1-2*. The Getty Conservation Institute, Los Angeles, USA

Casapulla C. & D'Ayala D. (2006). *In-plane collapse behaviour of masonry walls with frictional resistances and openings*. In: Proceedings of the 5th International Conference on Structural Analysis of Historical Constructions (SAHC06), New Delhi, India

Casolo S. & Milani G. (2010). A simplified homogenization-discrete element model for the non-linear static analysis of masonry walls out-of-plane loaded. *Engineering Structures*, 32, p.2352-2366

CEN (1991). *Timber structures - Joints made with mechanical fasteners – General principles for the determination of strength and deformation characteristics*. EN 26891, European Committee for Standardization (CEN), Brussels, Belgium

CEN (1991b). *Timber structures - Joints made with mechanical fasteners – General principles for the determination of strength and deformation characteristics*. EN 26891, European Committee for Standardization (CEN), Brussels, Belgium

CEN (2004). *Eurocode 8: design of structures for earthquake resistance. Part 1: general rules, seismic actions and rules for buildings*. EN 1998-1, European Committee for Standardization (CEN), Brussels, Belgium

CEN (2004b). *Eurocode 5: Design of timber structures. Part 1-1: general, common rules and rules for buildings.* EN 1995-1-1, European Committee for Standardization (CEN), Brussels, Belgium.

CEN (2005a). *Eurocode: Basis of structural design*. EN 1990:2002+A1, European Committee for Standardization (CEN), Brussels, Belgium

CEN (2005b). *Eurocode 8: Design of structures for earthquake resistance. Part 3: Assessment and retrofitting of buildings*. EN 1998-3, European Committee for Standardization (CEN), Brussels, Belgium

CEN (2008). Timber structures: dowel-type fasteners – requirements. EN14592, European Committee for Standardization (CEN), Brussels, Belgium

Chang W.S., Shanks J., Kitamori A. & Komatsu K. (2009). The structural behaviour of timber joints subjected to bi-axial bending. *Earthquake Engineering and Structural Dynamics*, 38, p.739-757

Chen W.F. & Han D.J. (1998). *Plasticity for structural engineers*. Springer

Chudyba K., Piszczek K., Stepień K., Szarliński J. & Urbański A. (1998). *Numerical modelling and experimental verification of the mechanical behaviour of masonry wallets*. In: Computer Methods in Structural Masonry, 4, E&FN Spon, UK

CIB 335 (2010). *Guide for the structural rehabilitation of heritage buildings*. Pompeu Santos S. (rep.), Modena C., Vientzileou E., Tomazevic M., Lourenço P., Capozucca R. Chidiac S. & Jaeger W., CIB Commission W023 – Wall structures, CIB Publication 335

Critchfield G.C., Willard K.E. & Connelly, D.P. (1986). Probabilistic sensitivity analysis methods for general decision models. *Computers and Biomedical Research*, 19, p.254-265

Croci G., D'Ayala D. & Liburdi R. (1995). History, observation and mathematical models in the seismic analysis of the Valadier abutment area in the Colosseum. *Annali di Geofisica*, Vol. XXXVIII, N. 5-6, November-December

Croci G. (2001). *Restoring the Basilica of St. Francis of Assisi*. CRM, no.8

Cundall P.A. (1971). *A computer model for simulating progressive large scale movements in blocky rock systems*. In: Proceedings of the Symposium of the International Society of Rock Mechanics, Vol. 1, Nancy, France

Chavesta Custodio M., Acevedo Mallque M. & Cano Delgado J.C. (2012). *Estudio Anatómico e identificación de especies forestales – Evaluacion estructural y especificaciones técnicas de las maderas de la Catedral de Ica*. Internal Report, Centro de Producción Forestal – Universidad Nacional Agraria La Molina (UNALM), Lima, Peru

D'Ayala D., Carriero A. (1995a). *Definition of the mechanical features of historic masonry and assessment of its seismic behaviour through analytical tools*. In: Proceedings of STREMA 1995, Crete, Greece

D'Ayala D., Carriero A. (1995b). *A numerical tool to simulate the non-linear behaviour of masonry structures*. In: Transactions on Modelling and Simulation, 10, WIT Press

D'Ayala D. (1998). *Numerical modelling of masonry structures reinforced or repaired*. In: Computer Methods in Structural Masonry, 4, E&FN Spon, UK

D'Ayala D. (2000). *Establishing correlation between vulnerability and damage survey for churches*. In: Proceedings of the 12th World Conference on Earthquake Engineering, Auckland, New Zeland

D'Ayala D. & Speranza E. (2003). Definition of collapse mechanisms and seismic vulnerability of historic masonry buildings. *Earthquake Spectra*, 19, p.479-509

D'Ayala D. (2005). Force and displacement based vulnerability assessment for traditional buildings. *Bulletin of Earthquake Engineering*, 3, p.235-265

D'Ayala D.F. & Forsyth M. (2007). *What is conservation engineering?* In: Structures & Construction in Historic Building Conservation, Blackwell Publishing, UK

D'Ayala D. & Tomasoni E. (2008). *The structural behaviour of masonry vaults: limit state analysis with finite friction*. In: Structural Analysis of Historic Construction, Taylor & Francis Group, London

D'Ayala D. & Benzoni G. (2012). Historic and traditional structures during the 2010 Chile earthquake: observations, codes, and conservation strategies. *Earthquake Spectra*, June 2012, 28(S1), p.S425-S451

D'Ayala, D. (2013). *Assessing the seismic vulnerability of masonry buildings*. In: Handbook of Seismic Risk Analysis and Management of Civil Infrastructure Systems, Woodhead Publishing in Materials

De Luca A., Giordano A. & Mele E. (2004). A simplified procedure for assessing the seismic capacity of masonry arches. *Engineering Structures*, 26, p.1915-1929

DeJong, M.J. (2009). *Seismic assessment strategies for masonry structures*. PhD dissertation, Massachusetts Institute of Technology, Massachusetts

Dorbath, L.; Cisternas, A.; Dorbath, C. (1990). Assessment of the size of large and great historical earthquakes in Peru. *Bulletin of the Seismological Society of America*, Vol. 80, No. 3, p. 551-576

Drucker D. C., Gibson R. E. & Henkel D. J. (1957). Soil mechanics and work hardening theories of plasticity. *Transactions*, ASCE, Vol.122, p.338-346

Drucker D.C. & Prager W. (1952). Solid mechanics and plastic analysis or limit design. *Quarterly of applied Mathematics*, 10, p.157-165

E.080 (2006). *Adobe*, Peruvian national building code. Lima, Peru

E.020 (2006). *Cargas*, Peruvian national building code. Lima, Peru

E.030 (2003). *National Building Code, Technical Standard of Building – earthquake-resistant design*. Lima, Peru

Fabbri F. (2010). *Analisi Numerica di volte in camorcanna e gesso rinforzate con materiali FRP*. Tesi di Laurea, Università di Bologna

Fernandez-Cabo J.L., Arce-Blanco M., Diez-Barra R. & Hurtado-Valdez P.A. (2012). *Theoretical and experimental structural studies of historical Latin-American laminated*

planked timber arches. In: Proceedings of the 12th World Conference on Timber Engineering, Auckland, New Zealand

Fernández-Golfín Seco J.I., Díez Barra M.R. & Hermoso Prieto E. (2003). Relaciones entre las variables clasificadoras de la madera estructural de los pinos silvestre y laricio procedencia española. *Materiales de Construccion*, 53 (270), p.45-55

Fonseca Ferreira, C, & D'Ayala D. (2012). *Numerical modelling and structural analysis of historical ecclesiastical buildings in Peru for seismic retrofitting*. In: Proceedings of SAHC 2012, Wroclaw, Poland

Fonseca Ferreira C., D'Ayala D., Fernandez-Cabo J.L. & Díez-Barra R. (2013). Numerical modelling of historic vaulted timber structures. *Advanced Materials Research, Structural Health Assessment of Timber Structures*, Trans Tech Publications, p.517-525

Franchin P., Emilio Pinto P. & Rajeev P. (2010). Confidence factor? *Journal of Earthquake Engineering*, 14, p.989-1007

Freeman S.A. (1998). *Development and use of capacity spectrum method*. In: 6th US NCEE Conference on Earthquake Engineering/EERI, Seattle, Washington

Frey H. C. & Patil S. R. (2002). Identification and review of sensitivity analysis methods. *Risk Analysis Journal*, Vol. 22, No.3, p.553-578

Furukawa A. & Ohta Y. (2009). Failure process of masonry buildings during earthquake and associated casualty risk evaluation. *Natural Hazards*, 49, p.25-51

Furukawa A., Spence R., Ohta Y. & So E. (2010). Analytical study on vulnerability functions for casualty estimation in the collapse of adobe buildings induced by earthquake. *Bulletin of Earthquake Engineering*, 8, p.451-479

Ganz H.R. (1985). *Mauerwerksscheiben unter normalkraft und schub*. Bericht Nr.: 148, Institut fnr Baustatik und Konstruktion, ETH Zurich

Gattulli V., Antonacci E., Vestroni F. (2013). Field observations and failure analysis of the Basilica S. Maria di Collemaggio after the 2009 L'Aquila earthquake. *Engineering Failure Analysis*, 34, p.715-734

Genna F., Pasqua M. & Veroli M. (1998). Numerical analysis of old masonry buildings: a comparison among constitutive models. *Engineering Structures*, 20 (1-2), p.37-53

Giardini, D.; Grünthal, G.; Shedlock, K. & Zhang, P. (1999). Global Map 1999. Produced by the Global Seismic Hazard Assessment Program (GSHAP) (http://www.seismo.ethz.ch/static/GSHAP/).

Gilbert M., Casapulla C. & Ahmed H.M. (2006). Limit analysis of masonry block structures with non-associative frictional joints using linear programming. *Computers and Structures*, 86, p.873-887

Giuriani E., Marini A., Plizzari G. (2005). Experimental behaviour of stud connected wooden floors undergoing seismic action. *Restoration of Buildings and Monuments*, 11(1), p.3-24

Giuriani E., Marini A. (2008). Wooden roof box structure for the anti-seismic strengthening of historic buildings. *International Journal of Architectural Heritage*, 2, p.226-246

Gómez Sánchez I. (2006). *Las estructuras de madera en los Tratados de Arquitectura (1500-1810)*. Asociación de Investigación Técnica de Industrias de la Madera y Corcho

Grünthal G. (Ed.) (1998). *European macroseismic scale 1998*. Conseil de L'Europe, Luxembourg

Gupta K.K. & J.L. Meek (1996). A brief history of the beginning of the finite element method. *International Journal for Numerical Methods in Engineering*, 39, p.3761‑3774

Hamburger R.O. (1996). *Implementing performance based seismic design in structural engineering practice*. In: 11th World Conference on Earthquake Engineering, Acapulco, Mexico

Hahmann L. (2006). *How stiff is a curved timber plank? Historical discussions about curved-plank structures*. In: Proceedings of the Second International Congress on Construction History; Queens' College, Cambridge, p.1501-1516

Helton J.C. (1993). Uncertainty and sensitivity analysis techniques for use in performance assessment for radioactive waste disposal. *Reliability Engineering and System Safety*, 41, p.327-367

Heyman J. (1966). The stone skeleton. *International Journal of Solids and Structures*, 2, p.249-279

Heyman J. (1967). Westminster hall roof. ICE Proceedings, Volume 37, Issue 1, p.137-162

Heyman J. (1995). *The stone skeleton: structural engineering of masonry architecture*. Cambridge University Press, Cambridge

Hoffman F.O. & Gardner R.H. (1983). *Evaluation of uncertainties in radiological assessment models*. In: Till J.E. & Meyer H.R. (Eds.), Radiological Assessment. A textbook on environmental dose analysis, Chapter 11, NUREG/CR-3332, ORNL-5968

Hofstetter K., Hellmich C. & Eberhardsteiner J. (2005). Development and experimental validation of a continuum micromechanics model for the elasticity of wood. *European Journal of Mechanics A/Solids*, 24, p.1030-1053

Holmberg S., Persson K. & Petersson H. (1999). Nonlinear mechanical behaviour and analysis of wood and fibre materials. *Computers and Structures*, 72 (4–5), p.459–480

Houben H. & Guillaud H. (1994). *Earth construction: a comprehensive guide*. Intermediate Technology Publications, London, UK

Huerta S. (2001). *Mechanics of masonry vaults: the equilibrium approach*. In: Historical Constructions, University of Minho, Guimarães, Portugal, p.47-69

Hume I. (2007). *The philosophy of conservation engineering*. In: Structures & Construction in Historic Building Conservation, Blackwell Publishing, UK

Hurtado Valdez P.A. (2011). *Bovedas encamonadas: origin, evolucion, geometria y construccion entre los siglos XVII y XVIII en el Virreinato de Peru*. PhD thesis, Universidad Politécnica de Madrid

ICOMOS (2004a). *The Burra Charter: the Australia ICOMOS Charter for Places of Cultural Significance (1979, revisions 1981, 1988, 1999)*. In: International Charters for Conservation and Restoration, Monuments and Sites I, 2nd edition, ICOMOS, München

ICOMOS (2004b). *The Venice Charter, International charter for the conservation and restoration of monuments and sites (1964)*. In: International Charters for Conservation and Restoration, Monuments and Sites I, 2nd edition, ICOMOS, München

ICOMOS (2004c). *Principles for the recording of monuments, groups of buildings and sites (1996)* (ratified by the 11th ICOMOS General Assembly in Sofia, October 1996).

In: International Charters for Conservation and Restoration, Monuments and Sites I, 2nd edition, ICOMOS, München

ICOMOS-ISCARSAH (2003). *Recommendations for the analysis, conservation and structural restoration of architectural heritage*. International Council on Monuments and Sites (ICOMOS), International Scientific Committee on the Analysis and Restoration of Structures of Architectural Heritage (ISCARSAH)

INC, Instituto Nacional de Cultura (2007). *Terremoto en el Sur: daños en el patrimonio. Gaceta Cultural del Peru*, Nº29, October 2007, INC, Lima, Peru.

INC, Instituto Nacional de Cultura (2008). *Manual de tecnicas constructivas tradicionales del poblado historico de Vilcashuaman*

Ingalls B. (2008). Sensitivity analysis: from model parameters to system behaviour. *Essays in Biochemistry*, Vol. 45, No. 1

Islam M.S. & Watanabe H. (2004). *FEM simulation of seismic behaviour of adobe structures*. In: Proceedings of the 13th World Conference on Earthquake Engineering, Vancouver, Canada

ISO 13822 (2010). *Bases for design of structures – assessment of existing structures*. International Organization for Standardization - ISO, Switzerland

ISRCHB (2006). *Guidelines for the conservation of historical masonry structures in seismic areas*. University of Minho, Technical University of Catalonia, Central Building Research Institute, Universita degli Studi di Padova, Project "Improving the Seismic Resistance of Cultural Heritage Buildings (ISRCHB)

Jalayer F., Iervolino I. & Manfredi G. (2010). Structural modelling uncertainties and their influence on seismic assessment of existing RC structures. *Structural Safety*, 32, p.220-228

Johansen K.W. (1949). *Theory of timber connections*. IABSE-International Association of Bridge and Structural Engineering Publications, 9

Kang H. & Willam K. (1999). Localization characteristics of triaxial concrete model. *Journal of Engineering Mechanics*, 125(8), p.941-950

Kececioglu D. (2002). *Reliability engineering handbook*. DEStech Publications Inc., Vol. 1, Lancaster, Pennsylvania, USA

Kohler J. (2010). *Modelling the performance of timber structures: recent research developments and future challenges*. In: 11th World Conference on Timber Engineering, Italy

Krstevska L., Tashkov Lj., Gramatikov K., Landolfo R., Mammana O., Portioli F. & Mazzolani, F. M. (2008). *Shaking table tests on the large scale model of Mustafa Pasha Mosque without and with FRP*. In: Structural Analysis of Historical Constructions, Taylor & Francis Group, London

Lagomarsino S. (1998). *A new methodology for the post-earthquake investigation of ancient churches*. In: Proceedings of the 11th European Conference on Earthquake Engineering, Paris, France

Lagomarsino S. & Resemini S. (2009). The assessment of damage limitation state in the seismic analysis of monumental buildings. *Earthquake Spectra*, 25(2), p.323-346

Lagomarsino S. & Cattari S. (2015). PERPETUATE guidelines for seismic performance-based assessment of cultural heritage masonry structures. *Bulletin of Earthquake Engineering*, 13, p.13-47

Lee J.S., Pande G.N., Middleton J. & Kralj B. (1996). Numerical modelling of brick masonry panels subjected to lateral loading. *Computers and Structures*, 61(4), p.735-745

Livesley R.K. (1978). Limit analysis of structures formed from rigid blocks. *International Journal for Numerical Methods in Engineering*, Vol.12, p.1853-1871

Lourenço P.B. (1996). *Computational strategies for masonry structures*. PhD thesis, Delft University of Technology, The Netherlands

Love A.E.H. (1888). The small free vibrations and deformation of a thin elastic shell. *Philosophical Transaction of Royal Society of London*, 179 A, p.491-456

Ma M.Y., Pan A.D.E., Luan M. & Gebara, J.M. (1996). *Seismic analysis of stone arch bridges using discontinuous deformation analysis*. In: Proceedings of the 11th World Conference on Earthquake Engineering, Acapulco, Mexico.

Málaga A.M. (1974). Las reducciones en el Perú durante el gobierno del virrey Francisco de Toledo. *Anuario de estudios Americanos*, 31, p.819-842

Mallardo V., Malvezzi R., Milani E. & Milani G. (2008). Seismic vulnerability of historical masonry buildings: a case study in Ferrara. *Engineering Structures*, 30, p.2223-2241

Mamaghani I.H.P., Aydan Ö. & Kajikawa Y. (1999). Analysis of masonry structures under static and dynamic loading by discrete finite element method. *Journal of Structural Mechanics and Earthquake Engineering*, No. 626/I-48, Japan Society of Civil Engineers-JSCE, p.1-12

Mann W. & Müller H. (1978). *SchubtragfShigkeit von mauerwerk*. In: *Mauerwerk Kalender*; Ernst and Sohn, Berlin

Martinez G., Roca P., Caselles O. & Clapés J. (2006). *Characterization of the dynamic response for the structure of Mallorca Cathedral*. In: Structural Analysis of Historical Constructions, Vol. I, p.601-608

Marussi Castellán F. (1981). *La quincha en las edificaciones monumentales del Virreinato del Perú*. PhD thesis, Universidad Politénica de Madrid, Madrid

Marussi Castellán F. (1989). *Antecedentes historicos de la quincha*. Documento tecnico, ININVI- Instituto Nacional de Investigacion y Normalizacion de la vivienda

Marzo A. (2006). Methodology for the analysis of complex historical wooden structures. *Pollack Periodica*, 1(1), p.35-52

Mayorca P. & Meguro K. (2004). *Proposal of an efficient technique for retrofitting unreinforced masonry dwellings*. In: Proceedings of the 13th World Conference on Earthquake Engineering, Vancouver, Canada

Meda A. & Riva P. (2001). *Strengthening of wooden floors with high performance concrete slabs*. International Journal for Restoration of Buildings and Monuments, 7(6), p.621-640

Mele E., De Luca A. & Giordano A. (2003). Modelling and analysis of a basilica under earthquake loading. *Journal of Cultural Heritage*, 4, p.355-367

Meli R. & Sánchez-Ramírez A.R. (1997). Rehabilitation of the Mexico City cathedral. *Structural Engineering International*, 7(2), p.101-106

Milani G. (2011). Kinematic FE limit analysis homogenization model for masonry walls reinforced with continuous FRP grids. *International Journal of Solids and Structures*, 48, p.326-345

Miller J.F. & Schmidt R.J. (2004). *Capacity of pegged mortise and tenon joinery*. Department of Civil and Architectural Engineering, University of Wyoming

Mishnaevsky Jr. L & Qing H. (2008). Micromechanical modelling of mechanical behaviour and strength of wood: State-of-the-art review. *Computational Materials Science*, 44, p.363–370

Mistler M., Butenweg C. & Meskouris K. (2006). Modelling methods of historic masonry buildings under seismic excitation. *Journal of Seismology*, 10, p.497-510

Morio J. (2011). Global and local sensitivity analysis methods for a physical system. *European Journal of Physics*, 32, p.1577-1583

NGM – National Geographic Magazine, January 2011

Novelli V. & D'Ayala D. (2011). *Seismic damage identification of cultural heritage assets*. In: Seismic Protection of Cultural Heritage, 13, p.

NRC-CNRC (1995). *Guideline for seismic upgrading of building structures*. National Research Council Canada, Institute for Research in Construction, Canada

NZSEE - New Zealand Society for Earthquake Engineering, (2011a). *Assessment and improvement of unreinforced masonry buildings for earthquake resistance*. Faculty of Engineering, University of Auckland, New Zealand

NZSEE - New Zealand Society for Earthquake Engineering, (2011b). *Commentary to assessment and improvement of unreinforced masonry buildings for earthquake resistance*. Faculty of Engineering, University of Auckland, New Zealand

OPCM 3431 (2005). *Primi elementi in materia di criteri generali per la classificazione sismica del territorio nazionale e di normative tecniche per le costruzioni in zona sísmica*. Ulteriori modifiche ed integrazioni all'Ordinanza n.3274 del 20/3/2003, Suppl. ord. n.85 alla G.U. n.107 del 10/5/2005

Orduña A. & Lourenço P.B. (2005a). Three-dimensional limit analysis of rigid blocks assemblages. Part I: torsion failure on frictional interfaces and limit analysis formulation. *International Journal of Solids and Structures*, 42, p.5140-5160

Orduña A. & Lourenço P.B. (2005b). Three-dimensional limit analysis of rigid blocks assemblages. Part II: load-path following solution procedure and validation. *International Journal of Solids and Structures*, 42, p.5161-5180

Ottosen N.S. & Ristinmaa M. (2005). *The mechanics of constitutive modelling*. Elsevier, UK

Pallarés F.J., Agüero A. & Ivorra S. (2009). A comparison of different failure criteria in a numerical seismic assessment of an industrial brickwork chimney. *Materials and Structures*, 42, p.213-226

Pande G.N., Liang J.X. & Middleton J. (1989). Equivalent elastic moduli for brick masonry. *Computers and Geotechnics*, 8, p.243-265

Parisi M.A. & Piazza M (2002). Seismic behaviour and retrofitting of joints in traditional timber roof structures. *Soil Dynamics and Earthquake Engineering*, 22, p1183-119

Piazza M. & Turrini G. (1983). *Il recupero static dei solai in legno*. Recuperare (7), p.396-407

Pilch M., Trucano T.G. & Helton, J.C. (2011). Ideas underlying the Quantification of Margins and Uncertainties. *Reliability Engineering and System Safety*, 96, p.965-975

Proaño R., Scaletti H., Zavala C., Olarte J., Quiroz L., Castro Cuba M., Lazares F., Rodriguez M. (2007). *Seismic vulnerabilty of Lima Cathedral, Peru*. In: Proceedings of the Conferencia Internacional en Ingenieria Sísmica, Universidad Nacional de Ingeniería, Centro Peruano Japonés de Investigaciones Sísmicas y Mitigación de Desastres, Lima, p.1-11

Quinn N., Fonseca Ferreira C. & D'Ayala D. (2015). *Performance-based approach for the seismic diagnosis of historic buildings*. In: Proceedings of SECED 2015 Conference – Earthquake Risk and Engineering towards a Resilient World, Cambridge, UK

Rao S.S. (2005). *The finite element method in engineering*. Elsevier Butterworth-Heinemann, Oxford

Roberti M.G., Donati L. & Fontana A. (2005). *Out-of-plane behaviour of multiple-leaf stone masonry*. In: Structural analysis of historical constructions, Taylor & Francis Group, London.

Roca P. (2001). *Studies on the structure of Gothic Cathedrals*. In: Historical Constructions, University of Minho, Guimarães, Portugal, p.71-90

Roca P., Cervera M. & Gariup L.P. (2010). Structural analysis of masonry historical constructions. Classical and advanced approaches. *Archives of Computational Methods in Engineering*, 17, p.299-325

Rowland I.D. & Howe T.N. (eds) (1999). *Vitruvius: Ten books on architecture*. Cambridge University Press

Saltelli A. (1999). Sensitivity analysis: Could better methods be used? *Journal of geophysical Research*, Vol. 104, No D3, p.3789-3793

Saltelli A., Chan K. & Scott M., eds. (2000). *Sensitivity analysis*. Wiley, New York

Saltelli A. (2005). *Global sensitivity analysis: an introduction*. In: Hanson K. M. & Hemez F.M. (Eds), Sensitivity Analysis of Model Output, Los Alamos National Laboratory, Los Alamos, NM, USA, p.27-43

Saltelli A. & Annoni P. (2010). How to avoid a perfunctory sensitivity analysis. *Environmental Modelling & Software*, 25, p.1508-1517

San Cristobal A. (2003). *Arquitectura virreinal de Lima en la primera mitad del siglo XVII*. Lima, Facultad de Arquitectura, Urbanismo y Artes, Universidad Nacional de Ingeniería

Senthivel R. & Lourenço P.B. (2009). Finite element modelling of deformation characteristics of historical stone masonry shear walls. *Engineering Structures*, 31, p.1930-1943

Sevim B., Bayraktar A., Altunişik A.C., Atamtürktür S. & Birinci, F. (2011). Assessment of nonlinear seismic performance of a restored historical arch bridge using ambient vibrations. *Nonlinear Dynamics*, 63, p.755-770

Shanks D., Chang W.S. & Komatsu K. (2008). *Experimental study on mechanical performance of all-softwood pegged mortice and tenon connections*. Biosystems Engineering, 100, p.562-570

Shi G.H. (1992). *Block system modelling by discontinuous deformation analysis*. Computational Mechanics Publication, UK

Shimada I. & Cavallaro R. (1985). Monumental adobe architecture of the late prehispanic Northern North coast of Peru. *Journal de la Société des Américanistes*, 71, p.41-78

Silva B., Guedes J.M., Arêde A. & Costa A. (2012). Calibration and application of a continuum damage model on the simulation of stone masonry structures: Gondar church as a case study. *Bulletin of Earthquake Engineering*, Vol. 10, Issue 1, p.211-234

Solis R.S., Haas J. & Creamer W. (2001). Dating Caral, a preceramic site in the Supe Valley on the Central Coast of Peru. *Science*, Vol. 292, p.723-726

Tarque N., Camata G., Spacone E., Varum H. & Blondet M. (2010). *Numerical modelling of in-plane behaviour of adobe walls*. In: Proceedings of the 8th National Congress on Seismology and Earthquake Engineering, Portugal

Tarque N.R., Camata G., Spacone E., Varum H. & Blondet M. (2013). Non-linear dynamic analysis of a full-scale unreinforced adobe model. *Earthquake spectra* (published online)

Taucer, F.; Alarcon, J.E. & So, E. (2009). 2007 August 15 magnitude 7.9 earthquake near the coast of Central Peru: analysis and field mission report. *Bulletin of Earthquake Engineering*, 7(1)

Tavera, H.; Salas, H.; Jiménez, C.; Antayhua, Y.; Fernández, E.; Vilcapoma, L.; Millones, J.; Bernal, I.; Zamudio, Y.; Carpio, J.; Agüero, C.; Pérez-Pacheco, I.; Rodríguez, S. & Aleman, H. (2002). *El terremoto de la región sur de Perú del 23 de Junio de 2001: aspectos sismológicos*. In: Tavera, H. (ed.), El terremoto de la región sur de Perú del 23 de Junio de 2001, Instituto Geofisico del Perú, Lima, Perú

Tavera, H.; Bernal, I.; Strasser, F.O.; Arango-Gaviria, M.C.; Alarcón, J.E.; Bommer, J.J. (2009). Ground motions observed during the 15 August 2007 Pisco, Peru, earthquake. *Bulletin of Earthquake Engineering*, 7(1)

Tolles E.L., Kimbro E.E. & Ginell W.S. (2002). *Planning and Engineering Guidelines for the Seismic Retrofitting of Historic Adobe Structures*. GCI Scientific Program Reports, The Getty Conservation Institute (GCI), Los Angeles, USA

Tondelli M., Rota M., Penna A. & Magenes G. (2012). Evaluation of uncertainties in the seismic assessment of existing masonry buildings. *Journal of Earthquake Engineering*, 16(S1), p.36-64

Torrealva D. & Vicente E. (2014). *Testing results*. Seismic Retrofitting Project in Peru, Internal Report, Pontificia Universidad Católica del Perú, Lima

Torrealva, D., J.V. Neumann, et al. (2006). *Adobe buildings at Pontificia Universidad Católica del Perú*. In: Proceedings of the Getty Seismic Adobe Project 2006 Colloquium. The Getty Conservation Institute, Los Angeles

Tsai P.H. & D'Ayala D. (2011) Performance-based seismic assessment method for Taiwanese historic Dieh-Dou timber structures. *Earthquake Engineering & Structural Dynamics*, 40(7), p.709-729

Turner M.J., Clough R.W., Martin H.C. & Topp L.J. (1956). Stiffness and deflection analysis of complex structures. *Journal of Aeronautical Sciences*, 23, p.805‑824

USGS historic world earthquakes list (available at: http://earthquake.usgs.gov/earthquakes/world/ historical _country .php #peru)

Utsu, T. (2002). *A list of deadly earthquakes in the world: 1500-2000*. In: Lee, W.H.K.; Kanamori, H.; Jennings, P.C.; Kisslinger, C. (2003), International Handbook of Earthquake & Engineering Seismology, Academic Press

Van der Put, T.A.C.M. and Leijten A.J.M. (2000). *Evaluation of perpendicular to the grain failure of beams, caused by concentrated loads of joints*. CIB-W18A/33-7-7, meeting 33, Delft, The Netherlands

Van der Put T.A.C.M. (2011). Fracture mechanics of wood and wood-like reinforced polymers. In: David E. Malach (ed.), *Advances in Mechanical Engineering Research*, Vol.2, Nova Science Publishers

Vargas J, Bariola J & Blondet M. (1983). *Informe final del proyecto resistencia sísmica de la mampostería de adobe*. Convenio AID-PUCP - Pontificia Universidad Católica del Perú, Lima

Vargas J, Bariola J & Blondet M. (1986). Seismic strength of adobe masonry. *Materials and structures*, 19(4), p.253-258

Vecchi S.S. (2009). *A finite element model evaluation of the dynamic behaviour of one-story adobe dwellings reinforced with polymer grid*. Master thesis, Swiss Federal Institute of Technology Zurich Master, Pontificia Universidad Católica del Perú, Zurich, Lima

Villacorta L. (2005). Las reducciones Toledanas (1570-1575). Reducciones indígenas en el valle de Lima. Poblados del siglo XVI en los alrededores de la capital. *Arkinka*, 121, p.37-45

Willam K. & Warnke E. (1975). *Constitutive model for triaxial behavior of concrete*. International Association for Bridge and Structural Engineering, Zurich, p.1-30

Yeomans D. (2003). *The repair of historic timber structures*. Thomas Telford

Zalewski W. & Allen E. (1998). *Shaping structures: statics*. John Wiley and Sons, New York

Zhuge Y. (2008). Distinct element modelling of unreinforced masonry wall under seismic loads with and without cable retrofitting. *Trans. TianJin Univ*, 14, p471-476

Zienkiewicz O.C & Cheung Y.K. (1967). *The finite element method in structural and continuum mechanics*. McGraw-Hill, London

Zienkiewicz O.C & Taylor R.L. (2000). *The finite element method*. Butterworth Heinemann, 5th edition, Oxford

Zimmermann T., Strauss A. & Bergmeister K. (2010). Numerical investigation of historic masonry walls under normal and shear load. *Construction and Building Materials*, 24, p.1385-1391

Zhou Z., Walker P. & D'Ayala D. (2008). Strength characteristics of hydraulic lime mortared brickwork. *Construction Materials*, 161 (CM4)

Annex I

Material properties of unfired brick (adobe) and rubble stone masonry existing in literature

TABLE I.1 Mechanical properties of adobe obtained from experimental tests

Literature	w (kN/m^3)	f_c (kPa)	f_t (kPa)	f_v (kPa)	E (MPa)	G (MPa)	υ	c (kPa)	f_b (kPa)	φ (rad)
Vargas *et al.* (1983) Peru				C: 60 [1] Cz: 96 HB: 54 H: 98 P: 72 L: 47 C: 51 (26) [2] Cz: 81 (76) HB: 54 H: 52 (46) P: 42 (27) L: 21 (12)						
Vargas *et al.* (1986) Peru				73 [3]						

LEGEND:

W: Specific weight	fv: Shear strength	υ: Poisson ratio	φ: Internal friction angle	C: Cajamarca	H: Huaraz
f_c: Compression strength	E: Young's modulus	c: Cohesion		Cz: Cuzco	P: Pisco
f_t: Tension strength	G: Shear modulus	f_b: Bond strength		HB: Huancayo Blanco	L: Lima (PUCP)

REMARKS:

[1] Results of diagonal compression tests.

[2] Results of indirect and direct (in brackets) shear tests.

[3] Mean value of diagonal compression tests performed with adobe masonry walls built with samples of soil gathered in different geographical areas of Peru (average of 45kPa, 55kPa, 70kPa, 95kPa, and 100kPa)

TABLE I.1 Mechanical properties of adobe obtained from experimental tests (cont.)

Literature	w (kN/m^3)	f_c (kPa)	f_t (kPa)	f_v (kPa)	E (MPa)	G (MPa)	υ	c (kPa)	f_b (kPa)	φ (rad)
Ottazzi *et al*. (1989) Peru		1640 [4]		70 [5]	181					
Loaiza *et al*. (2002) Peru		1200		25						
Tarque (2008) [6] Peru		840		70	174	78				
Vecchi (2009) [7] Peru	18.65		30							
Yamin *et al*. (2004) Colombia	18.00	1220		31 [8]	117	30.2				

LEGEND:
W: Specific weight
f_c: Compression strength
f_t: Tension strength
fv: Shear strength
E: Young's modulus
G: Shear modulus
υ: Poisson ratio
c: Cohesion
f_b: Bond strength
φ: Internal friction angle

REMARKS:
[4] Mean value of the results of uniaxial compression tests performed with adobe masonry piers.
[5] Mean value of the results of diagonal compression tests performed with walls strengthened by the introduction of straw.
[6] The values were collected in literature as results of experimental tests performed in PUCP.
[7] The values were collected in literature.
[8] The value was probably obtained from a diagonal compression test (the reference does not provide details).

TABLE I.1 Mechanical properties of adobe obtained from experimental tests (cont.)

Literature	w (kN/m^3)	f_c (kPa)	f_t (kPa)	f_v (kPa)	E (MPa)	G (MPa)	υ	c (kPa)	f_b (kPa)	φ (rad)
Kiyono & Kalantari (2004) Iran									2.9 [9] 4.6	0.56
Kuwata *et al.* (2005) [10] Iran		29400			42.857		0.25	49		0.35
Varum *et al.* (2006) Portugal		1130		109 [11]	183	33				
Liberatore *et al.* (2006) Italy				20.6 [12]				65 [13] 37		1 [13] 0.5
Quagliarini (2010) Italy		1000		140 [14] 270	33					

LEGEND:
W: Specific weight; fv: Shear strength; υ: Poisson ratio; φ: Internal friction angle
f_c: Compression strength; E: Young's modulus; c: Cohesion
f_t: Tension strength; G: Shear modulus; f_b: Bond strength

REMARKS:
[9] In-situ tests to evaluate the bond strength under shear (upper value) and tension (bottom value).
[10] No details of the experimental tests are reported by the authors.
[11] The value corresponds to the mean value of the results of diagonal compression tests. The shear strength was calculated assuming a pure shear stress state.
[12] The value was obtained from a diagonal compression test assuming a pure shear stress state.
[13] Values taken from Normal-Shear stress diagrams of direct shear tests. Upper value corresponds to a shearing phase and the bottom value to a re-shearing phase.
[14] Results of shear tests assuming a compression stress of 200kPa (upper value) and 400kPa (bottom value).

TABLE I.2 Mechanical properties of rubble stone masonry obtained from experimental tests

Literature	w (kN/m^3)	f_c (kPa)	f_t (kPa)	f_v (kPa)	E (MPa)	G (MPa)	υ	c (kPa)	f_b (kPa)	φ (rad)
Brignola *et al.* (2009) Italy				32 [15] 24 23						
Vasconcelos (2005) Portugal					2329.400		0.2	100		0.37

LEGEND:

W: Specific weight	fv: Shear strength	υ: Poisson ratio	φ: Internal friction angle
f_c: Compression strength	E: Young's modulus	c: Cohesion	
f_t: Tension strength	G: Shear modulus	f_b: Bond strength	

REMARKS:
[15] The values were obtained from diagonal compression tests in accordance with ASTM and RILEM standards.

Appendix

List of publications of the author

Fonseca Ferreira C., D'Ayala D., Fernandez-Cabo J.L., Arce-Blanco M., Díez-Barra R. & Hurtado-Valdez P. (2015). Numerical modeling and seismic assessment of historic planked timber arches. *International Journal of Architectural Heritage*, 9(6), p.712-729

Fonseca Ferreira C., Quinn N. & D'Ayala, D. (2014). *A logic-tree approach for the seismic diagnosis of historic buildings: application to adobe buildings in Peru.* In: Proceedings of the 2nd European Conference on Earthquake Engineering and Seismology, Istanbul

Fonseca Ferreira C. & D'Ayala D. (2014). *Structural analysis of timber vaulted structures with masonry walls*. In: Proceedings of SAHC2014: 9th International Conference on Structural Analysis of Historical Constructions, Mexico City, Mexico

Cancino C., Lardinois S., D'Ayala D., Fonseca Ferreira C., Quinn N., Torrealva D. & Vicente E. (2013). *Seismic retrofitting of historic earthen buildings: a project of the Earthen Architecture Initiative, The Getty Conservation Institute*. In: Proceedings of the UNESCO International Colloquium on the Conservation of World Heritage Earthen Architecture, UNESCO Headquarters, Paris, France

Fonseca Ferreira C., D'Ayala D., Fernandez-Cabo J.L. & Díez-Barra, R. (2013). Numerical modelling of historic vaulted timber structures. *Advanced Materials Research, Structural Health Assessment of Timber Structures*, Trans Tech Publications, pp. 517-525

Cancino C., Lardinois S., Michiels T., Balakrishnan P., D'Ayala D., Fonseca Ferreira C., Quinn N., Torrealva D. & Vicente E. (2013). *Earthen Architecture Initiative: Seismic Retrofitting Project – a bibliography*. The Getty Conservation Institute, Los Angeles, USA

Cancino C., Lardinois S., D'Ayala D., Fonseca Ferreira C., Torrealva D., Vicente E. & Villacorta Santamato L. (2012). *Seismic Retrofitting Project: assessment of prototype buildings.* Research Report, Volume 1 and 2. The Getty Conservation Institute, Los Angeles, USA

Fonseca Ferreira C. & D'Ayala D. (2012). *Seismic assessment and retrofitting of Peruvian earthen churches by means of numerical modelling*. In: Proceedings of the 15WCEE: 15th World Conference on Earthquake Engineering, Portugal

Fonseca Ferreira C. & D'Ayala D. (2012). *Numerical modelling and structural analysis of historical ecclesiastical buildings in Peru for seismic retrofitting*. In: Proceedings of SAHC2012: 8th International Conference on Structural Analysis of Historical Constructions, Poland

D'Ayala D. & Fonseca Ferreira C. (2012). *The Seismic Retrofitting Project: numerical modelling and analysis of earthen heritage buildings for seismic retrofitting*. In: Proceedings of the XIth International Conference on the Study and Conservation of Earthen Architecture Heritage, Pontificia Universidad Católica del Perú, Peru

Cancino C., Macdonald S., Lardinois S., D'Ayala D., Torrealva D., Ferreira C.F. & Vicente E. (2012). *The Seismic Retrofitting Project: methodology for seismic retrofitting of historic earthen sites after the 2007 earthquake*. In: Proceedings of the XIth International Conference on the Study and Conservation of Earthen Architecture Heritage, Pontificia Universidad Católica del Perú, Peru